

# Norwegian Petroleum Directorate **BULLETIN** No.11

2014



NORWEGIAN PETROLEUM  
DIRECTORATE



# Norwegian Petroleum Directorate Bulletin No. 11 2014

ISBN 978-82-7257-117-6

The NPD Bulletin is the journal of the Norwegian Petroleum Directorate (NPD). Its purpose is to enhance the understanding of the development of the Norwegian continental shelf. Contributors are from the NPD, the petroleum industry and academia. The journal is consecutively numbered and published at irregular intervals.

## Editor(s)

For the present volume, the editors are Atle Mørk, Bjørn Anders Lundschieen and Tore Høy.

## Instructions to authors

The present volume follows the standard of the *Norwegian Journal of Geology*.

## Subscription

The Bulletin is free of charge.

Please contact the NPD at: [postboks@npd.no](mailto:postboks@npd.no) for ordering copies of the bulletin.

Copies of individual papers can be downloaded at [www.npd.no/publikasjoner/](http://www.npd.no/publikasjoner/)

## Front cover

The Ichthyosaur ODa. The fossil is named after OD, the Norwegian abbreviation for the NPD, because it was found and excavated during NPD field expeditions to Svalbard. The fossil is described by Hurum et al. in this volume. A replica of the fossil is displayed in the entrance area of the NPD.

Photo: Jan A. Stenløkk, NPD.



## Thematic issue: Results from the Norwegian Petroleum Directorate's activities in the northern Barents Sea and Svalbard (2006 – 2014)

Geological field expeditions have been conducted in the Svalbard Archipelago in the period 2006 - 2014. The field expeditions were triggered by the Russian – Norwegian cooperation project, initialized in 2006, "*Late Mesozoic-Cenozoic Tectono-Magmatic History of the Shelf and Slope of the Barents Sea as a Key to Paleogeodynamic Reconstruction in the Arctic Ocean*", which included both onshore fieldwork and marine geology. The partners in the joint project were the Norwegian Petroleum Directorate (NPD) and the Russian institutions Geological Institute / Russian academy of Science, Moscow, and VNIIOkeangeologia, St. Petersburg. The first field expedition concentrated on the Festningen profile, western Spitsbergen, and was followed by several field expeditions and excursions to the eastern Svalbard. The various field activities are listed in the table below.

Year	Category	Locations
2006	Field expedition	Festningen: western Spitsbergen
2007	Field expedition	Hopen, Edgeøya, Barentsøya, Agard: eastern Svalbard
2007	Excursion	All around Spitsbergen including Edgeøya
2008	Field expedition	Hopen, Edgeøya, Barentsøya: eastern Svalbard
2009	Field expedition	Hopen, Edgeøya, Barentsøya: eastern Svalbard
2011	Field expedition	Hopen: eastern Svalbard
2012	Field expedition	Hopen: eastern Svalbard
2013	Field course	Isfjorden: central and western Spitsbergen
2013	Excursion	All around Spitsbergen including Edgeøya
2014	Field expedition	Hopen and Edgeøya: eastern Svalbard

The field activities have been organized in cooperation between NPD and SINTEF Petroleum Research, with SINTEF as operator (AM). In 2011 and 2012, the production licences PL609, PL438, PL492, PL533 and PL611 also supported the expeditions. The following institutions have participated in the field expeditions: NPD, SINTEF Petroleum Research, Norwegian University of Sciences and Technology, University of Oslo, University of Bergen, University Centre in Svalbard, Norwegian Polar Institute, Natural History Museum (Geology), Brekke Chemo, Geological Institute / Russian academy of Science, VNIIOkeangeologia – Federal State Unitary Enterprise, VSEGEI – A.P. Karpinsky Russian Geological Research Institute, Polish Academy of Science and Centre for Environmental Magnetism and Palaeomagnetism, Lancaster University, UK.

The data collected during the expeditions have been compared with seismic interpretation and reconnaissance studies based on stratigraphic cores in the northern Barents Sea. These comparative studies have resulted in a revised model of the palaeogeographic evolution of the entire Barents Shelf during the Triassic, which in turn has led to improved understanding of working Triassic petroleum systems in the Barents Sea as a whole. The field expeditions have also resulted in a new member of the upper Triassic De Geerdalen Formation, the Hopen Member, recently approved by the *Norwegian Committee on Stratigraphy*. The expeditions have been of considerable importance for improving scientific and cultural understanding between national resource managements, academia and industry; also across national borders since the participations have been international. They have led to, and contributed to four Master Theses and two PhD Theses. Master theses, PhD studies and post doc studies are still in progress. Several scientific articles, and popular science-articles, have been published in addition to those included in this volume.



Bente Nyland  
director general





# Triassic hydrocarbon potential in the Northern Barents Sea; integrating Svalbard and stratigraphic core data

Bjørn Anders Lundschien<sup>1</sup>, Tore Høy<sup>1</sup> & Atle Mørk<sup>2,3</sup>

<sup>1</sup> Norwegian Petroleum Directorate, P.O. Box 600, NO-4003 Stavanger, Norway

<sup>2</sup> SINTEF Petroleum Research, P.O. Box 4763 Sluppen, NO-7465 Trondheim, Norway

<sup>3</sup> Department of Geology and Mineral Resources Engineering, Norwegian University of Sciences and Technology, NO-7491 Trondheim, Norway

e-mails: Bjorn.Lundschien@npd.no Tore.Hoy@npd.no Atle.Mork@sintef.no

The Triassic to Middle Jurassic succession is a main target for exploration in the southern Barents Sea, where it has been explored for more than three decades. In the Norwegian part of the northern Barents Sea, the Triassic succession is quite important as the Jurassic is absent or thin, with incomplete stratigraphy, in large areas. The knowledge of the northern Barents Sea is limited since it is not yet opened for petroleum activity. However, by comparing extrapolations from the southern Barents Sea and onshore exposed strata from Svalbard with non-commercial seismic and stratigraphic cores in the northern Barents Sea, it is possible to suggest interpretations in this area.

Triassic oil-prone source rocks were first deposited in the southernmost Barents Shelf and have sourced several hydrocarbon traps, e.g. the Kobbe Formation reservoirs of the Goliat field. In the Svalis Dome area these source rocks (the Steinkobbe Formation) were established at least as early as in latest Olenekian (late Spathian) and span the entire Anisian. In the northern Barents Sea and on central and eastern Svalbard the correlative organic rich shales of the Botneheia Formation were deposited throughout the Anisian and Ladinian.

Triassic reservoir rocks were also first established in the southernmost Barents Shelf, in the Anisian, when the coastal sandstones of the regressive Kobbe Formation were deposited. The regressive trend continued during the deposition of the Snadd Formation from the Ladinian time close to the Norwegian mainland and in the Svalis Dome and Sentralbanken High areas. The prograding deltaic sediments of the Snadd Formation first reached the northernmost Barents Sea (off Kong Karls Land) and Svalbard in the Carnian. These regressive sandstones represent the main reservoir potential in large areas of the Barents Sea as seen by seismic interpretation. This evolution is favorable for Triassic play models with Lower and Middle Triassic source rocks of the Steinkobbe and Botneheia formations overlain by paralic sandstones of the Kobbe, Snadd and De Geerdalen formations.

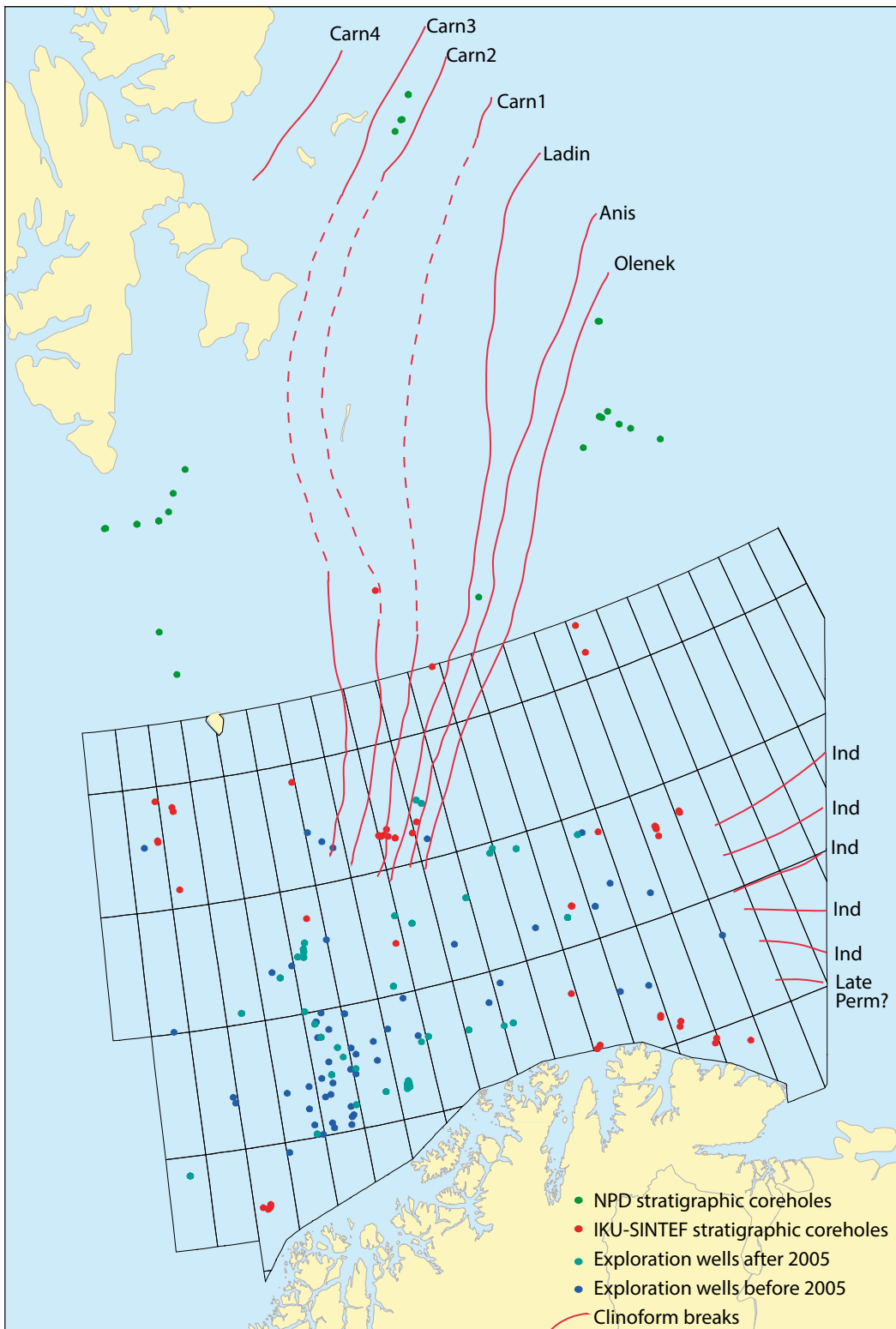
**Key words:** Barents Sea, Svalbard, Hydrocarbon potential, Triassic.

## Introduction

The southern part of the Barents Sea has been explored for hydrocarbons since the 1980s with the Triassic to Middle Jurassic as a main target. Several discoveries have been made, resulting in two hydrocarbon fields, Snøhvit and Goliat. A third, Johan Castberg, is currently under evaluation. In the Norwegian part of northern Barents Sea the Jurassic is absent in large areas. Where present, it is often thin and may contain incomplete stratigraphy, as observed in Norwegian Petroleum Directorate (NPD) stratigraphic boreholes, implying that the Triassic

becomes even more important. The northern Barents Sea, north of 74° 30', is not yet opened for petroleum activity, but seismic studies and reconnaissance studies with shallow stratigraphic drilling (down to 200 m below the sea bed) have been carried out by the NPD (Fig. 1), and form a basis for investigating this underexplored part of the Norwegian continental shelf.

During the Late Paleozoic, the Barents Sea evolved as a large embayment at the Northwestern corner of the supercontinent Pangea (Worsley, 2008; Buitter and Torsvik, 2007) (Fig. 2) and the fusion of the Laurentia



*Figure 1. Stratigraphic boreholes, exploration wells and seismically detectable breaks of prograding clinoforms in the Barents Sea. See Figures 3, 8 and 9 for seismic profiles displaying the prograding clinoform sequences.*

continent with Siberia during the Permian sealed off contact with southern areas (Tethys) and formed the Uralian Mountain chain. The erosion of the Uralian Mountains and basement rocks of Norway and the Kola peninsula filled the Barents Sea with sediments from the south-east during the Triassic (Worsley, 2008; Høy and Lundschieen, 2011; Riis et al., 2008; Glørstad-Clark et al., 2010). Seismic data show that systems of northward prograding clinoforms that define seismic sequences

(hereafter named clinoform sequences) probably were established already in the latest Permian close to the Finnmark coast. A set of clinoform sequences defines a clinoform belt. Clinoform belts prograded throughout the Barents Sea and reached the Svalbard Archipelago in the Late Triassic (Carnian) (Figs. 1, 3). This progressive development has previously been documented (Høy and Lundschieen, 2011; Riis et al., 2008; Glørstad-Clark et al., 2010, 2011), and will be further discussed herein.



Figure 2. The Pangea super continent (based on Torsvik and Cocks, 2005).

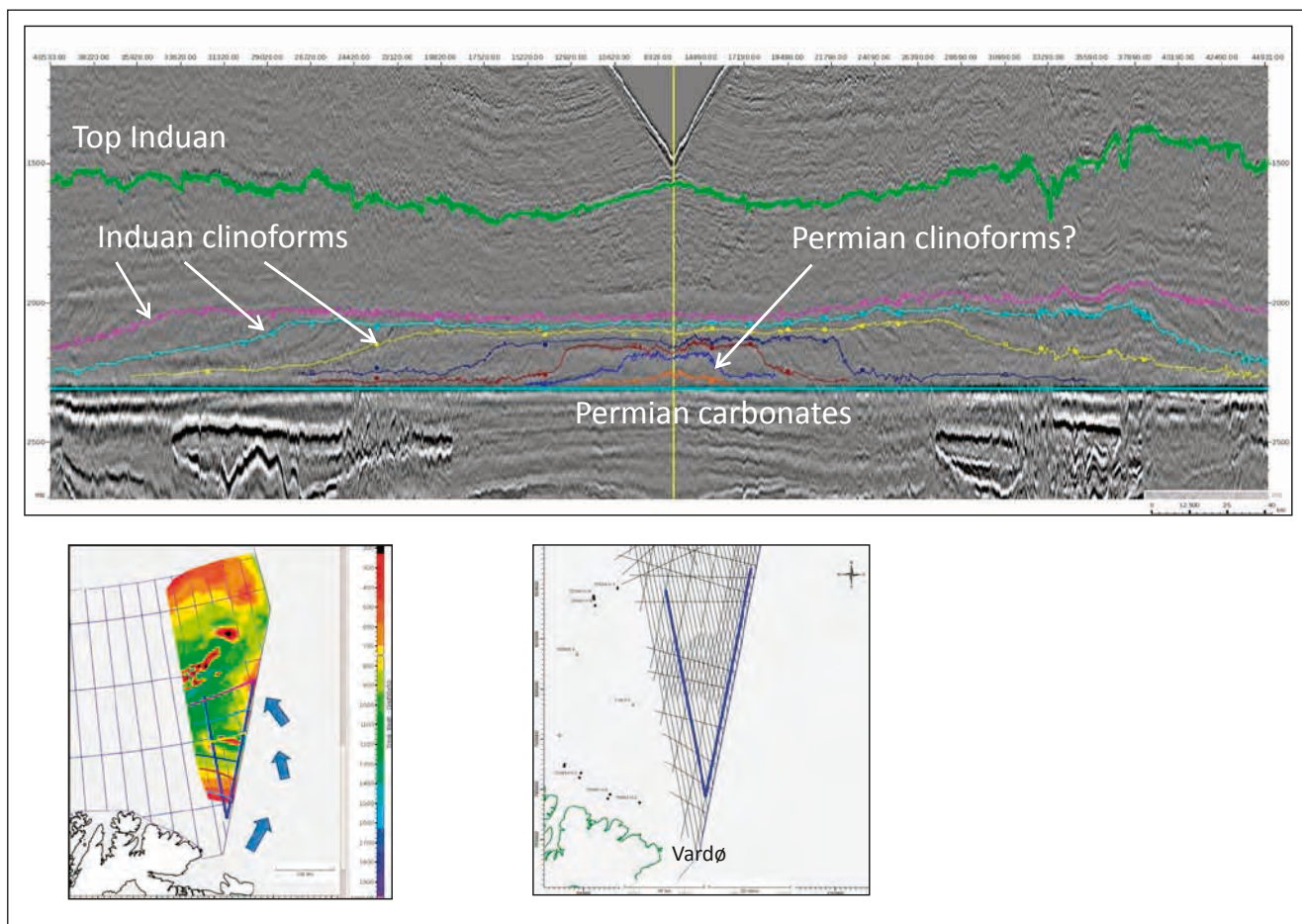
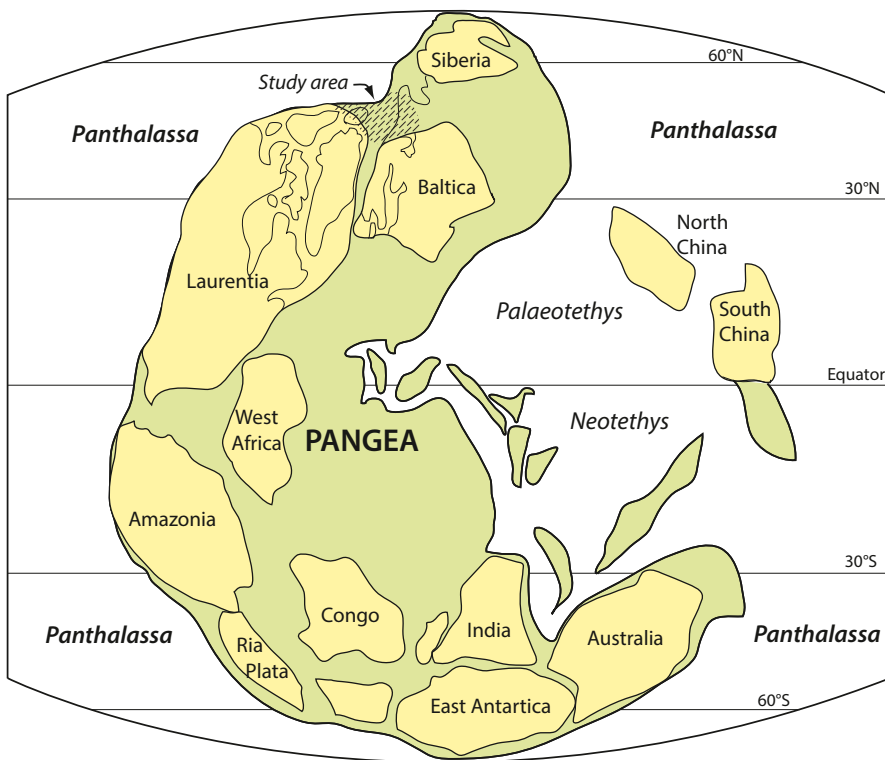


Figure 3. Seismic profile displaying clinoform sequences of latest Permian and Induan age, close to the eastern Finnmark coast, prograding towards north-northeast gradually changing to north basinwards (flattened on top Permian carbonates).

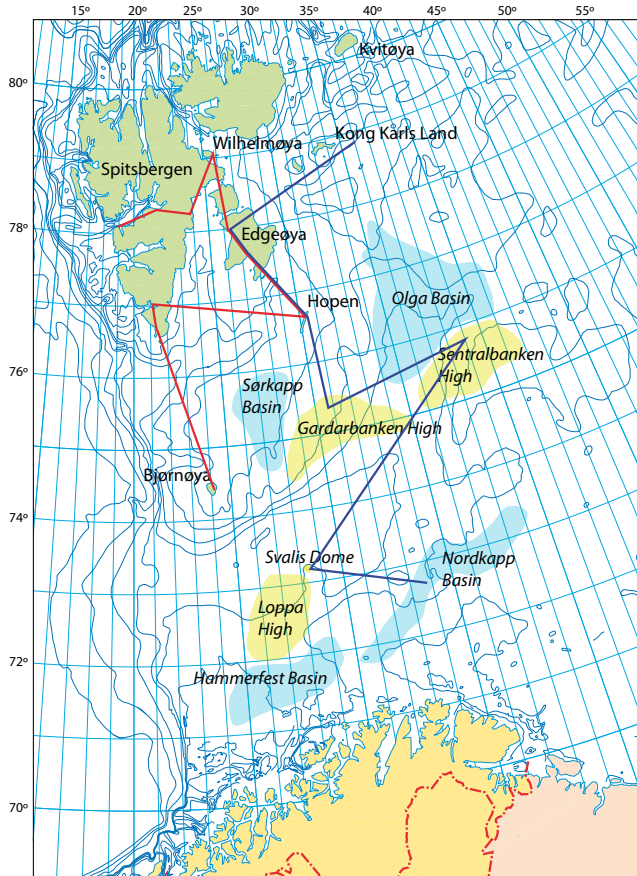


Figure 4. The main structural elements in the Barents Sea. The blue line marks the locations of stratigraphic boreholes and onshore sedimentological logs used in the geological profile in Figure 6. The red line marks the locations of onshore sedimentological logs used in the geological profile in Figure 7.

The tectonic development of the Barents Sea has been described in seismic studies (Faleide et al., 1984) and the main structures were mapped during the 1980s (Rønnevik and Jacobsen, 1984; Gabrielsen et al., 1990) (Fig. 4). Exploration drilling in the southern Barents Sea started in 1980 and focused mainly on the Jurassic succession (Larese et al., 1984; Olaussen et al., 1984; Berglund et al., 1986). Comprehensive overviews have been given (e.g. Johansen et al., 1993; Skjold et al., 1998).

Based on the first wells drilled, Worsley et al. (1988) established a local lithostratigraphy for the Mesozoic and Cenozoic succession of the southwestern Barents Sea. At present, more than a hundred exploration wells have been drilled in the southern Barents Sea. In addition, IKU/SINTEF Petroleum Research, on behalf of oil companies, has drilled c. 60 shallow stratigraphic

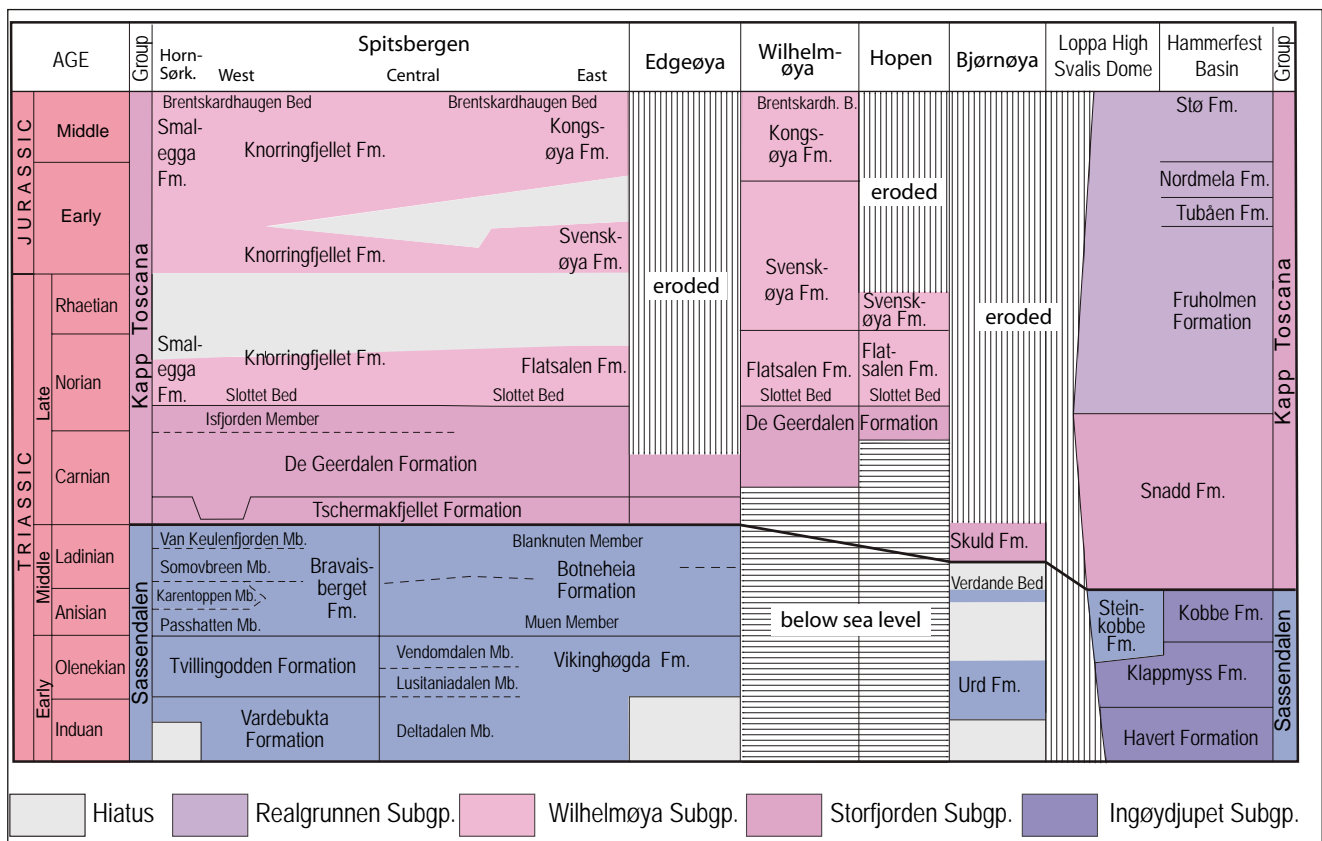


Figure 5. Lithostratigraphic scheme during the Triassic in Svalbard and the Barents Sea (modified from Mørk et al., 1999a).



cores on sub-cropping exposures below the Quaternary overburden. The NPD has carried out a similar program of stratigraphic coring in the northern, Norwegian part of the Barents Sea (Fig. 1), and 12 of these cores have penetrated the Triassic succession. In addition, the NPD has also gathered c. 130 000 km of non-commercial 2D seismic with line spacing typically 4 to 10 km, in the northern area. Triassic rocks were systematically cored and described at the Svalis Dome (Mørk and Elvebakk, 1999; Vigran et al., 1998) and in the Nordkapp Basin (Bugge et al., 2002) (Fig. 4). All these data were used to construct a common stratigraphy of Svalbard and the Barents Sea with the great similarities displayed at group level for the Paleozoic by Dallmann et al. (1999) and Larssen et al. (2002) and the Mesozoic by Mørk et al. (1999a) (Fig. 5).

The well exposed strata in Svalbard permit detailed stratigraphical and sedimentological studies. Triassic rocks in the archipelago provide data for interpreting the depositional environments. In this paper we will integrate interpretations from outcrop studies in Svalbard with seismic data and drilling information in the Barents Sea to comment on the petroleum potential of the northern Barents Sea.

## The Barents Shelf and Svalbard Triassic sediments

A review of the lithological and sedimentological development across the Barents Sea from the Nordkapp Basin to east of Kong Karls Land based on shallow stratigraphic cores and onshore sedimentological profiles is visualized in Figure 6. Different parts of the geological sections are available for this study technique in the different areas. At the Svalis Dome hydrocarbon source rocks are focused (Mørk and Elvebakk, 1999; Leith et al., 1993; Vigran et al., 1998), while in other areas like the Nordkapp Basin (Bugge et al., 2002) and the Sentralbanken High reservoir rocks have been in focus. In Svalbard, the whole succession has been studied considering both the hydrocarbon source and reservoir rocks. In Svalbard, exposures permit detailed studies of stratigraphy and sedimentology (Fig. 7) (Mørk et al., 1982, 1999a, b; Vigran et al., 2014) which help us to better understand also the Barents Shelf sediments (Fig. 6).

### Permian – Triassic boundary

The Permian – Triassic boundary forms a pronounced seismic reflector in the northern Barents Sea, as upper Permian carbonates are overlain by lower Triassic shale and siltstones. However, in parts of the southern Barents Sea this reflector represents a near top Permian boundary, since the uppermost Permian rocks in these areas are siliciclastic, sitting on top of carbonates. Although the Permian – Triassic boundary has been

penetrated in many exploration wells, it has only been cored by shallow stratigraphic drillings off Finnmark (Bugge et al., 1995) and at the Svalis Dome (Mørk and Elvebakk, 1999). The boundary is exposed on Bjørnøya (Mørk et al., 1990) and all along the western outcrop belt of Spitsbergen. Unconformities are documented at the Svalis Dome (Vigran et al., 1998) and at Bjørnøya (Mørk et al., 1990), both spanning the latest Permian and basal Triassic beds. On Spitsbergen continuous sedimentation may have taken place at Festningen and Vikinghøgda, whereas a pronounced hiatus occurs on Edgeøya where the Induan is missing (Pčelina, 1977; Mørk et al., 1982, 1999a, b; Vigran et al., 2014).

### Lower Triassic shelf sediment

Fine-grained clastics are deposited on top of the well cemented Permian sediments in the large embayment of the Barents Sea area. Clinoform sequences close to the Finnmark coast show that sediments were transported into the basin from Scandinavia and land areas to the southeast (Figs. 1, 3). Further out in the basin the shale dominated Havert Formation contains only minor sandstones, and the unit was deposited in marginal to open marine conditions (Worsley et al., 1988). Local areas like the Loppa High were emergent and partly emergent. Furthermore, Bjørnøya (Mørk et al., 1990), the Stappen High, the Svalis Dome (Mørk and Elvebakk, 1999), the Sørkapp-Hornsund High (Worsley and Mørk, 1978), southern Spitsbergen and Edgeøya are missing the lowest Triassic beds, on Edgeøya the oldest beds are dated to Olenekian (Pčelina 1977; Vigran et al., 2014). Except for basal conglomerates at the Sørkapp Hornsund High, fine-grained clastics rest directly on the well cemented Permian sediments. The only shallow stratigraphic core that contains Induan sediments is drilled at the Svalis Dome where laminated silt and claystone rests on Permian limestones (Mørk and Elvebakk, 1999).

Olenekian sedimentary rocks have been cored at the Sentralbanken High and the Svalis Dome, and are also present on all the major islands of Svalbard. At the Svalis Dome, two cores (7323/7-U-8 and 6) display a 70 m interval of the middle part of the Klappmyss Formation. According to Mørk and Elvebakk (1999), the cores contain bivalves and some ammonoids deposited in an open shelf environment. The lower 17 m of the lowermost core (U-8) is dominated by cross-bedded fining up thin sandstone beds that may represent storm deposits, while the remaining parts of these two cores are siltstone dominated. The next core (7323/7-U-3) occurs approximately 60 m higher in the succession and contains silty sandstone with abundant thin fining up sandstone lamina, representing distal turbidites or storm beds. At the Sentralbanken High strata of latest Olenekian age have been penetrated by two coreholes, 7532/2-U-1 and 7534/6-U-1. Core intervals are approximately 7 and 40 m thick, respectively. Both these coreholes also penetrate the Olenekian-Anisian boundary. The cored Olenekian

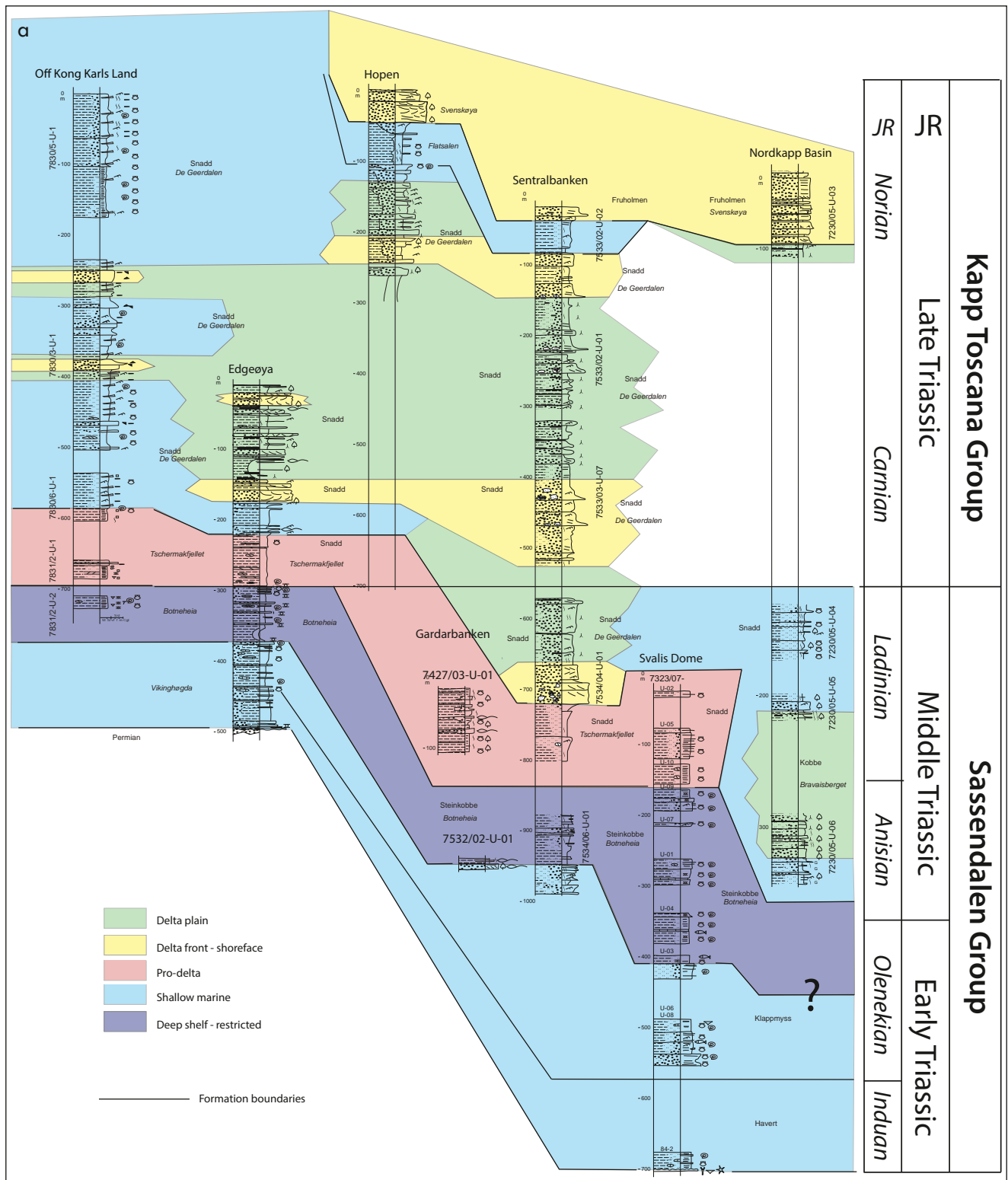


Figure 6. a) Review of the lithological and sedimentological development across the Barents Sea from the Nordkapp Basin to the area east of Kong Karls Land. Note the diachronous pattern of the facies development. See Figures 1 and 4 for stratigraphic boreholes and onshore locations. b) Legend.




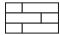
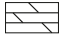


interval consists of silt and sandstones, the longest core displaying coarsening upward sequences and the shortest one being more uniform and upward fining in the very uppermost part. Bioturbation, palynofacies, coal debris and sedimentary structures indicate deposition

in two slightly different shallow marine environments. The shortest core may reflect deposition in a shallow marine channel or mouth bar system in a delta front environment while the longest one is likely to represent more distal prodelta conditions; these subtle variations



b

**Legend**

	Sand- and siltstone
	Mudstone / Debris flow
	Mud pebbles
	Limestone
	Siderite
	Coal
	Covered / partly covered
G	Glauconite
▽	Chert
□	Pyrite
⊕	Phosphate nodules
○	Nodules
⊗	Septarian nodules
~	Erosional surface
==	Planar lamination
≡	Cross-bedding
∩	Hummocky bedding
∧	Lenticular lamination
∩	Ripple lamination
★	Echinoderms
⊙	Ammonoids
⊕	Bivalves
▽	Brachiopods
Y	Bryozoans
T	Tasmanites
🐟	Fish remains
☞	Vertebrate remains
🌱	Plant fossils
🌳	Roots
{-}}	Increasing bioturbation

in depositional setting possibly reflecting auto cyclic switching of lobes in a large delta system. The interval is included in the Klappmyss Formation of Worsley et al. (1988).

In the Svalbard Archipelago, Olenekian sediments are found in the Urd Formation on Bjørnøya, the Tvillingodden Formation in western Spitsbergen and the Lusitaniadalen and the Vendomdalen members of the Vikinghøgda Formation on central Spitsbergen and eastern Svalbard.

The Tvillingodden Formation consists of dark grey, laminated shales coarsening upwards to laminated siltstones and sandstones and may display several (up to four) individual upward coarsening units. Bioturbation (e.g. *Rhizocorallium*) is common to abundant in the upper part of each unit. Macro fossils (bivalves, ammonoids and brachiopods) are sparse, except in two pronounced fossiliferous limestone beds. The entire formation is of marine origin, deposited in a moderately deep to shallow shelf environment, with the limestone beds representing bar deposits (Mørk et al., 1982).

The Vikinghøgda Formation consists of grey shales and silty to sandy shales with subordinate siltstones and carbonate beds (Mørk et al., 1999a, b; Vigran et al., 2014). The Lower Olenekian Lusitaniadalen Member consists of mudstones and siltstone beds and the upper Vendomdalen Member contains dominantly dark grey mudstones with dolomite beds. Abundant septarian nodules occur at several levels throughout the formation. The formation is interpreted as being deposited in moderately deep shelf environments with each member representing stacked, regionally transgressive-regressive successions (Mørk et al., 1999a, b).

#### Late Early and Middle Triassic hydrocarbon source rocks

The Middle Triassic (Anisian and Ladinian) succession occurs throughout the Barents Shelf and Svalbard. In most parts of the southern Barents Sea it is constituted by the Anisian Kobbe and the lower Ladinian to early Norian Snadd formations, representing one overall regressive unit each. In the Svalbard Archipelago, the Bravaisberget Formation, representing a major regressive coarsening upward sequence from shale to fine-grained sandstone, defines the Middle Triassic along western Spitsbergen (Mørk et al., 1982; Krajewski et al., 2007), while in central Spitsbergen and eastern Svalbard it is defined by the Botneheia Formation, dominated by dark organic rich shales (Krajewski, 2008; Mørk et al., 1982, 1999a). At the Svalis Dome, similar organic rich deposits dating from late Early Triassic (Spathian) throughout Anisian were drilled and prompted the definition of the Steinkobbe Formation, which is mostly correlative with the Botneheia Formation (Mørk and Elvebakk, 1999; Vigran et al., 1998). In view of this, we focus on the organic rich Steinkobbe and Botneheia formations and their potential as source rocks for hydrocarbons (Mørk and Bjørøy, 1984; Leith et al., 1993), but first we summarize the more proximal Kobbe Formation that hosts potential reservoir rocks.

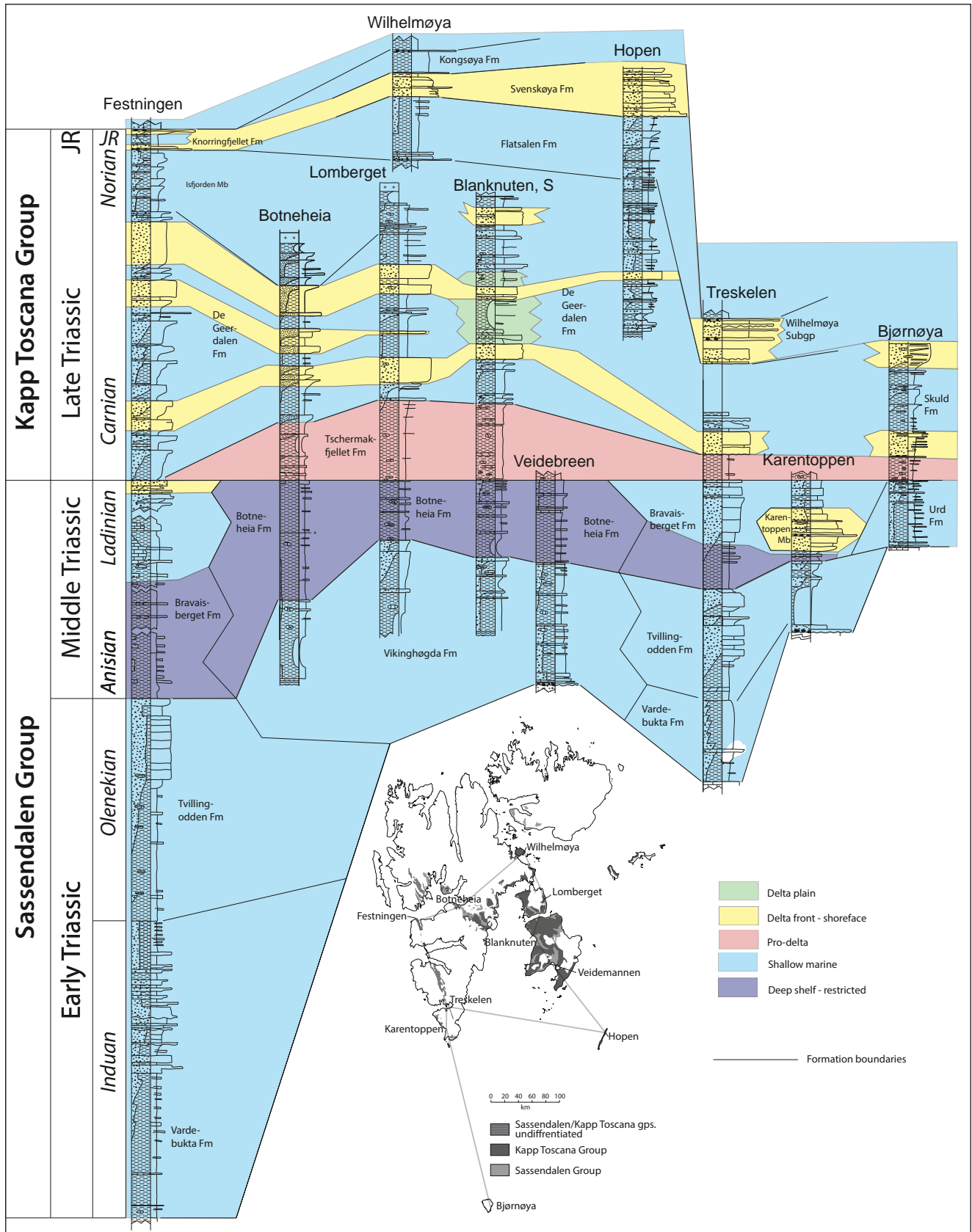


Figure 7. Review of the lithological and sedimentological development across the Svalbard Archipelago. See Figure 4 for onshore log locations. Legend in Figure 6b.

The Kobbe Formation defines an overall coarsening upwards succession initiated by marine shale that passes upwards into interbedded shales, siltstones and carbonate cemented sandstones. It spans the Anisian and earliest Ladinian, and rests on the base Anisian transgressive surface, which is well established from outcrop studies in Svalbard (Mørk et al., 1989, 1993) and also from seismic data, stratigraphic cores and exploration wells in the Barents Sea (Rasmussen et al., 1993; Van Veen et al., 1993; Skjold et al., 1998; Riis et al., 2008; Glørstad-Clark et al., 2010; Vigran et al., 2014). It displays coarse, proximal facies along the southern margin of the Hammerfest Basin and fines basinwards (Worsley et al., 1988). Close to the Troms Finnmark Fault Complex, fluvial to deltaic sandstones (Olaussen et al., 2010) of the Kobbe Formation constitute the main reservoirs of the Goliat oil and gas field. Coastal sandstones are also penetrated in the Nordkapp Basin by stratigraphic boreholes (Bugge et al., 2002) (Fig. 6) and by exploration wells in the southern part of the Bjarmeland Platform (e.g. 7225/3-1). In the eastern part of the Loppa High, the Kobbe Formation is initiated by the deposition of dark grey, organic rich marine shale coarsening upwards into interbedded shales and siltstones and a minor content of shallow marine sandstones in the uppermost part (e.g. exploration well 7222/6-1).

The Steinkobbe Formation was defined by Mørk and Elvebakk (1999) based on 5 cores that penetrated organic rich dark shale, representing 118 m of an interval of approximately 250 m at the Svalis Dome. The total organic carbon (TOC) varies between 2 and 6 %, but has intervals up to 8%. The organic material is dominated by type II/III kerogen characterized by high concentrations of extractable organic matter (Leith et al., 1993). The formation spans the late Spathian and the entire Anisian as dated by ammonoids and palynology (Vigran et al., 1998). The deposition of the Steinkobbe Formation starts earlier than the deposition of the Botneheia Formation in Svalbard (base Anisian), although they represent the same continuous depositional environments. This indicates that the preservation potential for organic matter with anoxic or periodic anoxic sea bottom conditions was established earlier in the central part of the Barents Sea (Svalis Dome) than in Svalbard. This restriction pattern in the Barents Sea embayment is supported by the Re-Os analysis (Xu et al., 2009) that shows more open marine conditions on Spitsbergen and water mass restrictions at the Svalis Dome in the late Anisian.

At the Sentralbanken High there is a marked change in lithology across the Olenekian-Anisian boundary in the two stratigraphic cores penetrating it, 7532/2-U-1 and 7534/6-U-1, from siltstones and sandstones to dark shale grading upwards into interbedded clayey siltstones and thin sandstones with a stable total TOC around 1%. We assign these Anisian successions of both cores to the Steinkobbe Formation of Mørk and Elvebakk (1999).

At Bjørnøya, the Verdande Bed is a phosphatic remanier conglomerate, indicating that an equivalent of the Steinkobbe/Botneheia Formation has been deposited and eroded as the overlying Skuld Formation resembles the Snadd Formation and is dated as Ladinian (Mørk et al., 1990).

In Svalbard, the Bravaisberget Formation comprises the whole Middle Triassic along western Spitsbergen (Weitschat and Dagys, 1989; Mørk et al., 1982, 1999a; Krajewski et al., 2007). It forms one overall coarsening upward succession with basal mudstones grading into siltstones and sandstones. Small phosphate nodules occur throughout the formation. Ammonoid, bivalve and brachiopod faunas are common. Trace fossils are present and display an upward increasing abundance reflecting improved living conditions through a regressive unit (Mørk and Bromley, 2008). The lower part of the formation, the Passhatten Member, is dominated by organic rich shale, and has similar hydrocarbon source rock properties as the Botneheia and Steinkobbe formations. The Bravaisberget Formation as a whole is interpreted as a deltaic influenced regressive unit (Mørk et al., 1989, 1999a).

The Botneheia Formation is dominated by organic rich shale (Mørk et al., 1982, 1999a; Krajewski, 2008). It forms one major coarsening upward section with basal mudstones grading into siltstones. The dominant lithology is black shale with abundant small phosphate nodules. Marine fossils and reptile bone fragments occur and are abundant in the upper part (the Blanknuten Member), which is also intensely bioturbated. The organic richness is high (TOC 1-10 %), especially within the Blanknuten Member and the formation represents the most important possible hydrocarbon source rock of Svalbard (Mørk and Bjørøy, 1984).

East of Kong Karls Land, the lowermost core in a series of five, 7831/2-U-2 (Figs. 1, 6), penetrated late Ladinian (Vigran et al., 2014) dark grey, laminated claystone of good to excellent organic richness (TOC 3.2 - 10.8 %) along with both phosphate and chert nodules. Fossils, dominantly bivalves, are present throughout the core, as are also layers of microcoquina (Mørk and Bromley, 2008), and the algae *Tasmanites* is abundant at several levels (Vigran et al., 2008). The high organic content of the claystone suggests a deep shelf depositional environment with restricted circulation and anoxic bottom water conditions. The core resembles the Botneheia Formation as exposed on Edgeøya (Krajewski, 2008; Lock et al., 1978; Mørk et al., 1982, 1999a) and is interpreted as the same.

The oil-prone hydrocarbon source rocks were first deposited in the southern Barents Shelf and have sourced several hydrocarbon traps, e.g. the Kobbe Formation reservoirs of the Goliat field. The age of the source rocks in the Goliat area is not specified, but they are



most likely defined by organic rich shales of Olenekian and early Anisian age, as observed in exploration wells, e.g. 7222/6-1 and 7121/1-1R (Olaussen et al., 2010), and indicate that the Steinkobbe Formation is present also in this area. The organic rich facies subsequently spread over major parts of the central and northern Barents Sea and Svalbard in the Early Anisian. Oxygenated conditions were established in the southernmost part of the Norwegian Barents Sea in the Anisian when the first coastal sandstones of the regressive Kobbe Formation were deposited. The oxygenated conditions and regressive trend continued during the deposition of the Snadd Formation throughout the Early Norian, only interrupted by the early Ladinian regional transgression (Worsley et al., 1988; Skjold et al., 1998; Glørstad-Clark et al., 2010). Contemporaneously organic rich shales continued to be deposited in the Svalis Dome area throughout the Anisian, and in the northern Barents Sea and in central and eastern Svalbard throughout the Ladinian. The prograding deltaic, oxidized sediments first reached the northernmost Barents Sea and Svalbard in the Carnian.

Organic rich Triassic sediments occur not only in the Barents Sea area. A similar development occurs in the Sverdrup Basin of Arctic Canada and in North Alaska (Leith et al., 1993). The organic rich deposits started first in the Barents Sea embayment at least as early as in the Spathian and then spread to all these areas after the base Anisian transgression. The organic rich episode also terminated first in the southern Barents Sea as advancing deltas filled the Barents Sea and finally at the early Carnian also covered Svalbard. In both the Sverdrup Basin and Alaska, the organic rich sediment deposition continued almost to the end of the Carnian.

### Late Middle and Late Triassic paralic sediments with reservoir potential

In the mid- Middle Triassic, in the Anisian, clastic sediments of the Kobbe Formation entered the southern Barents Sea embayment from south and southeast and terminated the organic rich deposition in this area, while organic rich sedimentation proceeded throughout the Middle Triassic in the northern Barents Sea and in Svalbard. Clinoform belts show how the paralic shelf and coast prograded towards the northwest (Fig. 1) (Høy and Lundschieen, 2011; Riis et al., 2008; Glørstad-Clark et al., 2010). In the southern Barents Sea the late Middle and early Late Triassic is constituted by the Snadd Formation. The Snadd Formation commences with relatively distal marine to prodelta shales, constituting most of the Ladinian section, passing upwards into large scale prograding deltaic systems forming the late Ladinian to early Norian succession. It represents a regressive succession that developed on top of the early Ladinian regional transgressive surface (Worsley et al., 1988; Glørstad-Clark et al., 2010).

At the Svalis Dome, only the basal part of the Snadd Formation (Ladinian) has been cored (Mørk and Elvebakk, 1999; Vigran et al., 1998) and displays open marine muddy, laminated siltstone with thin sandstone lamina shelf sediments like in the type well 7120/12-2 at Tromsøflaket. The lower core, 7323/7-U-10 (27 m), contains abundant bivalves and siderite nodules quite similar to the Tschermakfjellet Formation in Svalbard. The overlying core, 7323/7-U-5 (43 m), consists dominantly of shale and siltstone and abundant sandstone lamina varying from a few mm to 1.5 cm, representing distal storm layers in increasing abundance upwards. Together these cores indicate a regressive and slightly upward shallowing trend through this lower part of the Snadd Formation (Mørk and Elvebakk, 1999).

Close to the Gardarbanken High, the Snadd Formation in the core 7427/3-U-1 of Early Ladinian age, as dated by palynomorphs (Vigran et al., 2014), consists dominantly of shale comprising several coarsening upward units (5-20 cm) with dark grey parallel laminated shale at the bases, grading upwards into silty shale and occasionally into very fine sand with hummocky cross-bedding. These are sedimentary features indicative of deposition partly above storm wave base in a storm influenced shallow shelf to prodelta setting.

Paralic sediments constitute most of the cored sections of the Snadd Formation at the Sentralbanken High (Fig. 6). Delta plain deposits, often with thin coal beds and root horizons dominate, although channels and stacked channel systems also form significant parts of the succession. In core 7534/4-U-1, dated by palynology as late Ladinian (Vigran et al., 2014), the lowermost interval comprises two units, coarsening upward from slightly silty shale to sandy siltstone, containing open shelf ichnofauna like *Zoophycos*. A few bivalves and coquina layers occur associated with beds coarsening upwards from silt to fine-grained sandstone in the upper parts. The units are interpreted to represent prograding lobes within a delta system, at a locality within the reach of only the prodelta part. Across an erosional boundary on top of this interval there is an abrupt change in depositional environment. A 30 m thick channel complex of dominantly fine to medium grained sandstone contains abundant clasts of siltstone and claystone as well as mud clasts and coal debris (Fig. 6). This channel complex is interpreted to represent a delta front channel system. It is overlain by slightly more than 100 m of delta plain and estuarine sediments that display both fining and coarsening upwards successions characterized by several root horizons. In interbedded sandy siltstones, marine trace fossils like *Rhizocorallium*, *Paleophycus*, *Teichichmus*, and also a level with *Diplocraterion*, are present. Lenticular and wavy bedding dominate where bioturbation is sparse. Some levels with bivalve coquinas are present.

In the overlying core 7533/3-U-7, dated as early Carnian by palynology, the same alternation of bioturbated beds

and beds rich in coal debris are present in the lower part, while in the upper 60 m, coal beds are abundant. These beds are typically between a few cm to almost 1 m thick and often underlain by rootlets. Bioturbation is sparse within this upper part, and although sporadic bioturbation occurs, no clear marine indicators are observed. Hence, the core is interpreted as being deposited in an upper delta plain environment.

The same facies association continues in the next core (7533/2-U-1) of early and late Carnian age as dated by palynology (Vigran et al., 2014). However, some channel complexes, 10, 13 and 15 m thick, strongly resemble channel complexes of Hopen (Klausen and Mørk, 2014; Lord et al., 2014b) of approximately the same age. Coal beds and root horizons are abundant and desiccation cracks are present in the uppermost part. No marine indicators have been observed in this core either.

The top of the Snadd Formation is cored (7533/2-U-2) and consists of delta plain sediments of fine sand and silt with subordinate mud. Ripple lamination is abundant as is also desiccation cracks. The delta plain succession is abruptly overlain by a bed of muddy coarse calcite cemented sandstone that is bioturbated and capped with a thin siderite crust. This bed is overlain by a marine unit, palynologically dated as early Norian. On Hopen, the closest island, a correlative unit is named the Flatsalen Formation (Mørk et al., 2013; Lord et al., 2014a). The calcite cemented sandstone with the thin siderite crust resembles the Slottet Bed that marks the onset of the Wilhelmøya Subgroup in Svalbard, which is time equivalent with the Realgrunnen Subgroup in the southern Barents Sea (Mørk et al., 1999a).

East of Kong Karls Land, Triassic intervals from the late Ladinian to the early Late Carnian has been penetrated by five stratigraphic coreholes (Figs. 1, 6).

The stratigraphically lowest cores, 7831/2-U-2 and 7831/2-U-1, are short and span the Ladinian – Carnian boundary, as shown by macrofossils and palynology (Vigran et al., 2014). This boundary has also been numerically dated by Re/Os (Xu et al., 2014). There is a gap of some few tens of meters between these cores, but they represent a depositional continuity. The lower core is organic rich and assigned to the Botneheia Formation (see above). A regional seismic reflector is interpreted to correspond to the top of the Botneheia Formation, which is close to or just above this core (Riis et al., 2008, p. 323, fig. 5a). The lowermost part of the overlying core, 7831/2-U-1 (Late Ladinian), also represents deep shelf sediments, but is sparse in organic content and resembles the Tschermakfjellet Formations as it occurs on Edgeøya (Lock et al., 1978; Mørk et al., 1999 a). The overlying part (Carnian) contains sandstones and siltstones as well as coal fragments, typical for the Snadd Formation elsewhere in the Barents Sea.

The three overlying cores east of Kong Karls Land are all of Carnian age with the top of the uppermost one entering the late Carnian, as indicated by palynology, and are all referred to as the Snadd Formation. The lowermost of these cores, 7830/6-U-1 (c. 50 m), consists of dark grey silty shale with marine bivalves, some ammonoids and marine palynomorphs. The lower 13 m is rich in pyrite while sparse bioturbation and thin ripple laminated sandstone laminae with coal debris are common in the upper part. The core shows a gradual change from prodelta to more shallow depositional environments (Fig. 6).

The next core, 7830/3-U-1, is close to 200 m long and the uppermost core, 7830/5-U-1, is 120 m long. Both these cores represent variations between open shelf to delta front and shoreface conditions. Marine bivalves are present (abundant bivalves of the *Daonella/Halobia* group) in addition to some ammonoids. Bioturbation is sparse except for some few beds. A few, up to 5 m thick, sandstone beds are associated with mud flake conglomerates and minor coal debris, and represent delta front deposits. These deposits of mainly early Carnian age are clearly more distal than the early Carnian sediments at the Sentralbanken High.

In Svalbard, the Carnian to earliest Norian is represented by the Tschermakfjellet and the overlying De Geerdalen formations. The Tschermakfjellet Formation is dated as Early Carnian by ammonoids (Korčinskaja, 1982; Weitschat and Dagys, 1989; Dagys et al., 1993). The lower boundary is defined where grey, silty shale with red weathered thin beds and nodules of siderite sharply overlie the Bravaisberget and Botneheia formations. The formation consists of dark grey shales with an upward increasing content of siltstone and sandstone laminae. Fossiliferous beds with ammonoids, bivalves, gastropods and brachiopods occur in the eastern areas. It is interpreted to represent a pro-delta depositional environment (Mørk et al., 1982).

The De Geerdalen Formation is dated by ammonoids and palynology as Carnian to early Norian (Korčinskaja, 1982; Tozer and Parker, 1968; Vigran et al., 2014). The lower boundary is defined at the base of the first occurring prominent sandstone. The formation dominantly forms repeated coarsening upward successions from shale to sandstones. The sandstones may be grouped in two overall types of facies: 1) Coarsening upward units that are mostly massive, although some bioturbation and linguoid ripples occur, and 2) upward fining sharp based units, some with mud conglomerate or gravelstones. Ripple lamination and cross-bedding alternating with parallel bedding are common in both of these facies types. The formation as a whole is interpreted as deposited in shallow shelf to deltaic environments, being more proximal in eastern Svalbard (Edgeøya) than on central Spitsbergen (Mørk et al., 1982, 1999a; Rød et al., 2014).

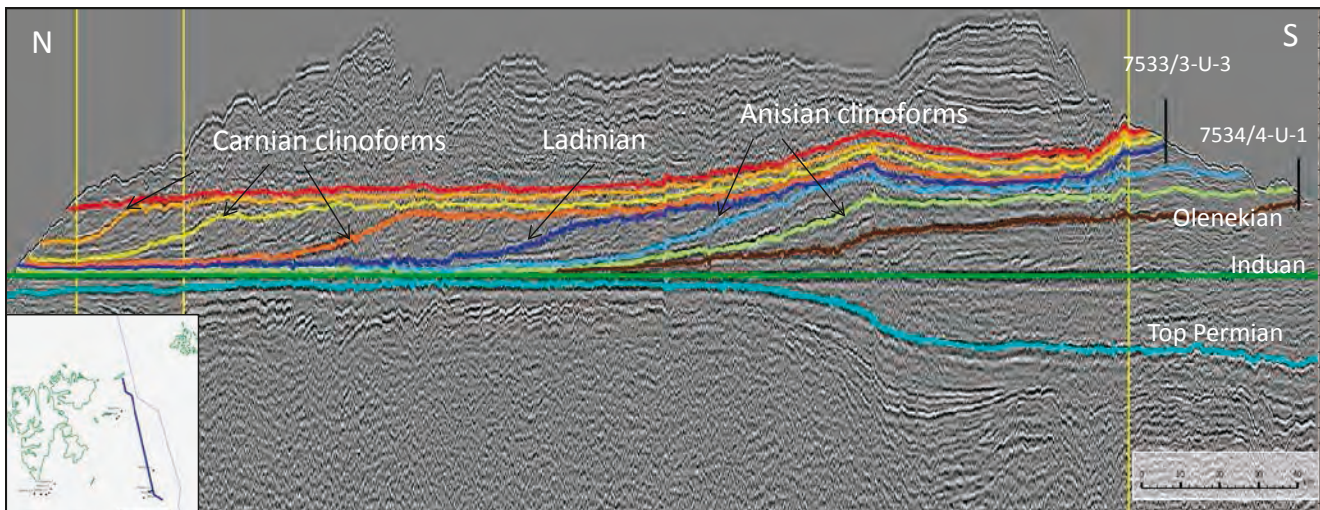


Figure 8. Prograding clinoform sequences north of the Olga Basin, being successively younger in the progradation direction (flattened on top Induan).

On top of the De Geerdalen Formation, the Slottet Bed represents a condensed shelf deposit due to the early Norian transgression of regional character, on which new regressive events represented by the Wilhelmøya and the Realgrunnen Subgroups evolved (Worsley, 2008; Bergan and Knarud, 1993; Mørk et al., 1999a). These subgroups of Late Triassic to Middle Jurassic age contain the hitherto most significant reservoir rocks in the Barents Sea. As stated above, the Realgrunnen Subgroup, of mainly Early to Middle Jurassic age, is absent in large areas in the northern Barents Sea and, where present, it is often thin and may contain incomplete stratigraphy, and is therefore not discussed further.

### Triassic clinoform sequences in the Barents Sea

In the Late Carboniferous and Permian, the Barents Sea was dominated by shallow marine carbonates (Worsley, 2008; Larssen et al., 2002). In deeper grabens such as the Nordkapp Basin and the Tiddlybanken Basin, large amounts of salt were deposited. The top of the Permian carbonates defines the basis for the uppermost Permian and Triassic accommodation space in the Barents Sea, and opened for prograding clinoform sequences all the way from the coast of the Norwegian mainland to Kvitøya northeast in the Svalbard Archipelago (Figs.1, 3, 8).

Regional seismic studies show that the thickness of Triassic clinoform belts in the Norwegian part of the Barents Sea range from 200 to 400 meter, which also indicates the same magnitude of water depth (Høy and Lundschieen, 2011). The distance of a single dipping clinoform surface, from the breaking point close to delta front down to the flat lying offshore basin floor beds, is in the range of 50-70 km, as observed in the Lower Triassic in the southeastern Barents Sea and the Middle and Upper Triassic in the northern Barents Sea (Figs. 3, 8). However, in some sub-basins the clinoform belts are thicker. In rim synclines, close to growing salt

diapirs in the Nordkapp and Tiddlybanken basins, the clinoform thickness expands significantly due to the sudden increase of accommodation space during the growth of the salt diapirs. The salt started to move when a clinoform belt reached an area with underlying salt and the load reached a critical weight. Growth faults in the Middle and Late Triassic related to salt collapse along the graben margins are a part of the increased accommodation space in the Nordkapp Basin.

The extensive Triassic clinoform sequences are derived from large river systems that filled the basin with sediments from southeast. As outlined above, this progressive infill included depositional environments ranging from deep basin to delta plain. The seismic response of this prograding system is a succession of clinoforms, being successively younger towards northwest (Høy and Lundschieen, 2011), in which lithological formation boundaries are diachronous.

In the southeastern part of the Norwegian Barents Sea, clinoform sequences are interpreted to have an early Triassic and possible late Permian age. In this area there is only one dominant clinoform belt, indicating that the sediment infill was faster than the basin subsidence. This interpretation is based on a change in seismic facies. Most of the Triassic succession overlying the marine clinoforms has a fluvial seismic character without any larger transgressions drowning the prograding delta. A succession of 10 or more clinoform sequences can be mapped in which the oldest clinoforms, close to the Finnmark coast, may have a late Permian age, representing the first major siliciclastic sediment supply to the Norwegian part of the Barents Sea.

Studies in the Pechora Basin show that the filling of the Eastern Barents Sea starts in Late Permian (e.g. Ostistiy and Fedorovsky, 1993, p. 244-246, figs. 1, 5), and this may also be the case along the coast, close to the



Scandinavian hinterland. The Ørret Formation of the latest Permian age is predominantly siliciclastic (Larsen et al., 2002) and may initiate the basin infill. From the seismic interpretation it is seen that the first clinoform belt in the Barents Sea predates the salt movement in the Tiddlybanken Basin. There is no thickening of the clinoform belt lateral to the salt diapir and no thinning of the belt on the flanks at the top of the salt structure. In the Middle Triassic, when the salt in the Tiddlybanken Basin started to move, the rim synclines provided increased accommodation space for the prograding clinoforms from south east.

In large areas in the central part of the Norwegian Barents Sea, there are two dominant clinoform belts of different age (Riis et al., 2008, p. 322, fig. 4c). The oldest belt is Early Triassic (Induan) in age and the youngest of Early and Middle Triassic age (Olenekian-Ladinian). Between the two belts there is a transgression of regional character on top of the Induan succession (Glørstad-Clark et al., 2010). The double set of clinoform belts may be caused by a fast subsidence in the area, which created renewed accommodation space and permitted a new filling of the basin in the same area. The Induan progradation reached the area North of the Olga Basin before it was drowned by

the base Olenekian transgression. In Olenekian and Middle Triassic time the bottomsets of the clinoform belt are likely to represent the organic rich shale of the Steinkobbe and Botneheia Formations. The bottom sets of the Induan clinoform belt may represent an additional and even older source rock, given low sedimentation rates (in fact likely in front of prograding clinoform sequences) and palaeo bathymetry favorable for anoxic bottom water conditions. Unfortunately, these beds have not been cored to date.

From the northern part of the Hoop area between the Bjarmeland Platform and the Fingerdjupet Sub Basin, the seismic data show progradation of the Triassic clinoforms (Fig. 9). On the Bjarmeland Platform the clinoforms are of Olenekian age while in the Hoop Fault Complex Anisian and Ladinian clinoforms dominate, and further west the Fingerdjupet Sub Basin comprises Late Triassic clinoforms. In well 7321/8-1, in the Fingerdjupet Sub Basin, the Early and Middle Triassic succession is highly condensed, only 36 m from top Permian to top Ladinian. This condensed section corresponds to the dramatic thinning of the Lower and Middle Triassic succession seen on the seismic line from the Bjarmeland Platform to the Fingerdjupet Sub Basin (Fig. 9). This thinning is compensated by a large thickness increase

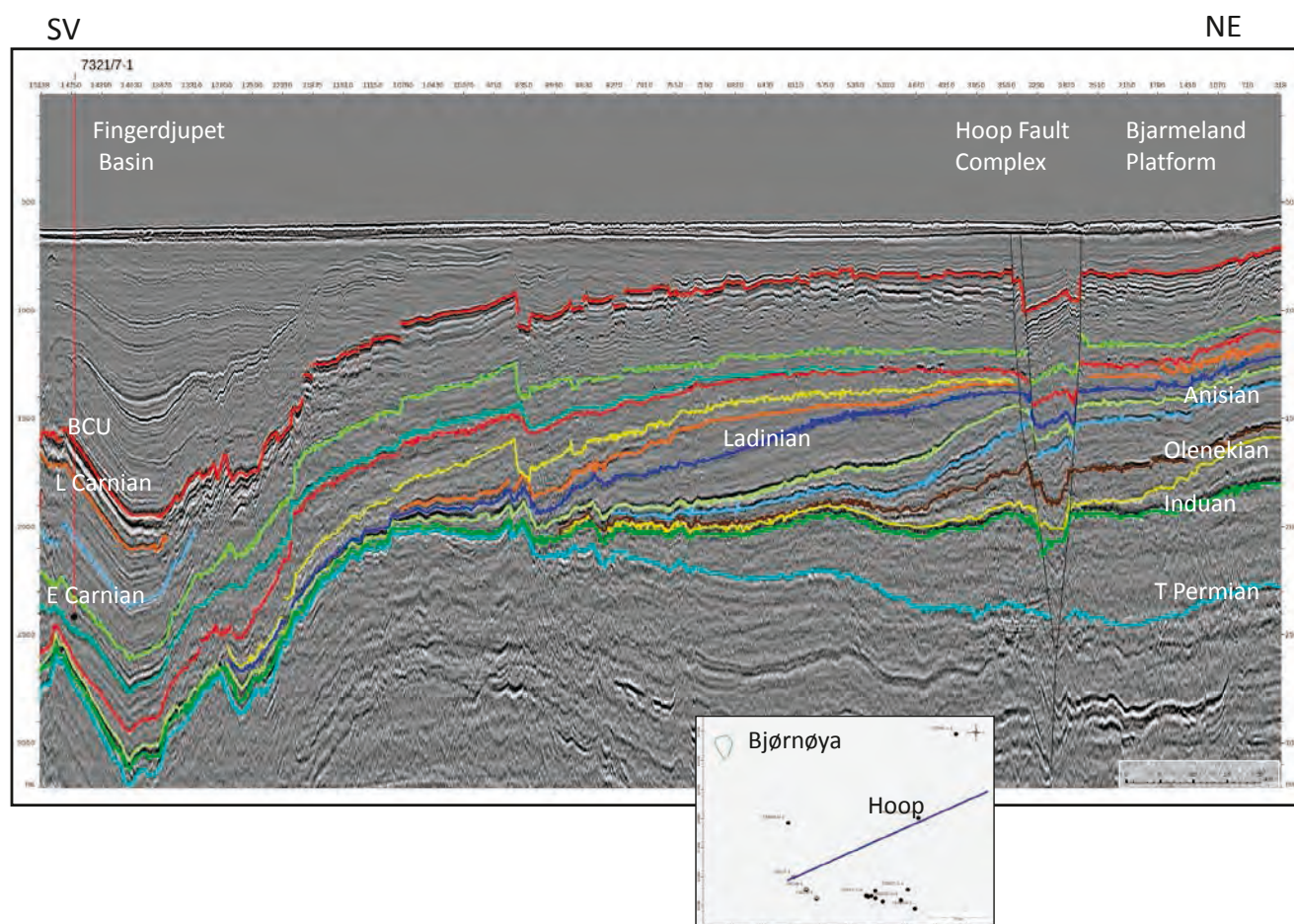


Figure 9. Prograding clinoform sequences in the Bjarmeland Platform, Hoop Fault Complex and the Fingerdjupet Sub Basin area, becoming successively younger in the progradation direction.

in the Late Triassic, and thus the thickness from top Induan to top Triassic on the Bjarmeland Platform and the Fingerdjupet Sub Basin is relatively equal, although timing of the infill is different.

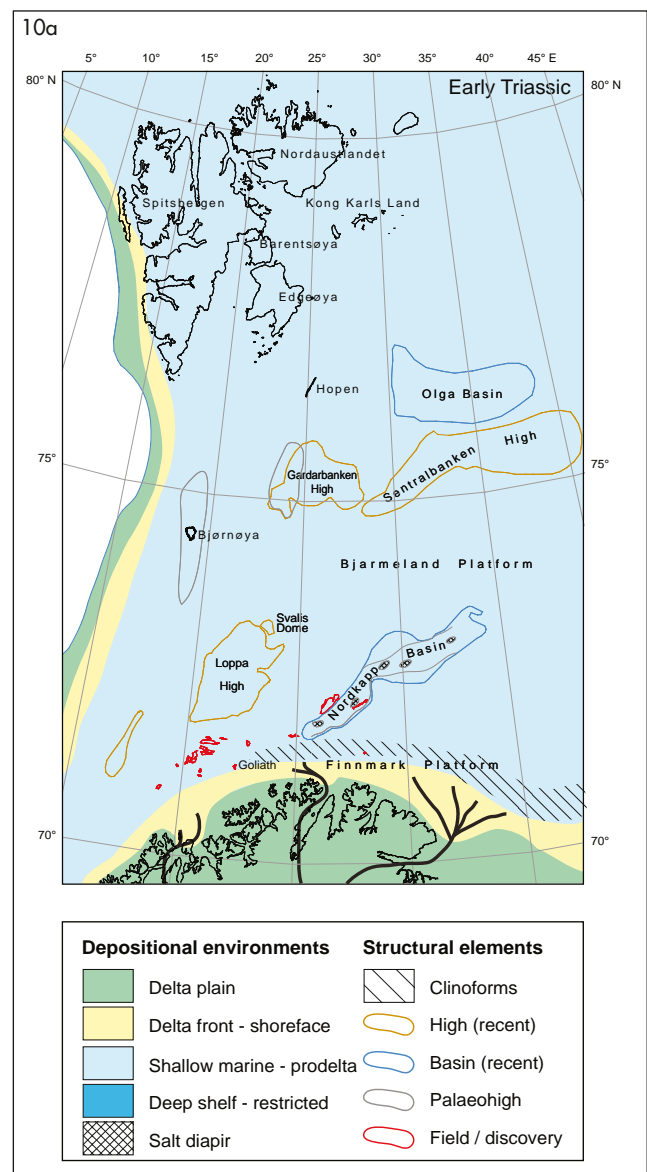
The seismic interpretation in the present study also demonstrates that the Hoop Fault Complex is of post Jurassic age in the northern part (Fig. 9). There are no major Triassic synsedimentary faults disrupting the clinoform sequences in this area. In contrast, synsedimentary growth faults can be observed along parts of this fault complex further south, adjacent to the Maud Basin and the Svalis Dome. A plausible explanation for this growth could be local salt movements during deposition creating increased accommodation space along the hanging wall of synsedimentary faults related to gravitational collapse when the salt moved from the Maud Basin to the Svalis Dome.

North of the Olga Basin, the Early and Middle Triassic clinoform sequences are successively thinning northwards. Only one dominant clinoform belt of Carnian age developed in this area (Fig. 8). A succession consisting of four Carnian clinoform sequences can be mapped in the northern part of the Barents Sea (Høy and Lundschieen, 2011, p. 251, fig. 15.4). The present seismic cover does not permit mapping further north and northwest, but paleocurrent measurements from the Svalbard Archipelago indicate that the Late Triassic progradation continued onto the islands of Svalbard and may have covered the whole archipelago (Høy and Lundschieen, 2011; Rød et al., 2014). This assumption is in accordance with provenance studies performed by Mørk (1999), and Pózer Bue and Andresen (2013) who suggested that Late Triassic sandstones of the De Geerdalen Formation were sourced from the south east, possibly the northern Uralides, with minor input from the Timanides. Close to Kvitøya, the Triassic clinoform beds crop out on the sea floor and are eroded as a response to the Cretaceous uplift, but there are no indications in the seismic data that Kvitøya was a basement high in the Triassic or an obstruction for further progradation towards northwest.

As stated before (Mørk, 1999; Høy and Lundschieen, 2011; Skjold et al., 1998; Riis et al., 2008; Glørstad-Clark et al., 2010), the Fenoscandian Shield as well as other land areas further east (the growing Uralian Mountains) were important provenance areas for the sediments that filled the Barents Sea basin in the earliest Triassic. Interpretation of the new seismic in the Norwegian part of the Barents Sea southeast, acquired in 2011, supports this hypothesis. Here, the uppermost Permian and lowermost Triassic clinoform sequences, close to the Finnmark coast, prograde towards north-northeast (Fig. 3). Further out in the basin, as the clinoform sequences are getting successively younger and gradually merge with the significantly more dominant clinoform succession building from the Uralides, the progradation

direction gradually changes towards north-west and finally towards west-north-west (Fig. 1).

In the Late Triassic, the northwesterly prograding paralic deposits covered most of the northern Barents Sea, including Svalbard, and may even also be the source for the northeastern supply of sediments to the Sverdrup Basin, explaining the missing Crockerland (Embry, 1993) and perhaps also the fluvial Triassic sediments on Franz Joseph Land (Preobrazhenskaya et al., 1985a, b). Hypothetically, such a large-scale delta system may also explain the indication of non-marine sediment supply to the Lomonosov Ridge which has been reported by Grantz et al. (2001).



## Hydrocarbon plays

A revised palaeogeographic evolution of the Barents Shelf during the Triassic is presented in Figure 10. The paleogeographic evolution is favorable for Triassic play models as Lower and Middle Triassic source rocks of the Steinkobbe and Botneheia formations are overlain by paralic sandstones of the Kobbe, Snadd and De Geerdalen formations, as well as the overlying Realgrunnen Sub Group. Such a development has been documented in exploration wells, stratigraphic cores and outcrops, as visualized by the correlation panels in Figures 6 and 7.

On the Barents Shelf, prolific hydrocarbon source rocks were deposited in an embayment later filled by prograding shelf edge deltas, forming a diachronous system. The

organic rich event initiated in the southernmost part, in Olenekian, representing the first occurrence of the Steinkobbe Formation, observed in the Svalis Dome area, while such sedimentation started in the Anisian further north and continued as the Botneheia Formation in Svalbard. Gradually, north-westward prograding shelf edge deltas with paralic sandstones also terminated the organic rich facies earlier in the southernmost Barents Sea, in Anisian, while it continued throughout the Anisian in the Svalis Dome area and throughout the Ladinian further north, east of Kong Karls Land and in Svalbard. This setting provides numerous possibilities for prolific hydrocarbon play models. In addition, the overlying Wilhelmøya and Realgrunnen sub-groups have excellent sandstones adding possible play models, not discussed further at this time.

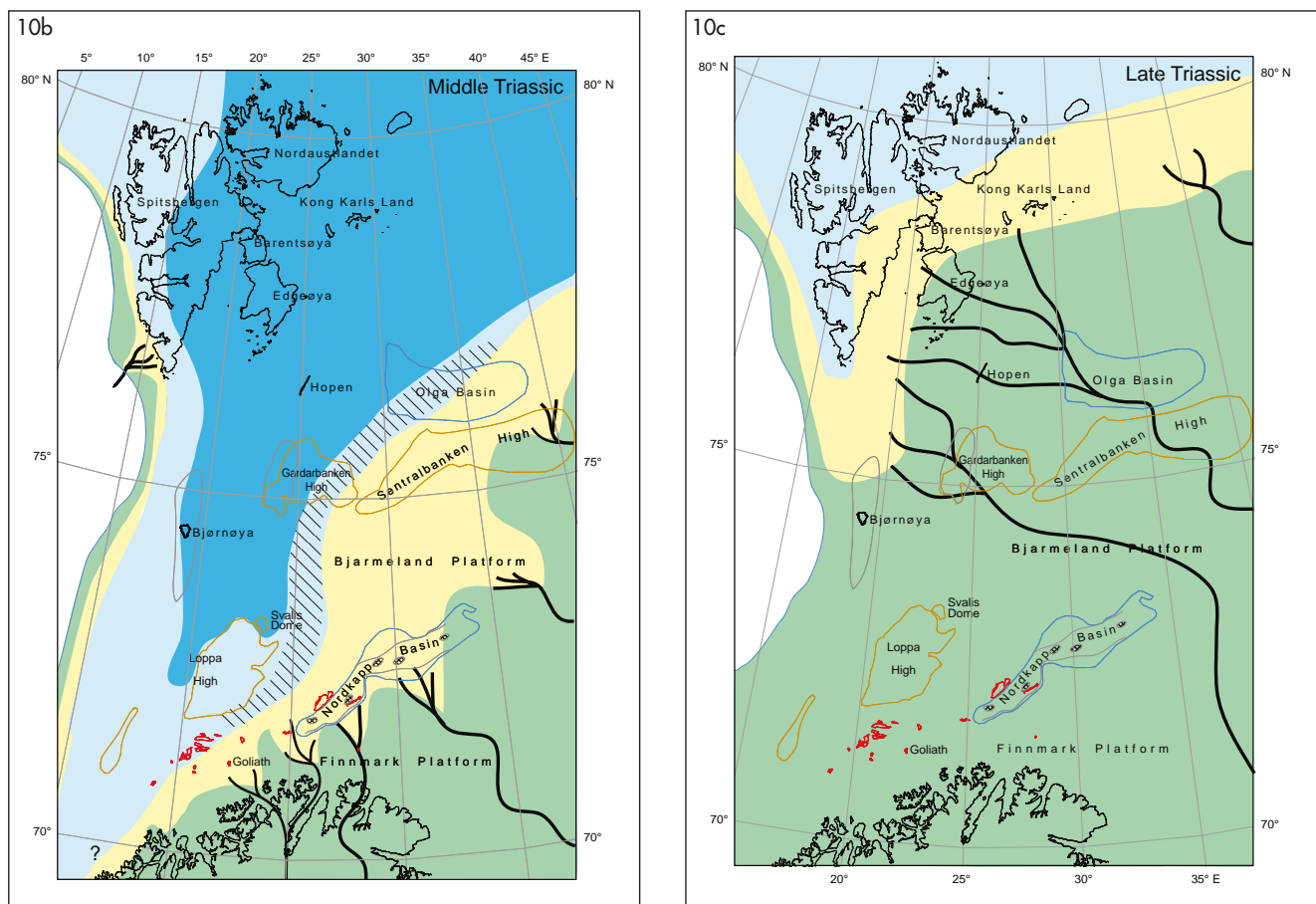


Figure 10. Palaeogeographic evolution of the Barents Shelf including Svalbard during the Triassic. a) Early Triassic, b) Middle Triassic and c) Late Triassic.



An additional older Lower Triassic source rock may also be represented by the bottomsets of the Induan clinoform belt (see above). However, sparse data, (no core information), make it difficult to model this possibility.

Klausen and Mørk (2014) have demonstrated how channel belt sandstones as observed on Hopen (Mørk et al., 2013, Lord et al., 2014b) are comparable with channel belts in the Snadd Formation, as interpreted from seismic data, further south in the Barents Sea. The two correlation panels (Figs. 6, 7) do not document any continuous sandstone sheets throughout this vast area, but rather indicate that these reservoir sandstone deposits may be present as more or less isolated sandstone bodies scattered over a large area.

The numerous thin coal beds in the Snadd and De Geerdalen Formation, as well as in the Kobbe Formation in the south-eastern part of the Norwegian Barents Sea, may hold some potential as gas-prone sources.

Extensive organic geochemical studies of cores (Leith et al., 1993) and material from Svalbard (Mørk and Bjørøy, 1984) have demonstrated the hydrocarbon potential; however the critical parameter in the different areas is the thermal maturation. The low thermal maturity seen for the Steinkobbe Formation on the Svalis Dome gives this unit a great potential also for larger areas of the Barents Sea. The data from Sentralbanken High also show moderate thermal maturation of shales in the Snadd Formation, implying that any underlying source rock will not be over-matured. On Svalbard, the Middle Triassic source rocks are over-matured on southern Spitsbergen, but in the oil window elsewhere. However, the maturity is quite low on eastern Barentsøya and Edgeøya (Mørk and Bjørøy, 1984), except for local maturation by intrusions over large areas (Brekke et al., 2014). This may indicate that low maturity Middle Triassic hydrocarbon source rocks may be widely present in the northern Barents Shelf.

The Kobbe Formation contains fluviodeltaic and shallow marine sediments along the Troms Finnmark Fault Complex, in the Nordkapp Basin and on parts of the Bjarmeland Platform and Loppa High, quite different from Kobbe Formation further to the northwest in the Barents Sea. This makes the formation of reservoirs possible in these areas; prominent reservoir quality is proven in the Goliat Field and the Nucula discovery. The overlying Snadd Formation, with similar reservoir possibilities, progrades towards the northwest across the entire Barents Shelf grading into the deltaic Tschermarkfjellet and De Geerdalen formations in Svalbard. These paralic deposits, including channel, delta front and shoreface sandstones form potential and promising reservoirs for hydrocarbons over wide areas of the Barents Sea.

## Conclusions

In the present study we have not looked at possible cap-rocks, however, interbedded shales may have cap rock capabilities and the pronounced marine inundation events that separate the different formations are all associated with widespread deposition of shale, providing a potent seal. The critical parameter for finding working Triassic hydrocarbon plays will thus be:

- Hydrocarbon source rock maturation level
- Recognising the paralic sandstones
- Assessing the integrity of cap rocks concerning the post-depositional tectonic history

The Triassic succession is outcropping on the sea floor or beneath the Quaternary overburden over large areas of the Barents Shelf, e.g. on the Sentralbanken High and southeast of Svalbard. Possible hydrocarbon plays may thus be found in areas with special tectonic development, for example downfaulted grabens, or it may be found at quite shallow levels. Exploration the last years has proven these assumptions, however, in the extensive area numerous such targets need to be tested.

### Acknowledgements.

This manuscript is based on seismic interpretation performed by the NPD, stratigraphic cores interpreted by SINTEF Petroleum Research and fieldwork in Svalbard. During the period 2006 to 2009 the fieldwork was carried out in cooperation between SINTEF Petroleum Research and the NPD. In 2011 and 2012 the fieldwork was also supported by the production licences PL609, PL438, PL492, PL533 and PL611. Snorre Olausen and Tore Grane Klausen are gratefully acknowledged for reviewing the manuscript. Their comments and suggestions have significantly improved this paper.

## References

- Bergan, M., & Knarud, R. 1993: Apparent changes in clastic mineralogy of the Triassic-Jurassic succession, Norwegian Barents Sea: Possible implications for palaeodrainage and subsidence. In Vorren, T.O. et al. (eds.): *Arctic Geology and petroleum potential: proceedings of the Norwegian Petroleum Society Conference, 15-17 August 1990, Tromsø, Norway*, 481-493. Elsevier, Amsterdam.
- Berglund, L., Augustson, J., Faereth, R., Gjelberg, J. & Ramberg, H.M. 1986: The evolution of the Hammerfest Basin. In Spencer A.M. (ed.): *Habitat of Hydrocarbons on the Norwegian Continental Shelf*. Graham & Trotman, London, 319-338.
- Brekke, T., Krajewski, K.P. & Hubred, J.H. 2014: Organic geochemistry and petrography of thermally altered sections of the Middle Triassic Botneheia Formation on south-western Edgeøya, Svalbard. *Norwegian Petroleum Directorate Bulletin*, 11, 111-128.
- Bugge, T., Mangerud, G., Mørk, A., Nilsson, I., Elvebakk, G., Fanavoll, S. & Vigran, J.O. 1995: The Upper Palaeozoic succession on the Finnmark Platform, Barents Sea. *Norsk Geologisk Tidsskrift*, 75, 3-30.
- Bugge, T., Elvebakk, G., Fanavoll, S., Mangerud, G., Smelror, M., Weiss, H.M., Gjelberg, J., Kristensen, S.E. & Nilsen, K. 2002: Shallow stratigraphic drilling applied in hydrocarbon exploration of the Nordkapp Basin, Barents Sea. *Marine and Petroleum Geology*, 19, 13-37.

- Buiter, S.J.H. & Torsvik, T.H. 2007: Horizontal movements in the eastern Barents Sea constrained by numerical models and plate reconstructions. *Geophys. J. Int.* 171, 1376–1389. doi: 10.1111/j.1365-246X.2007.03595.x
- Dagys, A.S., Weitschat, W., Konstantinov, A.G. & Sobolev, E.S. 1993: Evolution of the boreal marine biota and stratigraphy at the Middle/Upper Triassic boundary. *Mitteilungen, Geologisch-Paläontologisches Institut der Universität Hamburg*, 75, 249–256.
- Dallmann, W.K., Gjelberg, J.G., Harland, W.B., Johannessen, E.P., Keilen, H.B., Lønøy, A., Nilsson, I. & Worsley, D. 1999: Upper Palaeozoic lithostratigraphy. In Dallmann, W.K. (ed.): *Lithostratigraphic Lexicon of Svalbard. Review and recommendations for nomenclature use. Upper Palaeozoic to Quaternary bedrock*, 25–126. Norwegian Polar Institute, Tromsø.
- Embry, A.F. 1993: Crockerland – the northwest source area for the Sverdrup Basin, Canadian Arctic islands. In Vorren, T.O. et al. (eds.): *Arctic Geology and petroleum potential: proceedings of the Norwegian Petroleum Society Conference, 15–17 August 1990, Tromsø, Norway*, 205–216. Elsevier, Amsterdam.
- Faleide, J.I., Gudlaugson, S.T. & Jacquart, G. 1984: Evolution of the western Barents Sea. *Marine and Petroleum Geology*, 1, 123–150.
- Gabrielsen, R.H., Færseth, R.B., Jensen, L.N., Kalheim, J.E. & Riis, F. 1990: Structural elements of the Norwegian continental shelf. Part I: The Barents Sea Region. *Norwegian Petroleum Directorate Bulletin*, 6, 33 pp.
- Glørstad-Clark, E., Faleide, J.I., Lundschieen, B.A. & Nystuen, J.P. 2010: Triassic sequence stratigraphy and paleogeography of the western Barents Sea area. *Marine and Petroleum Geology*, 27, 1448–1475.
- Glørstad-Clark, E., Birkeland, E.P., Nystuen, J.P., Faleide, J.I. & Midtkandal, I. 2011: Triassic platform-margin deltas in the western Barents Sea area. *Marine and Petroleum Geology*, 28, 1294–1314.
- Grantz, A., Pease, V.L., Willard, D.A., Philips, R.L. & Clark, D.L. 2001: Bedrock cores from 89° North; implications for the geologic framework and Neogene paleogeography of Lomonosov Ridge and a tie to the Barents shelf. *Geological Society of America, Bulletin*, 113, 1272–1281.
- Høy, T. & Lundschieen, B.A. 2011: Triassic deltaic sequences in the northern Barents Sea. In Spencer, A.M., Embry, A.F., Gautier, D.L., Stopakova, A.V. & Sorensen, K. (eds.): *Arctic Petroleum Geology. Geological Society, London, Memoirs*, 35, 249–260.
- Johansen, S.E., Ostistiy, B.K., Birkeland, Ø., Federovsky, Y.F., Martirosjan, V.N., Christensen, O.B., Cheredeev, S.I., Ignatenko, E.A. & Margulis, L.S. 1993: Hydrocarbon potential in the Barents Sea region: play distribution and potential. In Vorren, T.O. et al. (eds.): *Arctic Geology and petroleum potential: proceedings of the Norwegian Petroleum Society Conference, 15–17 August 1990, Tromsø, Norway*, 273–320. Elsevier, Amsterdam.
- Klausen, T. G., & Mørk, A. 2014: The Upper Triassic paralic deposits of the De Geerdalen Formation on Hopen: Outcrop analog to the subsurface Snadd Formation in the Barents Sea. *American Association of Petroleum Geologists Bulletin*, 98, 1911–1941, doi:10.1306/02191413064.
- Korčinskaja, M.V. 1982: Ob'jasnitel'naja zapiska k stratigrafičeskoj scheme mezozoja (trias) Sval'barda (Explanatory note to the stratigraphic scheme of Mesozoic (Triassic) Svalbard), *PGO "Sevmorgeologija"*, 40–99. Leningrad. (In Russian).
- Krajewski, K.P. 2008: The Botneheia Formation (Middle Triassic) in Edgeøya and Barentsøya, Svalbard: lithostratigraphy, facies, phosphogenesis, paleoenvironment. *Polish Polar Research*, 29, 319–364.
- Krajewski, K.P., Karcz, P., Woźny, E. & Mørk, A. 2007: Type section of the Bravaisberget Formation (Middle Triassic) at Bravaisberget, western Nathorst Land, Spitsbergen, Svalbard. *Polish Polar Research*, 28, 319–364.
- Larese, R.E., Haskell, N.L., Prezbindowski, D.R. & Beju, D. 1984: Porosity development in selected Jurassic sandstones from the Norwegian North Seas, Norway. An overview. In Spencer, A.M. et al. (eds.): *Petroleum Geology of the North European Margin*. Norwegian Petroleum Society, Graham & Trotman, 81–95.
- Larssen, G.B., Elvebakk, G., Henriksen, L.B., Kristensen, S.E., Nilsson, I., Samuelsen, T.J., Svånå, T.A., Stemmerik, L. & Worsley, D. 2002: Upper Palaeozoic lithostratigraphy of the Southern Norwegian Barents Sea. *Norwegian Petroleum Directorate Bulletin*, 9, 76 pp.
- Leith, T.L., Weiss, H.M., Mørk, A., Århus, N., Elvebakk, G., Embry, A.F., Brooks, P.W., Stewart, K.R., Pchelina, T.M., Bro, E.G., Verba, M.L., Danyushevskaya, A. & Borisov, A.V. 1993: Mesozoic hydrocarbon source-rocks of the Arctic region. In Vorren, T.O. et al. (eds.): *Arctic Geology and petroleum potential: proceedings of the Norwegian Petroleum Society Conference, 15–17 August 1990, Tromsø, Norway*, 1–25. Elsevier, Amsterdam.
- Lock, B.E., Pickton, C.A.G., Smith, D.G., Batten, D.J. & Harland, W.B. 1978: The Geology of Edgeøya and Barentsøya, Svalbard. *Norsk Polarinstitutt skrifter*, 168, 64 pp.
- Lord, G.S. Solvi, K.H., Ask, M., Mørk, A., Hounslow, M.W. & Paterson, N.W. 2014a: The Hopen Member: A new lithostratigraphic unit on Hopen and equivalent to the Isfjorden Member of Spitsbergen. *Norwegian Petroleum Directorate Bulletin*, 11, 81–96.
- Lord, G.S., Solvi, K.H., Klausen, T.G. & Mørk, A. 2014b: Triassic channel bodies on Hopen, Svalbard: Their facies, stratigraphical significance and spatial distribution. *Norwegian Petroleum Directorate Bulletin*, 11, 41–59.
- Mørk, A. & Bjørøy, M. 1984: Mesozoic source rocks on Svalbard. In Spencer, A.M. et al. (eds.): *Petroleum geology of the Northwest European Margin*. Norwegian Petroleum Society, Graham & Trotman, London, 371–382.
- Mørk, A. & Bromley, R.G. 2008: Ichnology of a marine regressive systems tract: the Middle Triassic of Svalbard. *Polar Research*, 27, 339–359.
- Mørk, A. & Elvebakk, G. 1999: Lithological description of subcropping Lower and Middle Triassic rocks from the Svalis Dome, Barents Sea. *Polar Research*, 18, 83–104.
- Mørk, A., Knarud, R. & Worsley, D. 1982: Depositional and diagenetic environment of the Triassic and Lower Jurassic succession of Svalbard. In Embry, A.F. & Balkwill, H.R. (eds.): *Arctic Geology and Geophysics. Canadian Society of Petroleum Geologists Memoir*, 8, 371–398.
- Mørk, A., Embry, A.F. & Weitschat, W. 1989: Triassic transgressive-regressive cycles in the Sverdrup Basin, Svalbard and the Barents shelf. In Collinson, J.D. (ed.): *Correlation in Hydrocarbon Exploration*. Norwegian Petroleum Society, Graham & Trotman, 113–130.
- Mørk, A., Vigran, J.O. & Hochuli, P.A. 1990: Geology and palynology of the Triassic succession of Bjornøya. *Polar Research*, 8, 141–163.
- Mørk, A., Vigran, J.O., Korčinskaja, M.V., Pchelina, T.M., Fefilova, L.A., Vavilov, L.M. & Weitschat, W. 1993: Triassic rocks in Svalbard, the Arctic Soviet islands and the Barents Shelf: bearing on their correlations. In Vorren, T.O. et al. (eds.): *Arctic geology and petroleum potential: proceedings of the Norwegian Petroleum Society Conference, 15–17 August 1990, Tromsø, Norway*, 457–479. Elsevier, Amsterdam.
- Mørk, A., Dallmann, W.K., Dypvik, H., Johannessen, E.P., Larssen, G.B., Nagy, J., Nøttvedt, A., Olausen, S., Pchelina, T.M. & Worsley, D. 1999a: Mesozoic lithostratigraphy. In Dallmann, W.K. (ed.): *Lithostratigraphic Lexicon of Svalbard. Review and recommendations for nomenclature use. Upper Palaeozoic to Quaternary bedrock*, 127–214. Norwegian Polar Institute, Tromsø.
- Mørk, A., Elvebakk, G., Forsberg, A.W., Hounslow, M.W., Nakrem, H.A., Vigran, J.O. & Weitschat, W. 1999b: The type section for the Vikinghøgda Formation – a new Lower Triassic unit in Central and Eastern Svalbard. *Polar Research*, 18, 51–82.

- Mørk, A., Lord, G.S., Solvi, K.H. & Dallmann, W.K. 2013: *Geological map of Svalbard 1:100 000, sheet G14G Hopen*. Norsk Polarinstitutt Temakart No. 50.
- Mørk, M.B.E. 1999: Compositional variations and provenance of Triassic sandstones from the Barents Shelf. *Journal of sedimentary research*, 69, 690-710.
- Olaussen, S., Gloppen, T.G., Johannessen, E. & Dalland, A. 1984: Depositional environment and diagenesis of Jurassic reservoir sandstones in the eastern part of Troms I area. In Spencer, A.M. et al. (eds.): *Petroleum geology of the Northwest European Margin*. Norwegian Petroleum Society, Graham & Trotman, London, 61-80.
- Olaussen, S., Galimberti, R.F., Grindhaug, J.K., Heskkestad, B., Leutscher, J., Johnsen, E., Johnsen, S., Opsahl, E., Seldal, J. & Stensland, D. 2010: Hydrocarbon pools banked to the basin margin faults: harvesting a successful play model in the south-western Barents Sea. 29<sup>th</sup> Nordic Geological Winter Meeting. *Abstracts and Proceedings of the Geological Society of Norway*, 139-140.
- Ostistiy, B.K. & Fedorovsky, Y.F. 1993: Main results of oil and gas prospecting in the Barents and Kara Sea inspire optimism. In Vorren, T.O. et al. (eds.): *Arctic Geology and petroleum potential: proceedings of the Norwegian Petroleum Society Conference, 15-17 August 1990, Tromsø, Norway*, 243-255. Elsevier, Amsterdam.
- Pčelina, T.M. 1977: Permskie i triasovye otloženija ostrova Ėdž (Svalbard). (Permian and Triassic deposits of Edgeøya (Svalbard)). In *Stratigrafija i paleontologija dokembrija i paleozoja severa Sibiri (Stratigraphy and palaeontology of the Precambrian and Paleozoic of northern Siberia)*. Collection of scientific papers. NIIGA, 59-71. Leningrad. (In Russian).
- Pózer Bue, E. & Andresen, A. 2013: Constraining depositional models in the Barents Sea region using detrital zircon U-Pb data from Mesozoic sediments in Svalbard. *Geological Society Special Publication*, 386, 261-279. ISSN 0305-8719.
- Preobraženskaja, E.N., Škola, I.V. & Korčinskaja, M.V. 1985a: Stratigrafija triasovyh otloženij arhipelaga Zemlja Franca Iosifa (materialy burenija). Stratigraphy of Triassic deposits of the archipelago of Franz Josef Land (drill data). In *Stratigrafija i paleontologija mezozojskih osadočnyh bassejnov severa SSSR, Sbornik naučnyh trudov (Stratigraphy and paleontology of Mesozoic sedimentary basins of the North of the USSR, Collection of scientific papers)*, VNIIOkengeologija, Leningrad, 5-15. (In Russian).
- Preobraženskaja, E.N., Škola, I.V., Sergeev, O.V. & Možaeva, J.V. 1985b: Veščestvennyj sostav i uslovija formirovannija triasovyh otloženij arhipelaga zemli Franca Iosifa. Po materialam parametričeskogo burenija. (Triassic deposits of the archipelago of Franz Josef Land. Based on materials of parametric drilling). In *Geologičeskoe stroenie Barentsevo - Karskogo šelfa. Sbornik naučnyh trudov. (Geological structure of the Barents - Kara shelf. Collection of scientific papers)*, 74-86, Sevmergeologija, Leningrad (in Russian with Engl. abstr. p.119, translated into English 1986 by Norsk Polarinstitutt).
- Rasmussen, A., Kristensen, S.E., Van Veen, P., Stølan, T. & Vail, P.R. 1993: Use of sequence stratigraphy to define a semi-stratigraphic play in Anisian sequences, southwestern Barents Sea. In Vorren, T.O. et al. (eds.): *Arctic Geology and Petroleum Potential, Norwegian Petroleum Society (NPF) Special Publication no. 2*, 439-456. Elsevier Amsterdam.
- Riis, F., Lundschien, B.A., Høy, T., Mørk, A. & Mørk, M.B.E. 2008: Evolution of the Triassic shelf in the northern Barents Sea region. *Polar Research*, 27, 298-317.
- Rød, R.S., Hynne, I.B. & Mørk, A. 2014: Depositional environment of the Upper Triassic De Geerdalen Formation – An E-W transect from Edgeøya to Central Spitsbergen, Svalbard. *Norwegian Petroleum Directorate Bulletin*, 11, 21-40.
- Rønnevik, H.C. & Jacobsen, H.P. 1984: Structural highs and basins in the western Barents Sea. In Spencer, A.M. et al. (eds.): *Petroleum geology of the Northwest European Margin*. Norwegian Petroleum Society, Graham & Trotman, London, 19-32.
- Skjold, L.J., van Veen, P.M., Kristensen, S.E. & Rasmussen, A.R. 1998: Triassic sequence stratigraphy of the southwestern Barents Sea. *Special Publication - Society for Sedimentary Geology*, 60, 651-666.
- Torsvik, T.H. & Cocks, L.R.M. 2005: Norway in space and time: A Centennial Cavalcade. *Norwegian Journal of Geology*, 85, 73-86.
- Tozer, E.T. & Parker, J.R. 1968: Note on the Triassic biostratigraphy of Svalbard. *Geological Magazine*, 105, 526-542.
- Van Veen, P.M., Skjold, L.J., Kristensen, S.E., Rasmussen, A., Gjelberg, J. & Stølan, T. 1993: Triassic sequence stratigraphy in the Barents Sea. In Vorren, T.O. et al. (eds.): *Arctic Geology and Petroleum Potential, Norwegian Petroleum Society (NPF) Special Publication no. 2*, 515-538. Elsevier Amsterdam.
- Vigran, J.O., Mangerud, G., Mørk, A., Bugge, T. & Weitschat, W. 1998: Biostratigraphy and sequence stratigraphy of the Lower and Middle Triassic deposits from the Svalis Dome, central Barents Sea, Norway. *Palynology*, 22, 89-141.
- Vigran, J.O., Mørk, A., Forsberg, A.W., Weiss, H.M. & Weitschat, W. 2008: *Tasmanites*-algae contributors to the Middle Triassic hydrocarbon source rocks of Svalbard and the Barents Shelf. *Polar Research*, 27, 298-317.
- Vigran, J.O., Mangerud, G., Mørk, A., Worsley, D. & Hochuli, P.A. 2014: Palynology and geology of the Triassic succession of Svalbard and the Barents Sea. *Geological Survey of Norway Special Publication*, 14, 270 pp.
- Weitschat, W. & Dagys, A.S. 1989: Triassic biostratigraphy of Svalbard and a comparison with NE-Siberia. *Mitteilungen Geologisch-Paläontologisches Institut Universität Hamburg*, 68, 179-213.
- Weitschat, W. & Lehman, U. 1983: Stratigraphy and ammonoids from the Middle Triassic Botneheia Formation (*Daonella* Shales) of Spitsbergen. *Mitteilungen, Geologisch-Paläontologisches Institut der Universität Hamburg*, 54, 27-54.
- Worsley, D. 2008: The post-Caledonian development of Svalbard and the Western Barents Sea. *Polar Research*, 27, 318-338.
- Worsley, D. & Mørk, A. 1978: The Triassic stratigraphy of southern Spitsbergen. *Norsk Polarinstitutt Årbok*, 1977, 43-60.
- Worsley, D., Johansen, R. & Kristensen, S.E. 1988: The Mesozoic and Cenozoic succession of Tromsøflaket. In Dalland, A., Worsley, D. & Ofstad, K. (eds.): *A lithostratigraphic scheme for the Mesozoic and Cenozoic succession offshore mid- and northern Norway*. Norwegian Petroleum Directorate Bulletin, 4, 42-65. Stavanger.
- Xu, G., Hannah, J.L., Stein, H.J., Bingen, B., Yang, G., Zimmerman, A., Weitschat, W., Mørk, A. & Weiss, H.M. 2009: Re-Os geochronology of Arctic black shales to evaluate the Anisian-Ladinian boundary and global faunal correlations. *Earth and Planetary Science Letters*, 288, 581-587.
- Xu, G., Hannah, J.L., Stein, H.J., Mørk, A., Vigran, J.O., Bingen, B., Schutt, D.L. & Lundschien, B.A. 2014: Cause of Upper Triassic climate crisis revealed by Re-Os geochemistry of Boreal black shales. *Palaeogeography, Palaeoclimatology, Palaeoecology*, 395, 222-232. <http://dx.doi.org/10.1016/j.palaeo.2013.12.027>



# Depositional environment of the Upper Triassic De Geerdalen Formation – An E-W transect from Edgeøya to Central Spitsbergen, Svalbard

Rita Sande Rød<sup>1,2,3</sup>, Ingrid Bjørnerheim Hynne<sup>2,3,4</sup> & Atle Mørk<sup>2,5</sup>

<sup>1</sup> Norwegian Petroleum Directorate, P.O. Box 600, NO-4003 Stavanger, Norway, e-mail: rita.roed@npd.no

<sup>2</sup> Department of Geology and Mineral Resources Engineering, Norwegian University of Sciences and Technology (NTNU), NO-7491 Trondheim, Norway

<sup>3</sup> The University Centre in Svalbard (UNIS), Longyearbyen, Norway

<sup>4</sup> Statens vegvesen, Region vest, Askedalen 4, NO-6863 Leikanger, Norway

<sup>5</sup> SINTEF Petroleum Research, P.O. Box 4763 Sluppen, NO-7465 Trondheim, Norway

The depositional environment of the Upper Triassic De Geerdalen Formation has been studied through facies analysis of outcrop and core data, and geometric studies through photos and Lidar data. At various field localities across an east-west transect of Edgeøya and Spitsbergen, Svalbard, fluvial dominance and wave- and tidal influence have affected the sediments differently, resulting in lateral facies variability and different depositional elements. A proximal, fluvially dominated deltaic setting is interpreted on Edgeøya, where sandstone bodies have thick, ellipsoid geometries. On central Spitsbergen a more distal setting is found, with less generation of accommodation space and thus more wave modulation, resulting in thin, laterally continuous sandstone bodies. This study provides a detailed documentation of facies development of the De Geerdalen Formation, and support the recently suggested regional deltaic progradation across the Barents shelf from the southeast to the northwest.

**Key words:** Svalbard, Spitsbergen, Edgeøya, Triassic, Sedimentology, Facies, Depositional environments, De Geerdalen Formation.

## Introduction

The Triassic depositional environment of the entire Barents Shelf including Svalbard is interpreted as a wide shelf, in an embayment setting at the northern rim of Pangea (Worsley, 2008; Riis et al., 2008). While the sedimentation on Svalbard mainly was from westerly sources in the Early and Middle Triassic, this pattern changed in the Late Triassic when south eastern sources dominated (Worsley, 2008; Pozer Bue and Andresen, 2013; Mørk et al., 1982; Lundschieen et al., 2014; Vigran et al., 2014). The Barents Sea embayment was mostly filled along western Spitsbergen by the end of the Middle Triassic (Mørk et al., 1982, 1999; Krajewski et al., 2007), but was still a shelf depression further east and south with water depth around 400 m as judged by the height of clinofolds subsequently prograding into the basin (Lundschieen et al., 2014).

The Carnian to Early Norian De Geerdalen Formation is dominated by fine-grained sandstone and shale beds, and is underlain by the grey shales of the Early Carnian Tschermafjellet Formation and overlain by the Norian to Middle Jurassic Wilhelmøya Subgroup (Dagys and Weitschat, 1993; Mørk et al., 1999; Vigran et al., 2014).

Previous studies have presented a broad sedimentological model for the formation at Edgeøya (Lock et al., 1978), at Spitsbergen, Edgeøya and Barentsøya (Mørk et al., 1982), and throughout the Barents Shelf (Riis et al., 2008). Recent work on the Triassic regional geology of the Barents Sea (e.g. Høy and Lundschieen, 2011; Klausen and Mørk, 2014; Riis et al., 2008; Glørstad-Clark et al., 2010; Lundschieen et al., 2014) suggests a regional deltaic progradation across the Barents shelf from the southeast to the northwest.

The scope of the present study is to add more detailed documentation on facies development at Edgeøya

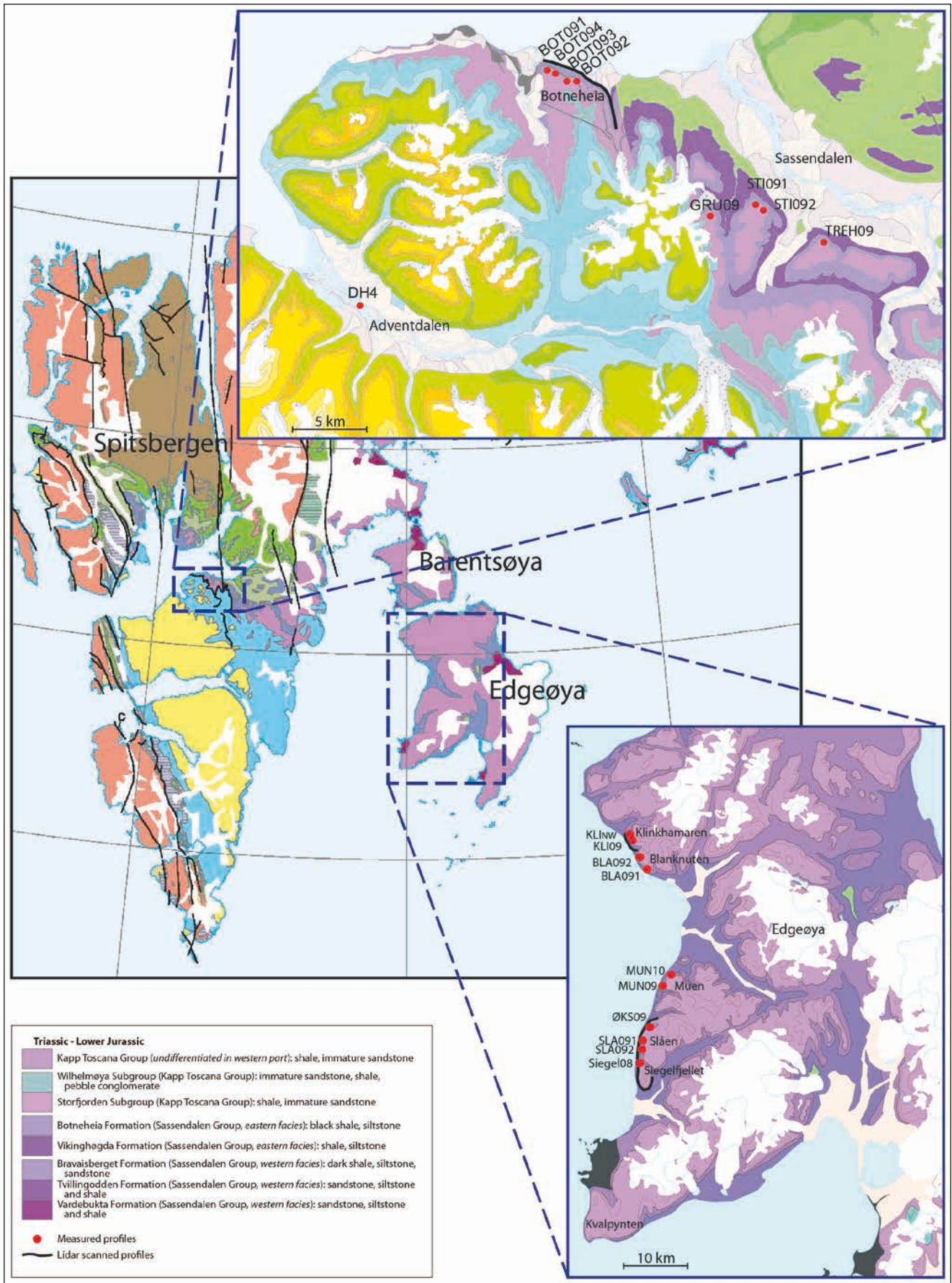


Figure 1. Map of Svalbard showing the two study areas at central Spitsbergen and at Edgeøya. Measured sections are indicated by red dots and Lidar scans by black lines. Maps are from the Norwegian Polar Institute.



and central Spitsbergen, focusing on: (I) creation and dynamic development of accommodation space, (II) sediment infill systems and processes, (III) depositional environments and facies belts and (IV) direction of sediment transport. Our work aims to document (1) the vertical transition from prodelta to delta front and delta plain depositional environments through the formation and (2) the lateral transition from proximal to distal depositional trend from east to west across Edgeøya and Spitsbergen. The upper part of the De Geerdalen Formation (mainly the Isfjorden Member) is eroded in most of this area and is consequently not studied.

## Methodology

Facies analysis has been used to systematize collected data in order to recognize depositional processes. The collected data are mainly sedimentological field logs (2009, 2010), in addition to the fully cored well DH4 of the UNIS CO<sub>2</sub> LAB (Braathen et al., 2012), and Lidar data (Fig. 1). Fifteen facies (A-O) are described mainly based on parameters such as sedimentary structures, grain size, unit thickness, bioturbation and organic content (Table 1).

The facies associations (1-6; Table 2), each defined by a set of facies occurring together, are deposits representing a sub-environment or a broader depositional environment (Fig. 2). They are described from a proximal (FA1: Fine-grained deposits in coastal areas) to a distal

position (FA6: Lower shoreface to offshore deposits) in the depositional model (Table 2).

The Lidar (Light detection and ranging) data are collected by helicopter-based laser scanning and provide digital terrain models of three of the visited localities (Slåen/Siegelfjellet, Klinkhamaren and Botneheia) seen as a black line on the locality map (Fig. 1). This Heli-map system is suitable to map both horizontal and vertical features with high resolution and accuracy (Skaloud et al., 2006). The system consists of a sensor block comprising digital camera, Lidar, an IMU (inertial measuring unit) and a GPS antenna, linked through supporting electronics (Vallet and Skaloud, 2004). The smallest features that can be measured are around 0.2 m.

Digital terrain models (DTM) are formed from the collected point clouds, and later textured with digital photographic images of the outcrop acquired simultaneously with the laser scan (Buckley et al., 2008b). The DTM makes geometric analyzing possible, and the image texturing make qualitative geologic interpretation possible (Buckley et al., 2008a).

Lidar data have been the main tool for the local spatial investigation of sandstone bodies. Together with field logs and photos, Lidar data have been used to recognize the depositional elements such as mouth bars and distributary channel complexes, and their dimensions, on the steep mountain faces.

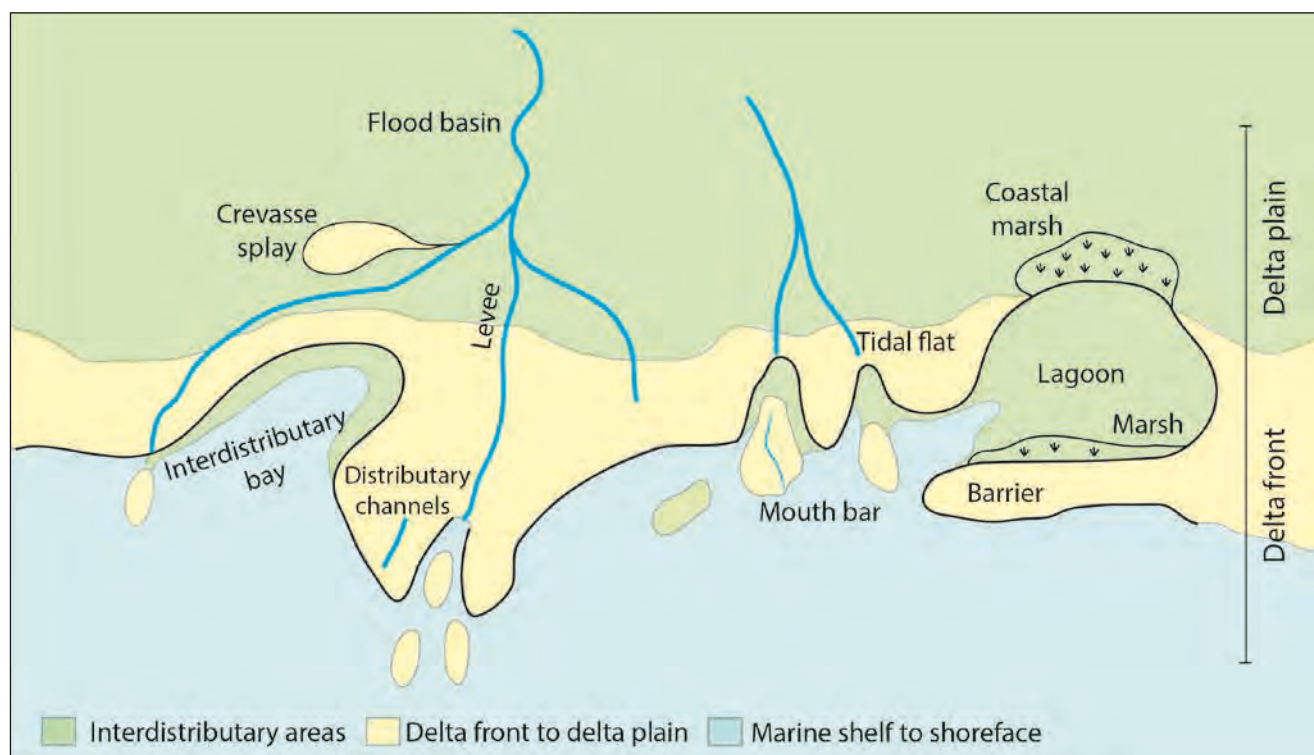


Figure 2. Conceptual sketch of sub-environments occurring in the De Geerdalen Formation. Features characteristic of fluvial, tide and wave influenced deltas are included. The delta environment is divided into interdistributary areas, delta front to delta plain and marine shelf to shoreface.



**Table 1.** Description of the fifteen Facies A-O based on measured sections from the De Geerdalen Formation at Edgeøya and central Spitsbergen. The facies are listed in order of decreasing grain size, and described based on parameters such as sedimentary structures, grain size, unit thickness, bioturbation and organic content. Abbreviations for grain size: vf=very fine, f=fine, m=medium.

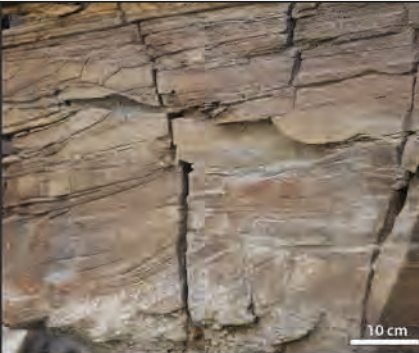

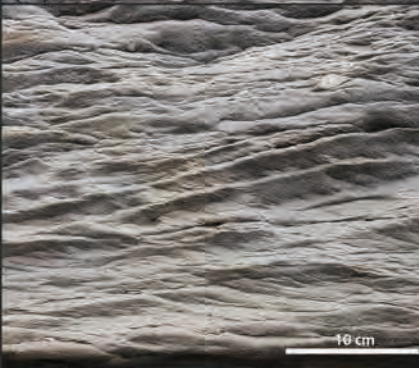


<p><b>A</b></p>	<p><b>Large scale cross stratified sandstone (f-m sand):</b></p> <p>Trough and tabular cross stratification (2D and 3D dunes). Often erosive based units with thicknesses from 0.5-7 m and set thicknesses from 0.1-0.2 m. Herringbone structures occur on Blanknuten and mud drapes in core material. Some units contain plant fragments, cementation, concretions and mud flakes. Grey, red to brown colour.</p> <p>3D dunes form at a higher flow velocity than 2D dunes. Herringbone structures are indicative of tidal influence.</p>	
<p><b>B</b></p>	<p><b>Small scale cross stratified sandstone (vf-m sand):</b></p> <p>Trough and tabular cross lamination (2D and 3D) ripples and herringbone lamination. Units have gradual or sharp contacts to associated facies, with thicknesses from 0.1-1.5 m and set thicknesses from 0.5-4 cm. Plant fragments occur, no bioturbation or cementation is observed. Grey to brown colour.</p> <p>Small scale 2D and 3D ripples form mainly by unidirectional flow in the lower flow regime.</p>	
<p><b>C</b></p>	<p><b>Climbing ripple cross laminated sandstone (f-m sand):</b></p> <p>Units are from 0.3-0.5 m in thickness with sharp contacts, and set thicknesses are from 1-3 cm. The angle of climb is from 15-30° (subcritical climb), and there are truncating boundaries between sets. Not observed bioturbation, organic material, mud flakes or cementation. Colour from grey to brown.</p> <p>Climbing ripples occur in environments of periodically high sediment accumulation and limited reworking in the lower flow regime.</p>	
<p><b>D</b></p>	<p><b>Symmetrical ripple laminated sandstone (vf-f sand):</b></p> <p>Include structures such as ripples, ripple cross lamination and plane parallel lamination. Units are from a few cm up to 0.5 m thick, their contacts are gradual or erosive and set thicknesses are 1-3 cm. <i>Rhizocorallium</i>, unspecified bioturbation and mud flakes are observed on localities on Spitsbergen and on Edgeøya. Plant fragments and calcite cementation are also observed. Colour from grey to red.</p> <p>The structures occur in environment of oscillatory flow produced by wave action in the lower flow regime. <i>Rhizocorallium</i> is a marine indicator.</p>	
<p><b>E</b></p>	<p><b>Low angle cross stratified sandstone (vf-f sand):</b></p> <p>Units are from 0.5-3 m thick, laminated or bedded and often with gradual contacts. Set thicknesses are from 5-15 cm. No observation of mud flakes or cementation, sparse bioturbation in outcrops, and plant fragments. Colour from grey to brown to red.</p> <p>The structure can develop in beach environments of both high and low energy or in fluvial environments.</p>	



Table 1. Continued

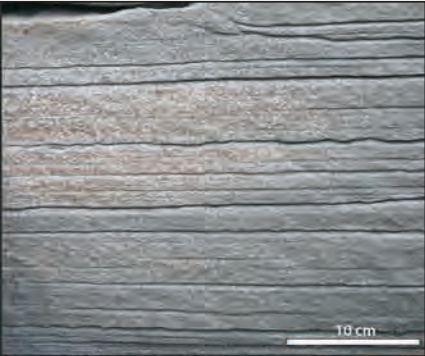




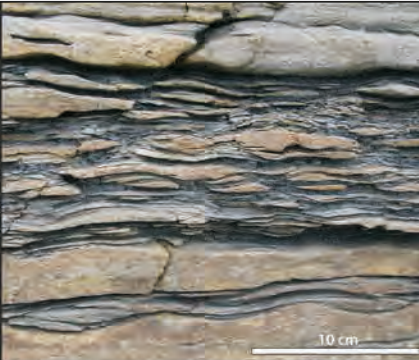




<b>F</b>	<p><b>Horizontal bedded sandstone (f sand):</b></p> <p>Units are from tens of cm up to a few metres, often with sharp contacts. Bed thicknesses are from 1-8 cm, and some beds are laminated. Bioturbation is observed on Klinkhamaren, mud flakes and calcite cementation in Sassendalen. Organic material is not observed. Grey colour.</p> <p>Horizontal bedding develops in the upper and lower flow regime.</p>	 <p>10 cm</p>
<b>G</b>	<p><b>Undulating fractured sandstone (f sand):</b></p> <p>Units are from 0.1-3 m thick, often erosive based. They appear massive with undulating fractures (see photo). Possible primary structures are large scale cross stratification or low angle cross stratification. Mud flakes are often found close to base of unit, as well as load structures. This facies occur in the lower growth faulted part of Klinkhamaren. Colour from grey to red to brown.</p> <p>Massive or structureless sand can form by liquefaction or rapid deposition from suspension. Mud flakes, erosive boundaries and load structures are often found in channel deposits.</p>	 <p>10 cm</p>
<b>H</b>	<p><b>Hummocky cross stratified (HCS) sandstone (vf-f sand):</b></p> <p>Small and large scale hummocks and swales structures, often overlain by symmetrical ripples. Units are often erosive based with thicknesses from 0.1-4 m, and set thicknesses from 1-20 cm. Bioturbation is common, e.g. <i>Diplocraterion</i>, <i>Skolithos</i>, <i>Rhizocorallium</i>, <i>Teichichnus</i> and <i>Ophiomorpha</i>. Mud flakes and deformation structures occur frequently. Little cementation and organic material observed.</p> <p>HCS occurs as a result of oscillatory and unidirectional flow combined, and is typical for storm deposits. The diverse ichnofauna is a clear marine indicator.</p>	 <p>10 cm</p>
<b>I</b>	<p><b>Mud flake conglomerate:</b></p> <p>Contains mud flakes in fine sand matrix. Clasts are 0.2-6 cm in diameter and of angular to subrounded shape. Units are from 0.5-4 m thick and erosive based. Bioturbation and organic material are not observed. Cementation occurs on Botneheia and Trehøgdene. Colour from grey to brown.</p> <p>Mud flakes are rip-up clasts from semiconsolidated mud and are common in tidal and fluvial environments. Can also form due to marine erosion. Indicative of high energy.</p>	 <p>10 cm</p>
<b>J</b>	<p><b>Fine grained rooted sandstone (vf sand):</b></p> <p>Vague ripple lamination and fracturing. Units are from 0.3-1.5 m thick with sharp contacts. Some units show heavy bioturbation. Plant fragments and roots are common and the colour is red to brown. Mud flakes are not observed.</p> <p>Root tracks and heavy bioturbation can occur in a low energy environment such as areas of emergence and flow stage in a continental environment.</p>	 <p>10 cm</p>



Table 1. Continued

<b>K</b>	<p><b>Heterolithic bedding (clay-f sand):</b> Lenticular bedding, wavy bedding and flaser bedding. Units are from 1-6 m thick, with sharp to gradual contacts. Sparse to heavy bioturbation and organic material found on Blanknuten. Mud flakes and cementation not observed. Colour from brown to grey.</p> <p>Heterolithic bedding often occurs in a setting of alternating energy regimes. The mud fraction is deposited from suspension and sand during periods of current activity. Common for tidal and fluvial environments.</p>	
<b>L</b>	<p><b>Carbonate rich sandstone (vf sand):</b> Carbonate concretions, cone in cone structures (see photo) and siderite layers. Fracturing and vague ripples are present in the concretions (0.1-2 m in diameter). The siderite layers are up to 0.4 m and form concretions at some localities.</p> <p>Secondary structures formed by diagenetic processes. Concretions and cone in cone form due to sediment pressure and compaction and siderite can form in waters of high Fe and low sulphate content.</p>	
<b>M</b>	<p><b>Coquina beds (shell banks):</b> Units are about 4 cm thick with sharp contacts. Consist of mainly fragmented bivalves (coquina). Colour from dark grey to brown.</p> <p>Fragmented bivalves can occur in high energy marine environments. Typical for the lower beds of the Isfjorden Member.</p>	
<b>N 1</b>	<p><b>Black shale (clay to silt): Laminated clay.</b> Units are from a few cm up to tens of meters, both with sharp and gradual contacts. Coal drapes in some outcrops. Dark grey colour.</p> <p>Occurs in low energy environment with fines and organic rich material settling from suspension.</p>	
<b>N 2</b>	<p><b>Silty shale (clay to vf sand):</b> Symmetrical ripples to planar lamination. Units are from a few cm up to 30 m, with sharp or gradual contacts. Grey colour. Low energy environment with settling of fines and little organic material.</p>	
<b>O</b>	<p><b>Coal and coal shale:</b> Units thicknesses from 10-20 cm, bounded by shale units. Sharp or gradual contacts. Dark grey to black colour.</p> <p>Coal form in environments with abundant vegetation and accumulation of organic material.</p>	



### Facies distribution

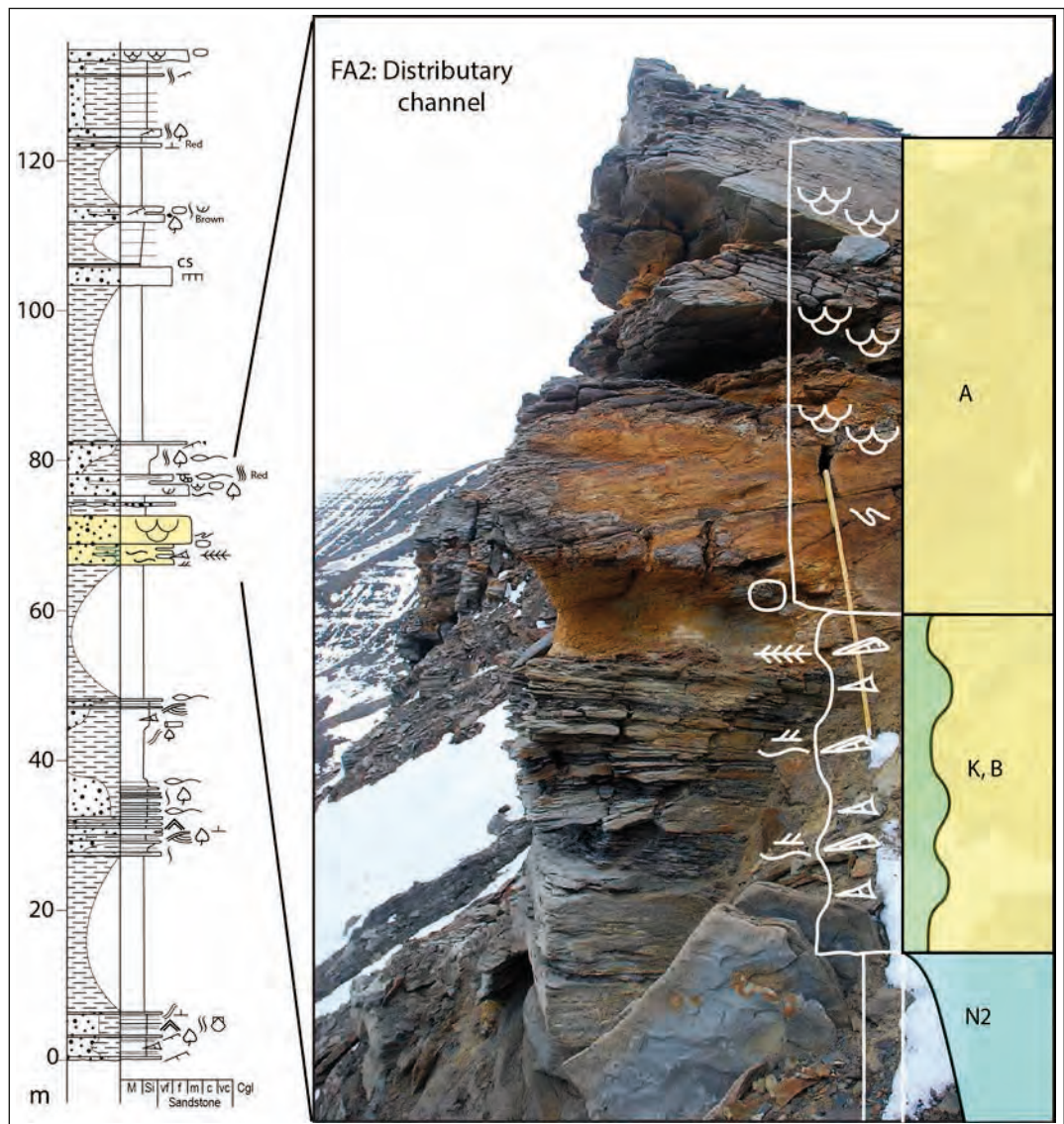
Facies association (FA) 6 is dominating the base of the De Geerdalen Formation and the FA1 the upper parts of sections throughout the field area. The FA2 and 3 (Table 2) occur both on Edgeøya and central Spitsbergen though more frequently in the east. The FA5 is unique to Edgeøya and FA4 is only observed on central Spitsbergen. The facies distribution within each FA is varying among the localities, with a trend of more proximal facies in the east and more distal facies in the west. This is demonstrated on Spitsbergen by for instance more prominent tidal signals such as herringbone structures (Facies B) in FA2 and 3 compared to the facies distribution within FA2 and 3 on Edgeøya which is more dominated by fluvial signals such as large scale trough cross stratified sandstone (Facies A).

Variability in facies distribution is also observed within FA1 where the Facies B (small scale cross stratified

sandstone), C (climbing ripples) and F (horizontal bedded sandstone) repeatedly occur on Botneheia, while on Edgeøya the Facies N1 (black shale), O (coal) and J (fine-grained rooted sandstone) are found at several levels in the formation.

FA2 occurs both on Edgeøya and central Spitsbergen (Fig. 3) and comprises fining up units of large scale cross stratification (Facies A), often erosively based with mud flakes (Facies I), heterolithic bedding (Facies K) and climbing ripples (Facies C). On Edgeøya the FA2 deposits are overlying FA3; while on central Spitsbergen FA2 is often occurring above FA1 or FA6. Heterolithic bedding, with both flaser-, wavy- and lenticular bedding (Facies K), is more frequently found in FA2 on central Spitsbergen than on Edgeøya. The heterolithic bedding, underlying the cross bedded sandstone, shows tidal signals such as double mud drapes and herringbone structures both on Botneheia and in the DH4 core.

**Figure 3.** Facies association 2 (Distributary channels) at Botneheia (BOT093, 65-73m above base of formation), Central Spitsbergen. The succession at Botneheia includes the facies K (Heterolithic bedding), facies A (Large scale cross stratified sandstone) and facies B (Small scale cross stratified sandstone). Legend in the Appendix.



**Table 2.** Description of six Facies associations (FA) in the De Geerdalen Formation, with localities at Edgeøya and central Spitsbergen. Main associated facies, occurrence and characteristics of the FA are included. They are listed in order of location in the depositional model, from a proximal to a distal position in a delta system.

	FA (Facies)	Occurrence	Characteristics
Interdistributary areas	1. Fine grained deposits in coastal areas (N, K, O, B, J, C, L)	Upper part of sections on Spitsbergen and Edgeøya. Frequently overlying FA2, and FA3.	Sub-environments such as tidal flats, lagoons, bays, floodplains. Crevasse splay and fining up units with rooted or coaly mudstone and thin possibly rippled sandstone with plant fragments are also typical.
Delta front to delta plain	2. Distributary channels (A, I, K, B, C)	Upper part of sections on Spitsbergen, including the DH4 core and middle to upper part of sections on Edgeøya. Overlying FA1 and FA3, and sometimes FA6.	Delta plain to delta front. Fining up units of fine- to medium-grained sandstone, often erosive based. Some degree of tidal influence (double mud drapes and herringbone structures) in the DH4 core and in Facies B at Botneheia.
	3. Mouth bars (A, B, D, E)	Middle to upper part of sections on Spitsbergen and Edgeøya. Overlying FA1, FA6 and underlying FA2.	Distal delta plain to proximal delta front. Upward coarsening units. Often a development from Facies B to Facies A upwards in the successions.
	4. Barrier bars (E, D, B, A, M)	In the DH4 core and lower to middle part of sections on Spitsbergen. Overlying FA6.	Delta front to upper shoreface setting. Upward coarsening units. Ripple lamination and low angle to cross stratified sandstone with some tidal signals at Spitsbergen. Erosive units observed in the DH4 core.
	5. Delta front channel sand (G, E, F, I, B)	Lower parts of sections on Klinkhamaren. Occuring within the growth faulted interval. Overlying FA6, and underlying FA6.	Fluvial delta front setting. Thickness of units varies between the different fault blocks suggesting syntectonic deposition.
Marine shelf to shoreface	6. Lower shoreface to offshore deposits (N, H, L, D, M, K)	Dominating in lower to middle parts of sections on Spitsbergen and lower parts of sections on Edgeøya.	Lower shoreface to shelf conditions. Mudstone dominated successions with storm beds, HCS structures and wave rippled very fine- to fine-grained sandstone.

Vertically stacked upward coarsening successions, separated by fine-grained deposits (FA1) are typical for the De Geerdalen Formation and are represented by FA3 (Fig. 4). On Edgeøya it is characterized by symmetrically

rippled sandstone (Facies D) overlain by low angle and trough cross stratified units (Facies E and A), sometimes with thin coal seams (Facies O) interbedding the successions. Minor bioturbation is observed at Blanknuten and



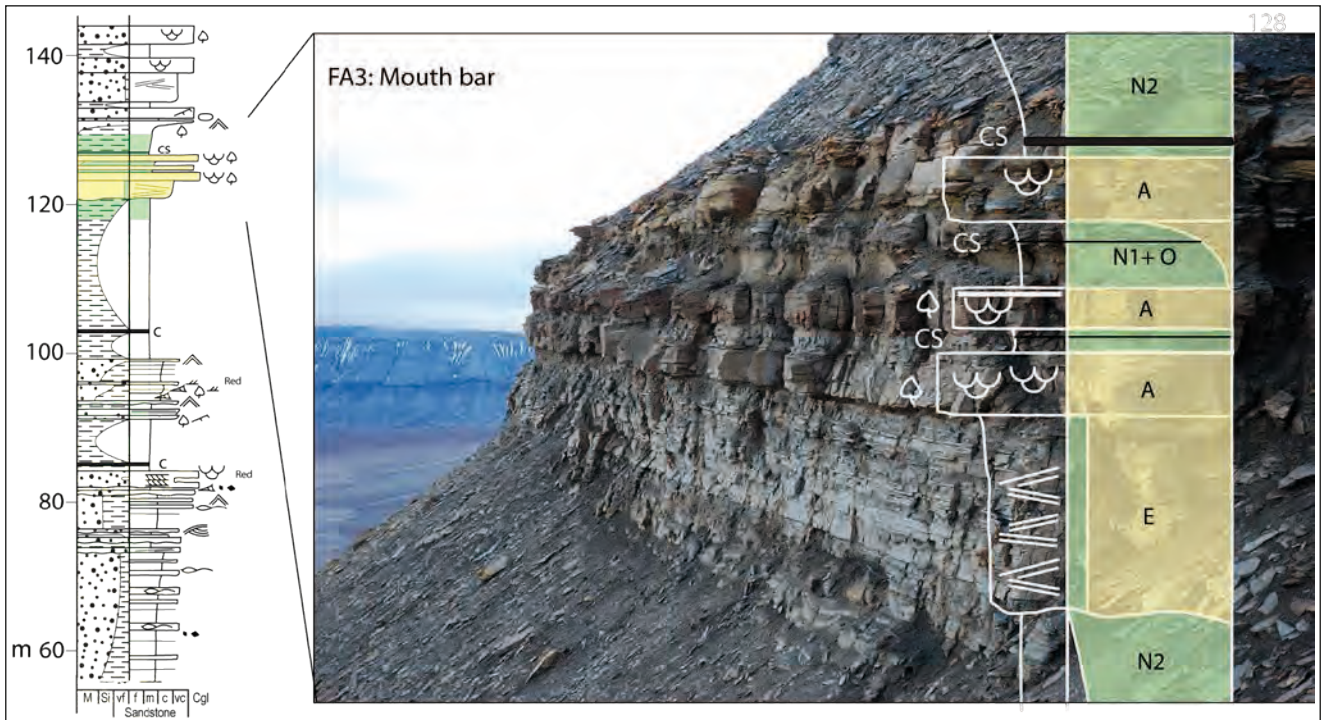


Figure 4. Facies association 3 (Mouth bar) in the De Geerdalen Formation at Blanknuten (BLA091, 120-130m above base of formation), Edgeøya. The succession is upward coarsening, with facies E (Low angle cross stratified sandstone) and facies A (Large scale cross stratified sandstone) at Blanknuten. At this locality the facies association is overlying facies N2 (silty shale), and interbedded with facies N1 (Black shale) and O (Coal). Legend in the Appendix.

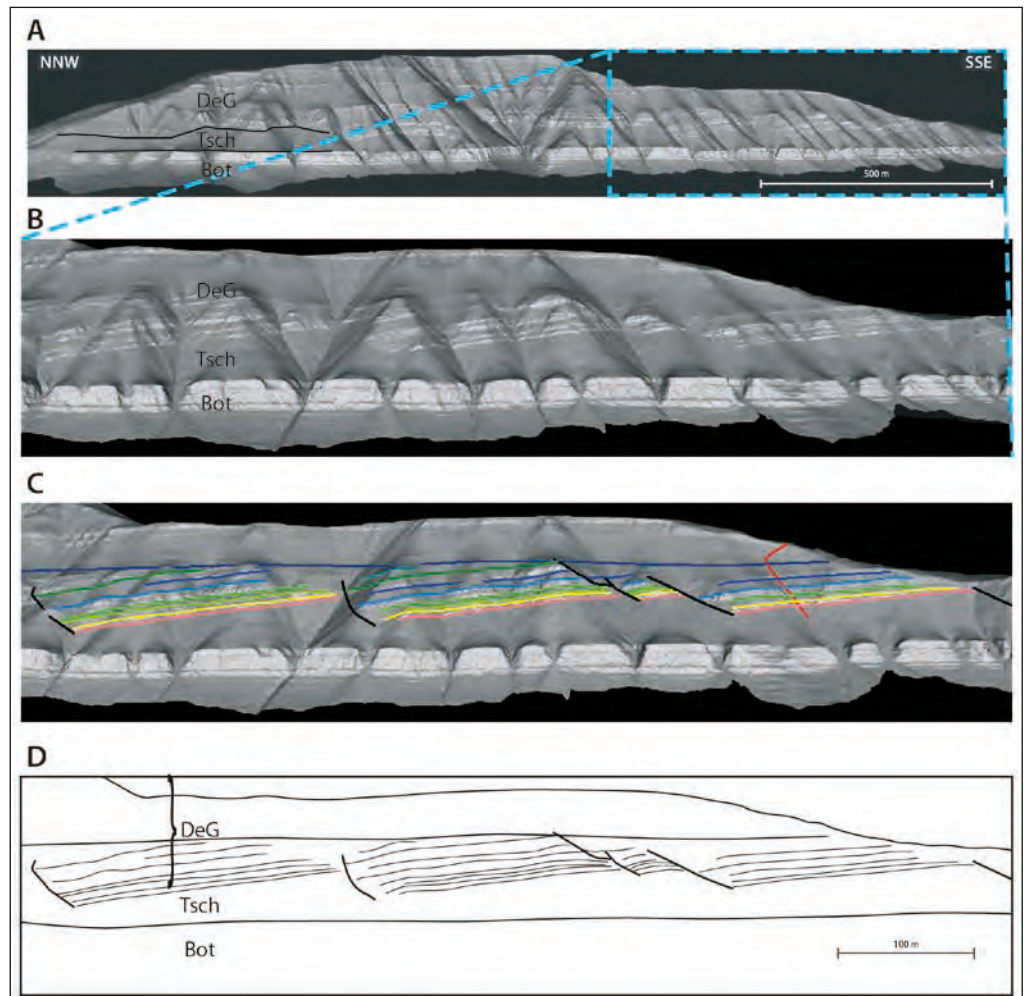
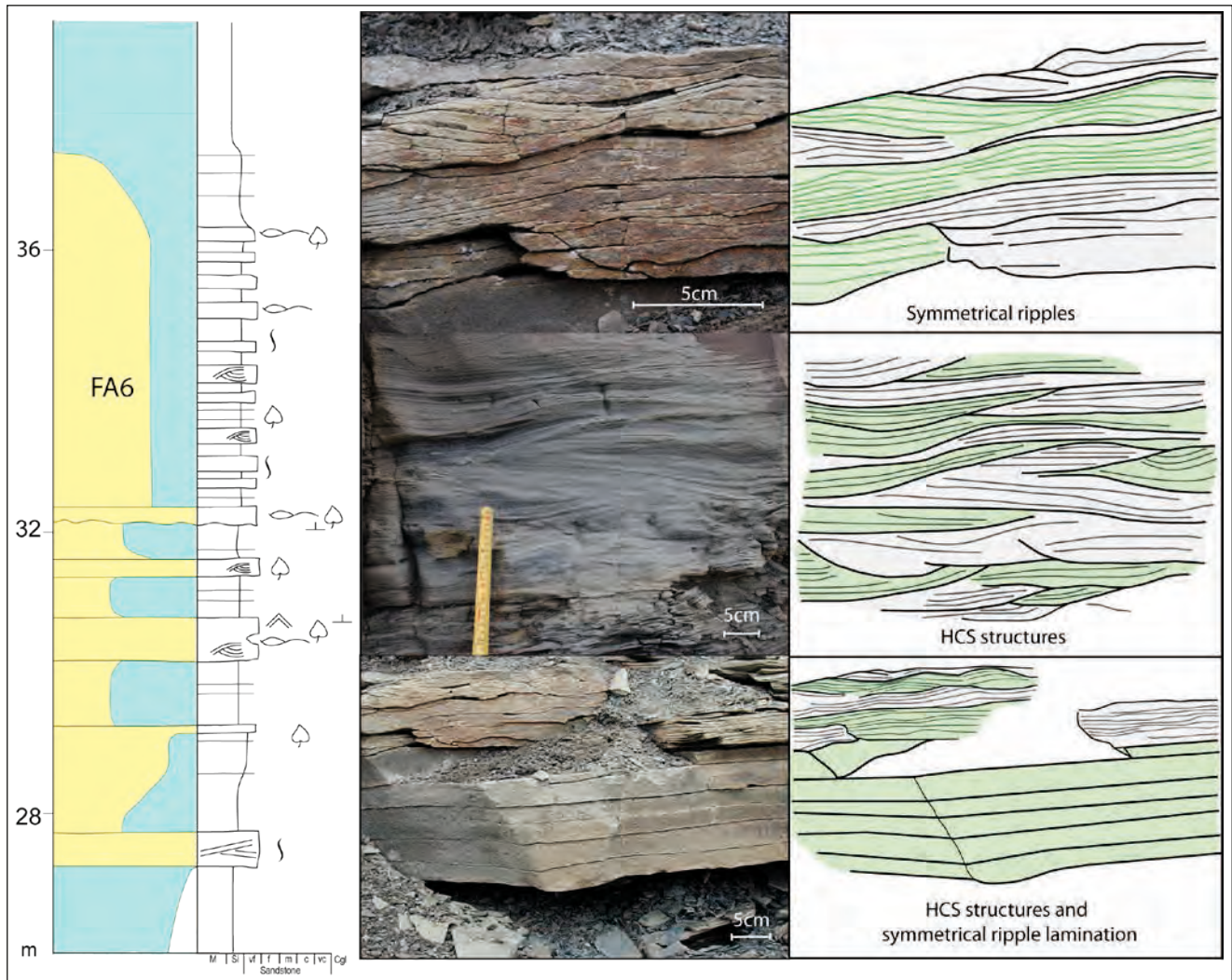


Figure 5. A) The Lidar model of the Klinkhamaren locality with formations indicated; the Botneheia (Bot), Tschermakfjellet (Tsch), and De Geerdalen (DeG) Formations. B) Zooming in on the southern part of the mountain (blue box) tilted strata are visible in the lower part of the De Geerdalen Formation. C) The position of the field log (red) is shown together with the interpretation of strata (various colours), faults (black) and a flooding surface (dark blue). D) The interpretation shows plane to listric faults with parallel strata and a small wedging toward the top of each fault block. No sandstone is observed within these wedges.





**Figure 6.** Facies Association 6, Lower shoreface to offshore deposits. The profile is from the lower part of the De Geerdalen Formation on Botneheia (BOT093), central Spitsbergen, showing interbedded sandstone layers and shale. Structures in the sandstones are shown in photos and corresponding drawings, where the symmetrical ripples and HCS overlain by symmetrical ripples are from Sassendalen (TREH09) and the plain HCS structures are from Botneheia (BOT091). Legend in the Appendix.

Klinkhamaren. On central Spitsbergen the FA3 succession has a less distinct upward coarsening trend. These successions have tidal signals, are erosive based and lack the coal units.

FA4 and FA5 are always found overlying FA6. Vaguely upward coarsening units on central Spitsbergen, showing symmetrical ripple lamination (Facies D) and low angle cross stratification (Facies E) are typical of the deposits described as barrier bars (FA4), which is not observed at Edgeøya. At Klinkhamaren massive sandstone beds with undulating fractures (Facies G), load structures and mud flakes (Facies I) are interbedded with shale (Facies N2). These deposits are described as delta front channel sand (FA5), but are poorly understood. They may be the result of mass transport or resedimentation related to fault activity. Thickness variations are evident within some of these units. At Klinkhamaren there are faults occurring in the lower part of the De Geerdalen Formation that tilt

the strata within the fault blocks. Some of the strata are wedge shaped indicating syntectonic deposition (Fig. 5). The wedge deposits on Klinkhamaren are mostly siltstone and shale, unlike the more famous locality Kvalpynten where the wedges mostly consist of sandstone (Edwards, 1976; Osmundsen et al., 2014). Determining whether the FA5 is disturbed or influenced by active faulting is beyond the scope of this article. However, syndimentary faulting seems likely due to the massive appearance of the sandstone.

Successions dominated by shale, siltstone and fine-grained sandstone (FA6) are found both at Edgeøya and on central Spitsbergen (Fig. 6). Thickness variations of the successions are greater on Edgeøya than on central Spitsbergen, indicating more variation in accommodation space in the east than in the west. The sandstone occurs as thin ripple- to planar laminated units (Facies D), often overlying hummocky cross stratified (HCS)

units (Facies H). At Botneheia some successions in the upper reaches of the formation show an upward coarsening trend from heterolithic bedding and small scale HCS to large scale HCS.

The results of the facies analysis are summarized in two correlation panels; one for Edgeøya, eastern Svalbard (Fig. 7) and the other for central Spitsbergen, western Svalbard (Fig. 8).

## Results and interpretations - Edgeøya

At Edgeøya eleven profiles are measured (Fig. 7) and two Lidar scans are performed at Klinkhamaren and Slåen/Siegelfjellet (Fig. 1). In the lower parts of the De Geerdalen Formation at Blanknuten and at Muen the environment is interpreted as marine (FA6), with symmetrical ripples, HCS structures and mudstone domination. At Klinkhamaren the deposits have been affected by faulting, and the facies and the sandrich lithology suggest a more proximal delta front setting (FA3 and 5), as compared to the prodelta setting of Blanknuten and Muen at this level. At the same stratigraphic level at Slåen/Siegelfjellet the sandstone dominated interval (FA2 and 3) reflects a local point source with depositional elements such as mouth bars and distributary channels.

At Blanknuten and Klinkhamaren the upper parts of sections comprise thin, upward coarsening, laterally continuous units (FA3; Fig. 7). They consist of low angle cross stratification, trough cross bedding, ripples, bioturbation and lenticular bedding. The variety of facies at these localities indicates a rapidly changing environment. The thickest coarsening upward sandstone beds are interpreted as mouth bars/deltaic lobes, and the shale interbedded with thin siltstone and sandstone beds are interpreted as interdistributary areas influenced by tide, waves and a fluvial component. As the upper part of Edgeøya is eroded and thus do not expose the uppermost part of the De Geerdalen Formation, this level is missing at Slåen/Siegelfjellet and Muen.

At Blanknuten paleocurrent measurements were taken systematically on ripples, troughs and foresets through the two measured profiles (BLA091 and BLA092; Fig. 9). They have been corrected for a magnetic declination of 11°E. The monodirectional paleocurrent data indicate a sediment transport from an eastern source, with both SW and NW progradational directions.

### An example from Slåen/Siegelfjellet

The Slåen/Siegelfjellet locality is an 8 km long west facing section (Fig. 1). Four profiles are measured and a Lidar scan is collected. The vertically exaggerated sketch of the Slåen/Siegelfjellet locality shows the different intervals interpreted as shelf/shoreface, delta front/plain and interdistributary areas, represented in blue, yellow and green respectively (Fig. 10A). The boundaries of these intervals were interpreted in the Lidar model.

The measured sections at Slåen (ØKS09, SLA091 and SLA092) shown in the Figs. 7 and 10, display a 10 m thick succession of coarsening upward units of large scale fine to medium cross stratified sandstone with sharp possibly erosive bases (Fig 10D; 8-18 m). Upward fining units with small scale cross stratification are overlying these units (Fig 10D; 18-21 m). Paleocurrent measurements indicate a NW sediment transport direction. The upward coarsening units are believed to reflect sand deposited in a large standing body of water, transported by a unidirectional flow, and the upward fining units to reflect channel deposits. Underlying the sandstone interval is mud dominated units with thin upward coarsening sandstone units with symmetrical ripples interpreted as prodelta environment. The sandy parts of the sections are therefore interpreted as delta front deposits, prograding across the prodelta, with the lower sand units interpreted as mouth bar deposits (FA3) and the upward fining sands as distributary channel deposit (FA2). The equivalent succession at Siegelfjellet (Siegel08) shown in Figs. 7 and 11, is consisting of upward coarsening units of shale and rippled sandstone (FA6), upward fining units of large scale cross stratified sandstone (FA2), and on top repeated upward coarsening units with some coal and plant fragments (FA1). This was interpreted as fluvially dominated delta front/plain by Glørstad-Clark (2011).

At the north face of the Siegelfjellet large-scale troughs are observed (Fig. 11B). At the corresponding level the measured profile (Siegel08) shows fining up sandstone units with unidirectional cross bedding, such as tangential and trough cross stratification and asymmetrical ripples. Such a combination of different scale troughs are referred to as compound cross stratification and occur as superimposed bedforms migrate over a larger parent bedform (cf. Reading, 1996; Reesink and Bridge, 2007). In a distributary system this could represent dunes migrating across a channel floor represented by the larger troughs.

The middle sandstone dominated interval has the largest variation in thickness from a minimum thickness of about 8 meters, to a maximum thickness of about 45 meters, as shown in yellow in Fig. 11A. This is indicating significant lateral facies changes, typical of a delta front to delta plain environment. The Lidar model indicates that the interval consists of flat based sandstone bodies with flat or convex tops. This differs significantly from the typical channel (complex) morphology with a concave base and a flat top as seen in the upper part of the De Geerdalen Formation on Hopen (Klausen and Mørk, 2014; Lord et al., 2014). The positive relief of sandstone bodies indicates absence of significant erosion and dominance of stacking of sand body elements. This indicates progradation into existing accommodation space as opposed to scour and fill, and is thus interpreted as a distributary system with mouth bars and distributary channels. The same external shape of architectural elements

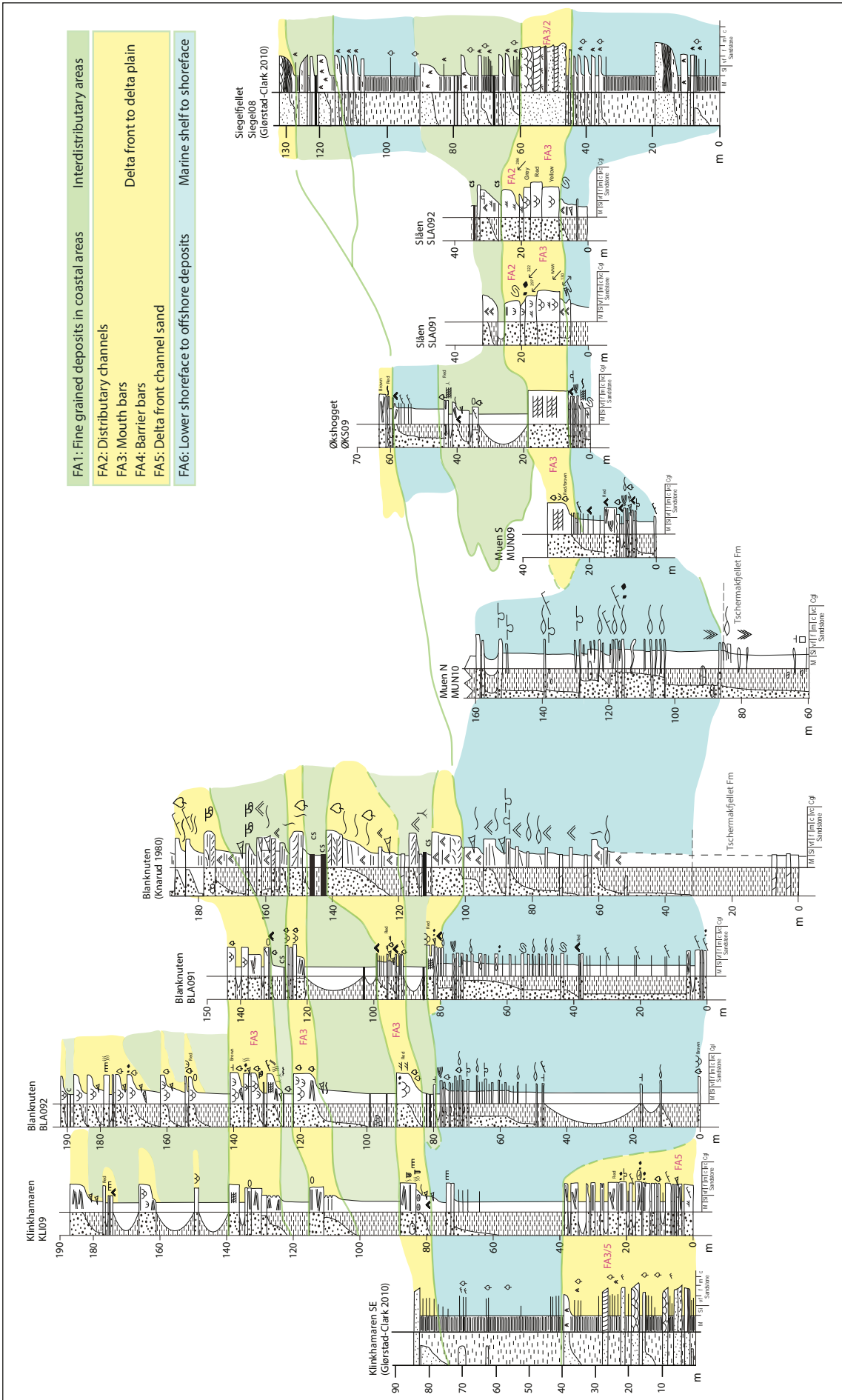


Figure 7. Correlation panel of measured sections on Edgeøya with interpreted facies associations. Location of localities in Figure 1. Legend in the Appendix.



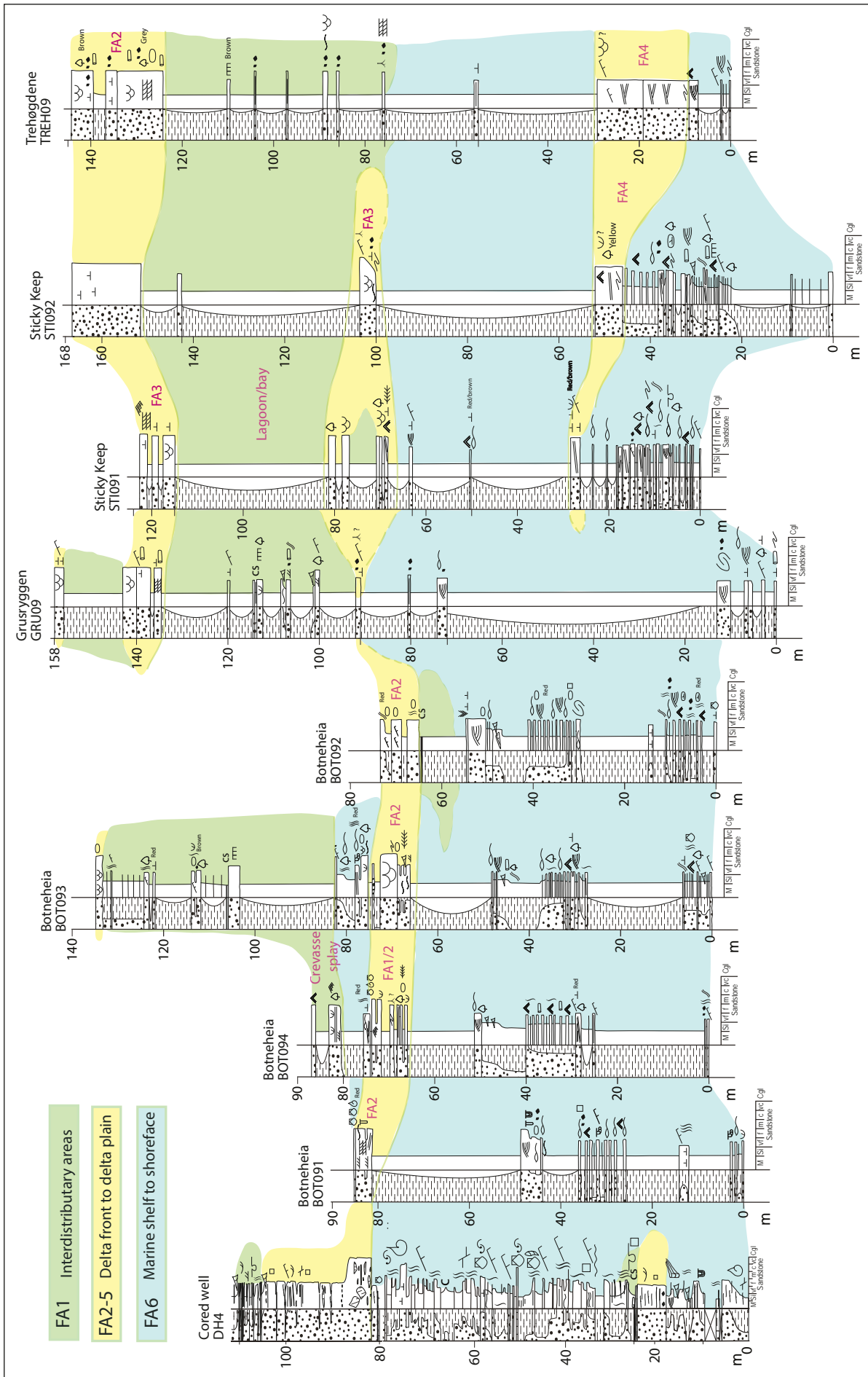


Figure 8 Correlation panel of measured sections on Central Spitsbergen with interpreted facies associations. Location of localities in Figure 1. Legend in the Appendix.

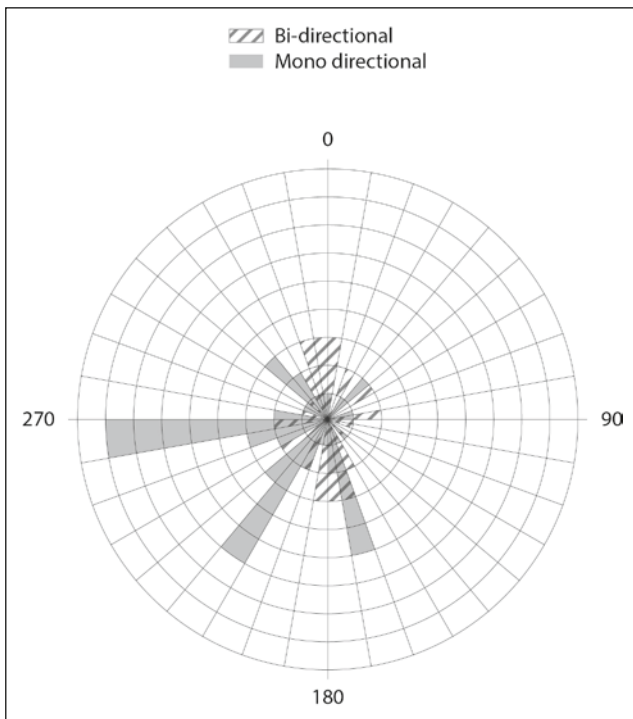


Figure 9. The 53 monodirectional and 20 bidirectional paleocurrent measurements from the sections at Blanknuten, Edgeøya (BLA 091 and 092) are presented above. The data range mainly between 160° and 330°, indicating a dominant paleocurrent direction towards the west.

is reported by Chakraborty and Sarkar (2005) who interpreted plano-convex sandstone bodies as delta front bars. Such geometries are only observed at Edgeøya, at Siegel-fjellet and Blanknuten (Fig. 12).

These sandstone bodies have outcrop dimensions of 30-45 m thickness and 300-500 m width, which yields a thickness to width ratio of about 1:10. Some of these distinct morphologies are observed on the other side of the mountain as well, thus indicating an elongate shape with an east-west depositional trend, supporting the western transport direction given by the paleocurrent data.

Above the sandstone dominated interval, thin upward coarsening rippled sandstone units interbedded with thin mudstone and coal shale units occur within FA1. Plant fragments and thin heterolithic bedded units indicate interdistributary areas that are close to a sediment source, but not receiving the main clastic input (e.g. FA1).

### Results and interpretations – Central Spitsbergen

In central Spitsbergen nine profiles are measured including one core from Adventdalen (DH4) near Longyearbyen and a Lidar scan is collected at Botneheia (Fig. 8). The geometries observed here are for the most part thin meter-scale units where laterally continuous blocky sandstone and siltstone layers are interbedded with shale (Fig. 12).

In the lower parts of the De Geerdalen Formation mudstone dominates and is interbedded with thin hummocky cross stratified sandstone beds. In TREH09 and DH4 thicker low angle cross stratified sandstone units occur, interpreted as barrier complexes (FA4). This is quite similar to the lower parts of sections at Edgeøya, with thick prodelta deposits and locally developed thicker sandstone units with more proximal facies (e.g. FA3 and 5). The difference is that in the east the fluvial component dominates, whereas in the west the deposits seem to be increasingly wave influenced. In fluvially dominated delta front to delta plain environments, depositional elements such as distributary channels and mouth bars are common. In a wave modulated setting these elements will be reworked, and the mouth bars will be formed as barrier bars (Bhattacharya, 2006).

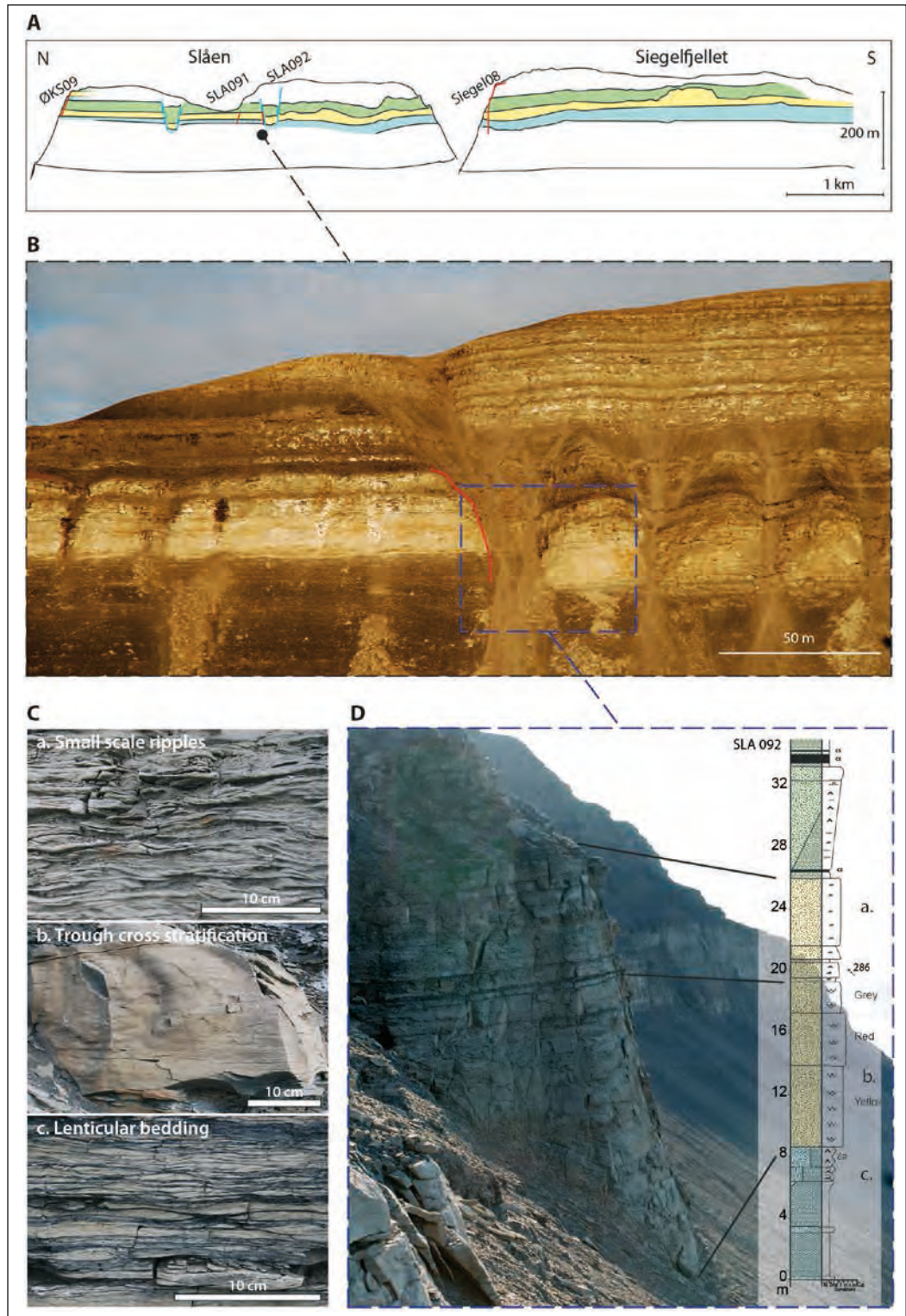
A distinct 10 m thick sandstone bench at about 70 meters above base of the formation is continuous along the whole section on Botneheia (Fig. 8). With its meter thick rippled and trough cross stratified sandstone interbedded with thinner siltstone and shale layers (Facies A, K), it is interpreted as distributary channel deposits (FA2). Distributary channel deposits are also interpreted in the DH4, level 80-100 m. In Sassendalen (STI091, STI092, and GRU09) thin trough cross bedded units (Facies A, B) are interpreted as mouth bars. These deposits are thinner than their equivalent distributary channel and mouth bar units at Edgeøya. The deposits on central Spitsbergen also differ from their eastern equivalents by having tidal signals such as herringbone structure and double mud drapes. This is believed to be a result of a weaker fluvial component distally which allows the wave and tidal signals to become more prominent.

Interdistributary areas (FA1) are interpreted as the main depositional environment in the upper part of sections on Central Spitsbergen. The thin rippled sandstone beds (Facies B, K) are interpreted as crevasse splays and the thicker sharp based units with unidirectional cross bedding including climbing ripples (Facies A, C) as distributary channels. This level shares characteristics with the equivalent level in the east, such as coal shale stringers, similar facies and repetitive successions of interbedded thin sandstone units and shale units. The upward coarsening of most of the sandstone units in the east is different; as few such trends are observed in the west.

### Discussions – Depositional model

Facies associations in the lower part of the De Geerdalen Formation vary from offshore-shoreface deposits (FA6) to the proximal delta deposits of FA2, FA3 and FA5 in the east and to FA4 and FA2 in the west. In the upper part of the formation interdistributary area deposits (FA1), such as lagoon, bay, back barrier and delta plain deposits dominate. At Edgeøya these deposits are interbedded

**Figure 10.** A) Overview composite figure with a vertically exaggerated sketch from the Lidar data of the Slåen/Siegelfjellet locality; B) a photo showing where the SLA092 profile (red line) was measured; C) close up photos of representative facies in log (Facies B, A and K respectively) and D) a photo of the outcrop with the SLA092 log. The colors blue, yellow and green represent the depositional environments marine shelf/shore-face (FA6), delta front/plain (FA2-5) and interdistributary areas (FA1) respectively.

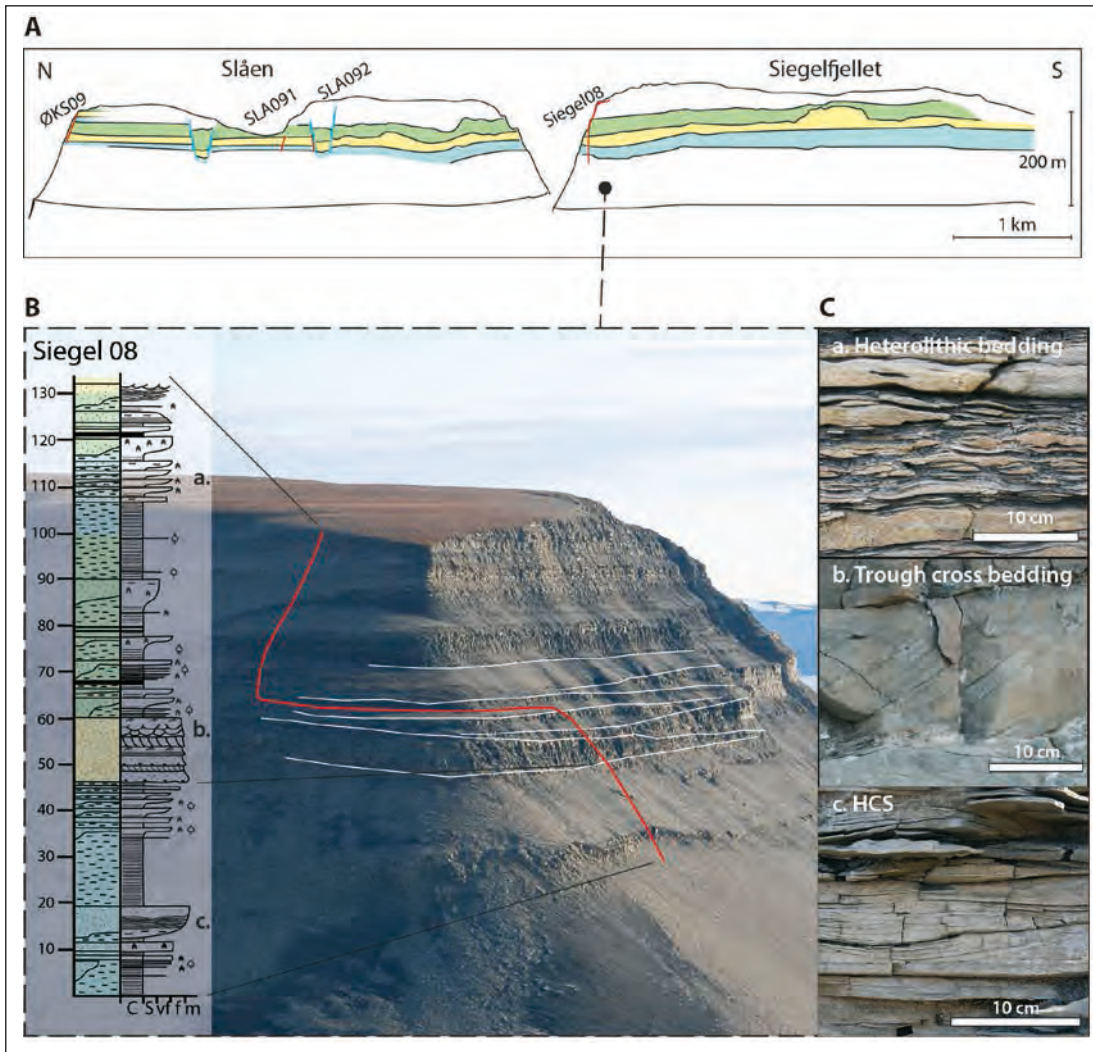


with upward coarsening sandstone packages (e.g. FA3). In central Spitsbergen the interbedded packages of sandstone are generally thinner and mostly upward fining (e.g. FA2).

Hummocky cross stratification is believed to be one of the diagnostic sedimentary structures of storm

dominated shallow marine environments. Variations in coast and delta morphologies can create different type of HCS successions, as observed within the FA6. The upward coarsening HCS successions at Botneheia can represent reworked mouth bars at the delta front (cf. Bhattacharya, 2006), sand sheets in the offshore area between fair-weather- and storm-wave base (cf. Willis





**Figure 11.** A) Overview figure from Siegfjelllet. The vertically exaggerated sketch shows the three discussed intervals, and the location of the measured profiles (in red). B) The overview photo shows the north face of Siegfjelllet with the observed large-scale troughs drawn with white lines. The corresponding 48-60 m interval in the log (in yellow) shows fining upward units of tangential and trough cross stratified and rippled sandstone. C) The close-up photos show representative facies from each of the intervals in the log (Facies K, A and H respectively). Legend in the Appendix.

and Gable, 2001) or proximal banks as interpreted by Knarud (1980). The thickening and increasing of amalgamation of HCS units upwards in the successions can be a result of delta margin progradation. Such HCS units are deposited in the transition to shoreline sands as in the way described from other areas by Dott and Bourgeois (1982) and Duke and Prave (1991). Successions with dominance of shale and thin ripple- and plane laminated sands may represent distal tempestite sandstone deposited in an offshore setting (cf. Duke and Prave, 1991).

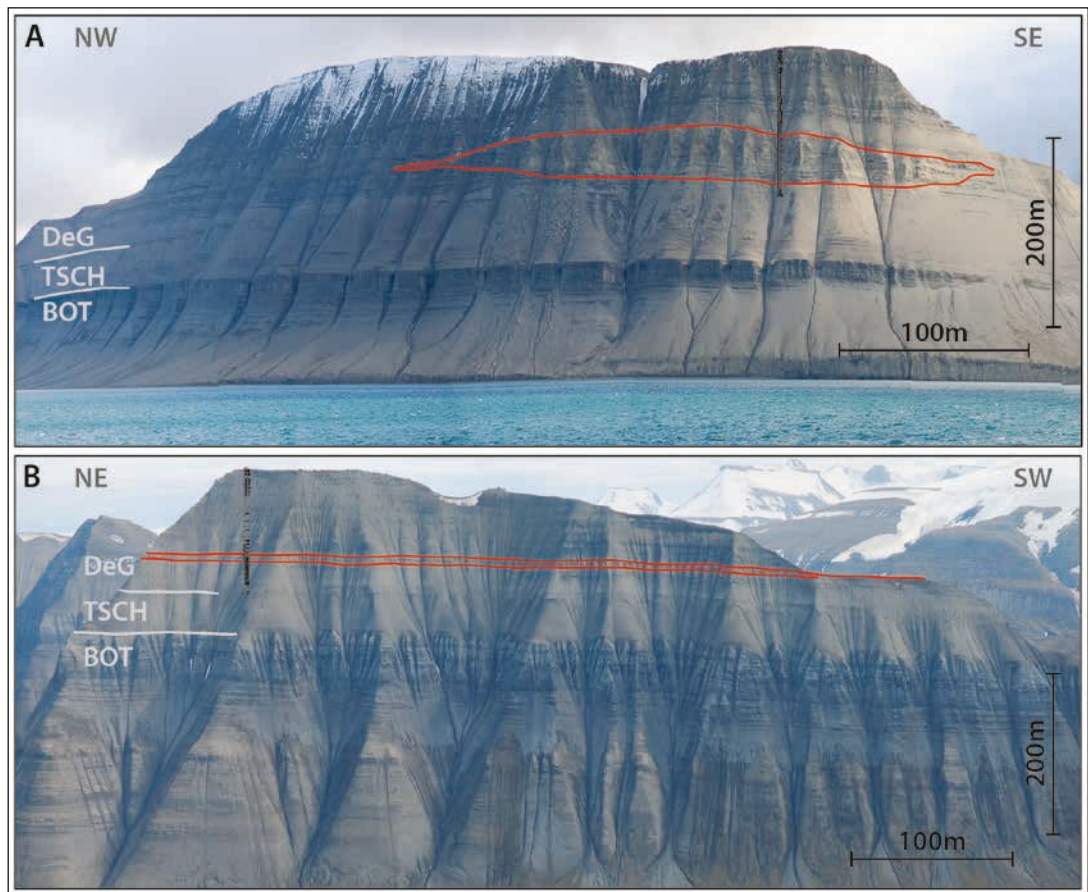
Upward coarsening units and low bioturbation rates as observed within FA3 and FA4 are typical in a delta front setting (Hori et al., 2002), and can develop from prograding deltaic lobes and mouth bars or from barrier island systems developing in a changing regressive and transgressive setting (Bhattacharya, 2006). Heterolithic bedding, mainly occurring on Edgeøya within FA2, can form on delta front or in interdistributary areas on a delta plain (Martino, 1996; Bhattacharya, 2006; Dalrymple and Choi, 2007). In fluvially dominated delta front to delta plain environments, depositional elements such as distributary

channels (FA2) and mouth bars (FA3) are common. In a wave modulated setting these elements will be reworked, and the mouth bars will be formed as barrier bars (FA4) (Bhattacharya, 2006).

Mouth bars (FA3) occur more frequently on Edgeøya than on central Spitsbergen. In the latter localities distributary channels (FA2) are more frequent. Barrier bars (FA4) have only been interpreted on central Spitsbergen. This reflects fluvially dominated areas in the east where mouth bars could develop and a coastline more prone to wave modulation in the west. This indicates slower generation of accommodation space in the west compared to the east.

Distributary channels are distinguished from other sandstone successions by the erosive base and the characteristic mud flake conglomerate. Mud flake conglomerates are typical for channel deposits, as described in several studies (cf. Dalrymple and Choi, 2007). Mud drapes, herringbone structures and heterolithic bedding present both in the DH4 core and on Botneheia, indicates significant

**Figure 12.** Variations in geometry of sandstone bodies (red) in the east compared to the west illustrated by (A) Blanknuten, Edgeøya with an ellipsoid shaped sandstone body and B) the 682 m asl summit of Trehøgden, central Spitsbergen with a thin but laterally extensive sandstone body. The different formations Botneheia (BOT), Tschermakfjellet (TSCH) and De Geerdalen (DeG) Formations are indicated.



tidal influence on the Spitsbergen deposits. Distributary channels on Edgeøya are erosively based and contain mud flakes in some successions, but lack distinct diagnostic tidal signatures. According to Nakajo (1998) upper distributary channels generally display only minor tidal signals compared to lower distributary channels; this gives additional indication that the depositional environment at Spitsbergen is more distal than at Edgeøya.

**Width:** Thickness ratio (W/T) has previously been studied to separate architectural elements from each other (c.f. Reynolds, 1999; Gibling, 2006). Reynolds (1999) found that fluvial trunk channels are in general wider than the distributary channels, and have a W/T range of 25-100. Distributary channels which share many of the characteristics of fluvial trunk channels can be separated from purely fluvially affected channels by having a lower W/T (Reading and Collinson, 1996). Gibling's (2006) dataset compiled from several studies shows that delta distributaries have W/T ratios mainly less than 50. Higher W/T ratios reported in certain studies are related to weaker incision and broader distribution and therefore appear to represent terminal distributary systems (Gibling, 2006).

The observed W/T of 10 in the interpreted FA3/2 interval at Siegfjället is hence within the same order of

magnitude as the distributary channel ratios found by Reynolds (1999). Comparable W/T ratios for channels on Hopen are reported by Klausen and Mørk (2014). The elongate planoconvex geometry and facies analysis suggest, however, that this is mouth bar deposits. As recorded by several logs at Edgeøya the mouth bar deposits are often overlain by distributary channel deposits, so the geometry might reflect a combination of the two depositional elements.

The paleocurrent measurements have shown a western component to the sediment transport direction of this system. At Blanknuten the paleocurrent directions range mainly between 160° and 330°, with a dominant western component. This indicates a sediment source in the east and a delta progradation with delta lobe switching. Few measurements were taken at other localities; however, most of these indicate a NW paleocurrent direction (e.g. SLA091 and SLA092, Fig. 9). A large number of paleocurrent measurements were collected by Knarud (1980) at localities across Svalbard (Blanknuten, Agardhfjellet, Dalsnuten among others). The directions are widespread; however the dominant direction is towards the northwest. Høy and Lundschiën (2011) presented paleocurrent measurements from various localities in eastern Svalbard (Hopen, Negerfjellet, Kvalpynten, Slåen, Blanknuten, Barentsøya and Agardhbukta) indicating N to



NW paleocurrent directions. The few exceptions were interpreted to be related to point bars or delta lobes. In this study, the dominant direction at Blanknuten was found to be towards the W and WSW, the same result as presented in Figure 9. The overall NW and W paleocurrent directions are consistent with the NW delta progradation through the Barents Sea from the Uralides proposed by several workers (Glørstad-Clark, 2011; Høy and Lundschieen, 2011; Riis et al., 2008) and also supported by provenance studies (Mørk, 1999; Pozer Bue and Andreassen, 2013).

Ellipsoid shaped and thick sandstone bodies, typical for fluviially dominated delta fronts, occur on Edgeøya. As previously discussed thickness of a mouth bar depend on accommodation space (Reynolds, 1999). On Spitsbergen, thin, laterally extensive sandstone bodies occur, typical of shoreface environments where wave action redistributes sediments. These deposits are thinner than their equivalent distributary channel and mouth bar units in the east, probably due to less accommodation space. The facies association development observed from Edgeøya to central Spitsbergen reflects a change from proximal to distal depositional environment with more accommodation space in the east than in the west where there is less sedimentation and more wave modulation.

## Conclusions

The depositional environment of the De Geerdalen Formation is of regressive nature with evidence of deltaic influence. At the various localities, fluvial dominance and wave- and tidal influence have affected the sediments differently, resulting in lateral facies variability and different depositional elements.

A more proximal deltaic setting is interpreted on Edgeøya than on central Spitsbergen, indicating delta progradation from the (south) east. The depositional environment is a storm and wave influenced coast, with tidal influence, and fluvial domination in the east where the generation of accommodation space enables preservation of the depositional elements such as mouth bars and distributary channels. In the proximal setting the sandstone bodies therefore have thick, ellipsoid geometries. In the more distal setting in the west, there is less generation of accommodation space, and the sandstone bodies tend to be thin and laterally continuous due to more wave and tide influence.

The present study is adding more detailed documentation on facies development at Edgeøya and central Spitsbergen, and the results support the suggested regional deltaic progradation across the Barents shelf from the southeast to the northwest.

## Appendix – Legend to sections.

	Sandstone
	Claystone / mudstone
	Covered / partly covered
	Mud- and claystone clasts
	Coal
<b>CS</b>	Coal-shale
	Current ripples (3D)
	Current ripples (2D)
	Symmetrical ripples
	Unspecified ripple lamination
	Herringbone lamination
	Climbing ripples
	Planar lamination
	Low angle cross-bedding
	Lenticular lamination
	Lenticular and ripple lamination
	Large scale trough cross-stratification
	Large scale tangential cross-stratification
	Large scale angular cross-stratification
	Large scale hummocky bedding
	Small scale hummocky bedding
	Double mud drapes
	Mud drape
	Mud flakes
	Erosional surface
	Desiccation cracks
	Loading (major)
	Loading (minor)
	Soft sediment deformation
	Convolute lamination
	Small fault
	Nodule
	Pyrite
	Cone in cone
	Calcite cementation
	Siderite cementation
	Unspecified cementation
	Bidirectional paleocurrent measurement
	Monodirectional paleocurrent measurement
	Unidentified fossil fragment
	Bivalves
	Coquina
	Gastropods
	Wood / Plant fragments
	Roots
	Increasing bioturbation
	<i>Skolithos</i>
	<i>Rhizocorallium</i>
	<i>Diplocraterion</i>
	<i>Teichichnus</i>
	<i>Palaeophycus</i> (+ unidentified tunnels)

### Acknowledgements.

This work was supported by the NPD, and performed while all authors had affiliation to NTNU and UNIS. Thanks to the reviewers Johan Petter Nystuen and William Helland Hansen for constructive feedback that helped improve and clarify the manuscript. Thanks also to NPD colleagues for good ideas and discussions.

## References

- Bhattacharya, J.P. 2006: Deltas. In Posamentier, H. W. & Walker, R. G. (eds.): Facies models revisited, *Special Publication*, 84, Society of Sedimentary Geology, 237-292.
- Braathen, A., Bælum, K., Christiansen, H.H., Dahl, T., Eiken, O., Elvebakk, H., Hansen, F., Hanssen, T.H., Jochmann, M., Johansen, T.A., Johnsen, H., Larsen, L., Lie, T., Mertes, J., Mørk, A., Mørk, M.B., Nemeč, W., Olaussen, S., Oye, V., Rød, K., Titlestad, G.O., Tveranger, J. & Vagle, K. 2012: The Longyearbyen CO<sub>2</sub> Lab of Svalbard, Norway—initial assessment of the geological conditions for CO<sub>2</sub> sequestration. *Norwegian Journal of Geology*, 92, 353–376. ISSN 029-196X.
- Buckley, S.J., Howell, J.A., Enge, H.D. & Kurz, T.H. 2008a: Terrestrial laser scanning in geology: data acquisition, processing and accuracy considerations. *Journal of the Geological Society of London*, 165, 625–638.
- Buckley, S.J., Vallet, J., Braathen, A. & Wheeler, W. 2008b: Oblique helicopter-based laser scanning for digital terrain modelling and visualisation of geological outcrops. *International Archives of the Photogrammetry, Remote Sensing and Spatial Information Sciences*, 37 (B4), 493–498.
- Chakraborty, T. & Sarkar, S. 2005: Evidence of lacustrine sedimentation in the Upper Permian Bijori Formation, Satpura Gondwana basin: Palaeogeographic and tectonic implications. *Journal of Earth System Science*, 114, 3, 303–323.
- Dagys, A.S. & Weitschat, W. 1993: Correlation of the Boreal Triassic. *Mitteilungen Geologisch-Paläontologisches Institut Universität Hamburg*, 75, 249–256.
- Dalrymple, R.W. & Choi, K. 2007: Morphologic and facies trends through the fluvialmarine transition in tide-dominated depositional systems: A schematic framework for environmental and sequence stratigraphic interpretation. *Earth Science Reviews*, 81, 135–174.
- Dott, R.H. & Bourgeois, J. 1982: Hummocky stratification: Significance of its variable bedding sequences. *Geological Society of America Bulletin*, 93, 663–680.
- Duke, W.L. & Prave, A.R. 1991: Storm- and tide-influenced prograding shoreline sequences in the Middle Devonian Mahantango Formation, Pennsylvania. In Smith, D.G., Reinson, G.E., Zaitlin, B.A. & Rahmani, R.A. (eds.): *Clastic Tidal Sedimentology*, *Canadian Society of Petroleum Geologists*, 19, 625–628.
- Edwards, M.B. 1976: Growth Faults in Upper Triassic Deltaic Sediments, Svalbard. *American Association of Petroleum Geologists Bulletin*, 60, 341–355.
- Gibling, M.R. 2006: Width and thickness of fluvial channel bodies and valley fills in the geological record: A literature compilation and classification. *Journal of Sedimentary Research*, 76, 731–770.
- Glørstad-Clark, E. 2011: Depositional dynamics in an epicontinental basin: De Geerdalen Formation on Edgeøya, Svalbard. In Glørstad-Clark, E.: *Basin analysis in the western Barents Sea area: The interplay between accommodation space and depositional systems*, PhD thesis, University of Oslo, 215–262.
- Glørstad-Clark, E., Faleide, J.I., Lundschieen, B.A. & Nystuen, J.P. 2010: Triassic seismic sequence stratigraphy and paleogeography of the western Barents Sea area. *Marine and Petroleum Geology*, 27, 1448–1475.
- Glørstad-Clark, E., Birkeland, E.P., Nystuen, J.P., Faleide, J.I. & Midtkandal, I. 2011: Triassic platform-margin deltas in the western Barents Sea area. *Marine and Petroleum Geology*, 28, 1294–1314.
- Hori, K., Saito, Y., Zhao, Q. & Wang, P. 2002: Architecture and evolution of the tidedominated Changjiang (Yangtze) River delta, China. *Sedimentary Geology*, 146, 249–264.
- Høy, T. & Lundschieen, B.A. 2011: Triassic deltaic sequences in the northern Barents Sea. In Spencer, A. M., Embry, A., Gautier, D. L., Stoupakova, A. & Sørensen, K. (eds.): *Arctic Petroleum Geology*, 35, 249–260.
- Klausen, T. G., & Mørk, A. 2014: The Upper Triassic paralic deposits of the De Geerdalen Formation on Hopen: Outcrop analog to the subsurface Snadd Formation in the Barents Sea. *American Association of Petroleum Geologists Bulletin*, 98, 1911–1941, doi:10.1306/02191413064.
- Knarud, R. 1980: *En sedimentologisk og diagenetisk undersøkelse av Kapp Toscana Formasjonens sedimenter på Svalbard*. Unpublished Cand.Real thesis, University of Oslo, 208 pp.
- Lock, B.E., Pickton, C.A.G., Smith, D.G., Batten, D.J. & Harland, W.B. 1978: The geology of Edgeøya and Barentsøya, Svalbard. *Norsk Polarinstitutt Skrifter*, 168, 64 pp.
- Lord, G.S., Solvi, K.H., Ask, M., Mørk, A., Hounslow, M.W. & Paterson, N.W. 2014: The Hopen Member: A new member of the Triassic De Geerdalen Formation, Svalbard. *Norwegian Petroleum Directorate Bulletin*, 11, 81–96.
- Lundschieen, B.A., Høy, T. & Mørk, A. 2014: Triassic hydrocarbon potential in the Northern Barents Sea; integrating Svalbard and stratigraphic core data. *Norwegian Petroleum Directorate Bulletin*, 11, 3–20.
- Martino, R.L. 1996: Stratigraphy and depositional environments of the Kanawha Formation (Middle Pennsylvanian), southern West Virginia, U.S.A. *International Journal of Coal Geology*, 31, 217–248.
- Mørk, A., Knarud, R. & Worsley, D. 1982: Depositional and diagenetic environments of the Triassic and Lower Jurassic succession of Svalbard. In Embry, A.F. & Balkwill, H.R. (eds.): *Arctic Geology and Geophysics, Canadian Society of Petroleum Geologists Memoir*, 8, 371–398.
- Mørk, A., Embry, A.F. & Weitschat, W. 1989: Triassic transgressive-regressive cycles in the Sverdrup Basin, Svalbard and the Barents Shelf. In Collinson, J.D. (ed.): *Correlation in Hydrocarbon Exploration, Norwegian Petroleum Society*, Graham & Trotman Ltd, 113–130.
- Mørk, A., Dallmann, W.K., Dypvik, H., Johannessen, E.P., Larsen, G.B., Nagy, J., Nøttvedt, A., Olaussen, S., Pchelina, T.M. & Worsley, D. 1999: Mesozoic lithostratigraphy. In Dallmann, W. K. (ed.): *Lithostratigraphic lexicon of Svalbard. Review and recommendations for nomenclature use. Upper Palaeozoic to Quaternary bedrock*, Tromsø, Norwegian Polar Institute, 127–214.
- Mørk, M.B.E. 1999: Compositional variations and provenance of Triassic sandstones from the Barents Shelf. *Journal of Sedimentary Research*, 69, 690–710.
- Nakajo, T. 1998: Tidal influences on distributary-channel sedimentation of the Tertiary delta in the Taishu Group, Tsushima Islands, southwestern Japan. *Journal of Geosciences*, 41, 37–46.
- Osmundsen, P.T., Braathen, A., Rød, R.S. & Hynne, I.B. 2014: Styles of normal faulting and fault-controlled sedimentation in the Triassic deposits of Eastern Svalbard. *Norwegian Petroleum Directorate Bulletin*, 11, 61–69.
- Pozer Bue, E. & Andresen, A. 2013: Constraining depositional models in the Barents Sea region using detrital zircon U–Pb data from Mesozoic sediments in Svalbard. *Geological Society of London, Special Publication*, 386, 261–279. ISSN 0305-8719.
- Reading, H.G. & Collinson, J.D. 1996: Clastic coasts. In Reading, H.G. (ed.): *Sedimentary Environments: Processes, Facies and Stratigraphy*, Oxford, Blackwell Science Ltd, 154–231.
- Reynolds, A.D. 1999: Dimensions of paralic sandstone bodies, *American Association of Petroleum Geologists Bulletin*, 83, 211–229.
- Riis, F., Lundschieen, B.A., Høy, T., Mørk, A. & Mørk, M.B.E. 2008: Evolution of the Triassic shelf in the northern Barents Sea region, *Polar Research*, 27, 318–338.



- Skaloud, J., Vallet, J., Keller, K., Veyssi re, G. & K obl, O. 2006: An eye for Landscapes – Rapid Aerial Mapping with Handheld Sensors, *GPS World*, 17(5), 26-32.
- Steel, R.J. & Worsley, D. 1984: Svalbard's post-Caledonian strata. An atlas of sedimentological patterns and palaeogeographic evolution. In Spencer, A.M. et al (eds.): *Petroleum Geology of the North European Margin*, Norwegian Petroleum Society, Graham & Trotman Ltd, 109-135.
- Vallet, J. & Skaloud, J. 2004: Development and experiences with a fully-digital handheld mapping system operated from a helicopter. The International Archives of the Photogrammetry, *Remote Sensing and Spatial Information Sciences*, 35, Part B, Commission 5. Istanbul. 791-796.
- Vigran, J.O., Mangerud, G., M ork, A., Worsley, D. & Hochuli, P.A. 2014: Palynology and geology of the Triassic succession of Svalbard and the Barents Sea. *Geological Survey of Norway Special Publication*, 14, 270 pp.
- Willis, B.J. & Gabel, S. 2001: Sharp-based, tide-dominated deltas of the Sege Sandstone, Book Cliffs, Utah, USA. *Sedimentology*, 48, 479-506.

# Triassic channel bodies on Hopen, Svalbard: Their facies, stratigraphic significance and spatial distribution

Gareth S. Lord<sup>1,2</sup>, Kristoffer H. Solvi<sup>1</sup>, Tore G. Klausen<sup>3</sup> & Atle Mørk<sup>1,4</sup>

<sup>1</sup> Department of Geology and Mineral Resources Engineering, Norwegian University of Science and Technology (NTNU), NO-7491 Trondheim, Norway. e-mail: gareth.lord@ntnu.no

<sup>2</sup> The University Centre in Svalbard (UNIS), Longyearbyen, Norway.

<sup>3</sup> University of Bergen, Norway.

<sup>4</sup> SINTEF Petroleum Research, Trondheim, Norway.

Channelized deposits are observed in the steep cliff sections on the island of Hopen in SE Svalbard. This presents a unique opportunity to study the geometry and spatial distribution of these channel bodies within the paralic depositional environment of the Carnian aged De Geerdalen Formation.

In this study we have combined field observations with a 3D geological model of the island. Utilising PhotoModeler™ software, with an extensive photo database of the study area, it has been possible to identify the presence of 25 channel bodies on the island. 12 have been observed directly in the field, with the remainder being identified with photo mosaics and by implementing the 3D geological model. Analysis has shown that the channels were deposited in three different depositional environments; fluvial, tidal and estuarine. Channel deposits that have not been observed in the field are interpreted based on their geometries and visible internal architectures seen within high resolution outcrop photographs.

Channel bodies are seen to be confined to discrete stratigraphical intervals within the De Geerdalen Formation, defined as channel zones. Three zones are described, based upon the concentration of channels within each interval. These intervals are categorised as a lower fluvial zone, a middle tidal zone and an upper fluvial zone.

These zones are subsequently overlain by a marine flooding event represented by the Hopen Member. An overall paralic depositional environment for the De Geerdalen Formation on Hopen is maintained, however the nature of channels clearly shows a greater influence of fluvial deposition for the formation in this region of Svalbard. This indicates deposition in a more proximal position relative to the source area, than elsewhere on Svalbard.

**Key words:** Channels, Stratigraphy, Hopen, Svalbard, Triassic.

## Introduction

The presence of cliff forming sandstone bodies, initially deposited in a continental fluvial environment, have long been known to form the island of Hopen, in the SE part of the Svalbard archipelago (Flood et al., 1971; Smith et al., 1975; Mørk et al., 2013). Economic interests in the northern Barents Sea have also increased scientific activity in the Upper-Triassic succession of Svalbard. Recent expeditions to Hopen have thus placed a greater interest in the understanding of these sandstone bodies, due to their potential as hydrocarbon reservoirs

(Johansen et al., 1993; Riis et al., 2008; Lundschieen et al., 2014). The sandstone bodies are laterally extensive, often seen in cross section and in some instances can be observed on both sides of the island. These represent ancient fluvial and estuarine channel systems which can be considered analogous to the upper part of the Snadd Formation in the Barents Sea (Klausen and Mørk, 2014).

Multiple short geological expeditions to Hopen have been conducted by SINTEF Petroleum Research, NPD and participant companies of production licences in the Barents Sea (PL438, PL533, PL609 and PL611),



herein referred to as the *Hopen Geology Project*. These expeditions have visited the island annually since 2007 and this timespan has allowed for the acquisition of new geological data from the island, albeit by numerous workers. This includes an improvement on sedimentological knowledge from extensive logging, photographic modelling of the island, the creation of a new stratigraphical interval and an updated geological map (Mørk et al., 2013; Lord et al., 2014).

The objective of this paper is to add further documentation of these channel features seen on the island of Hopen. By positioning them accurately within the stratigraphy of the De Geerdalen Formation, it is possible to understand their spatial distribution in relation to the paralic environment which characterises the De Geerdalen Formation on Hopen. This is achieved through the combination of geological modelling and outcrop studies. This is intended to provide a firm basis of geological understanding and support future studies with onshore-offshore correlation of the Late-Triassic sediments, into the northern Barents Sea.

## Geological Setting and Stratigraphy of Hopen

The island of Hopen lies in the SE corner of the Svalbard archipelago (Fig. 1) at approximately N76°35' E25°20' in the Norwegian high arctic. It is a small island of only 34 km in length and 0.5-2.5 km in width consisting entirely of Triassic aged strata, which protrude to a maximum height of 371 m above sea level. Its origin probably relates to the nature of deep rooted faulting in NE region of the Barents Sea (Doré, 1995; Grogan et al., 1999). The crustal structure around Hopen is dominated by a series of NE-SW trending lineaments, oblique to the regional N-S trend of structures in Spitsbergen (Doré, 1995; Grogan et al., 1999).

The island features regionally and gently northwards dipping strata, dissected by a series of NW-SE trending normal faults dipping to both the SW and NE. The stratum of the island also display gentle synclinal and monoclinical structures, with limbs dipping to both the NE and SW (Smith et al., 1975; Mørk et al., 2013; Klausen and Mørk, 2014).

Exposures of the island represent three formations (Fig. 2) of the Late-Triassic in Svalbard (Mørk et al., 1999). These include; the uppermost of the De Geerdalen Formation, with its heterolithic nature of alternating sandstone and siltstone deposited in a paralic deltaic setting (Klausen and Mørk, 2014). The entirety of the overlying Flatsalen Formation, with the Slottet Bed at its base can be observed at Lyngfjellet in the NE of the island. Lyngfjellet is capped by a c. 35 m thick cliff forming succession of the Svenskøya Formation of

Norian and possibly Rhaetian age (Mørk et al., 2013; Vigran et al., 2014) and is the only locality at Hopen where this formation is present (Mørk et al., 1999; 2013).

The De Geerdalen Formation on Hopen is dated as Late-Triassic, Carnian to Norian in age, based on the presence of ammonites, palynology and magneto-stratigraphy (Pčelina, 1972; Korčinskaja, 1980; Tozer and Parker, 1968; Launis et al., 2014; Lord et al., 2014; Vigran et al., 2014). The uppermost part of the De Geerdalen Formation on Hopen is interpreted as showing an increasing marine influence, exhibiting lower net-to-gross succession, dominated by hummocky cross-stratification. This upper part of the De Geerdalen Formation has been defined as the Hopen Member (Mørk et al., 2013; Lord et al., 2014), a time equivalent unit to the Isfjorden Member of central Spitsbergen.

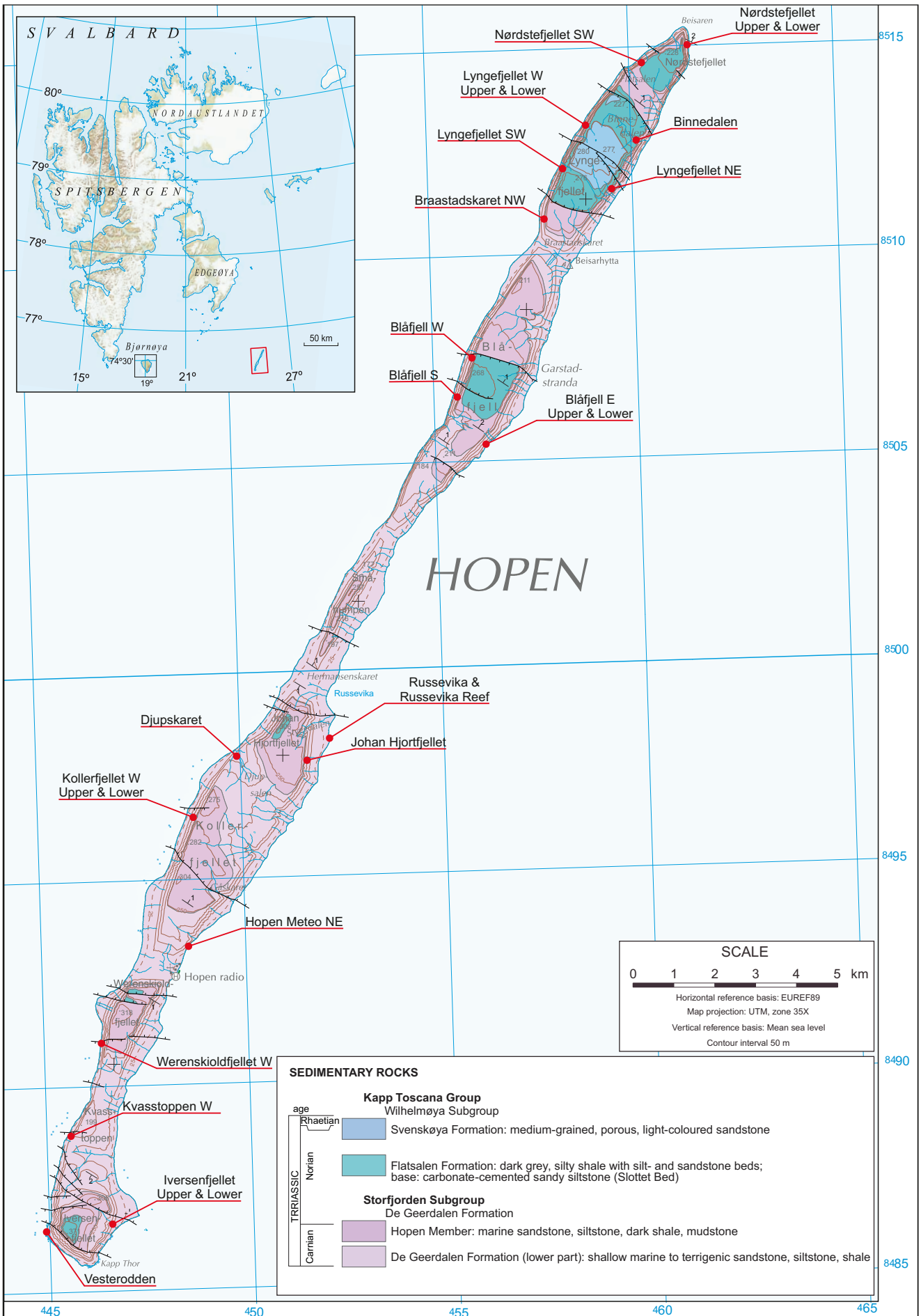
Recent advances in the understanding of the development of the De Geerdalen Formation throughout the Triassic (see Worsley, 2008; Klausen and Mørk, 2014; Glørstad-Clark et al., 2010; Lundschieen et al., 2014, Lord et al., 2014; Rød et al., 2014) show that the Triassic strata of Hopen represent some of the youngest and most regressive onshore exposures, of a large-scale deltaic system, that gradually filled the Barents shelf during the Triassic (Worsley, 2008; Glørstad-Clark et al., 2010; Lundschieen et al., 2014). The palaeogeographic map in Figure 2 illustrates a reconstruction of this deltaic environment during the Late-Triassic.

This enclosed shelf, in the northern coastline of the Pangean supercontinent stretched out to the boreal Panthalassa Sea and was gradually filled with sediments, derived from the Uralian mountain chain (Puchkov, 2009; Pózer Bue and Andresen, 2013; Lundschieen et al., 2014). The Ural Mountains were uplifted as a series of tectonic and orogenic events throughout the Late Devonian, Late Carboniferous and Permian (Puchkov, 2009), as the Siberian Plate collided with the smaller landmasses of Kazakhstania and Pangea itself.

The outcrops that represent the most distal parts of this deltaic system are observed on central Spitsbergen within the De Geerdalen Formation, whereas the corresponding paralic and proximal part of this delta within the Triassic succession can be found on the islands of Barentsøya, Edgeøya and Hopen. The axis of Hopen lies relatively perpendicular to the interpreted NW direction of deltaic progradation (Klausen and Mørk, 2014; Lundschieen et al., 2014).

The youngest Triassic exposures found in Svalbard are present on Spitsbergen and Hopen and are not exposed on

*Figure 1. Location map and geological map of Hopen after Mørk et al. (2013). Channel locations are denoted.*





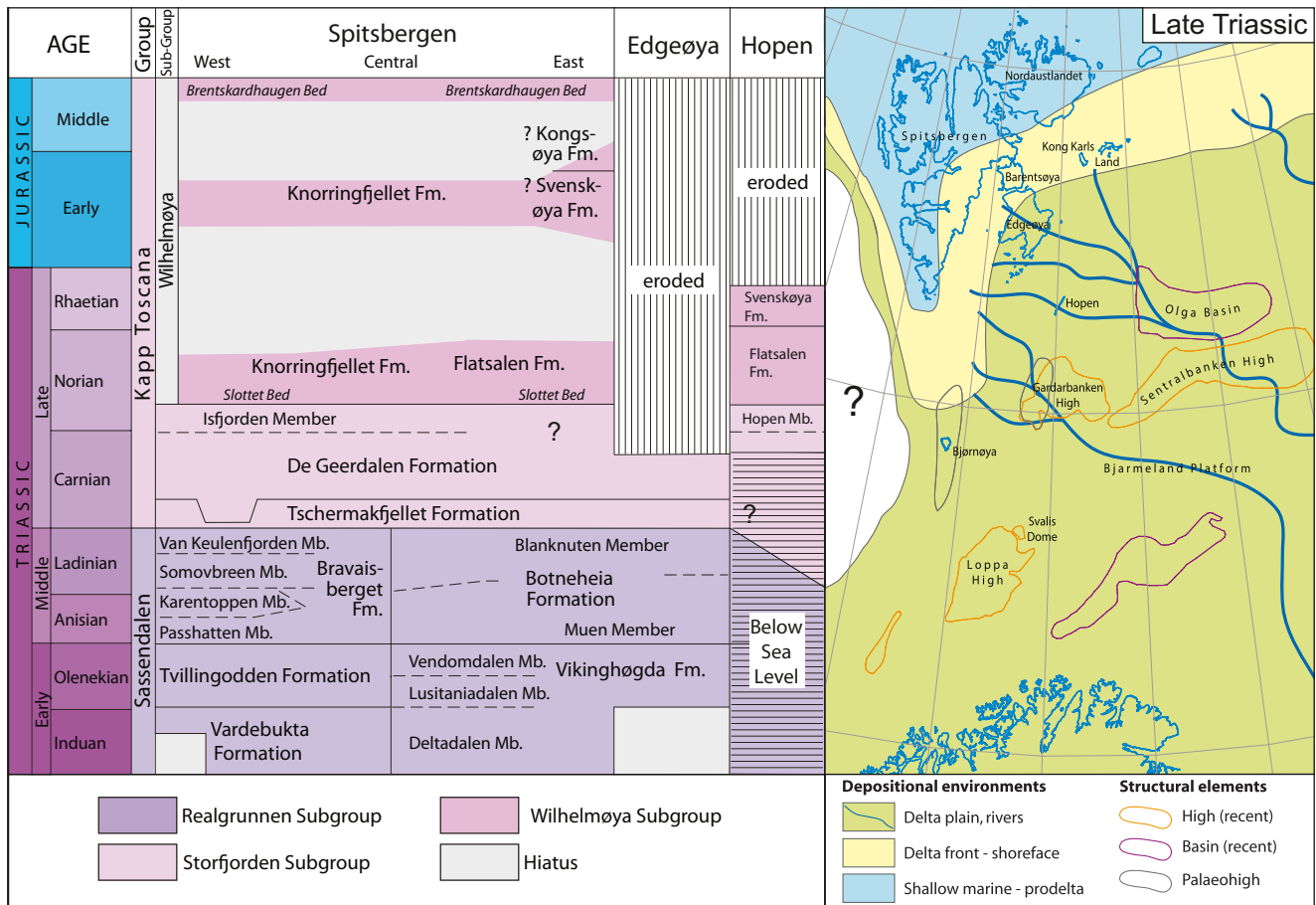


Figure 2. Stratigraphic chart over Svalbard after Mørk et al. (2013) and palaeogeographic map of the Late Triassic after Lundschieen et al. (2014).

Edgeøya or Barentsøya. The Triassic strata of the eastern islands represent a proximal position within this delta system, relative to central Spitsbergen. The observation of extensive channel bodies within the strata of Hopen fits well with the regional Triassic development (Klausen and Mørk, 2014; Riis et al., 2008; Rød et al., 2014).

## Channel Types and Architecture

Rivers and channels are a major pathways of sediment routing through a terrestrial environment and their nature can be considered complex (Collinson, 1996). Here we provide a simple overview of channel types seen in the rock record and the ways in which they can be interpreted in outcrop.

Ancient channels are generally classified with regards to their internal architectures (Collinson, 1996; Gibling, 2006; Miall, 1988, 1996, 2013). As no vertical sequence is diagnostic of any specific channel type, their architecture and geometry become major facets in determining the channel facies (Miall, 1985).

The description of channel sand body geometries is based primarily on the visual characteristics observed

from photo mosaics and measured in the 3D model. Channel sand bodies can be seen to range in size and shape considerably and thus an overview of the terminology used for describing both sandstone channel bodies is presented in Figure 3. Individual sandstone channel bodies can be described as forming several distinctive geometrical shapes, being symmetrical, asymmetrical and lenticular. These become complex within channel systems involving multiple channels, where they can become multilateral, stacked or are seen to form laterally extensive sheets.

Channel forms and architecture can range from simple individual sandstone channels to multilateral channels or stacked channel systems. Individual channels can represent small systems with little or no avulsion. Multilateral / laterally accreting channels generally represent the lateral migration of a channel due to erosion on the outside of a bend and deposition on the inside. This often results in the presence of heterolithic channel bodies with notable accretion surfaces (Collinson, 1996). Stacked channel systems represent the repeated activation of a watercourse over time showing evidence of a primary sediment pathway where numerous rivers repeatedly erode into earlier underlying channels.

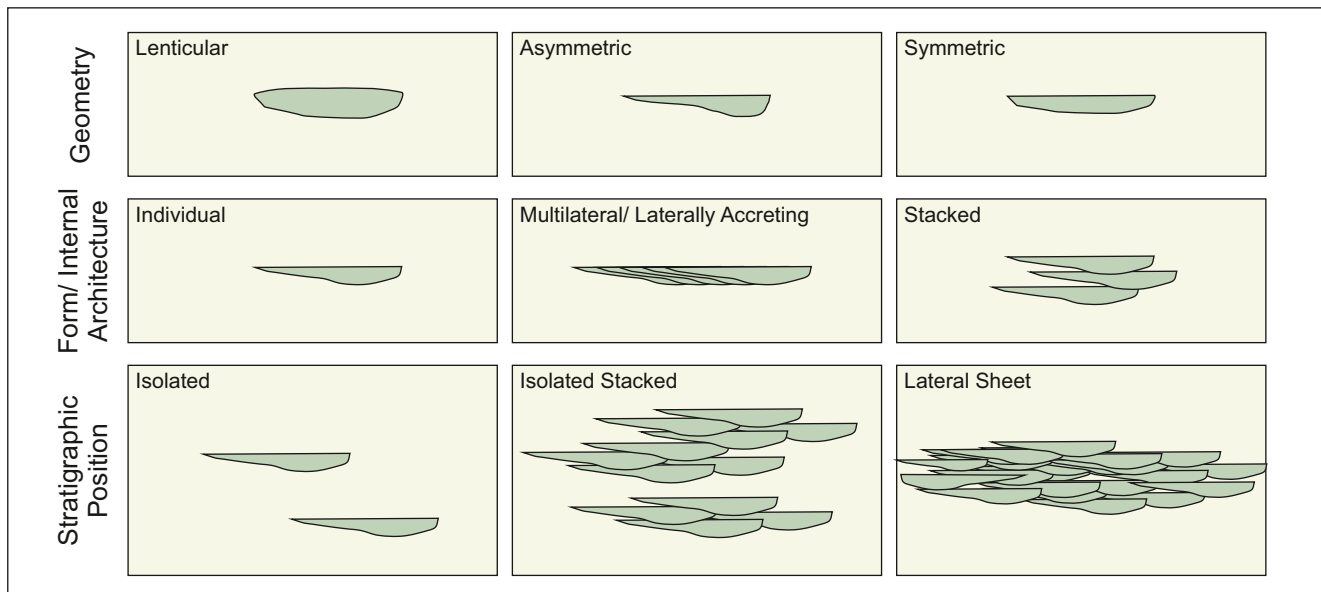


Figure 3. Simple overview figure showing channel geometry and forms for ancient channel nomenclature after Collinson (1996).

Channels can be isolated within the stratigraphy or be amalgamated into systems representing a major watercourse, sediment routing pathway. These amalgamated systems can themselves be isolated within floodplain deposits or form widespread lateral sheet sands composed of multiple channel systems that spread over a wide area.

## Methodology

### PhotoModeler™ 3D Geological Model

A 3D geological model of the island has been produced utilising PhotoModeler™ software from EOS Systems (Solvi, 2013). The model applies a large database of high resolution digital photographs to make a 3D visualisation of the island, overlying a digital elevation model (provided by the Norwegian Polar Institute). This model can be manipulated and used to interpret the islands geological characteristics.

The method of constructing the model uses a series of photographs taken with a high resolution camera, using 85 mm or 300 mm lenses. In total 4900 photographs of the island have been used. Visual interpretation of these images was used to document the occurrence and distribution of channel bodies throughout the De Geerdalen Formation.

These photographs are then used in panoramic combinations within the PhotoModeler™ program, where known points are selected to reference their locations to a digital elevation model. The addition of aerial photographs of the island, provided by the Norwegian

Polar Institute, allowed for a greater level of detail and accurate geometrical measurements of the geology to be made. Formation thicknesses have been calibrated based on stratigraphical log data recorded in the field and height reference points measured by GPS, to ensure feature are accurately represented in the model.

The criteria for the identification of channel bodies, observed within the geological model, rely on the identification of features evidently formed by an erosive process. Vertically incising and laterally constrained features that are seen within the model are interpreted as channel bodies, with the addition of evidence from their internal architectures.

### Field Studies

Conventional field studies form the bulk of the geological understanding of Hopen. Sections are provided by the *Hopen Geology Project* and have been drawn by small team operating throughout the island over relatively short periods of time; herein we integrate these sections.

Those channels that have been logged and their sedimentary structures analysed to determine their facies association are displayed in Figure 4. Field studies are used to assist the interpretation of channels that have not been directly observed in the field. Understanding of channels seen within the geological model is based on observed channel architecture and geometry, whilst the nature of the depositional environment is inferred by extrapolating the stratigraphical level of the channel laterally towards logged sections.

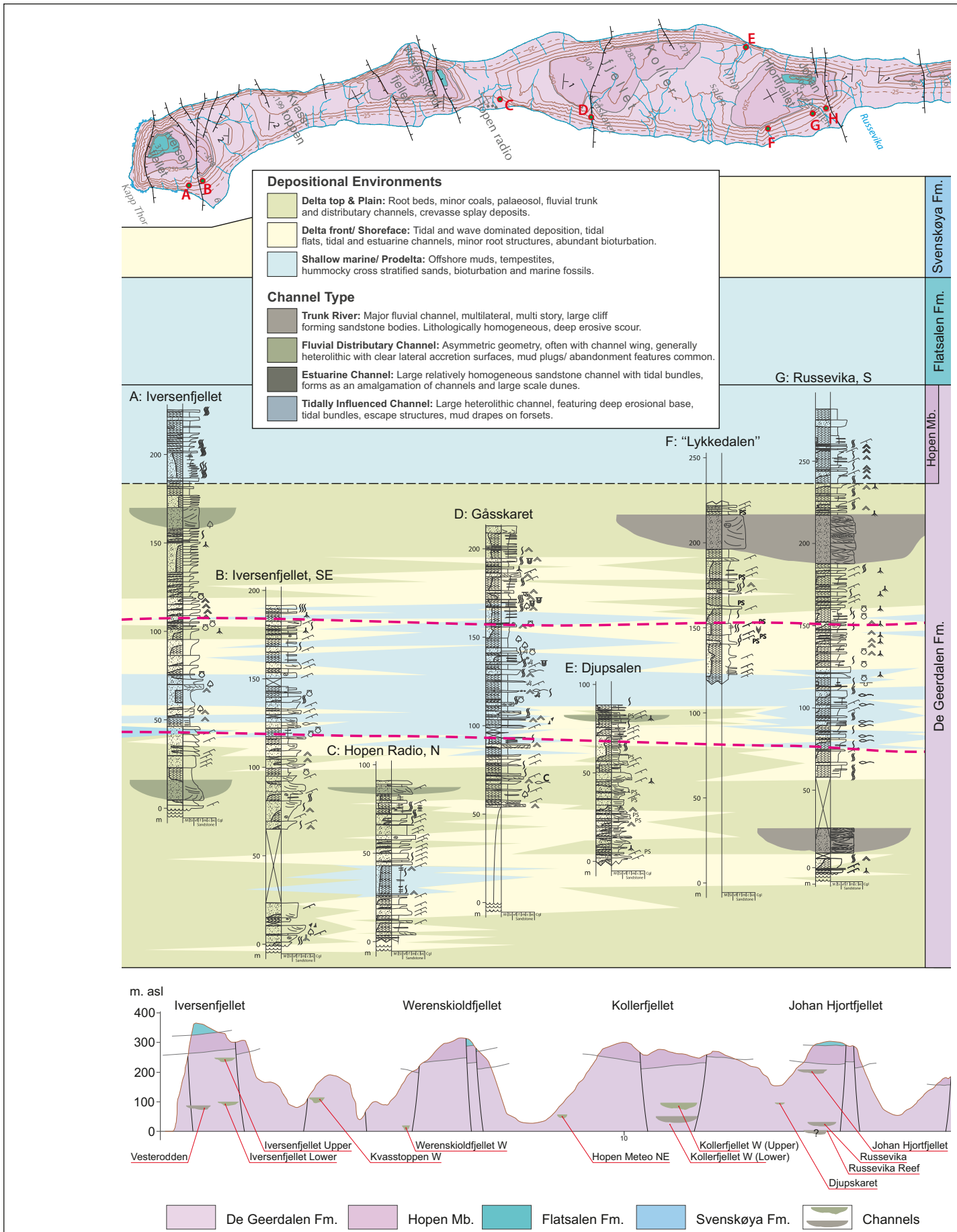
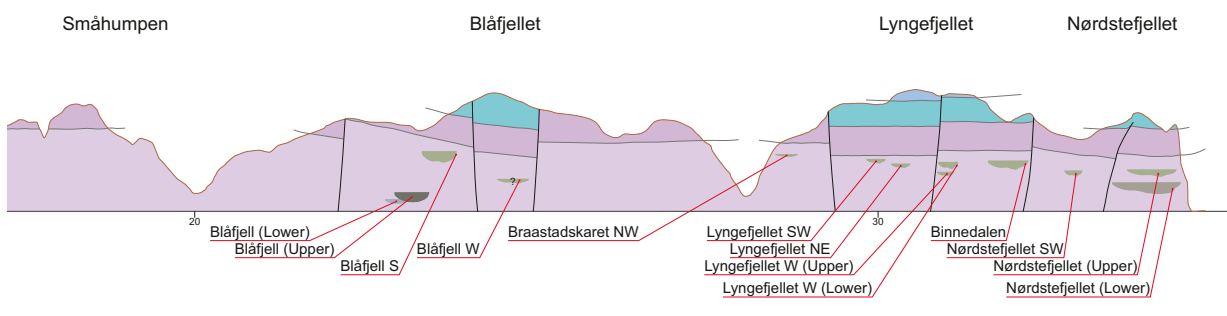
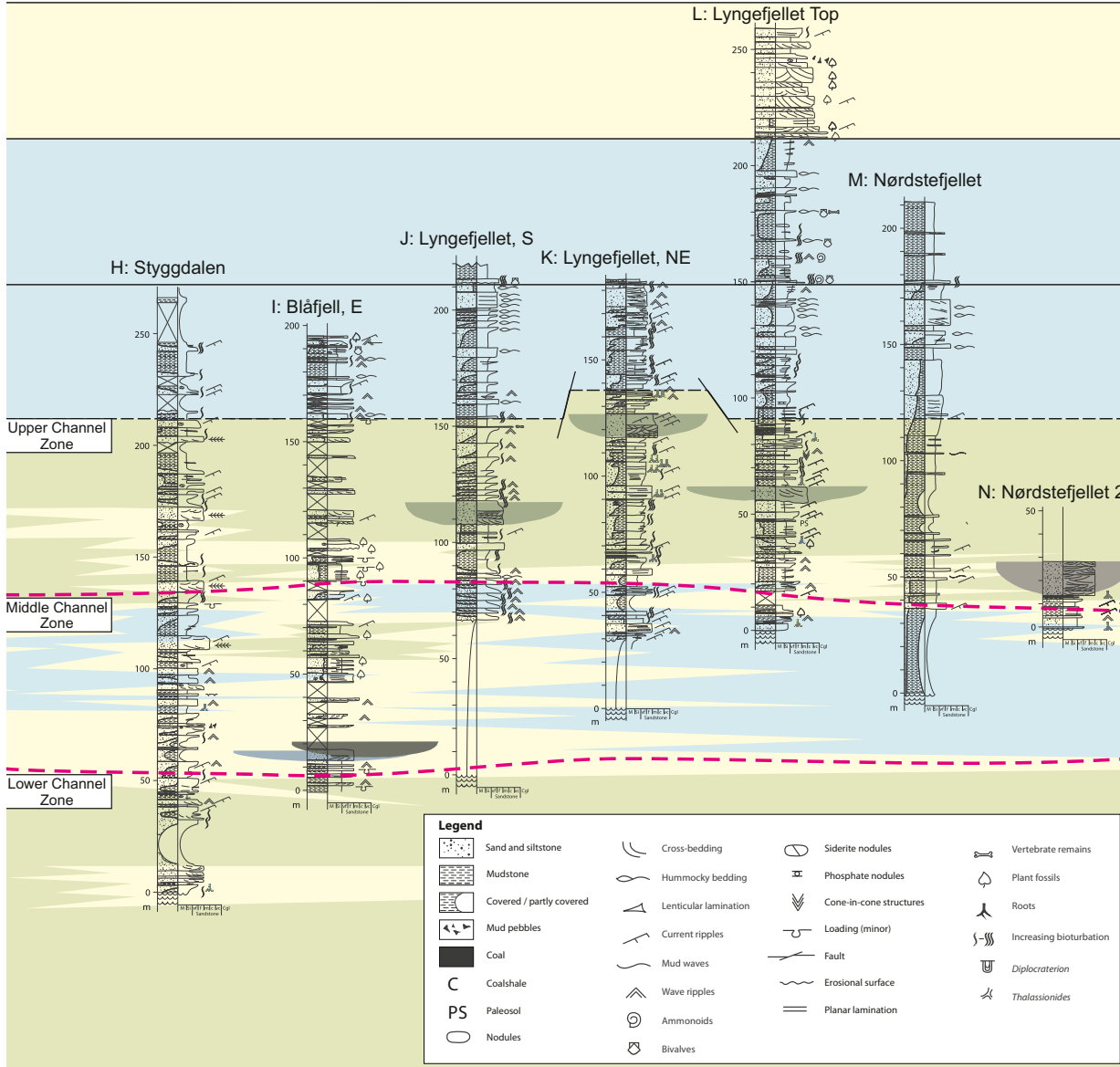
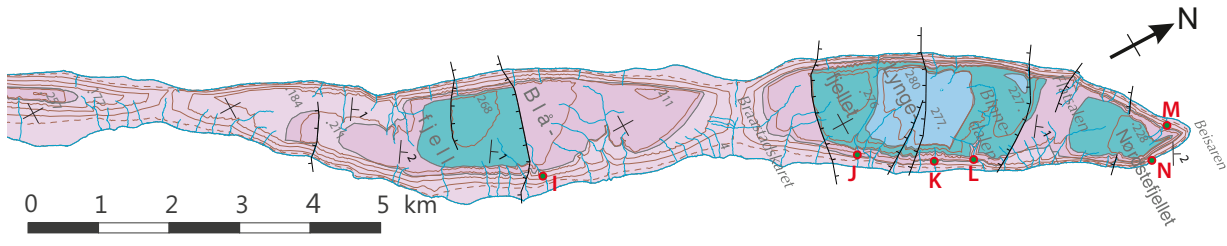


Figure 4. Overview of stratigraphical logs from Hopen, locations are marked on the map and stratigraphy is flattened at the base of the Hopen Member. Logged channels are highlighted and a simplified interpretation of depositional environment is given. Each channel zone is denoted





based on the depositional environments and the position of all channels identified is shown in the cross section. Logs are provided by the Hopen Geology Project with map, cross section and facies after Mørk et al. (2013).

## Channels and the Stratigraphy

Throughout the stratigraphy channel sandstone bodies can be arranged into a relatively discrete stratigraphy (Solvi, 2013; Klausen and Mørk, 2014), herein we provide greater evidence for this trend and discuss the type of channels found at the varying stratigraphical intervals. When flattening the stratigraphy of the island in relation to the Slottet Bed and also the recently defined Hopen Member, to avoid disruption by faulting (Mørk et al., 2013; Lord et al., 2014); the stratigraphical relationships and the lateral extent of depositional environments can be seen (Fig. 4).

25 channel bodies have been identified on the island of which 12 have also been directly observed in the field. Those that have not been directly observed in the field have been identified within the 3D model and their nature is determined based on their visual characteristics. Here, we explain the basis for classifying the different channels and where they are located in the stratigraphy. Table 1 presents a complete overview of channel characteristics, geometries and architectures. These are ordered into three defined stratigraphical intervals and channels are ordered in relation to their stratigraphic position below the Hopen Member. These stratigraphic intervals are defined as the lower, middle and upper channel zones as shown in the correlation on Figure 4.

In most instances channel features are seen to scour into underlying, soft, highly heterolithic sediments and feature a lateral pinch out. Based on the observations presented in Table 1, three primary channel types are interpreted. Fluvial channels are observed and assist the definition of overall depositional environments for various stratigraphic intervals. Fluvial, tidally influenced fluvial and estuarine channels are also observed and defined based upon their internal channel heterogeneity and sedimentological characteristics. Fluvial channels are the most abundant and are seen to vary in facies type, with trunk rivers, distributary channels and individual channels often displaying abandonment features.

Strata of the De Geerdalen Formation, initially deposited within a shallow marine environment or prodelta environment (See legend in Fig. 4), are comprised of highly heterolithic beds formed in several marine facies types. These include: Sediments deposited in a low energy environment, consisting of fine grained mud and silt, with fine laminae containing distal storm beds host to minor hummocky cross-stratification. In addition bioturbated thin sandstones and shales often seen in conjunction with abundant wave ripple structures are common within this facies. This depositional environment also incorporates the uppermost unit of the De Geerdalen Formation, the Hopen Member, which represents a widespread flooding surface visible throughout the island (Mørk et al., 2013; Lord et al., 2014).

Some sections of Hopen's stratigraphy is interpreted to represent tidally dominated sedimentation within a delta front environment and here sediments are seen to be richer in sand, featuring abundances of bioturbation and hummocky cross-stratified sands (Fig. 4). Heterolithic packages of shale interspersed with minor cross stratified sand beds are present suggesting a greater influence of wave and tidal re-working of sediments. Minor root structures are present within this facies association and are interpreted as a tidal marsh environment.

The delta top setting present within the De Geerdalen Formation is evident based on the presence of notable root beds, minor coal beds and an abundance of plant fragments (Launis et al., 2014). Dominant facies within this environment are crevasse splay deposits, floodplain deposits of non-marine mud and shale, and minor root beds alongside palaeosol horizons.

### The Upper Channel Zone

#### Fluvial Channels in the Upper Zone

At the SW cliff section of Lyngfjellet (Fig. 5A) some 4 m from the base of the Hopen Member a channel body with a thickness of 8 m and a lateral extent of 240 m is observed in the 3D geological model. The sandstone comprising this feature is laterally extensive for 90 m, whilst the pinch outs appear to consist of finer grained sediments. This channels architecture reveals that the NE pinch out is represented by a channel wing, whilst lateral accretion surfaces are present. This channel is interpreted as being a fluvial distributary channel.

On NE Lyngfjellet a channel body has been observed in the field and is shown in log K: Lyngfjellet NE (Fig. 4) and Figure 5B. This laterally extensive channel sandstone is 11 m in thickness and of unknown width, featuring trough cross stratified medium to coarse grained sand, upwards fining to current rippled fine sand. The log does not suggest any evidence for a stacked channel complex or, this having a multilateral architecture. However, the sandstone is capped by a succession of fines that coarsen upwards and include root horizons, probably representing abandonment features. This channel is interpreted as being a major fluvial channel, most probably a distributary although a trunk channel cannot be ruled out.

18 m below the base of the Hopen Member, on the mountain of Johan Hjortfjellet lays a 28-32 m thick sandstone body, measuring approximately 950 m in width (Fig. 5C). Its exact lateral extent is undetermined due to its northern pinch out (when observed from the eastern side of the island) being very discrete. This channel has been logged in its entirety, log G: Russevika, S which shows the fine to medium grained sandstone channel eroding into soft underlying shales. Its internal architecture is dominated by large scale trough-cross

**Table 1.** An overview of the individual channels observed on Hopen including geometries, characteristics and interpretation. Channels are ordered by their stratigraphical position in relation to the base of the Hopen Member. Three zones are evident.

Channel Location	Fig.	Position below Hopen Member	Width / Thickness	Notes	Channel Type
Upper Channel Zone					
Lyngefjellet SW	5A	4 m	240 m / 8 m	Asymmetrical channel scour with channel wing, features lateral accretion surfaces terminating at the base of the channel. Visual characteristics suggest relatively homogeneous composition.	Fluvial Distributary Channel
Lyngefjellet NE	5B	10 m	Undetermined / 11 m	Trough cross-stratified medium/ coarse grained sandstone fining up wards to medium grained current rippled sandstone.	Fluvial Distributary Channel of potential Trunk River
Johan Hjortfjellet	5C	18 m	c. 600 m / 32 m	Single storey channel, with an erosive base and lithological homogeneity, featuring large scale trough cross stratification.	Trunk River (after Klausen & Mørk 2014)
Binnedalen	5D	24 m	Undetermined / 7-15 m	Prominent trough and cross trough bedding, mud clasts line the base of troughs. Gentle upwards fining observed into current rippled sandstone with rootlets.	Fluvial Distributary Channel
Braastadskaret NW	5E	25 m	100 m / 7 m	Amalgamated, multi lateral channel body with laterally accreting beds, channel wing and potential mud plug.	Fluvial Distributary Channel
Blåfjell	5F	c. 28 m	325-475 m / 13-19 m	Heterolithic composition with near symmetrical geometry. Laterally accreting beds present. No channel wing or evidence for mud plug. Features sand lenses.	Fluvial Distributary Channel
Lyngefjellet W (Upper)	5G	29 m	210 m / 11 m	Single storey, medium grained channel sandstone. Featuring an erosive base, extensive cross stratification with the uppermost fining to massive fine sand. Notable lateral accretion surfaces present with potential mud plug.	Fluvial Distributary Channel
Iversenfjellet (Upper)	-	29 m	Undetermined / 12 m	Trough and planar cross stratified sandstone with plant fragments. Fining upwards to small upwards coarsening deposits, representing lateral accretion beds.	Fluvial Distributary Channel
Nordstefjellet (Upper)	5H	30 m	Undetermined / 10-15 m	Appears at similar stratigraphical level to the channel body in Binnedalen.	Fluvial Distributary Channel
Nordstefjellet SW	-	42 m	200 m / 15 m	Symmetrical body. No notable internal structures, geometry is highly lenticular with a concave base and top. Bending of overlying beds suggests a component of differential compaction.	Major Fluvial Channel (Possible Trunk River)
Lyngefjellet W (Lower)	5I	50 m	145 m / 6 m	Heterolithic composition with accretion surfaces and mud plug, asymmetric geometry and isolated in the stratigraphy.	Fluvial Distributary Channel
Kvasstoppen W	5J	50 m	Undetermined / 30 m	Scouring sandstone body, truncated by fault however shows evidence for feint lateral accretion surfaces suggesting multilateral channel architecture with relative lithological homogeneity.	Fluvial Distributary Channel
Nordstefjellet (Lower)	5K	60 m	1000 m / 36 m	Multilateral channel sandstone, laterally accreting surfaces, with an erosive base and lithological homogeneity. Minor trough cross stratification is observed, but is not prominent.	Trunk River (after Klausen & Mørk 2014)
Blåfjell W	5L	Undetermined	Undetermined	Asymmetrical geometry with notable channel wing. Laterally accreting beds terminating at the base of channel scour, heterolithic composition with a mud plug.	Fluvial Distributary Channel
Middle Channel Zone					
Kollerfjellet W (Upper)	5M	130 m	815 m / 25 m	Prominent cliff forming sandstone, deep scour and lenticular geometry, possible upwards fining trend with lateral accretion surfaces evident.	Fluvial Channel (with potential marine influence)
Djupskaret	-	135 m	150 m / 5 m	Lateral accretion surfaces are prevalent consisting clearly of lighter coloured sediments within finer grained (darker) material. Indication for possible mud plug.	Fluvial Distributary Channel
Blåfjell E (Upper)	5N	c. 140 m	415 m / 30 m	Amalgamated channel bodies, tidal bundles.	Estuarine Channel
Blåfjell E (Lower)	5N	145 m	100 m / 7 m	Erosional base, mud drapes, wave ripples and large scale trough-cross stratification.	Tidally Influenced Fluvial channel
Lower Channel Zone					
Iversenfjellet (Lower)	-	178 m	Undetermined / 15 m	Thick trough and planar cross bedded medium grained sandstone, fining upwards.	Fluvial Distributary Channel
Kollerfjellet W (Lower)	5O	179 m	915 m / 20 m	Highly vegetated, fractured and weathered exposure. Potential multilateral channel system with lateral accretion surfaces evident.	Trunk River
Vesterodden	5P	183 m	Undetermined / 15 m	Notable cliff forming sandstone, no apparent internal architecture, however a potential mud-plug is observed.	Trunk River
Werenskioldfjellet W	5Q	190 m	210 m / 22 m	Erosional scour, no obvious internal structures due to extensive fracturing and weathering of this exposure.	Fluvial Distributary Channel
Hopen Meteo NE	5R	200 m	232 m / 15 m	Asymmetrical geometry. Deep scour and mud plug, potentially stacked channel with some minor lateral accretion surfaces present.	Fluvial Distributary Channel
Russevika	5S	200 m	Undetermined / 13 m	Symmetrical channel geometry. Trough and cross stratified bedding within channel sandstone suggesting multilateral architecture. Deposited atop terrestrial sediments with coal and root beds.	Potential Trunk River Channel
Russevika Reef	5T	230 m	c. 150 m / unknown	Cross stratified medium grained sandstone with large tree fossils. Cutting into heterolithic sediments.	Potential Trunk River Channel



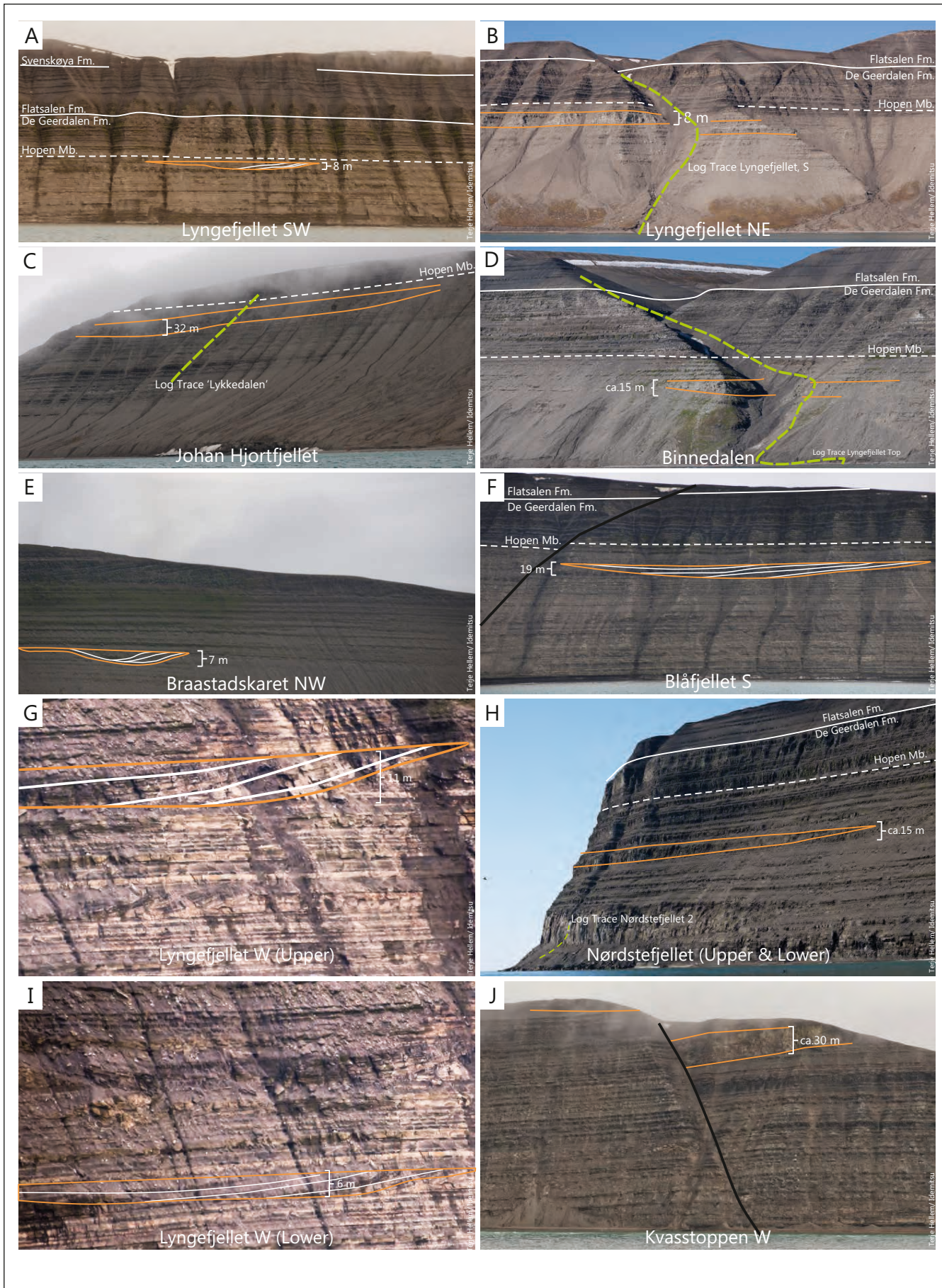
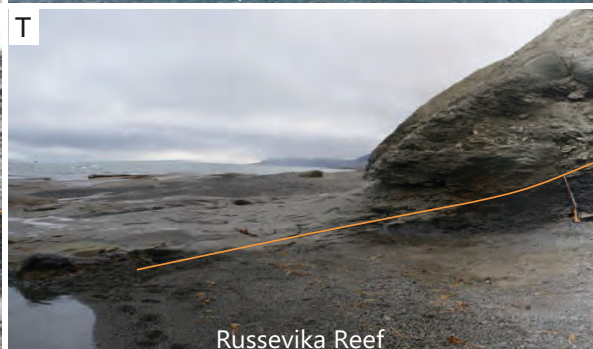
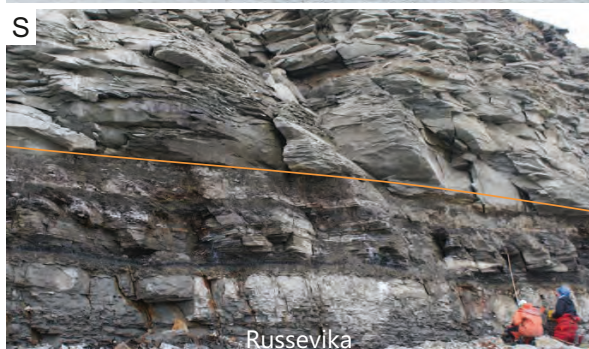
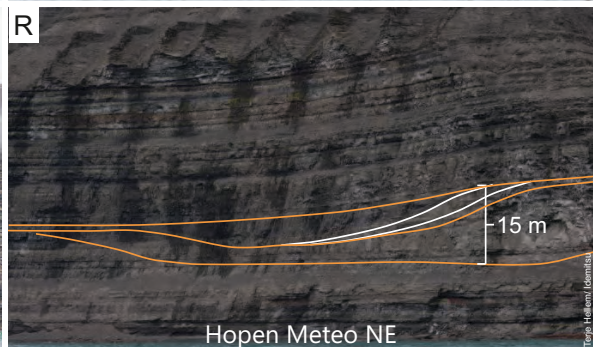
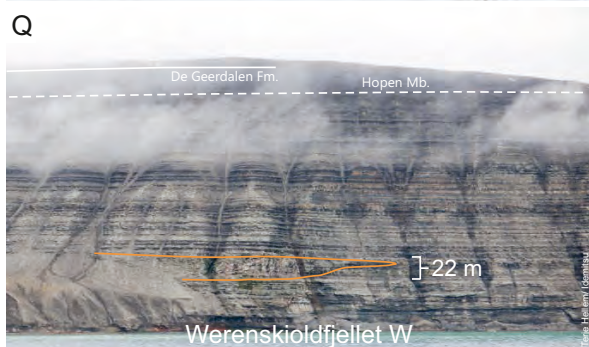
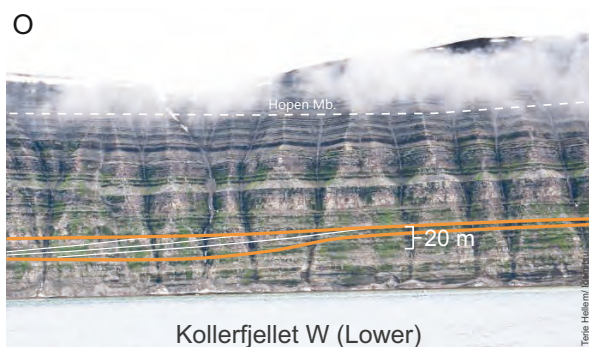
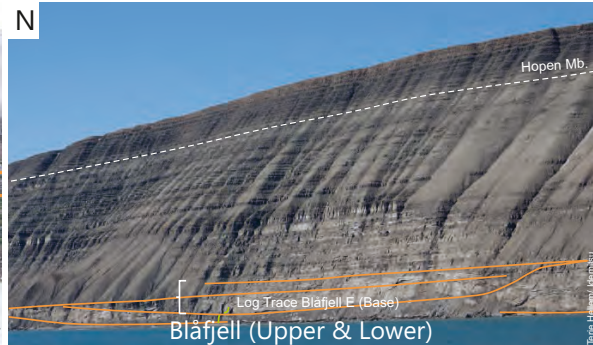
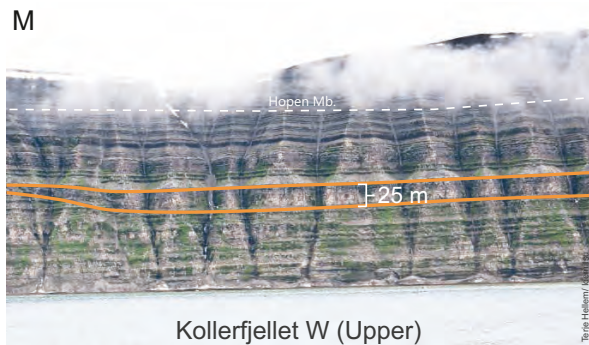
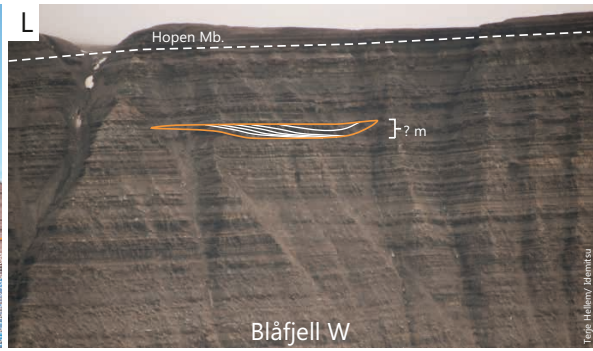
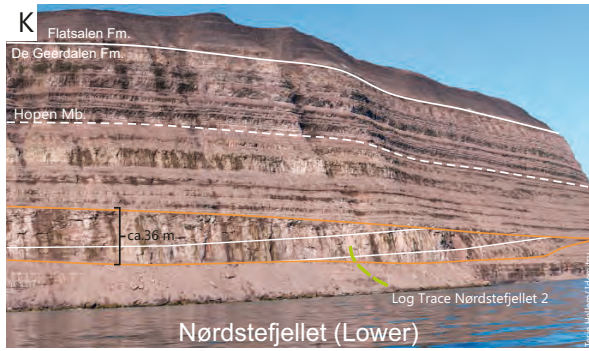


Figure 5 A-T. Images of channel bodies observed on Hopen. Photos relate to those indicated in Table 1 and channel positions are marked on the map in Figure 1. See text for detailed explanation of channels.





stratification. Due to this channels exposure being at a higher position in the stratigraphy, foresets of these troughs have formed a weathering surface and de-lamination is prominent. This inherently adds difficulty in the observation of larger structures due to the highly irregular expression of this sandstone and thus no lateral accretion surfaces are observed, nor evidence for this channel being component to a stacked complex. This channel body represents a large trunk river channel, following the interpretation of Klausen and Mørk (2014). This is based on the large channel geometry, its lateral extent and despite no visual evidence for lateral accretion surfaces, the log shows that the body is comprised of multiple packages trough cross and planar cross bedded sandstones, suggesting a component of lateral migration.

The sandstone channel body seen within the valley of Binnedalen in the northern end of Hopen is laterally discontinuous; 7 m in thickness and featuring a clear erosional scour (Fig. 5D). The width is undetermined as scree inhibits lateral tracing of this channel body. The sandstone lies 24 m below the base of the Hopen Member within heterolithic, laminated shale and thin sandstones. Beds below the base of this body consist of siltstones, with minor root beds and loading structures. The internal architecture of the sandstone shows pronounced large scale trough cross bedding with an abundance of rip up mud clasts and organic material observed at the base of the troughs. Internal bed packages show a tendency for gentle fining upwards and the uppermost parts of these are dominated by uni-directional current ripples. The channel is topped by a minor upwards fining package of sand to silt, featuring coalified root structures and desiccation cracks. These characteristics suggest a delta top environment in a fluvial dominated system. The channel lack marine or tidal influence and the internal architecture of the sandstone, suggest that this channel body represents a fluvial distributary channel.

On the western cliff section, on the NW flank of Braastadskaret (Braastadskaret NW, Fig. 5E), a channel scour is seen to erode into the underlying strata some 25 m below the base of the Hopen Member. Measurements indicate that this feature is 7 m thick and 100 m wide. The internal architecture of this channel is seen to display a series of laterally accreting, dipping bedding planes that terminate at the base of the scour. This channel may represent a laterally accreting body similar to several others observed on the island. In addition, interpretation from the model suggests the channels features a mud plug suggesting that the dipping beds may represent a migrating point bar within the bend of a fluvial distributary channel, which has then been abandoned.

On Blåfjell a channel scour estimated at approximately 13-19 m thick and 325 – 475 m in width is observed at approximately 28 m below the base of the Hopen Member (Blåfjell, S Fig. 5F). The internal architecture of this channel scour is dominated by a series of gently

dipping sandstone beds intermittently dispersed with finer grained material, suggesting that this channel is multilateral in nature. Furthermore, observations made from the model show evidence for sand lenses within the scour and there is also potential for this channel being part of a stacked channel complex, with a younger channel scouring into an older channel body at the same stratigraphical interval. This is interpreted as representing a fluvial distributary channel, showing evidence of abandonment with potential reactivation of the watercourse at a later time.

The uppermost channel on the western coastline of Lyngefjellet (Lyngefjellet W, Upper) is situated approximately 29 m below the base of the Hopen Member and its dimensions are 11 m in thickness and 210 m in lateral extent (Fig. 5G). The channel is present in the log taken at Lyngefjellet (J: Lyngefjellet, S), on the eastern side of Hopen. This channel features a scouring base into soft underlying sediments and its internal architecture is also well defined in the 3D geological model. A series of laterally dipping beds of medium grained sandstone can be seen. The presence of fine grained material suggests that this channel has undergone abandonment at some stage and subsequent filling by fine grained flood deposits. The sandier accretion packages were deposited by the migration of a point bar. This is interpreted as a fluvial distributary channel.

In the upper sections of Iversenfjellet in southern Hopen features a sandstone channel body of 12 m thickness and an undetermined width, lying 29 m below the Hopen Member. The channel is homogeneous, composed of medium grained sandstone featuring trough and planar cross bedding. The uppermost of this body is defined by minor upwards coarsening packages. This channel is interpreted as representing a fluvial distributary channel. At Nørdstefjellet, 30 m below the base of the Hopen Member a channel sandstone body is observed, (Nørdstefjellet Upper, Fig. 5H). This channel is not logged but does appear at a similar interval to that in Binnedalen and appears isolated within the surrounding strata. It is laterally extensive with no noticeable internal architecture. The thickness is determined to be some 10-15 m whilst the lateral extent is unknown. Given the relative homogeneity of this sandstone body, with no evidence for lateral accretion surfaces or obvious fines formed during abandonment, this channel is interpreted as being a fluvial distributary channel.

On the SW flank of Nørdstefjellet a laterally discontinuous, lenticular shaped sandstone channel body is observed to be down cutting some 8 m into underlying sediments. Stratigraphically, it occurs 42 m below the base of the Hopen Member at a similar interval to the fluvial channel observed in the coastal cliff section at NE Nørdstefjellet. The sandstone has a thickness of 15 m and a width of 200 m. This deep scour and symmetrical geometry suggest that this channel represents a major



watercourse, with no evidence for lateral migration being seen. The channel is interpreted as representing a major fluvial channel, possibly a trunk river.

The lowermost channel on the western coastline of Lyngfjellet (Lyngfjellet W, Lower) occurs some 50 m below the base of the Hopen Member and its geometry forms a laterally discontinuous scour, of 6 m in thickness and 145 m in lateral extent (Fig. 5I). The channel displays two prominent characteristics with regards to its internal architecture. First and foremost, a series of notable, sandy accretion surfaces are observed dipping laterally within the channel scour. Alongside, a series of fine grained sediments are observed. These are interpreted as the accreting planes of point bar deposits within a meandering river system, with fine grained sediments representing the ultimate abandonment of this channel and subsequent filling by sediments over time, suggesting this river is a fluvial distributary channel branching from a major watercourse.

On the western side of the mountain of Kvasstoppen (Kvasstoppen W) on southern Hopen, a 30 m thick sandstone body has been observed (Fig. 5J). Its lateral extent is undetermined due to fault displacement. Its position in the stratigraphy is 50 m below the Hopen Member. Despite Kvasstoppen not being capped by the Hopen Member, the position has been determined by laterally tracing prominent beds across the fault to Iversenfjellet. This places the body within delta plain sediments seen in the upper parts of the De Geerdalen Formation, beneath the Hopen Member. Although not logged, subtle bed packages are observed. Given its stratigraphical position, thickness and homogeneity, this sandstone might represent a fluvial, distributary channel deposit.

At Nørdstefjellet in the northern end of the island is a 36 m high and 1000 m wide sandstone body evident in the lower cliff section, shown in log N: Nørdstefjellet 2, (Fig. 5K). This single storey, multilateral channel body shows a clear lateral pinch out to fine grained sediments and a scour of some 17-20 m. It is present on both sides of the island as a notable cliff and is subject to minor oblique fault displacement. Within this channel body, the sandstone is relatively homogeneous with trough cross bedding surfaces being visible. The base is sharp, with an irregular contact into the underlying shale, which comprise minor, laterally discontinuous coals and coalified root structures. This channels stratigraphical position is determined to be approximately 60 m below the base of the Hopen Member. Given the multilateral nature, geometry and sheer size of this channel it is interpreted as representing a trunk river.

A channel scour is observed on the southern side of Blåfjell, named as Blåfjell, W (Fig. 5L). Within this scour, lateral accretion surfaces are observed in the 3D geological model, with a discontinuous layer of darker and presumably more mud rich deposits being evident.

The position in the stratigraphy and extrapolation of the level to nearby logs, suggest this channel lies within delta top sediments and therefore it may represent a minor, formerly meandering fluvial distributary channel, with a mud plug formed as a result of channel abandonment.

## The Middle Channel Zone

### Fluvial, Tidal and Estuarine Channels in the Middle Zone

The upper cliff section on the western side of Kollerfjellet (Kollerfjellet W Upper, Fig. 5M) is seen to enclose a laterally discontinuous cliff forming sandstone body. Its position in the stratigraphy is measured as being 179 m below the base of the Hopen Member. This channel is determined to be 20 m thick and with an estimated width of 915 m (which cannot be accurately determined due to faulting). The cliff section of the channel itself is seen to be highly vegetated and weathered, thus no internal characteristics can be observed. This channel is interpreted as being a fluvial channel, however given its stratigraphical position, the potential remains for this to represent a tidally dominated or estuarine channel.

Within the narrow and steep sided gully of Djupskaret, a 5 m thick and 150 m wide channel occurs at a stratigraphic level some 135 m below the base of the Hopen Member. A section slightly north of this is logged at Djupsalen (Log E: Djupsalen), where a minor component of this channel body has been observed at the same stratigraphic level. The logged strata display a clear palaeosol horizon with intermittent current ripple laminated sandstones and root structures. Within the De Geerdalen Formation at various locations throughout Svalbard, most noticeably on the eastern island Edgeøya, palaeosols are common and they are characterised by bleached zones (Miall, 2006). On Hopen, however, they are observed to primarily be thin oxidised beds often seen in conjunction with coal shale, minor coal beds and coalified roots. Palaeosols can also be defined as a common flood plain facies (Miall, 2006; Kraus and Aslan, 1993), which suggests that this channel is deposited within a delta plain environment. Analysis of the internal architecture shows evidence for lateral accretion surfaces, indicating the lateral migration of a point bar. The heterolithic composition shows evidence for a mud plug. The relatively small lateral extent and minor thickness of this body, alongside the associated facies, indicate that this channel is representative of a relatively minor fluvial distributary channel. Given the position in the stratigraphy which is dominated by marine influenced facies it is likely this channel was initially flowing in a very near shore environment, where major channel paths have branched into smaller systems.

Along the coastline at Blåfjell two channels are observed to form a stacked channel system, where one is seen to scour into one below as shown in Figure 5N. The uppermost channel forms a vertical cliff of 30 m

height, with an overall width of 415 m. This prominent sandstone body incising into the channel beneath it and its approximate stratigraphical position is c. 175 m below the base of the Hopen Member. The internal architecture of this channel body displays a series of prominent erosional scours along individual bed boundaries, which are observed to be of thicknesses between 3-5 m. They are interpreted as representing the amalgamation of small channels, with a minor lateral extent of some 10-15 m. This channel system has been logged (Blåfjell, E) and the upper part of this section reveals the presence of mud drapes along wave ripple crests, loading structures in the form of flame casts and Klausen and Mørk (2014) report the presence of tidal bundles within the lower packages of the channel body. This package is defined by Klausen and Mørk (2014) to be the deposits of an estuarine system where dune migration within a confined channel system represents scour and fill.

The lowermost channel of this stacked system and also this channel zone occurs some 180 m below the base of the Hopen Member and is seen to scour into underlying sediments. This channel body is 7 m thick and is documented in the stratigraphical log I: Blåfjell, E and in Figure 5N. The width is measured at some 100 m despite this channel being incised by an overlying channel body. The internal channel architectures, observed in the 3D geological model, shows that the channel contains a series of beds, where multiple erosional scours form their basal geometry. This can thus be considered as a stacked channel system, composed of minor stacked and amalgamated channels. Further information is provided from the sedimentological log Blåfjell, E where the lowest exposures of this channel have been logged along with the overlying channel body. The log shows a gentle upwards fining trend of fine to medium grained sandstone with an erosional base. Internal structures show the presence of large scale trough-cross stratification and mud-drapes. Mud drapes are common features in tidally influenced environments (Bhattacharya, 2006). Based on the presence of mud drapes, suggesting a bi-directional flow, this lower channel body is interpreted as being deposited within a tidally influenced environment and is defined as a tidal channel.

## The Lower Channel Zone

### Fluvial Channels in the Lower Zone

The basal sections of the mountain of Iversenfjellet in southern Hopen are seen to contain a sandstone channel body of 15 m thickness. The extent of this channel is undetermined due to extensive cover in the lower slopes of the mountain in this area. The channel consists of medium grained trough and planar cross bedded sandstone, seen to fine upwards into siltstone. This upwards fining trend suggests a slow abandonment of this channel. No evidence for a multilateral architecture is observed and no erosional surfaces are seen within the

channel itself. This channel is within a zone dominated by delta top sediments and is interpreted as representing a fluvial distributary channel.

The cliff section on the western side of Kollerfjellet is seen to enclose a laterally discontinuous cliff forming sandstone body (Table 1, Fig. 5O). Its position in the stratigraphy is measured as being 179 m below the base of the Hopen Member. This channel is determined to be 20 m thick and with an estimated width of 915 m. The cliff section of the channel itself is seen to be highly vegetated and weathered, thus no internal characteristics can be observed. This channel appears to have a homogeneous composition, its geometry and scale suggests it represents a very large channel system and is thus interpreted as representing a trunk river.

At the SE tip of Hopen, a prominent cliff forming sandstone is present in the section at Vesterodden, approximately 183 m below the base of the Hopen Member (Table 1, Fig. 5P). This channel has been subject to faulting thus its lateral extent is undetermined; its thickness is measured to be 15 m. No sedimentological logs cover this channel; however neighbouring strata show that this interval is dominated by fine grained sediments with current ripple lamination. The stratigraphical interval here also contains an upwards fining sandstone bed with an erosional base, interpreted in this case to be a crevasse splay. The channel body is interpreted to be a fluvial trunk river, within a delta top setting.

The western flank of Werenskioldfjellet, to the SW of the Hopen meteorological station contains a 22 m thick and 210 m wide channel sandstone body, clearly eroding into the underlying sediments (Fig. 5Q). The channel body is present in the stratigraphy approximately 190 m below the base of the Hopen Member and correlates well to the stratigraphical level of the log taken at Iversenfjellet SE (Fig. 4). Strata in this interval consist of fine grained sediments containing wave and current ripple laminations, along with minor bioturbation. No direct environment indicators are evident; however the presence of symmetrical wave ripples and the occurrence of bioturbation suggest that this channel has been deposited in an environment with close proximity to wave or potentially tidal influence, such as a lower delta plain environment. This channel is thus interpreted as representing fluvial distributary channel at a point in the delta system where rivers have branched or anastomosed into smaller channels.

To the NE of the Hopen meteorological station a channel scour is present in the stratigraphy, approximately 200 m below the base of the Hopen Member (Fig. 5R). Its dimensions are measured to be 15 m in thickness and 232 m in overall width, however, a potential pinch out laterally to the north cannot be determined due to the presence of a deeply incised gully. The internal

architecture as observed in the geological model shows the presence of an 8 m thick package of dark, fine grained sediments forming what is interpreted to be a mud plug. This channel was presented in Nystuen et al. (2008) although with no additional interpretation. No other prominent internal structures are noted. It is interpreted that this channel represents an abandoned fluvial distributary channel.

Sandstone channel bodies are also evident on the beach section at Russevika in central east Hopen, where a 13 m thick channel is observed to scour into soft underlying shales. Field observations show that this underlying stratum contains wave rippled siltstone with mud drapes, minor coals, root beds and small stream scours (see Figs. 5S and 6A-C). The channel consists entirely of sandstone, with large scale trough and cross-trough bedding present. Due to cover the full lateral extent is undetermined. The stratigraphical position of this channel body is 200 m below the base of the Hopen Member. The channel facies is representative of a fluvial channel with no evidence for any tidal influence being seen within the channel body itself; however wave ripples and bioturbation is seen in the underlying beds in addition to a minor coal bed and coalified root structures. The channel is interpreted to be a fluvial distributary channel based on the primarily heterogenic composition of the sand and lack of evidence for external environmental influences being present.

A further sandstone that is classified as fluvial in origin is observed to protrude from the island as a shallow, wave cut platform beneath the channel at Russevika (Fig. 5T), termed 'Russevika Reef' in Table 1. The exact geometries are unknown, yet it is laterally discontinuous in the order of ca. 75-100 m, and lithologically homogenic (when observed at low tide). This sandstone is considered to have similarity with those channels seen at Nørdstefjellet and Johan Hjortfjellet. It is suggested on this basis that this sandstone is almost certainly representative of a fluvial channel, possibly representing a trunk river. Furthermore, field observations show that this channel is seen to be transporting large trees (Fig. 6D), a feature also seen in the trunk river channel at Johan Hjortfjellet.

## Discussion

The nature of channel sandstone bodies on the island of Hopen can be interpreted as being indicative of three different depositional environments. Fluvial trunk river channels and fluvial distributary channels are seen to be present within delta top dominated sediments, whilst tidal and estuarine channels are seen within sediments dominated by a delta front environment. The geometry of these bodies and their architectures also vary in this regard. Fluvial trunk rivers are seen to be homogeneous in composition and form either lenticular or near symmetrical sandstone bodies, that typically feature a greater width to thickness ratio (Gibling, 2006). Fluvial

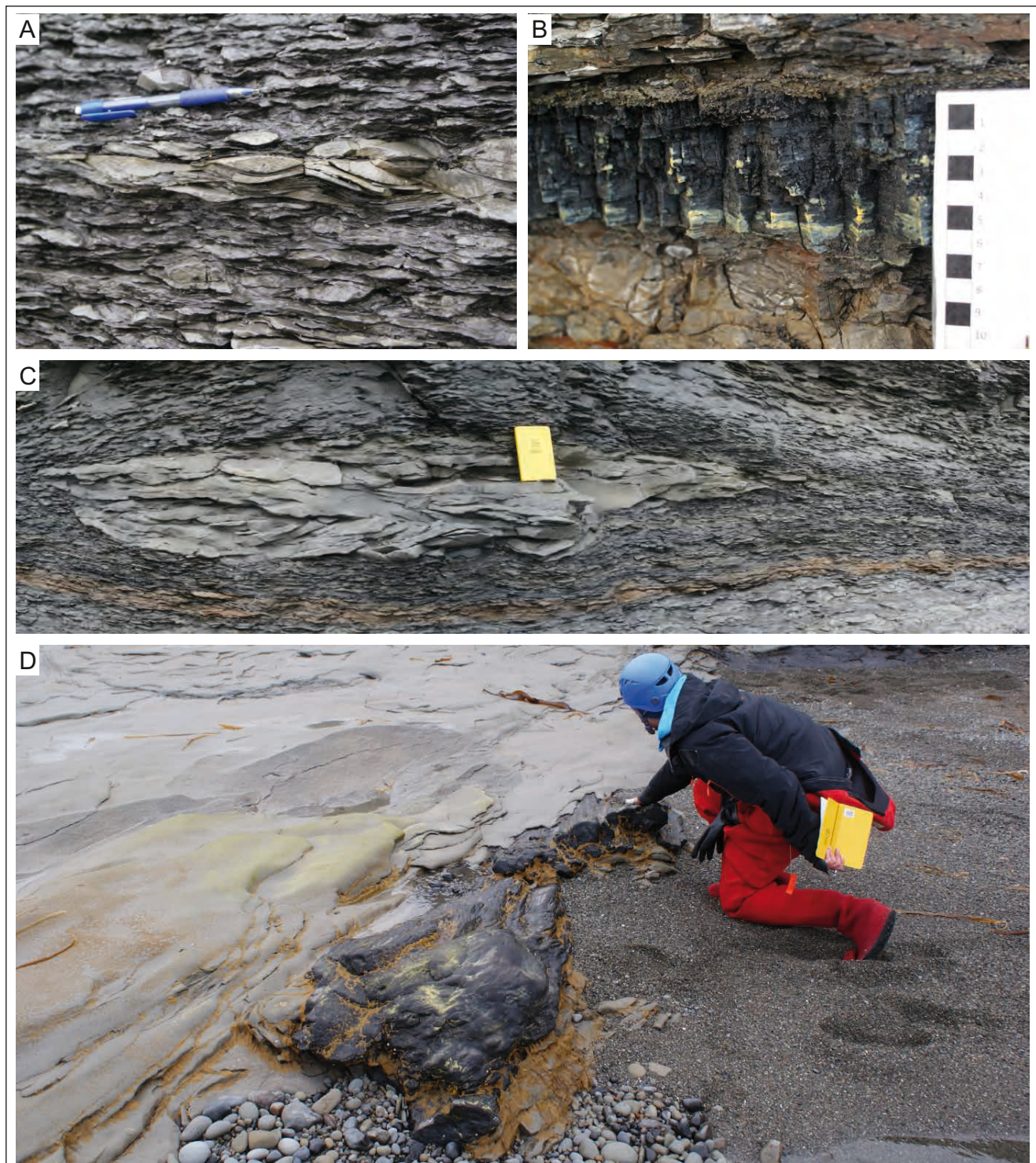
distributary channels are in comparison characterised by their asymmetric geometry. At some locations, such as those seen at Lyngfjellet SW, Braastadskaret NW or Blåfjell S (Figs. 5A, E, L) the potential for the presence of a channel wing is evident. This is observed by the noticeable thinning of the channel's form laterally away from the scour, however this has only been observed in photomosaics. Both types of fluvial channels are seen to be isolated within the stratigraphy and do not form stacked systems or lateral sheets (Fig. 3). Channels of both types however, show evidence for lateral accretion surfaces, with these being most evident in the heterolithic sediments seen in fluvial distributary channels.

Fluvial channels can be seen to represent both meandering rivers systems and also anastomosed systems, based on the presence of lateral accretion surfaces seen in distributary channels. Fluvial trunk channels are suggested to represent a moderate sinuosity, multi-channel system flowing through an area characterised by extensive vegetation with a large proportion of overbank deposits. A number of channels also display abandonment features, characterised by their overall heterolithic composition, internal architecture and evidence for abandonment based on the presence of mud plugs. This is most evident in the channels at Lyngfjellet SW, Braastadskaret NW and Blåfjell W (Figs. 5A, E, L). These channel features are suggested to have formed on or near the apex of a bend in a meandering river system. Meanders are eroded through leaving an oxbow lake or meander scar that is later in-filled with fine grained sediments, through lake like deposition (Collinson, 1996).

The lowermost exposures present on the island of Hopen are dominated by terrestrial floodplain sediments, in which 7 channels incising into heterolithic sediments have been identified. These channels are shown within the lower channel zone in Table 1, which corresponds to interval 1a of Klausen and Mørk (2014) and is determined to occur approximately 180-200 m below the Hopen Member. These channels are located at Hopen Meteo NE, Kollerfjellet W (Lower), Iversenfjellet (Lower), Vesterodden, Werenskioldfjellet W, Russevika and protruding out to sea at Russevika Reef (Fig. 4). Only the channels at Hopen Meteo NE and the two at Russevika have been observed in the field, the remainder are identified in the 3D geological model.

This lower zone is of unknown thickness, as the De Geerdalen Formation continues in the subsurface. The presence of the fluvial Russevika Reef channel coupled with the Iversenfjellet SE and Hopen Radio N logs in Figure 4 suggest that the interval remains predominantly within a delta-top to delta front environment continuing in the immediate subsurface. A minor marine incursion of unknown lateral extent is interpreted within this zone (as shown in Figure 4), however, channels in this lower zone are dominantly distributary channels.





**Figure 6.** A, Mud draped wave ripples seen in the tidally dominated delta front sediments below the channel at Russevika. B, Minor coal seam directly beneath the Russevika channel. C, Cross stratified micro channels seen in wave rippled, tidal sediments underlying the Russevika channel. D, Excellently preserved tree trunk trapped in the outer edge of the trunk river at Russevika Reef.

The strata dominating the middle section of the stratigraphy, between c. 70 and 180 m below the Hopen Member, is interpreted as being dominated by facies that display a marine influence. This ca. 100 m thick interval consists primarily of shallow marine and delta front facies associations. Here abundant bioturbation, wave ripples and

laterally discontinuous sandstone beds featuring hummocky cross-stratification are prevalent. This is a visually discrete interval and corresponds closely to interval 1b of Klausen and Mørk (2014). It is considered laterally extensive, spanning the entirety of the island; however, fault displacement and scree cover make facies correlation difficult.



The middle zone is also interspersed with minor occurrences of delta front and delta top facies as show in Figure 4. Here channels are interpreted to be influenced to a greater extent by marine processes, given the individual channel architecture, geometries and sediment characteristics. Two primarily marine channels are observed at Blåfjell, where a lower tidally dominated channel is present, which is seen to be subsequently eroded into by an estuarine channel system. The two remaining channels seen in the middle zone are deemed to be fluvial distributary channels. They feature internal characteristics inherent of a fluvial system and in the case of the channel at Djupskaret are in close relation to delta top sediments. Given their stratigraphical position, however, an aspect of marine influence cannot be ruled out, as this interval is dominated by marine processes, suggesting fluvial channels are a result of delta switch.

The uppermost strata of the De Geerdalen Formation on Hopen, below the Hopen Member, are interpreted as being dominated by delta top and delta plain sediments, with minor marine influenced intervals being present where delta front facies are observed. This is defined as the upper channel zone (Table 1) which corresponds to intervals 2b and 2c of Klausen and Mørk (2014). Within this zone a total of 14 fluvial channels are observed. Of these 14 channels, 6 have been logged and their depositional facies has been determined through direct observation whilst the remaining channels are interpreted with evidence from photographs and the 3D geological model.

The De Geerdalen Formation on Svalbard was reported as a shallow marine to fluvial succession by Buchan et al. (1965) and Mørk et al. (1982). Deltaic conditions were reported from Barentsøya and western Edgeøya (Knarud, 1980; Lock et al., 1978; Mørk et al., 1982) and fluvial to delta top with coal beds further east on Edgeøya (Lock et al., 1978). Sedimentological data from Hopen was not presented, but the general depositional conditions as reported on the other main Svalbard islands were assumed to continue also to Hopen. In the Barents Sea, the correlative Snadd Formation was also reported as shallow marine to deltaic, however it is more fluvial in nature, especially in its upper part and this is noted by many authors (e.g. Høy and Lundschieen, 2011; Klausen and Mørk, 2014; Riis et al., 2008; Glørstad-Clark et al., 2010).

The abundant presence of channels, within the De Geerdalen Formation on Hopen was first reported by Mørk et al. (2013) and these channels was compared with channels detected by seismic methods in the southern Barents Sea in the Snadd Formation by Klausen and Mørk (2014). Observations supported by shallow drilling data in the northern Barents Sea (Lundschieen et al., 2014) show that this area was covered by extensive paralic deposits from mainland Norway through to Hopen. Authors interpreting seismic data demonstrated that

during the Carnian four seismic sequences, up to 400 m thick, were progressing across the Barents Sea and passed Hopen in the uppermost sequence (e.g. Lundschieen et al., 2014). The Hopen exposures thus display the nature of these prograding sequences with its arrangement of different channel belts.

The exposed Hopen succession as a whole is younger than the section at Edgeøya (Riis et al., 2008; Lord et al., 2014; Lundschieen et al., 2014) and together they give a view of the total Late Triassic succession on the eastern Svalbard Islands. Hopen provides excellent exposures along a near perpendicular plane to the major palaeoflow direction of rivers during the Carnian. Klausen and Mørk (2014) show a clear trend of channels seen in seismic migrating to the W and NW. The perpendicular aspect of the island to this palaeoflow and the steep sections allow for excellent studies to be made. On Edgeøya, outcrops are generally oblique to the orientation of channels and thus their abundance may be under reported as their presence is not evident as with channels seen on Hopen.

On Spitsbergen; the Triassic succession is mostly complete (Buchan et al., 1965; Mørk et al., 1982, 1999), although the uppermost part (Wilhelmøya Subgroup) is quite condensed, especially in the central and western areas. Detailed facies studies by Rød et al. (2014) demonstrate that the paralic nature of the De Geerdalen Formations extends from Edgeøya into central Spitsbergen. Delta front sediment is, however, more abundant in these areas than distinct channels as seen on Hopen.

In comparison to the wider extent of the De Geerdalen Formation in Svalbard, the facies seen at Hopen is comparable to that on Edgeøya, despite being younger in age. Rød et al. (2014) document a paralic environment in the upper parts of the De Geerdalen Formation seen in western Edgeøya. A significantly greater extent of delta front and shore face facies is observed in central Spitsbergen with an inherently greater abundance of inter-distributary facies. In addition, a greater tidal influence is seen within distributary channels in Spitsbergen. Rød et al. (2014) report mud drapes and herringbone structures in distributary channels found in Spitsbergen, while distributary channels on Edgeøya lack diagnostic features that suggest any tidal influence (Rød et al., 2014) has been overprinted by a stronger fluvial signal.

The Triassic of western Spitsbergen cannot be correlated directly with the units of eastern Svalbard due to a different development of these sediments. This shows a clear regressive development of a paralic environment into the latter part of the Triassic, both on Spitsbergen, Edgeøya and Hopen. The depositional environment seen on Hopen represents the most regressive stage of this development seen in Svalbard, but similar to observations in cores from the Northern Barents Sea (Lundschieen et

al., 2014), and seismic data in the southern Barents Sea (Klausen and Mørk, 2014).

The offshore development of the Late Triassic is also well documented by Klausen and Mørk (2014), who present the De Geerdalen Formation at Hopen as an analogue to the Triassic Snadd Formation in the subsurface. The clear evidence for the development of meandering river systems in the Carnian (Klausen and Mørk, 2014) provides good evidence for a regressive deltaic system at this time. Hopen features sandstone channel bodies, of similar scale to those observed in the Barents Sea Snadd Formation and thus provides a good analogue to the Late-Triassic in the Barents Sea. Palaeoflow indicators also suggest a primarily westwards direction, with a provenance source to the east (Mørk, 1999; Rød et al., 2014) consistent with the trend of deltaic progradation seen in seismic (Høy and Lundschieen, 2011; Riis et al., 2008; Glørstad-Clark et al., 2010).

The creation of the Hopen Member (Mørk et al., 2013; Lord et al., 2014) and its evident correlation to the Isfjorden Member in central Spitsbergen, displays one of the regional sequence stratigraphic intervals within the De Geerdalen Formation. The gentle onset of a transgression, shown by the development of marine influenced strata overlying the paralic sediment, further highlights the fact that the sediments in the De Geerdalen Formation at Hopen are the youngest and most regressive stage of this Carnian deltaic system.

## Conclusions

25 sandstone channel bodies are observed on the island of Hopen. Stratigraphical positioning of channels show they form discrete intervals, dominated by a particular depositional style. The channels are dispersed throughout the stratigraphy and are numerous in the upper part of the De Geerdalen Formation, below the Hopen Member. Channels observed lower in the succession are less frequent and estuarine and tidal influence is observed for some of these channels.

Channels are isolated within the stratigraphy, forming individual bodies or multilateral/ stacked systems. Internal architecture and heterogeneities of channels vary considerably; from massive or highly cross-stratified, laterally accreting sandstone bodies deposited within a terrestrial fluvial environment, to more heterolithic stacked channel systems indicative of a tidally influenced system.

The upper channel zone occurs at 0-60 m below the base of the Hopen Member, the middle channel zone occurs 130-145 m, whilst the lower channel zone occurs 180-200 m. These zones are interpreted as representing a fluctuating sea level, inherent within a paralic environment (Klausen and Mørk 2014; Riis et al., 2008;

Glørstad-Clark et al., 2010; Lundschieen et al., 2014; Rød et al., 2014). The middle and upper zones together represent an overall shallowing upwards sequence, overlain by the Hopen Member.

The presence of trunk river and distributary channels on Hopen indicates a fluvially influenced setting, for the De Geerdalen Formation in this region. This is in contrast to central Spitsbergen where a stronger tidal signal is observed (Rød et al., 2014) and Edgeøya where diagnostic tidal features are sparse. In eastern Svalbard a paralic depositional environment is evident in the upper part of the succession (Lundschieen et al., 2014; Rød et al., 2014). This allows for a composite of the stratigraphy of these locations to give a strong indication of the overall nature of the Triassic succession in the northern Barents Sea.

The depositional environment for the De Geerdalen Formation on Hopen is a fluvial dominated and tidally influenced delta plain, given the highly heterolithic nature of sediments and rapid fluctuations between terrestrial and marginal marine facies. The De Geerdalen Formation is present throughout Svalbard, becoming increasingly distal towards the NW. This gradual development is controlled by the W and NW direction of delta progradation as defined by Riis et al. (2008), Høy and Lundschieen (2011), Glørstad-Clark et al. (2010) and Lundschieen et al. (2014).

### Acknowledgements.

Geologists from SINTEF Petroleum Research, NTNU, UNIS, UiB, NPD, NPI and supporting companies have participated in fieldwork and excursions. Terje Hellem is responsible for the collection of photographs provided for use in the PhotoModeler™ Geological Model. Thanks are extended to the reviewers Evy Glørstad-Clark and Erik P. Johannessen for their valued input and Rita Sande Rød for thoughtful advice.

## References

- Bhattacharya, J.P. 2006: Deltas. In Posamentier, H.G., & Walker, R.G. (eds.): *Facies models revisited, Society of Sedimentary Geology, Special publication, 84*, 237-292.
- Buchan, S.H., Challinor, A., Harland, W.B & Parker, J.R. 1965: The Triassic stratigraphy of Svalbard: *Norsk Polarinstitutt Skrifter, 135*, 92 pp.
- Collinson, J.D., 1996: Alluvial sediments. In Reading, H.G. (ed.): *Sedimentary environments: Processes, Facies and Stratigraphy*. Blackwell Publishing, 5-57.
- Doré, A.G. 1995: Barents Sea Geology, Petroleum Resources and Economic Potential. *Arctic, 48*, 3, 207-221.
- Flood, B., Nagy, J. & Winsnes, T.S. 1971: The Triassic succession of Barentsøya, Edgeøya and Hopen (Svalbard). *Norsk Polarinstitutt Meddelelser, 100*, 20 pp.
- Gibling, M.R. 2006: Width and thickness of fluvial channel bodies and valley fills in the geological record: A literature compilation and classification. *Journal of Sedimentary Research, 76*, 731-770.
- Glørstad-Clark, E., Faleide, J.I., Lundschieen, B.A. & Nystuen, J.P. 2010: Triassic seismic sequence stratigraphy and paleogeography of the western Barents Sea area. *Marine and Petroleum Geology, 27*, 1448-1475.



- Grogan, P., Østvedt-Ghazi, A.-M., Larssen, G.B., Fotland, B., Nyberg, K., Dahlgren, S. & Eidvin, T. 1999: Structural elements and petroleum geology of the Norwegian Sector of the Barents Sea. In Fleet, A.J. & Boldy, S.A.R. (eds.): *Petroleum Geology of Northern Europe, Proceedings of the 5<sup>th</sup> Conference*, 247-259.
- Høy, T. & Lundschieen, B.A. 2011: Triassic deltaic sequences in the northern Barents Sea. In Spencer A.M., Embry, A F., Gautier, D.L., Stopakova, A.V. & Sørensen, K. (eds.): *Arctic Petroleum Geology. Geological Society, London, Memoirs*, 35, 249-260.
- Johansen, S.E., Ostisty, B.K., Birkeland, Ø., Fedorovsky, Y.F., Martirosjan, V.N., Brunn Christensen, O., Cheredeev, S.I., Ignatenko, E.A. & Margulis, L.S. 1993: Hydrocarbon potential in the Barents Sea region: Play distribution and potential. In Vorren, T.O. et al. (eds.): *Arctic Geology and Petroleum Potential, NPF Special Publication no. 2*, Elsevier Scientific Publications, 273-320.
- Klausen, T. G., & Mørk, A. 2014: The Upper Triassic paralic deposits of the De Geerdalen Formation on Hopen: Outcrop analog to the subsurface Snadd Formation in the Barents Sea. *American Association of Petroleum Geologists Bulletin*, 98, 1911-1941, doi:10.1306/02191413064.
- Knarud, R. 1980: *En sedimentologisk og diagenetisk undersøkelse av Kapp Toscana Formasjonens sedimenter på Svalbard*. Cand. Real thesis, University of Oslo, 208 pp.
- Korčinskaya, M.V. 1980: Early Norian Fauna of the Archipelago of Svalbard. In Geologiya osadochnogo chekhla arhipelaga Svalbard (*Geology of the Sedimentary Cover of the Archipelago of Svalbard*), Leningrad: NIIGA, 30-43.
- Kraus, M.J. & Aslan, A. 1993: Eocene hydromorphic paleosols; Significance for interpreting ancient floodplain processes. *Journal of Sedimentary Petrology*, 63, 453-463.
- Launis, A., Pott, C. & Mørk, A. 2014: A glimpse into the Carnian: Late Triassic plant fossils from Hopen, Svalbard. *Norwegian Petroleum Directorate Bulletin*, 11, 129-136.
- Lock B.E., Pickton C.A.G., Smith D.G., Batten D.J. & Harland W.B. 1978: The geology of Edgeøya and Barentsøya, Svalbard. *Norsk Polarinstittutt Skrifter*, 168, 64 pp.
- Lord, G.S. Solvi, K.H., Ask, M., Mørk, A., Hounslow, M.W. & Paterson, N.W. 2014: The Hopen Member: A new lithostratigraphic unit on Hopen and equivalent to the Isfjorden Member of Spitsbergen. *Norwegian Petroleum Directorate Bulletin*, 11, 81-96.
- Lundschieen, B.A., Høy, T. & Mørk, A. 2014. Triassic hydrocarbon potential in the Northern Barents Sea; integrating Svalbard and stratigraphic core data. *Norwegian Petroleum Directorate Bulletin*, 11, 3-20.
- Miall, A.D. 1985: Architectural-element analysis; a new method of facies analysis applied to fluvial deposits. *Earth Sciences Review*, 22, 261-308.
- Miall, A.D. 1988: Reservoir heterogeneities in fluvial sandstones; lessons from outcrop studies. *American Association of Petroleum Geologists Bulletin*, 12, 682-697.
- Miall, A.D. 1996: *The geology of fluvial deposits*. Springer-Verlag, New York, 582 pp.
- Miall, A.D. 2006: *The Geology of Fluvial Deposits: Sedimentary Facies, Basin Analysis and Petroleum Geology*. 4<sup>th</sup> Corrected Printing, Berlin, 582 pp.
- Miall, A.D. 2013: *Fluvial Depositional Systems*, Springer Geology, Springer International Publishing Switzerland 2013, 316 pp.
- Mørk, A., Knarud, R. & Worsley, D. 1982: Depositional and diagenetic environments of the Triassic and Lower Jurassic succession of Svalbard. In Embry A.F. & Balkwill, H.R. (eds.): *Arctic Geology and Geophysics, Canadian Society of Petroleum Geologists Memoir*, 8, 371-398.
- Mørk, A., Dallmann, W.K., Dypvik, H., Johannessen, E.P., Larssen, G.B., Nagy, J., Nøttvedt, A., Olaussen, S., Pčelina, T.M. & Worsley, D. 1999: Mesozoic Lithostratigraphy. In Dallmann, W.K. (ed.): *Lithostratigraphic Lexicon of Svalbard, Upper Palaeozoic to Quaternary Bedrock – Review and recommendations for nomenclature use*. Norwegian Polar Institute, Tromsø.
- Mørk, A., Lord, G.S., Solvi, K.H. & Dallmann, W.K. 2013: *Geological Map of Svalbard 1:100 000, sheet G14G Hopen. Norsk Polarinstittutt Temakart No. 50*.
- Mørk, M.B.E. 1999: Compositional variations and provenance of Triassic Sandstones from the Barents Shelf. *Journal of Sedimentary Research*, 69, 690-710.
- Nystuen, J.P., Mørk, A., Müller, R. & Nøttvedt, A. 2008: From desert to floodplain – from land to sea. In Ramberg, L., Solli, A. & Nordgulen, Ø. (eds.): *The Making of Land: Geology of Norway*, The Geological Society of Norway, Trondheim, 328-353.
- Pózer Bue, E. & Andresen, A. 2013: Constraining depositional models in the Barents Sea region using detrital zircon U-Pb data from Mesozoic sediments in Svalbard. *Geological Society Special Publication*, 386, 261- 279.
- Puchkov, V.N. 2009: The evolution of the Uralian orogeny. *Geological Society, London, Special Publications*, 327, 161-195.
- Pčelina, T.M. 1972: Concerning the age of sedimentary strata on Hopen. In Sokolov, V.N. & Vasilevskaya, N.D. (eds.): *Mesozoic deposits in Svalbard*. Leningrad, 75-81.
- Riis, F., Lundschieen, B.A., Høy, T., Mørk, A & Mørk, M.B.E. 2008: Evolution of the Triassic shelf in the northern Barents Sea region. *Polar Research*, 27, 318-338.
- Rød, R.S., Hynne, I.B. & Mørk, A. 2014: Depositional environment of the Upper Triassic De Geerdalen Formation – An E-W transect from Edgeøya to Central Spitsbergen, Svalbard. *Norwegian Petroleum Directorate Bulletin*, 11, 21-40.
- Smith, D.G., Harland, W.B. & Hughes, N.F. 1975: Geology of Hopen, Svalbard. *Geological Magazine*, 112, 1-23.
- Solvi, K.H. 2013: *Visualize and interpret the geometry, heterogeneity and lateral continuation of channel bodies in the De Geerdalen Formation at Hopen*. Master Thesis, Norwegian University of Science and Technology, 122 pp.
- Tozer, E.T., & Parker, J.R. 1968: Notes on the Triassic biostratigraphy of Svalbard. *Geological Magazine*, 105, 526-542.
- Vigran, J.O., Mangerud, G., Mørk, A., Worsley, D. & Hochuli, P.A. 2014: Palynology and geology of the Triassic succession of Svalbard and the Barents Sea. *Geological Survey of Norway Special Publication*, 14, 270 pp.
- Worsley, D. 2008: The post-Caledonian development of Svalbard and the western Barents Sea. *Polar Research*, 27, 298-317.



# Styles of normal faulting and fault-controlled sedimentation in the Triassic deposits of Eastern Svalbard

Per Terje Osmundsen<sup>1,2</sup>, Alvar Braathen<sup>2,3</sup>, Rita Sande Rød<sup>2,4,5</sup>  
& Ingrid Bjørnerheim Hynne<sup>2,4</sup>

<sup>1</sup> Geological Survey of Norway, N-7491 Trondheim, Norway, e-mail: per.osmundsen@ngu.no

<sup>2</sup> University Centre in Svalbard (UNIS), N-9171 Longyearbyen, Norway.

<sup>3</sup> Department of Geoscience, University of Oslo, N-0316 Oslo, Norway;

<sup>4</sup> Norwegian University of Science and Technology, N-7491 Trondheim, Norway.

<sup>5</sup> Norwegian Petroleum Directorate, N-4003 Stavanger.

In the eastern Svalbard archipelago, two main types of E-W and NW-SE trending normal faults are exposed in the Upper Triassic, prodelta Tschermakfjellet and paralic/deltaic De Geerdalen formations. One is clearly syndepositional, confined to the Tschermakfjellet and lower parts of the De Geerdalen formations and associated with substantial fault-block rotation and fault-related sedimentation patterns. The other appears to be post-sedimentary with respect to the De Geerdalen Formation. At two key localities in Eastern Svalbard, the De Geerdalen Formation can be subdivided into a growth-faulted lower part and a more gentler dipping, much less faulted upper part, respectively, separated by an unconformity and by units that filled and draped the remnant topography. Above this level, the upper parts of the De Geerdalen Formation consists of interbedded shales and sandstones, shown elsewhere to represent fluvial channel, bar and tidal deposits. Below the unconformity, structural styles include 2-3 generations of moderately dipping, planar and listric faults with syn-sedimentary displacements that range between metres and tens of metres. The dominating syn-sedimentary fault set dips towards the south and southwest. A number of faults detach in the underlying Tschermakfjellet or Botneheia formations.

At Kvalpynten on southern Edgeøya, structural and stratigraphic relationships indicate at least two stages of syndepositional faulting, with listric and more planar faults causing rotation of bedding, erosion of fault crests and deposition of complex sand units in half-graben basins. Inside the basins, sediment transport and distribution, and thus resultant sedimentary architecture, was controlled by the normal faults. Based on photographic analysis and field observations, composite sandstone units in the half-graben can be subdivided into building-blocks that consist of distinct sandbody types. These show different relationships to the bounding faults and to underlying strata, most likely related to variable rates of accommodation creation and sediment supply along the syndepositional faults. The underlying cause of faulting may tentatively be the collapse of a local, southwards prograding delta that competed with the more regional, northwestwards prograding one. Another, perhaps more likely explanation would be the collapse of parts of the regional delta front that had an anomalous orientation. However, the consistent fault orientations over many kilometers and the systematic repetition of sedimentary architectures over several half-graben basins lead us to suggest that faulting was influenced by a tectonic stress field.

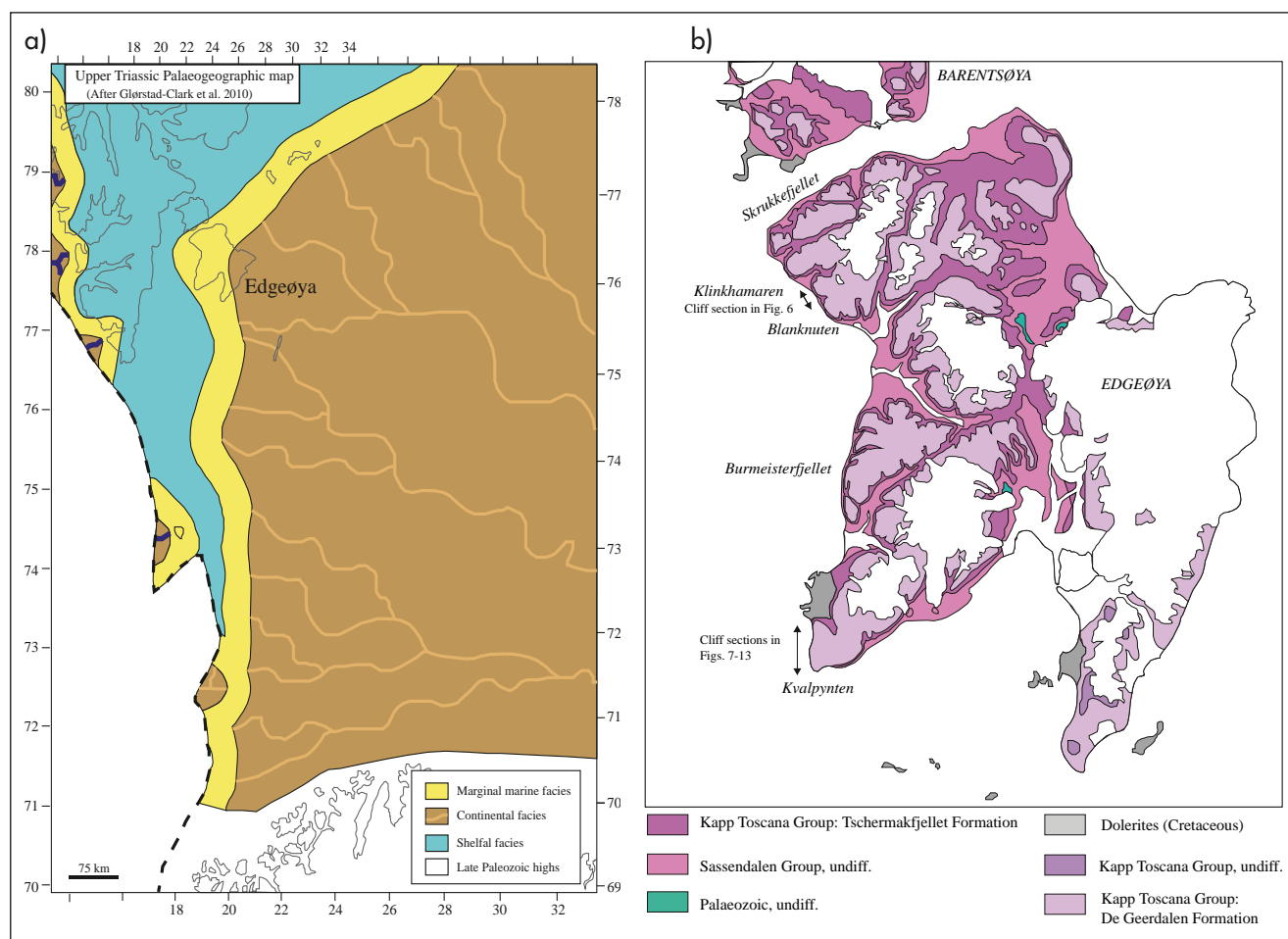
**Key words:** Svalbard, Triassic, Edgeøya, Fault-controlled sedimentation, Growth faults.

## Introduction

We present new structural and stratigraphic data that describe fault styles, kinematics and half-graben filling patterns associated with reservoir-scale faults that deform a Triassic paralic/deltaic succession in eastern Svalbard. The data were recorded during a field expedition to East Svalbard in the summer of 2009, with a

limit to the time spent on a number of outcrops. Interpretations of lithology and structure are based on photographic evidence and benchmark observations from a restricted number of localities. They should therefore be regarded as preliminary. Considerable further research potential resides in the several kilometers of excellent, but variably accessible exposures provided by the cliff faces of the study area.





**Fig. 1.**

a) Upper Triassic palaeogeographic map showing Triassic progradation over the western Barents Sea area.

b) Map of Edgeøya ([www.polarinstituttet.no/interactive\\_maps](http://www.polarinstituttet.no/interactive_maps)) with key localities described in this paper.

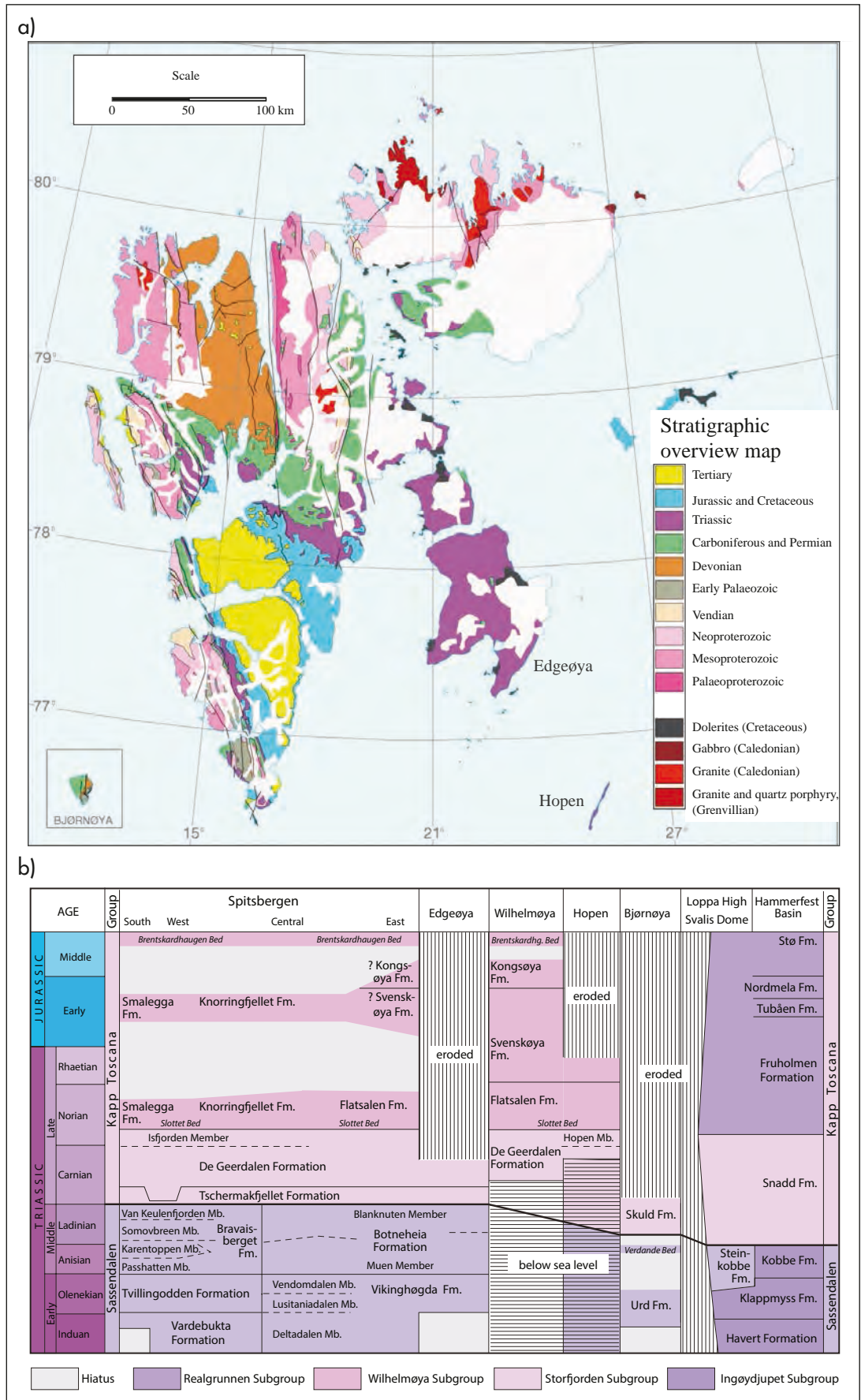
The Triassic period in the western Barents Sea was characterized by gradual progradation and infill from a main sediment source in the east, southeast, and south, as evidenced by northwestwards-dipping clinoforms recognized in seismic reflection data (Fig. 1a, e.g. Høy and Lundschieen 2011; Riis et al., 2008; Glørstad-Clark et al., 2010; Anell et al., 2014). Glørstad-Clark et al. (2010) interpreted the Triassic succession (Fig. 2) as divided into 5 second-order sequences separated by maximum flooding surfaces, in turn controlled by regional relative sea-level changes. In the Late Triassic, uplift changed to subsidence in areas such as the Loppa High, where a westerly sediment source became prominent (op. cit.). At this time, rifting commenced again between Norway and Greenland, and although local sediment sources were probably active, Greenland was likely a sediment source for parts of the Barents Sea area in the Late Triassic (Glørstad-Clark et al., 2010). Other parts were apparently still dominated by a steady sediment supply from the southeast, and palaeocurrent readings from eastern Svalbard (Hopen, Edgeøya, E. Spitsbergen) reported by Høy and Lundschieen (2011) support west- to northwest-directed palaeocurrents in parts of the Triassic in that area. Consistent with Edwards (1976), we argue that in

areas of syndepositional normal faulting, this pattern was more complicated than hitherto recognized, and that unresolved issues remain regarding the stratigraphy and structure of eastern Svalbard. Below, we aim to provide more data from this complex area.

### The De Geerdalen Formation

The deltaic Carnian to Early Norian De Geerdalen Formation is excellently exposed in a series of cliff exposures on Spitsbergen, Hopen and Edgeøya (Figs. 1, 2). The formation consists of paralic deposits, alternating fluvial and upper shoreface sandstones, heterolithic sandstone-shale successions and dark silty shales that overlie the prodelta shales of the Tschermafjellet Formation and the organic rich, marine shales of the Botneheia Formation (Mørk et al., 1982, 1999). The De Geerdalen Formation reaches thicknesses of up to c. 400 metres on Edgeøya, increasing towards Hopen where only the upper part is exposed (e.g. Mørk et al., 2013, Anell et al., in press). Sections in Spitsbergen are generally less thick, with the type section in De Geerdalen being 238 metres. Boreholes drilled for a CO<sub>2</sub> project in Longyearbyen do, however, offer thicknesses

**Fig. 2.**  
**a)** Geological overview map of Svalbard (Dallmann et al., 2002).  
**b)** Overview of the Triassic stratigraphy in Svalbard and the Barents Sea (From Mørk et al., 2013)



larger than 280 metres (Braathen et al., 2012). In large parts of the De Geerdalen Formation, fluvial and shallow

marine sand bodies occur as laterally persistent, trough- and planar cross-bedded and ripple laminated sandstone

sheets, variably capped by coal beds and encased in dark shales further described by Rød et al. (2014). Based on palaeocurrent readings, Høy and Lundschieen (2011) reported general west- and northwestwards flow directions in the De Geerdalen Formation in Hopen and eastern Spitsbergen, in accordance with the seismic evidence for northwesterly progradation over much of the western Barents Sea (op. cit. and Glørstad-Clark et al., 2010).

Based mainly on photographs of the cliff faces, an array of mainly south-facing normal faults in the De Geerdalen Formation on southern Edgeøya were interpreted as syndepositional 'growth faults' by Edwards (1976), and related to the collapse of a south-sloping delta front. More recent work has challenged this interpretation, based on the mapping of Triassic, northwest-prograding clinoforms over much of the western Barents Sea (Høy and Lundschieen, 2011). We focus in particular on the syn-sedimentary faults and basins and on the sedimentary architectures associated with them. Recent developments in our understanding of the Triassic regional geology of the Barents Sea (e.g. Worsley, 2008; Høy and Lundschieen, 2011; Riis et al., 2008; Glørstad-Clark et al., 2010; Anell et al., 2013), as well as of fault-controlled sedimentary architecture in rifts (e.g. Prosser, 1993; Ravnås and Steel, 1998; Gawthorpe and Leeder, 2000) and deltaic settings (Bhat-tarchaya and Davies, 2001; Garcia-Garcia et al., 2005) invite a re-investigation of this spectacular area.

## Styles of normal faulting

Faults that affect the Triassic succession in the study area are mainly E-W to NW-SE oriented and show normal separation. The faults are of two main types: 1) faults with dominating south- and southwest dips that control thickness variations and sedimentary architecture in half-graben basins in the lower parts of the De Geerdalen Formation and 2) steep, planar faults that do not appear to affect sedimentation in the De Geerdalen Formation. The latter display sharply defined, planar fault planes and thin fault cores, commonly constituted by centimeter to tens of centimeters thick fault gouge or shale gouge (Fig. 3), and cut high stratigraphic levels in the De Geerdalen Formation exposed at Hopen, (see stratigraphic correlation in Riis et al. 2008). Displacements are normally in the order of meters. At least one such fault appears to have affected deposition in the overlying Flat-salen Formation, in terms of an extensional fault monocline (Fig. 3). Below, we report observations of fault style, kinematics, and impact on the contemporaneous sedimentary system for a number of studied faults and fault arrays in the study area. We focus on the more detailed evidence for fault-controlled sedimentary architecture observed at Klinkhamaren and, in particular, at Kvalpynten on Edgeøya, where such features are particularly well exposed.

## Fault kinematics

Slickensided faults on Hopen and Edgeøya show that the faults are mainly normal, sometimes with a minor strike-slip component (e.g. Figs. 3, 4), and that they record N-S to NNE-SSW extension. Based on the dataset presented below, this kinematic pattern appears as associated with both the main types of faults; the kinematics of the planar faults do not appear as significantly different from those of faults that are demonstrably syndepositional (see below). One exception is a subhorizontal fault, associated with a metre-thick zone of shale gouge and a number of moderately dipping splay faults, found in southern Hopen (Fig. 3h). The most important faulting events are, however, restricted to the lower half of the exposed succession between the Botneheia Formation and the top of the De Geerdalen Formation.

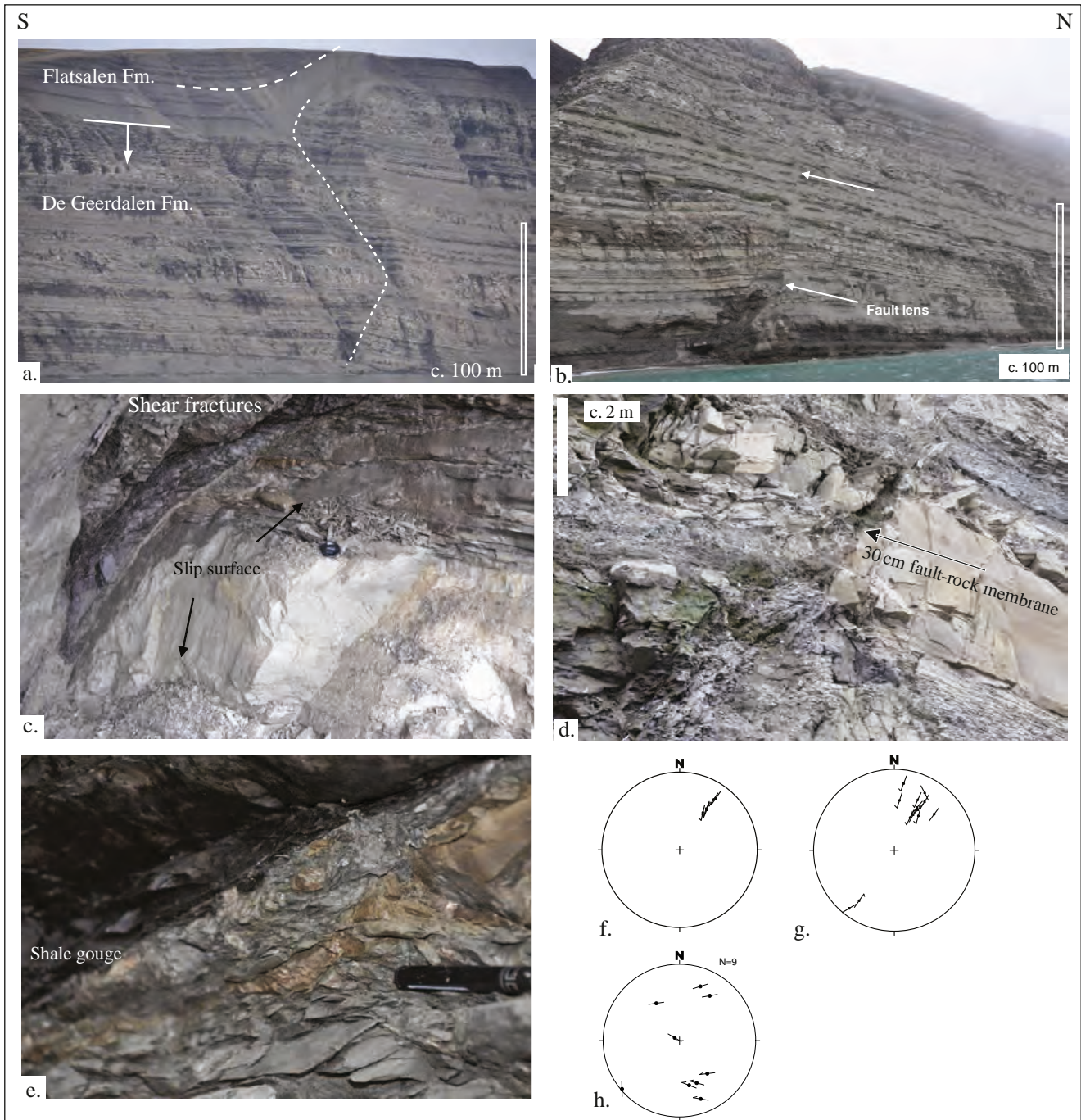
## Shallow-rooted normal faults at Skrukkefjellet and Klinkhamaren

At Skrukkefjellet, northwestern Edgeøya, a more than 100 m thick succession in the Tschermakfjellet and De Geerdalen formations are involved in a km-scale rollover anticline in the hanging wall of a normal fault that detaches along the top of the Botneheia Formation (Fig. 5). The succession involved in the rollover is shale-dominated with laterally discontinuous sandstone bodies and a few more continuous, amalgamated sandstone sheets. From the photographic analysis, it appears that an unconformity occurs at a level intermediate between the top of the Botneheia Formation and the top of the exposed section. This remains to be verified in the field, but such an unconformity would indicate that the hanging wall experienced two main phases of fault-induced rotation. No exposed faults with sliplines were recorded at this locality, but readings of bedding indicate rotation around a subhorizontal, NW-SE trending axis that likely reflects the strike of the fault that caused the rotation (Fig. 5b). The fault itself dips towards the west or southwest as interpreted from cutoffs of beds in the mountainside.

At Klinkhamaren, the De Geerdalen Formation changes from a thick lower part with variable sand content to varying shaly shallow marine and continental deposits in the upper part (Fig. 6). An array of tilted blocks is bound by normal faults that detach near the top of the Botneheia Formation. Similar to the locality at Skrukkefjellet, the faults were interpreted based on cutoffs of rotated beds exposed in the mountainside, and on the abrupt transition of bedding orientations across the fault-lines. Growth wedges, thickening towards the faults, were interpreted in the southern parts of the exposure (Rød, 2011).

Again, the rotated bedding gives clues to the orientation(s) of the array of faults (Fig. 6c). An unconformity separates rotated half-graben basins from an overlying subhorizontal succession. The lower 40 metres of the De Geerdalen Formation recorded



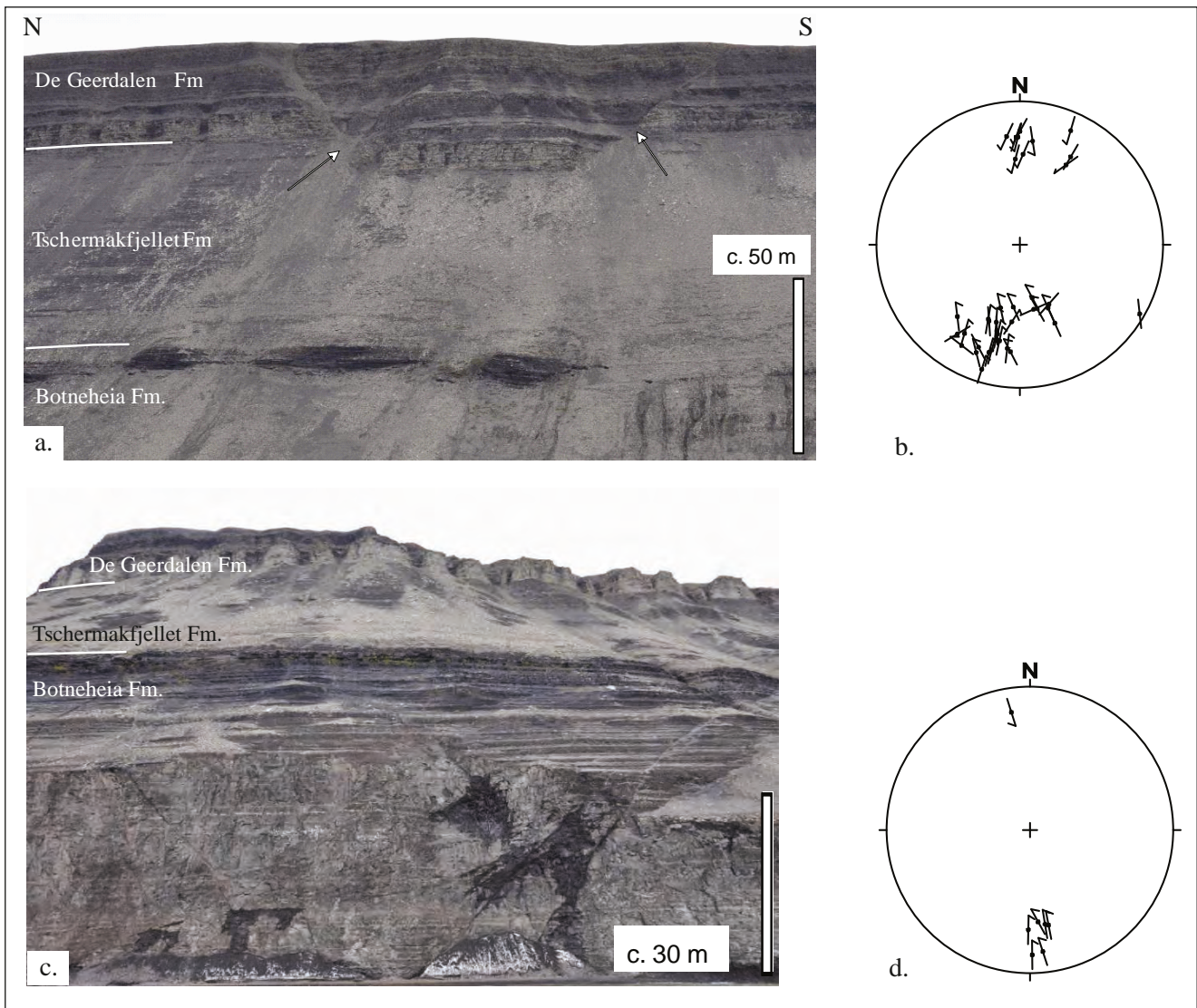


**Fig. 3.** Planar steep normal faults in Hopen. **a)** A normal fault or linked array of normal faults appears as transitional into a monocline in the overlying Flatsalen Formation. Albeit cutting the De Geerdalen Formation without notable syn-sedimentary effects, the fault may have been syn-sedimentary at the level of the Flatsalen Formation, producing a growth fault monocline of the type described for instance from the Gulf of Suez (e.g. Gawthorpe et al., 1997). **b)** Bifurcation of a small fault producing a fault lens. **c)** Details from the fault in **b)**, including a striated slip surface and a suite of associated faults and shear fractures that give evidence for downdip normal movements. **d)** and **e)** show details of fault cores with up to 30 cm of fault-rock membrane and part of a fault core with fault shale gouge that hosts sandstone clasts. In the stereograms (lower hemisphere, equal area Schmidt-nets) the faults are represented as slip-line plots. Plots in **f)** ( $N=6$ ) and **g)** ( $N=13$ ) show kinematic data from faults in **a)** and **b)** respectively. These are WNW-ESE trending normal faults with a near dip-slip sense of movement. The plot in **h)** shows kinematic data from a flat-lying fault associated with a metres-scale shale gouge in southern Hopen. This fault and associated normal splays appear to have experienced hangingwall-to-the-west movement. The role of this fault is uncertain, but the fault slip data do not conform to the general NE-SW-directed extension indicated by the other planar faults reported from Hopen, and it may be associated with post-Triassic deformation.

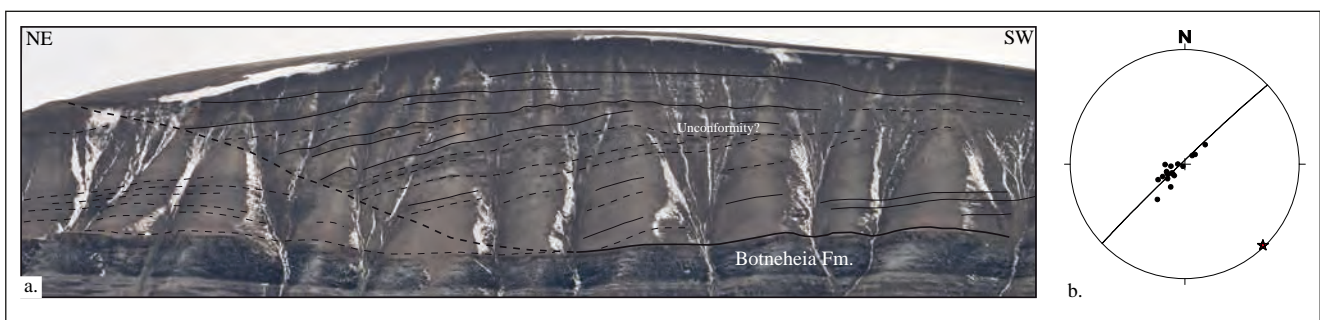
by Hynne (2010) at Klinkhamaren rest on the shales of the Tschermakfjellet Formation and are involved in the faulting described above. The sandstones, which are

generally fine-grained and erosive-based with small-scale, unidirectional cross bedding and contain plant fragments, were interpreted to represent delta front and

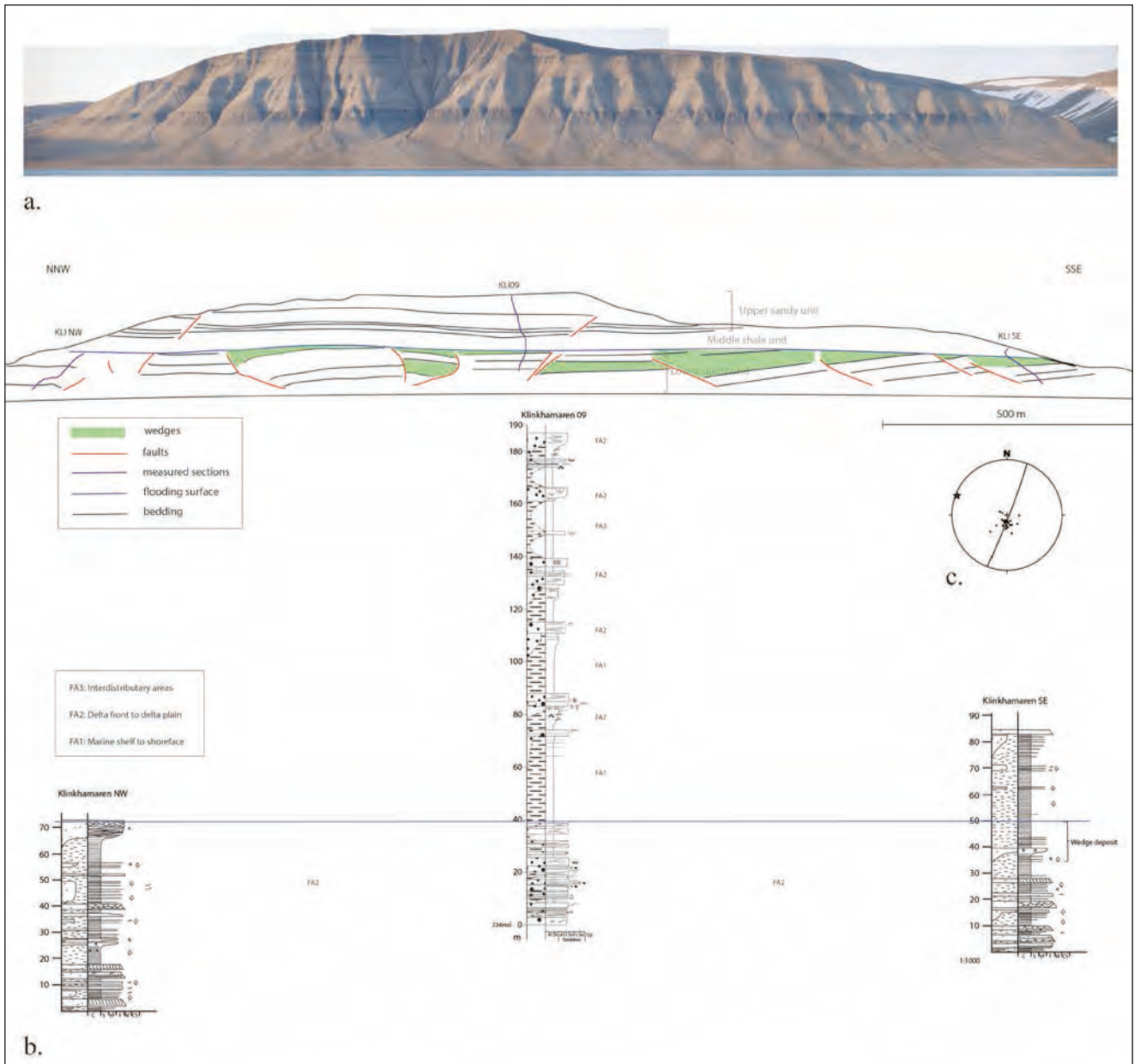




**Fig 4.** Planar, moderately to steeply dipping faults at western Edgeøya. **a)** Graben structure in Burmeisterfjellet, affecting parts of the Tschermakfjellet and De Geerdalen formations. Arrows point to the main fault planes. The faults are conjugate, generally E-W to ESE-WNW-striking, brittle faults of which some die out or terminate in the Tschermakfjellet Fm. **b)** Slip-linear stereographic representation of E-W oriented faults and shear fractures in the Burmeisterfjellet graben (N=35). The faults are overall showing normal kinematics. **c)** Faults and fractures cut the Botneheia Fm., which in a number of localities acts as a basal detachment surface for syn-sedimentary normal faults. **d)** Slip-linear stereographic representation of faults and shear fractures that cut the Botneheia Fm. (N=7). Based on these few readings, the kinematic pattern appears as comparable to that recorded in the Burmeisterfjellet graben. Thus, not all the faulting soled out at the top of the Botneheia Fm.



**Fig. 5.**  
**a)** Rollover structure above detachment at Skrukkefjellet, Edgeøya. The detachment follows the upper boundary of the Botneheia Fm. Shale-rich stratigraphy above the Botneheia Formation contains some sandstone layers and isolated sandstone bodies and displays a wedge shape as outlined on the line-drawing, indicating syntectonic sedimentation.  
**b)** Plot of bedding in the area of the rollover indicating deflection around a NW-SE-trending axis, consistent with the rollover forming along a NW-SE-trending fault.



**Fig 6.** Photomosaic *a*) and line drawing *b*) showing rotated fault-blocks above basal detachment at the top of the Botneheia Fm. at Klinkhamaren, Edgeøya. Lower diagram in *b*) also shows the correlation by Rød (2011) of the local stratigraphy between logs KLI NW and KLI SE (Glørstad-Clark, 2011) and the longer KLI 09 by Rød (2011; FA - Facies association). The faults are generally not exposed but a southwest-dipping orientation would be consistent with the observed northwards rotation of bedding, tentatively around the WNW-ESE-trending axis calculated from the stereogram in *c*) (star = pole to best-fit great circle for poles to bedding). Note unconformity above which faulting and block rotation generally cannot be observed (blue, line). *c*) shows stereographic plot of bedding measured at Klinkhamaren and the NW-SE-trending calculated fold axis.

top (channel) sandstones by Hynne (2010) and fluviially dominated delta front deposits by Glørstad-Clark (2011). In the interpretation of Rød (2011), a flooding surface marks the incipient burial of the faulted succession. Evidence for soil formation, recorded by Glørstad-Clark (2011) may tentatively represent processes that took place on the rotated fault blocks as they were eroded and weathered prior to burial below the strata in the upper parts of the section. Stratigraphically higher in the section, thick shales separate upwards-coarsening sandbodies with ripples and low-angle

cross-stratification; these were interpreted to represent fluctuations between lower shoreface/offshore deposition and delta lobe progradation, respectively (Hynne, 2010). Almost 150 out of 190 metres of the logged section consists of these facies associations.



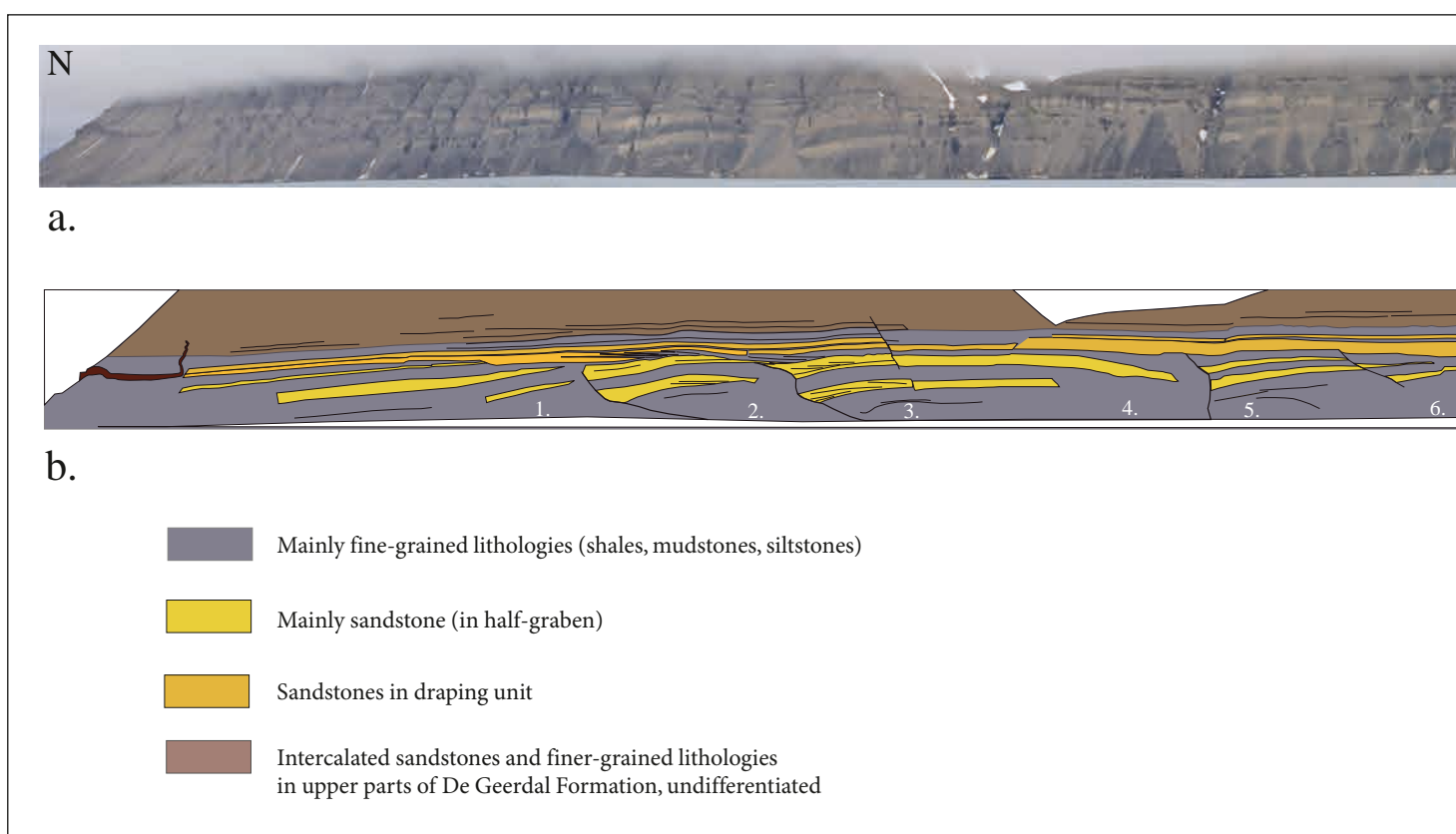


Fig. 7.

a) Photomosaic showing array of syndepositional faults in Kvalpynten. The section is approximately 8 kilometres long in total.

b) Simplified interpretation of mozaic in a, showing the subdivision of the De Geerdalen Formation into a lower part with composite sandstone units in half-graben basins, the draping unit and the upper shale and the less faulted upper parts of the De Geerdalen Formation. Numbers of individual half-graben as used in the text. Landings were made in the areas of half-graben 7-10. Logs in Figure 13 were constructed in half-graben 10.

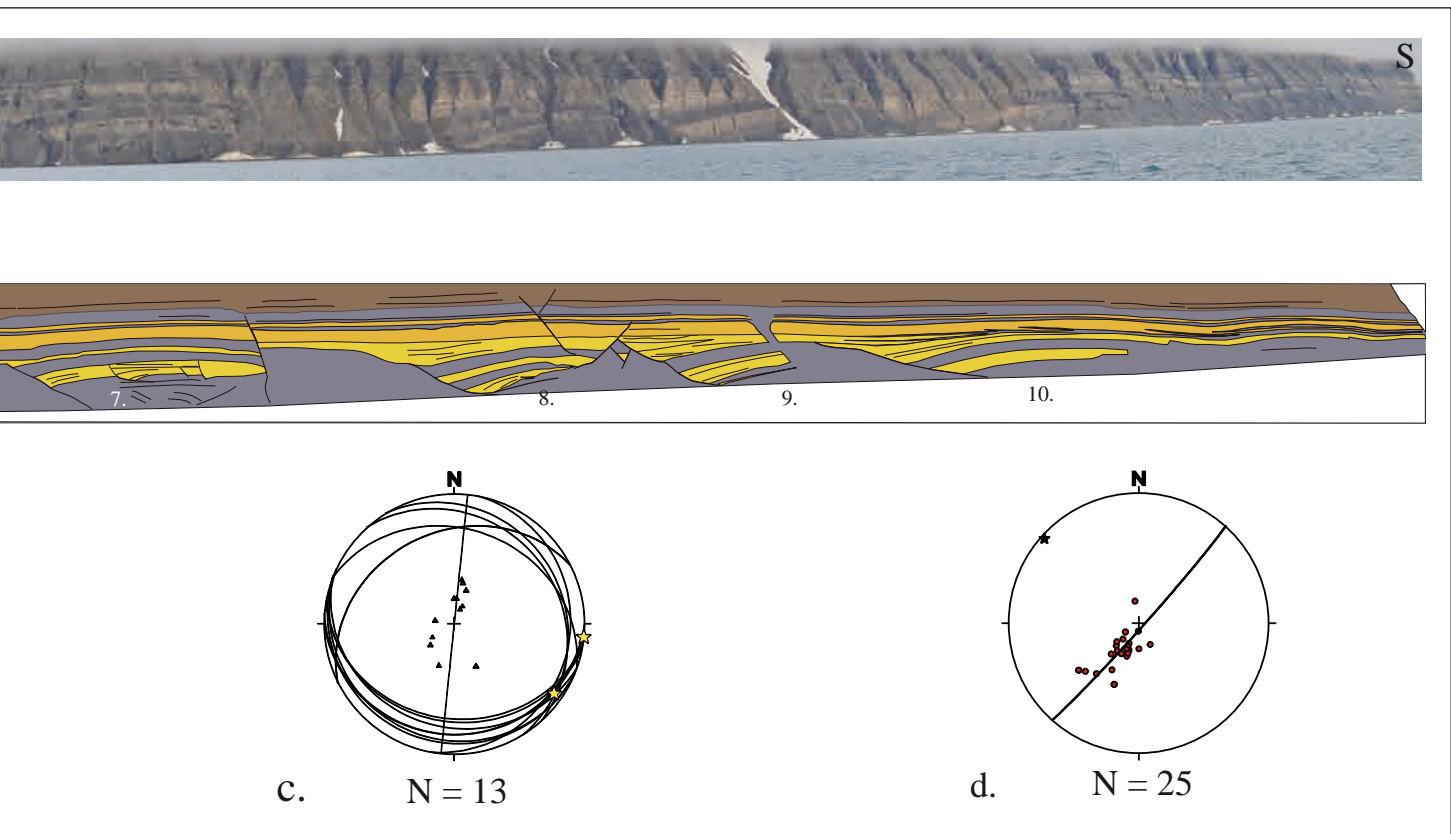
## Fault system at Kvalpynten

An approximately 8 kilometres long cliff exposure along the west side of Kvalpynten, southern Edgeøya, offers spectacular sections through an array of half-graben and their bounding normal faults (Fig. 7) that affect the De Geerdalen Formation. The dominating set of southerly facing faults has rotated bedding to northerly dips in their hanging walls. In more detail, the fault system is complex, with both syn- and antithetic (i.e. N-dipping) faults affecting stratigraphic levels from the base of the exposure in the Tschermakfjellet Formation to the unconformity that occurs at mid stratigraphic levels in the De Geerdalen Formation. Especially, the shales of the Tschermakfjellet Formation appear to be deformed in a complex way (see below).

The faults in the De Geerdalen Formation are commonly characterized by normal separations in the order of tens of meters. In the study area, fault orientations are E-W to NW-SE, and bedding appears as deflected around NW-SE-trending axes, likely reflecting rotation in the hangingwall of faults with a general NW-SE strike (Fig. 7). The general scarcity of fault slip data from these

localities reflects limited time at the outcrop. Also, kinematic indicators were difficult to obtain from some faults. This hampers our interpretation of accurate slip direction. However, judging from the observed stratigraphic separation, rotation of bedding, and by analogy with faults at other localities in the area (Figs. 5, 6, 7), the faults appear as mainly normal, and will be referred to as such in the following.

The fault system exposed at Kvalpynten is complex, with more than one generation of faults. Cross-cutting relationships provide relative ages between faults in a number of localities. In half-graben 7 and 8, for instance (Fig. 8), which were both visited by us in the field, two, or possibly, three generations of normal faults were identified. These are (1) an early set of north- or northwest-dipping faults that rotated bedding in (prodelta) shales towards the south at the lowermost exposed stratigraphic levels (Fig. 8a). These faults do not appear to be associated with sand deposition, and are overlain by subhorizontal or gently dipping shale successions. A reservation has to be made with respect to the contact between the rotated fault blocks and the overlying shales, which could not be accessed by



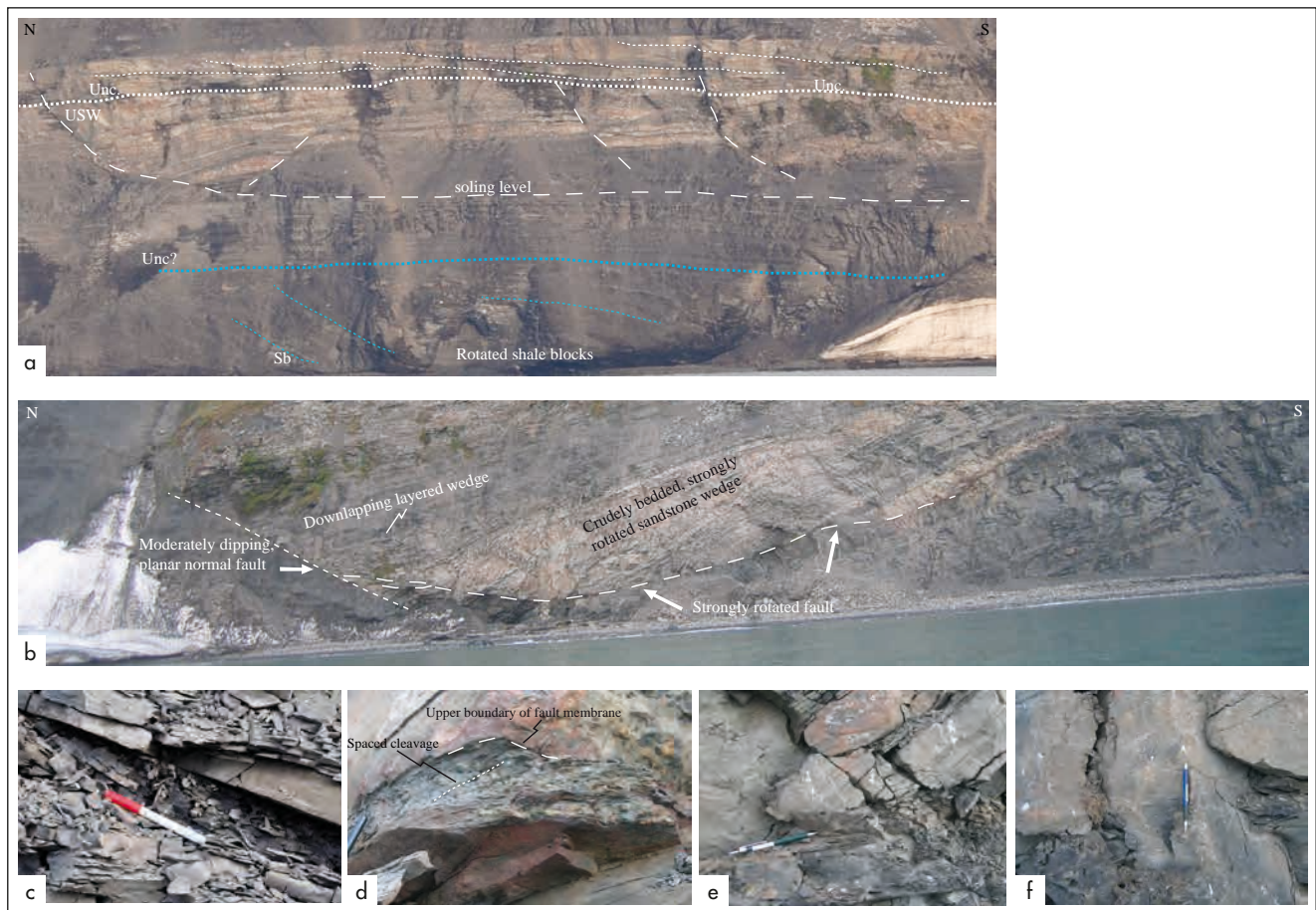
- c) Stereogram (Schmidt-net) with syn-sedimentary faults at Kvalpynten represented by great circles as well as by poles. Measured faults have shallow to moderate dips to the south-southwest and to the north-northeast. Calculated fault intersections (stars) plunge ESE and SE.
- d) Stereographic representation of poles to bedding at Kvalpynten, with best-fit great circle and pole to best-fit great circle (star). The latter indicates deflection of beds around a NW-SE-trending axis, consistent with faulting along NW-SE trending faults.

us in the field. The above interpretation is valid if the subhorizontal shales are overlying the rotated fault-blocks unconformably, without an intervening shale detachment. (2) Listic faults that detach in subhorizontal shale beds within the exposed section, and that are associated with deposition of sandy growth wedges (Figs. 8a, b). Where detaching along shale bedding, the core of one such fault displayed no discrete slip surface, but a dm-thick, cohesive sandstone membrane with mixed-in clay and cm-sized rounded, diagenetic pyrite. This fault core is laterally continuous with a more shaly membrane containing fault-parallel lamina, and is interpreted as evidence for listric faulting under hydroplastic conditions (Fig. 8). In the case shown in Figure 8a, the sandstone unit offset by listric faults contains internal unconformities against which faults terminate or lose displacement. The top of the sand unit is planar and unaffected by the faults. The sand unit is, however, in turn, cut by younger, more planar faults (3) that cut the entire lower half of the exposed section, including older listric faults and their soling levels, and that dominate the section in Kvalpynten. In detail, many of the faults show a brittle style of deformation with slip surfaces with mm-to dm-thick shale or sand gouge or mixtures between the two. One such fault cuts the

listric fault in Figure 8b and was likely responsible for its rotation past the horizontal. The planar faults were clearly associated with several periods of sand deposition and the adjacent hanging wall half-graben normally contain 2-3 composite sand units (e.g. Fig. 9).

The fault populations described in half-graben 7 and 8 reveal what appears to be a polarity change from dominantly north(east)-facing in the shale-dominated, lower exposed stratigraphic levels to dominantly south(west)-facing at the higher, more sandstone-rich levels in the De Geerdalen Formation. The upper parts of the formation, characterized by intercalated sandstones and shales, cap the faulted succession (Figs. 7, 9) and mark the cessation of significant normal faulting in the Kvalpynten section.

The top of the Botneheia Formation, which served as a basal detachment for syn-sedimentary faults in Skrukkefjellet and Klinkhamaren (Figs. 5, 6) is not exposed at Kvalpynten, and it is uncertain whether the third set of faults described above cross-cut this stratigraphic level or detached along it. The limited rotation displayed by their hanging walls may, however, indicate a deeper level of detachment than the top of the Botneheia Formation.



**Fig. 8.** Styles of faulting observed at different stratigraphic levels at Kvalpynten give clues to a polyphase faulting evolution. With reference to Fig. 7, faults in a) and b) are located in half graben 7 and 8, respectively.

a) At low stratigraphic levels in a), shale bedding is rotated southwards adjacent to north-dipping faults. The rotated shales appear to be overlain unconformably by (sub)horizontal shales, on top of which listric, outcrop-scale faults detach. In the composite sandstone unit at mid levels in the photograph, these listric faults offset lower parts of the unit. They detach in subhorizontal to gently dipping shales ('soling level'). The faults are cut by an unconformity occurring in the upper part of the sandstone body, and that incises gently southwards. Above the unconformity, beds display apparent southwards dips in a low-angle progradational pattern. The top of the sandstone unit is flat, indicating cessation of listric faulting at this time. Note uniform sandstone wedge thickening towards the footwall of the fault, similar to those observed along the younger, more planar faults in fig. 10. The composite sandstone unit is cut and displaced by the more planar faults that bound half-graben 7 in the north and south, respectively.

b) Rotated, soft-sedimentary fault at low levels in half graben at Kvalpynten (# 8, see Fig. 7). Note older listric fault strand, soling out parallel to bedding in the silty shales and rotated past horizontal to northerly apparent dips. A younger, more planar south-dipping fault segment cuts the first. Two wedge-shaped sandstone bodies are associated with the fault(s); the most sand-rich one is associated with the rotated fault, the more shale-rich layered wedge that downlaps onto the top of it appears to be associated either with the latest movements on the rotated fault or, alternatively, with the younger fault that cuts it. Photos c-f show details of the rotated fault plane. Along its northern parts.

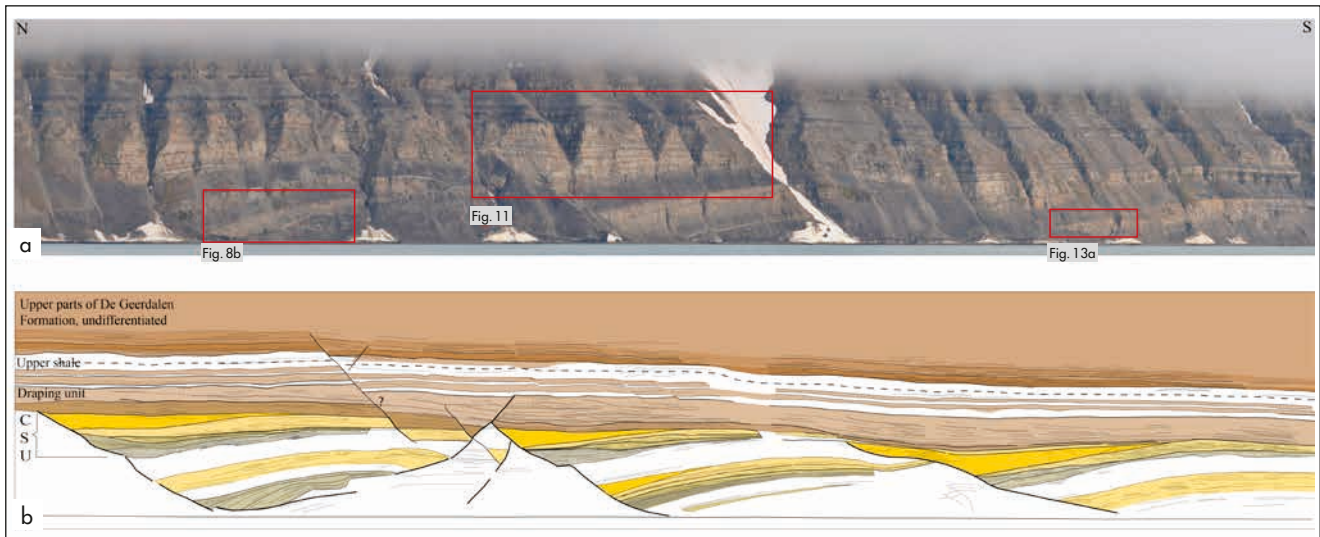
c), a fracture is developed along the slip surface between foot- and hanging wall, characterized by a 2-5 cm of sheared sand membrane on the hanging wall side and a 5-10 cm of sheared shale membrane on the footwall side. Where sandstones are juxtaposed across the fault, a 10-15 cm sheared sand membrane is observed, containing mixed-in clay and cm-sized diagenetic pyrite balls d). A weak, oblique cleavage is locally associated with the sand membrane. More distally, the contact between foot- and hanging wall is comprised mainly by sheared sand and shale membranes that are generally thin, leaving rotated hanging wall sandstones in contact with subhorizontal shales e) over only a few centimetres of fault membrane, commonly without a brittle fracture to mark the slip plane f). Our observations point towards hydroplastic conditions locally during faulting, maybe related to fluid overpressure in the shales.

## Fault-controlled sedimentary architecture at Kvalpynten

The section exposed along the southwest coast of Edgeøya reveals world-class examples of fault-controlled sedimentary architecture. In the following, we focus on the geometry and architecture of composite sandstone units in and immediately above the array of half-graben

basins. Our description and analysis is based on interpretation of photomosaics combined with work on selected beach sections. Thus, we emphasize that more field work is needed to provide a more complete sedimentological analysis of the section. However, the combination of photomosaics and field observations already provide some useful information that is described below.





**Fig. 9.**

- a) Photomosaic of three adjacent half-graben at Kvalpynten (# 8, 9 and 10 in Fig. 7), showing composite sandstone units banked against the half-graben bounding normal faults as well as overlying units.
- b) Line-drawing interpretation of photomosaic in a, emphasizing architecture of composite sandstone units (CSU) and the overlying draping unit. Note similarities in the architecture of the upper CSU in the half-graben; each is composed of an aggradational to southerly prograding lower part (greenish grey = heterolithic wedges, light yellow = hangingwall-prograding units) and an upper part that consists of a uniform sandstone wedge (bright yellow). This pattern indicates that the evolution of the three adjacent half-graben involved similar stages of fault-related rotation, subsidence and deposition, see text.

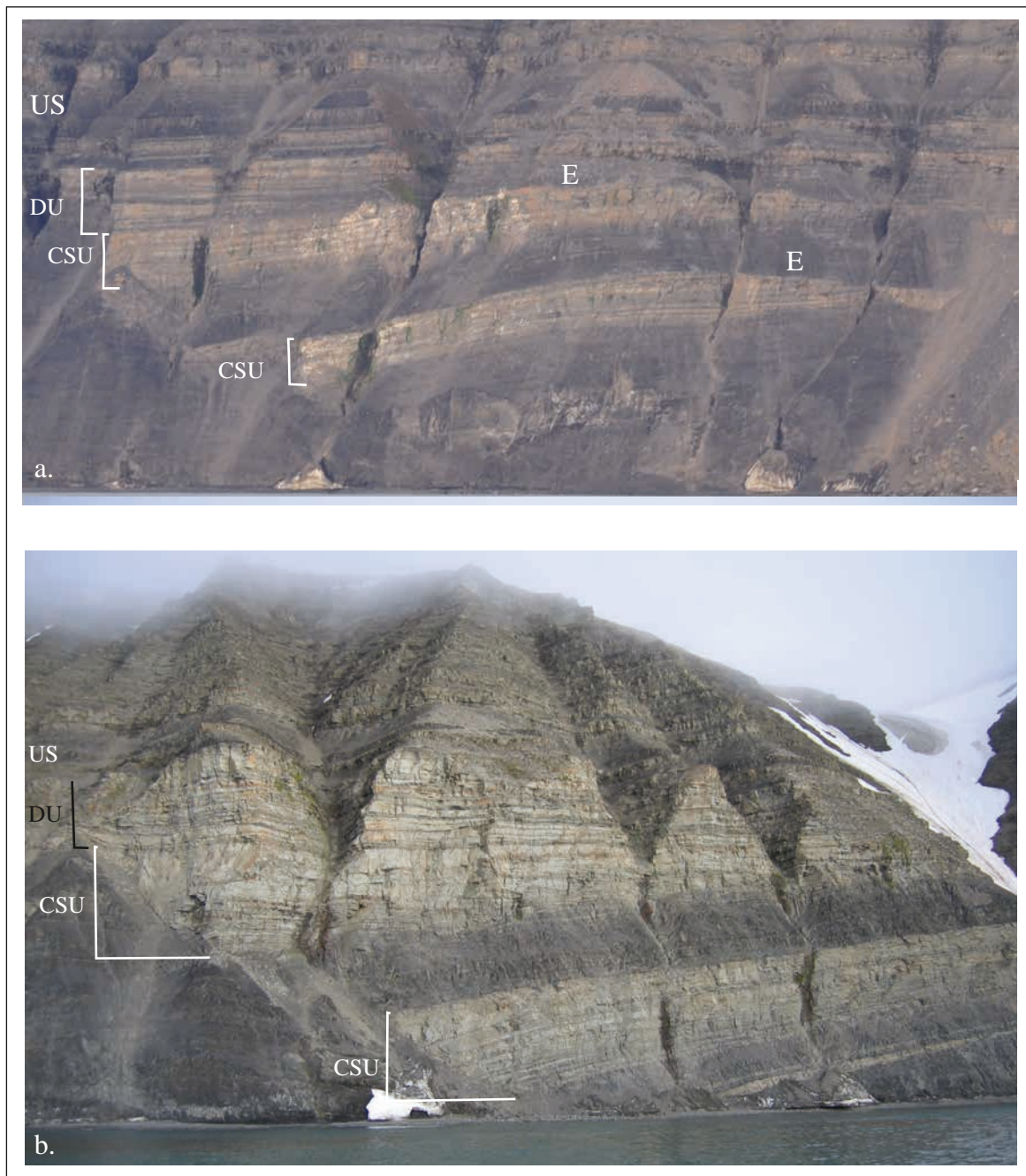
The section at Kvalpynten can be divided into a lower, faulted part, characterized by stratigraphic growth towards the faults and an upper (almost) unfaulted part characterized by more widespread intercalated shales and sandstones. The upper and lower parts are separated by, firstly, a stratigraphic interval with variable but commonly abundant sandstone content that fills in remnant topography in the half-graben basins and onlaps the highs between them. We term this unit informally the draping unit. Channel fill units are clearly defined in sand-dominated, central parts of the draping unit, and in both the northern and the southern parts of the section, it reveals an apparent southwards prograding theme, with downlap onto rotated beds in the underlying half-graben. Secondly, in the southern parts of the section, the draping unit is capped by two thin shale-rich intervals, but these wedge out northwards in the section. Thirdly, the most prominent marker in the section between the upper and lower parts of the De Geerdalen Formation is a dark-coloured fine-grained interval that can be traced across the entire exposure (the upper shale, Figs. 7, 9). This unit appears to entirely post-date the syndepositional faulting observed in the lower parts of the section. Together, the draping unit and overlying shales cap the underlying half-graben and accordingly provide a unit that reflects the termination of faulting. The De Geerdalen Formation at Kvalpynten thus appears to record deposition in fault-controlled half-graben basins, followed by cessation of faulting and infill of remnant topography from a sandy source (deposition of the draping unit). This was followed by a temporary cessation of sand deposition, perhaps facilitated by a transgressional event, and by later widespread sand and shale deposition unaffected by fault-related slopes.

### Sandbody architecture and stacking patterns in the half-graben basins

The half-graben in Figure 7 displays somewhat variable infill patterns with the most sand-rich half-graben in the south of the section. Some fundamental stacking patterns do, however, appear as characteristic for several adjacent half-grabens. An observation made by Edwards (1976) as well as by ourselves is that the shoulders of some rotated fault-blocks contain unconformities consistent with erosion into sandy intervals (Fig. 10). In some localities, such unconformities are stacked upon each other and separated by incised sandstone and shale beds, giving evidence for several phases of fault-block rotation, uplift and subsidence. Unconformities also occur inside some of the composite sandstone bodies (see below). Whereas the fine-grained, dark-coloured intervals are mainly plane-bedded and show little evidence for growth adjacent to the normal faults, the sandstones reveal a range of architectures and stacking patterns. This is interpreted to reflect their proximity to the basin-bounding normal faults and the variation in sediment supply and transport.

Each half-graben commonly contains 2-3 sandstone-dominated, composite units, in which a range of sandbody types are stacked as building-blocks (e.g. Figs. 9, 11, 12). Based on our analysis of photographs from Kvalpynten and on limited observations in the field, we identify a number of different sandbodies inside the composite sandstone units (Figs. 9, 11, 12).

1. A sandbody type recognised in several of the half-graben is triangular in cross-section and consists of thin



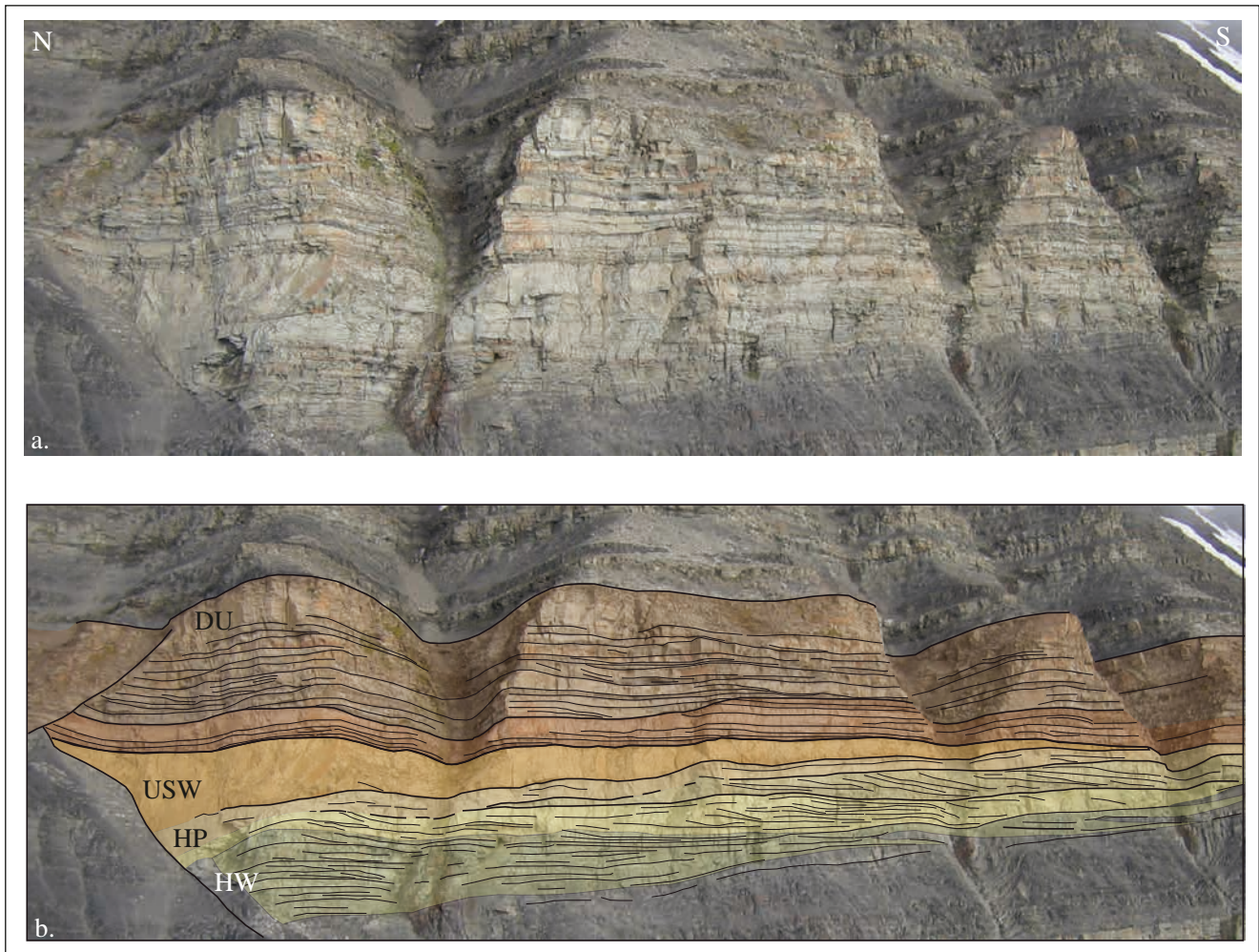
**Fig. 10.** Comparison of architecture in half graben 2 and 9 in Fig. 7; note subdivision into composite sandstone units (CSU) inside the half-graben and their relations to the overlying draping unit (DU). Also, the architecture of the draping unit is different in the two cases. In **a**), mixed sandstone-shale foresets downlap onto the upper CSU, in **b**), the lower boundary of the draping unit appears as less unconformable, but just above the base, it contains erosive channel boundaries. US - Upper shale unit.

sandstone beds separated by darker, more fine-grained intervals. Based on their apparent lithological content we will refer to these sandbodies as heterolithic wedges (Figs. 11, 12). Their internal architecture is characterized by growth towards the controlling fault and by a corresponding convergence of strata in the direction of the hanging wall. The stratal pattern inside some of the wedges does, however, indicate some progradation in the direction of the hanging wall (i.e. in a southerly direction). We interpret the heterolithic wedges to represent deposition under alternating energy conditions

in periods with high aggradation rates close to the fault planes. Moderate progradation onto the hanging wall may have been driven by a gentle slowdown in fault subsidence rates or by a moderate increase in sediment supply.

2. Sand bodies that are lenticular or thinly wedge-shaped in cross-section and characterized by foresets that dip in the direction of the hanging walls (i.e. southwards) occur inside several of the composite sandstone units. We will refer to these as hangingwall-prograding sandbodies





**Fig. 11.**

**a)** Close-up of upper part of half-graben 9 at Kvalpynten (see location in Fig. 9), with interpretation.

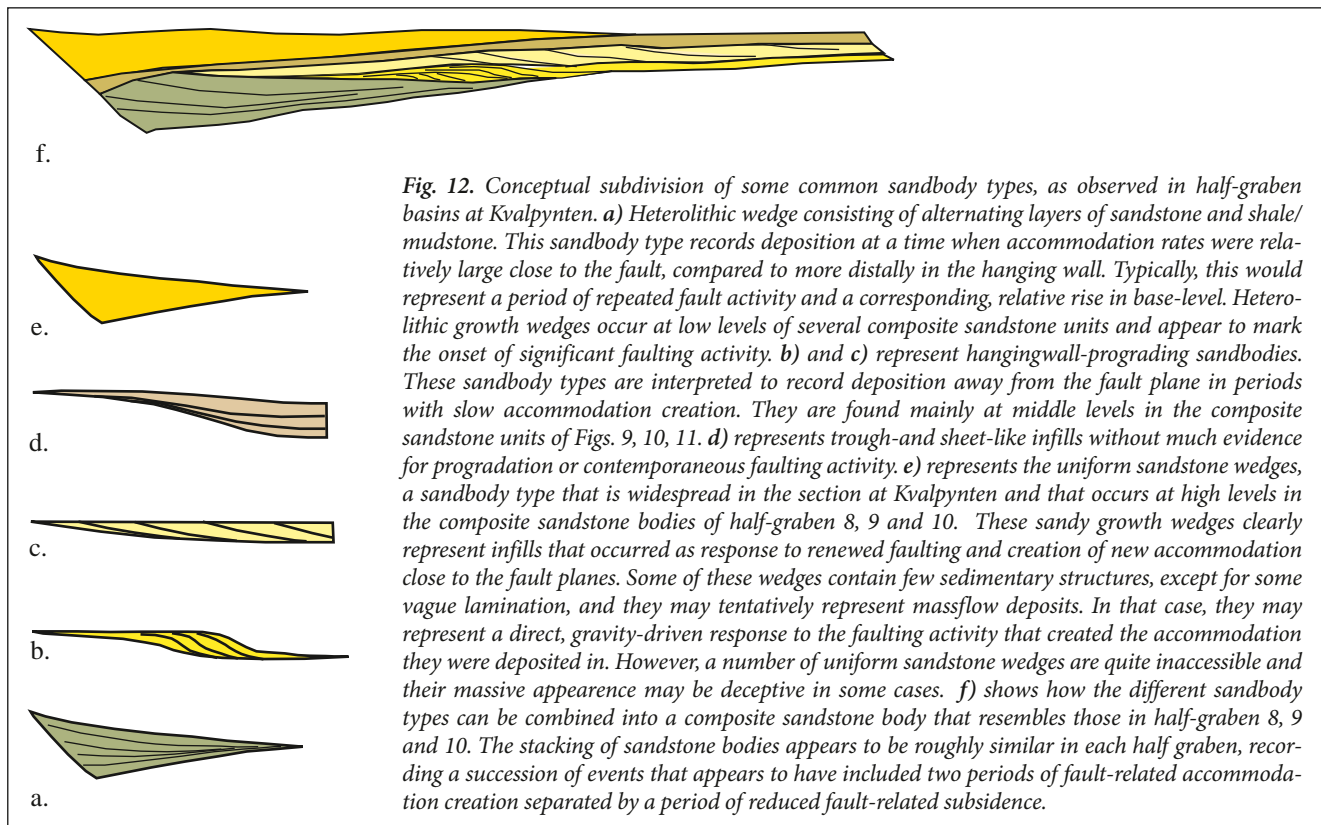
**b)** Note sedimentary architecture in the composite sandstone unit including a lower, heterolithic wedge (HW) with beds that downlap onto underlying shales, strongly progradational, more lenticular sandbodies rooted in massive sandstone close to the fault (HP) and an upper, uniform sandstone wedge (USW). The sandy draping unit (DU) that covers the half-graben shows multiple evidences for channel erosion. At this locality, the draping unit appears as conformable on the underlying composite sandstone body and as such as part of it, but on the larger scale, it downlaps or erodes strata in the underlying half-graben and is sometimes separated from underlying composite sandstone units by a shale-rich interval (see Fig. 10).

(Figs. 11, 12). They are commonly deposited on top of heterolithic wedges, but contrary to them, they do not show significant thickening towards the subbasin-controlling fault(s). Rather, several such sandbodies show a tendency to become thicker in the hanging wall direction (e.g. Fig. 11). Our tentative interpretation of the hanging-wall-prograding sandbodies is that they were deposited at times when sediment supply may have exceeded the accommodation creation rates near the faults. The degree of obliquity between the sediment transport direction and the fault planes is, unfortunately, unknown. The hanging-wall-prograding sandbodies are locally overlain by thin units that contain gently flexed or parallel strata indicating passive infill of remnant accommodation.

3. A characteristic sandbody type occurring close to the top of composite sandstone units in half-graben 8, 9 and

11 comprises massive to weakly stratified sandstone growth wedges that are banked against southerly-dipping normal faults and that become thicker towards them (Figs. 8, 9, 10, 11 and 12). These wedges appear to contain very little fine-grained material, and sedimentary structures, if present at all, are hard to classify at range. We refer to these sandbodies as uniform sandstone wedges, contrary to the heterolithic wedges described above. Where we studied such a wedge in half-graben 11, it was composed of fine- to medium-grained massive sandstone with some plane-laminated intervals. A thin conglomerate horizon marked the area adjacent to the bounding fault. The scarcity of sedimentary structures, the absence of shale-dominated intervals and the wedge shape lead us to interpret this body as a massflow unit deposited into accommodation space that was produced adjacent to the controlling normal fault during or shortly after





fault movement. It is thus possible that deposition of this and other units with similar characteristics were triggered directly by the faulting. A special case that occurs in the same half-graben is illustrated in Figure 13, where a well-defined sandbody occupies a trough-shaped depression defined by the underlying beds. The concave base and the flat top of the sandbody indicates infill of topography, in this case a hanging wall syncline produced by a ramp in the underlying fault plane, as described by McClay and Scott (1991).

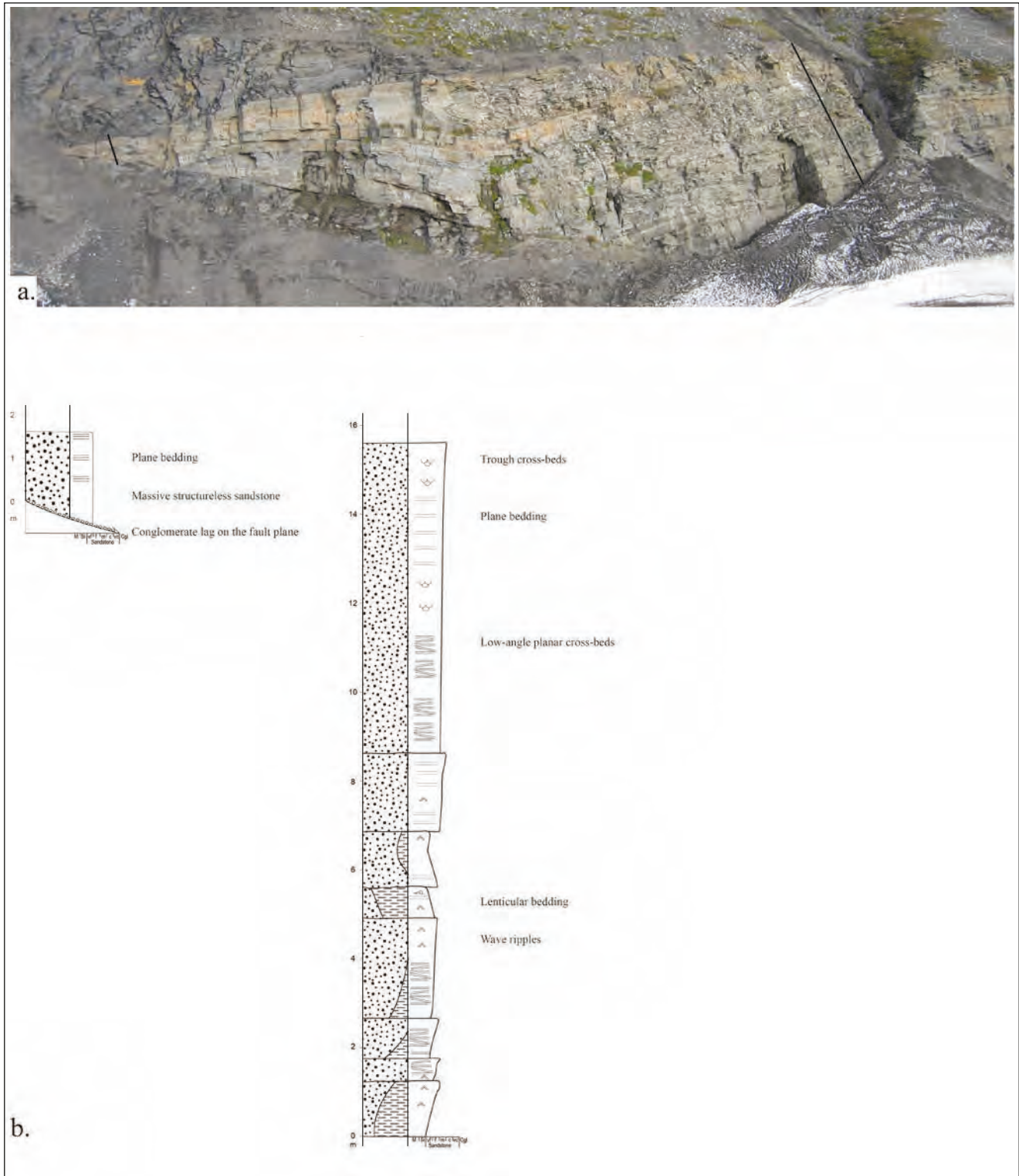
In detail, the sandbodies may reveal a complex architecture, such as the logged interval from the lower composite sandstone unit in half graben 10 (Fig. 13). This section comprises metre-thick upwards-coarsening units of very fine to fine-grained sandstones with plane beds, wave ripples and low-angle cross-strata overlain by several metres of fine-grained, low-angle and trough cross-bedded sandstones. Lenticular bedding occurred in a thin interval. Most likely, these are tidally influenced marine shoreface deposits.

The southerly direction of progradation observed inside the half-graben as well as in the draping unit is at odds with the generally northwest-directed sediment transport associated with Triassic progradation across the Barents shelf. At Kvalpynten, the lateral extent of southerly prograding sets are in the order of tens to hundred(s) of meters. However, the exact progradation direction was not recovered, and thus, the component of transport parallel to the fault planes (i.e. in a more east-west direction)

cannot be validated. However, northwards progradation in accordance with the regional model can be excluded as a main component inside the individual half-graben at Kvalpynten. The consistent observation of apparent southwards progradation also makes it less likely that the foresets represent, for instance, epsilon cross-bedding from sinuous channels. Our preliminary conclusion is therefore that the foresets represent a real southwards component of sand progradation along the south-dipping faults. This is consistent with observations from the Blanknuten area by Rød et al. (2014). Further work on facies analysis and palaeocurrents is necessary to obtain a full understanding of sediment transport and deposition inside the half-graben at Kvalpynten.

## Discussion

The fault styles and kinematic patterns reported in this paper give evidence for north-south to northeast-southwest oriented extension in the Triassic succession of East Svalbard. Based on the present dataset, the kinematic pattern displayed by the syn-sedimentary faults at Kvalpynten cannot be properly separated from that of the later, steeper faults. The most significant normal separations observed by us were associated with deposition of the lower parts of the De Geerdalen Formation. At Klinkhamaren and Kvalpynten on Edgeøya, an unconformity followed by an apparently transgressive shale interval separates the faulted lower parts of the De Geerdalen Formation from the overlying,



**Fig. 13.**

- a) Sandstone infill in synclinal depression in lower composite sand unit in half graben 10. We interpret the sandbody to fill in a hanging wall syncline (Hws) that likely developed over a ramp in the underlying fault plane; the geometry of the infilling sandbody shows that hanging-wall deformation was syn-sedimentary.
- b) Log through proximal and more distal parts of the composite sandbody (Rød, 2011, log traces marked on photograph in a) reveals that it consists mostly of massive, low-angle and trough-cross bedded sandstones with wave ripples and one interval showing lenticular bedding. It was likely deposited in a shallow marine (shoreface) environment and the massive to vaguely plane-laminated character of a uniform sandstone wedge close to the half-graben bounding fault (left) may represent massflow deposition into the sandy shoreface environment. The abrupt change back to a deeper marine (prodelta) environment indicates that sand supply was abruptly shut off after cessation of faulting.

less faulted parts (Figs. 6, 7, 8). Our observations at Skrukkefjell and Klinkhamaren (Figs. 5, 6) show that in those locations, the top of the black shales in the Botneheia Formation provided a detachment for higher-level normal faults. Small normal faults do, however, also cut down into the Botneheia Formation (Fig. 4), providing evidence for modest extension also of this unit. The sense of shear on this detachment was overall top-south or southwest, judging from the south- to southwestwards-facing polarity of the majority of syn-sedimentary faults. This shear sense is also compatible with the regional, gentle southwards dipping top of the Botneheia Formation. The presence of a northwards-displacing fundamental detachment, proposed for Kvalpynten by Høy and Lundschieen (2011), has not been confirmed by us. If an underlying detachment exists at Kvalpynten, it is more likely to be dominated by south- or southwest-directed displacement of the hanging wall, similar to the detachment at Klinkhamaren.

As well as providing direct evidence for syndepositional normal faulting (e.g. Edwards, 1976), the intricate stacking patterns recorded by the De Geerdalen Formation at Kvalpynten provide clues to the movement history of individual faults, as well as to the processes that eventually led to burial of the fault array.

We emphasize that the discussion below is based mainly on metre- or larger-scale sandbody architecture and stacking patterns, based in turn on observations and photographs on the scale of entire mountainsides. More detailed outcrop investigations are necessary to perform a full sedimentological analysis of the sections. Detail observations from accessible beach sections at Kvalpynten and from other parts of the De Geerdalen Formation (Hynne, 2010 and Rød et al., 2014) do, however, put some further constraints on the interpretation. Parts of the De Geerdalen Formation logged at Blanknuten contain laterally persistent sandy channel units with trough and planar cross-bedding, asymmetric ripples, abundant plant fossils and capping coal layers (Hynne, 2010, Rød et al., 2014), indicating repeated delta lobe progradation with fluvial and marsh environments separated by prodelta shales. Parts of the composite sandbodies observed in the half-graben may have been deposited in a marine shoreface environment, and the thick successions of finer-grained units that separate them indicate return to deeper (?) marine environments for considerable periods of time.

The stacking pattern that occurs in composite sandstone units at 2-3 levels in several of the half-grabens typically comprise (base to top):

- 1) an aggradational to weakly prograding heterolithic wedge,
- 2) 2-3 stacked, hangingwall-prograding units, sometimes associated with more passively draping strata and
- 3) a uniform sandstone wedge in the upper part of the composite sandstone unit (e.g. Figs. 11, 12).

Variations over this theme are particularly observed in the most sand-rich half-graben, notably those in Figure 9. As noted above, the exact direction of progradation has not been recorded from the sandbodies, but consistent apparent southward dips in the N-S-trending Kvalpynten section shows that in the half-graben bound by south-dipping faults, progradation occurred in the direction of the hanging wall.

Based on their tripartite sandbody architecture, the upper composite sandstone units in the half-grabens 8, 9 and 10 appear to record a similar faulting evolution. We propose the following general formation scenario: initial movements on the faults caused differential accommodation creation with the highest magnitudes and rates close to the fault planes. Sand deposition at this stage occurred in pulses, creating a layered, heterolithic growth wedge that displays a diffuse downlap or onlap onto underlying shales, often with a more parallel bedded distal part. The overall architecture of the heterolithic wedge is aggradational to weakly progradational. This configuration appears to have been followed by a slowdown in the accommodation creation rate close to the faults, as shown by the thinner prograding sandbodies, which have foresets that dip in the direction of the hanging wall and that tend to become thicker in that direction. In all three half-graben in Figure 9, deposition of progradational units was followed by deposition of relatively uniform sandstone wedges with growth towards the controlling faults. The geometry of the uniform wedges demonstrates that they filled differential accommodation with maximum values close to the fault planes and the massive nature of some of the wedges indicates, tentatively, deposition by massflow processes. Thus, the inferred slowdown of fault slip rates and associated hangingwall-directed progradation was followed by what appears to have been a rapid increase in accommodation creation rates and the filling of this accommodation by massflow-type deposits.

Some of the composite sandstone bodies that occur at low stratigraphic levels in the half graben appear to record a similar evolution. For instance, in half-graben 9, a progradational unit underlies a uniform sandstone wedge. The sandstone wedge is, in turn, overlain directly by tens of metres of darker, finer-grained lithologies. Thus, after an initial phase of faulting that resulted in footwall-directed rotation of strata and fault-related (massflow?) sedimentation, the composite sandbody was buried in a less sand-prone, maybe deeper marine environment. Renewed activity on the fault became responsible for deposition of the stratigraphically higher composite sandbody in Figure 11. Cessation of this fault activity was, however, followed by southwards progradation of the draping unit.

With exception of the lowermost stratigraphic levels (below), it appears that the thick, dark coloured and finer-grained deposits preserved in the half graben



were less affected or unaffected by faulting during sedimentation. Thus, it appears that in the half graben, the main periods of fault activity are represented by sandbody construction. Eventually, as faulting ceased, regional processes took control over deposition in the Klinkhamaren and Kvalpynten areas.

The draping unit that buried the half-graben at Kvalpynten rests unconformably on its substrate over much of the section, and its outcrop-scale architecture shows evidence for southerly progradation, downlap and channel incision. We interpret the draping unit to have filled in remnant topography created by previous faulting. Also, it appears to have been affected by gentle sags that developed above some of the half-graben (e.g. Figs. 9, 10), perhaps as a result of differential compaction. In these areas, downlap/onlap in a southerly direction is observed in the draping unit. Similar to the composite sandbodies in the half graben, the southward direction of progradation excludes only a northwards component; southwest, southeast and southwards progradation directions are possible. Southwestwards palaeocurrents were reported from lower parts of the De Geerdalen Formation in the Blanknuten area (east Edgeøya) by Knarud (1980), by Rød (2011), by Høy and Lundschieen (2011) and by Rød et al. (2014). It is possible that the above observations from low stratigraphic levels of the De Geerdalen Formation at Kvalpynten reflect the same pattern, but this remains a speculation until more palaeocurrent data are available. In the uppermost parts of the draping unit, two northward pinching shale horizons are intercalated with sheet sandstones and herald the onset of deposition of the thicker, upper shale unit that separates the draping unit from the overlying complex of intercalated sandstones and shales. The latter could be the equivalent of the fluvial and tidal channel, marsh and tidal flat deposits described by other workers in the De Geerdalen Formation (e.g. Rød et al., 2014). From the unconformable top of the rotated half-graben, the draping unit, the upper shale and the less faulted upper parts of the De Geerdalen Formation record erosion and draping of previously faulted strata. The draping and burial of the growth-faulted succession involved deposition of southerly prograding sandstones over a regional unconformity, transgression of these by conditions corresponding to more fine-grained deposition and finally, deposition of a fluvial/deltaic/tidal complex that constitutes much of the De Geerdalen Formation. We speculate that a maximum flooding surface may be located inside the upper shale unit and that the De Geerdalen Formation above the unconformity may represent parts of a depositional sequence where the lowstand systems tract is represented by the draping unit.

Several suggestions have been made with respect to the underlying cause(s) of faulting in the De Geerdalen Formation at Edgeøya. Edwards (1976) concluded that the faults at Kvalpynten represented collapse of

a south-facing delta front. This would be consistent with the observations of the southerly progradation of sandbodies as well as with the overall dominance of southward facing faults. The mapping of clinoforms in the Triassic succession in much of the western Barents Sea (Høy and Lundschieen, 2011; Glørstad-Clark et al., 2010; Anell et al., 2014; Lundschieen et al., 2014) shows that on the regional scale, progradation was towards the northwest. Thus, if the faults represent delta collapse, more local progradation with a southwards component prevailed in the Edgeøya area, due to either a competing delta with a northern source and different sediment transport, or a deflection of the main northwest transport direction in the main delta. The latter could occur due to faulting along a part of the delta front that had an anomalous orientation. Riis et al. (2008) suggested that a Triassic palaeohigh may have occupied parts of the future Svalbard area, as further highlighted by Anell et al. (in press). This may have led to the deflection of the generally northwest-prograding delta front and associated sediment transport directions. Another model for faulting, discussed by Høy and Lundschieen (2011) was that it was less directly related to the delta front but still caused by the sediment loading on soft clays. In such a case, they argued that faults may not have their orientations directly controlled by the orientation of the delta front. A third model suggests a regional driving force: deeply rooted Triassic faults have been observed in the Barents Sea south of Svalbard, and it has been argued that tectonics may be responsible, directly or indirectly, for parts of the observed faulting (e.g. Anell et al., 2013). In such a scenario, faulting may have been due to delta collapse that was either caused by or influenced by a tectonically generated stress field. Such an interpretation may be supported by the consistency in fault orientation and the generally south-facing polarity of the majority of the syn-sedimentary faults, as well as by the systematic variations in sedimentary architecture over several half-graben basins. More data, from the offshore as well as the onshore are needed to constrain better the fundamental causes of faulting.

## Conclusions

Two families of faults exposed on Hopen and Edgeøya in the eastern Svalbard archipelago indicate N-S to NE-SW extension. These are: 1) syndepositional faults with low to moderate dips, that are confined to the lower parts of the De Geerdalen Formation, exposed on Edgeøya and 2) steeper faults that are post-sedimentary with respect to the De Geerdalen Formation, but that affect higher stratigraphic levels, as seen on Hopen. For parts of the syndepositional fault system, the top of the Botneheia Formation acted as a basal detachment, as evidenced by the soling of faults at this level at Skrukkefjell and Klinkhamaren. At Kvalpynten, some syn-sedimentary low-angle faults detach in the Tschermakfjellet Formation. At Klinkhamaren and Kvalpynten, an

unconformity divides the De Geerdalen Formation into a lower part with syn-sedimentary faults and associated rotated strata and a much less faulted upper part. Thus, the apparently anomalous pattern of sediment transport and deposition in the hanging walls of south-facing faults may be restricted to the lower parts of the De Geerdalen Formation.

In detail, the fault systems are complex and at Kvalpynten, up to three populations of syn-sedimentary faults have been recorded. These include an early, north-facing generation that appears to affect only the lowermost stratigraphic levels (i.e. the Tschermakfjellet Formation) and that appear to be associated with shaly basin fills. The second fault population shows listric faults rooted in the underlying shales and were associated with sand deposition, and a dominating set of more planar faults that cut deeper than the exposed section and are associated with deposition of composite sandstone bodies tens of metres thick. All three populations were active prior to deposition of the draping unit (DU), which filled in remnant topography prior to deposition of a widespread shaly marker horizon.

At Kvalpynten, composite sandstone bodies display consistent evidence for southerly directed components of progradation in the half-graben and for strongly fault-controlled sandbody stacking patterns. This is in contrast with the sedimentary architecture that dominates above the draping units and elsewhere in the generally northwestwards-prograding Triassic sequence. The external and internal geometry of fault-controlled sandbodies point towards a similar evolution in several of the half-graben.

The sandstone unit that drapes the half graben shows apparent southwards progradation locally, where it downlaps or onlaps onto rotated strata in the upper parts of the half-graben. Other parts of the DSU show evidence for channel erosion. It appears that the DSU was deposited through south- or southwestwards progradation. The apparent transgression of this complex by a widespread shale unit marks a period of less sand-prone conditions before onset of the repeated cycles of delta progradation and retreat that makes up the upper, less faulted parts of the De Geerdalen Formation.

The consistency in orientation and the generally south-facing polarity of the majority of the syn-sedimentary faults, as well as the systematic variations in sedimentary architecture over several half-graben basins may indicate a tectonic influence on the syn-sedimentary fault systems.

#### Acknowledgements.

We thank Atle Mørk (SINTEF, NTNU) and the Norwegian Petroleum Directorate for logistic support. The above interpretations do, however, remain the sole responsibility of the authors. The captain and crew of M/S Kongsøy are thanked for 2 weeks of accommodation and good catering on board. We thank Arild Andresen, Winfried Dallmann and Fridtjof Riis for their thorough and insightful reviews.

## References

- Anell, I., Braathen, A., Olaussen, S. & Osmundsen, P.T. 2013: Evidence of faulting contradicts a quiescent northern Barents shelf during the Triassic. *First Break*, 31, 67-76.
- Anell, I., Midtkandal, I. & Braathen, A. 2014: Trajectory analysis and inferences on geometric relationships of an Early Triassic prograding clinoform succession on the northern Barents shelf. *Marine and Petroleum Geology*, 54, 167-179.
- Anell, I., Braathen, A. & Olaussen, S., in press. The Triassic of the northern Barents Shelf: A regional understanding of the Longyearbyen CO<sub>2</sub> reservoir. *Norwegian Journal of Geology*.
- Bhattacharya, J.P. & Davies, R.K. 2001: Growth faults at the prodelta to delta-front transition, Cretaceous Ferron sandstone, Utah: *Marine and Petroleum Geology*, 18, 525-534.
- Braathen, A., Bælum, K., Christiansen, H.H., Dahl, T., Eiken, O., Elvebakk, H., Hansen, F., Hanssen, T.H., Jochmann, M., Johansen, T.A., Johnsen, H., Larsen, L., Lie, T., Mertes, J., Mørk, A., Mørk, M.B., Nemec, W., Olaussen, S., Oye, V., Rød, K., Titlestad, G.O., Tveranger, J. & Vagle, K. 2012: The Longyearbyen CO<sub>2</sub> Lab of Svalbard, Norway—initial assessment of the geological conditions for CO<sub>2</sub> sequestration. *Norwegian Journal of Geology*, 92, 353–376. ISSN 029-196X.
- Dallmann, W.K., Ohta, Y., Elvevold, S. & Blomeier, D. (eds.) 2002: *Bedrock map of Svalbard and Jan Mayen*. Norsk Polarinstitutt Temakart no. 33, 1:750 000.
- Edwards, M. 1976: Growth faults in Upper Triassic Deltaic Sediments, Svalbard. *American Association of Petroleum Geologists, Bulletin*, 60, 341-355.
- Glørstad-Clark, E. 2011: *Basin analysis in the western Barents Sea area: The interplay between accommodation space and depositional systems*. PhD thesis, University of Oslo, Oslo, 262 pp.
- Glørstad-Clark, E., Faleide, J.I., Lundschie, B.A. & Nystuen, J.P. 2010: Triassic seismic sequence stratigraphy and paleogeography of the western Barents Sea area. *Marine and Petroleum Geology*, 27, 1448-1475.
- Gawthorpe, R.L. Sharp, I., Underhill, J.R & Gupta, S. 1997: Linked sequence stratigraphic and structural evolution of propagating normal faults. *Geology*, 25, 795-798.
- Gawthorpe, R.L. & Leeder, M.R., 2000: Tectono-sedimentary evolution of active extensional basins. *Basin Research*, 12, 195-218.
- Garcia-Garcia, F., Fernández, J., Viseras, C. & Soria, J.M. 2006: Architecture and sedimentary facies evolution in a delta stack controlled by fault growth (Betic Cordilleras, southern Spain, Late Tortonian). *Sedimentary Geology*, 185, 79-92.
- Hynne, I. 2010: *Depositional environment on eastern Svalbard and central Spitsbergen during Carnian time (Late Triassic): A sedimentological investigation of the De Geerdalen Formation*. Master's thesis, Norwegian University of Science and Technology, Department of Geology and Mineral Resources Engineering, 144 pp.
- Høy, T. & Lundschie, B.A. 2011: Triassic deltaic sequences in the northern Barents Sea. In Spencer, A.M., Embry, A.F., Gautier, D.L., Stoupakova, A.V. & Sørensen, K. (eds.): *Arctic Petroleum Geology*. Geological Society, London, Memoirs, 35, 249-260.
- Knarud, R. 1980: *En sedimentologisk og diagenetisk undersøkelse av Kapp Toscana Formasjonens sedimenter på Svalbard*. Cand.Real thesis, University of Oslo, 208 pp.

- Lundschieen, B.A., Høy, T. & Mørk, A. 2014: Triassic hydrocarbon potential in the Northern Barents Sea; integrating Svalbard and stratigraphic core data. *Norwegian Petroleum Directorate Bulletin*, 11, 3-20. ISBN 978-82-117-6
- McClay, K.R., & Scott, A.D. 1991: Experimental models of hanging wall deformation in ramp-flat listric extensional detachment systems. *Tectonophysics*, 188, 85-96.
- Mørk, A., Knarud, R. & Worsley, D. 1982: Depositional and diagenetic environments of the Triassic and Lower Jurassic succession of Svalbard. In Embry, A.F. & Balkwill, H.R. (eds.): *Arctic Geology and Geophysics, Canadian Society of Petroleum Geologists Memoir*, 8, 371-398.
- Mørk, A., Dallmann, W., Dypvik, H., Johannessen, E.P., Larsen, G.B., Nagy, J., Nøttvedt, A., Olaussen, S., Pchelina, T.M. & Worsley, D. 1999: Mesozoic Lithostratigraphy. In W.K. Dallmann (ed.): *Lithostratigraphic lexicon of Svalbard. Review and recommendations for nomenclature use. Upper Palaeozoic to Quaternary bedrock: Norwegian Polar Institute, Tromsø*, 127-214.
- Mørk, A., Lord, G.S., Solvi, K.H. & Dallmann, W. 2013. *Geological map of Svalbard 1:100 000, sheet G14G Hopen. Norsk Polarinstitutt Temakart No. 50.*
- Prosser, S. 1993: Rift-related depositional systems and their seismic expression. In Williams, G.D. & Dobb, A.: *Tectonics and seismic sequence stratigraphy. Geological Society Special Publications*, 71, 35-66.
- Ravnås, R. & Steel, R.J. 1998: Architecture of Marine Rift-basin successions. *American Association of Petroleum Geologists, Bulletin*, 82, 110-146.
- Riis, F., Lundschieen, B.A., Høy, T., Mørk, A. & Mørk, M.B. 2008: Evolution of the Triassic shelf in the northern Barents Sea region. *Polar Research*, 27, 318-338.
- Rød, R.S. 2011: *Spatial occurrence of selected sandstone bodies in the De Geerdalen Formation, Svalbard, and their relation to depositional facies.* Master Thesis, Norwegian University of Science and Technology, Department of Geology and Mineral Resources Engineering, 123 pp.
- Rød, R.S., Hynne, I.B. & Mørk, A. 2014: Depositional environment of the Upper Triassic De Geerdalen Formation – An E-W transect from Edgeøya to Central Spitsbergen, Svalbard. *Norwegian Petroleum Directorate Bulletin*, 11, 21-40. ISBN 978-82-117-6.
- Worsley, D. 2008: The post-Caledonian development of Svalbard and the western Barents Sea. *Polar Research*, 27, 298-317.





# The Hopen Member: A new member of the Triassic De Geerdalen Formation, Svalbard

Gareth S. Lord<sup>1,2</sup>, Kristoffer H. Solvi<sup>1</sup>, Marianne Ask<sup>3</sup>, Atle Mørk<sup>1,4</sup>,  
Mark W. Hounslow<sup>5</sup> & Niall W. Paterson<sup>3</sup>

<sup>1</sup> Department of Geology and Mineral Resources Engineering, Norwegian University of Science and Technology (NTNU), NO-7491 Trondheim, Norway.  
e-mail: gareth.lord@ntnu.no

<sup>2</sup> The University Centre in Svalbard (UNIS), Longyearbyen, Norway.

<sup>3</sup> The University of Bergen (UiB), Bergen, Norway.

<sup>4</sup> SINTEF Petroleum Research, NO-7465 Trondheim, Norway.

<sup>5</sup> The Lancaster Environment Centre, Lancaster, United Kingdom.

Hopen is a solitary island of Upper Triassic strata in the south-eastern most corner of the Svalbard archipelago. Outcrop studies throughout the island, supported by palynology, magnetostratigraphy and geological modelling have led to the identification of a new member unit within the upper part of the De Geerdalen Formation, the Hopen Member. Based on the distinctive visual properties of the strata observed in the mountain sides of Hopen, a recorded change in sediment style and an increase in the concentration of marine palynomorphs, the unit is well expressed. The Hopen Member represents an extensive, ~70 m thick succession of marine influenced shale and subordinate sandstones, distinguishing itself from the paralic and non-marine clastic sediment packages of the remaining part of the De Geerdalen Formation. The Hopen Member is traceable throughout the entire island, given its prominent darker colouration due to the lateral extent of its marine mudstones, unlike the bed packages below, which are laterally inextensive and more sandstone rich. Palynological and magnetostratigraphic studies have indicated an age of latest Carnian to earliest Norian for the member. With the age and stratigraphical position of the member being taken into account, it is possible to define this unit as a time equivalent to that of the Isfjorden Member of central Spitsbergen. However, its distinctively different lithological properties call for the creation of a new lithostratigraphic unit as opposed to simple correlation.

**Key words:** Hopen Member, Stratigraphy, Triassic, Svalbard.

## Introduction

Expeditions organised by SINTEF Petroleum Research and the Norwegian Petroleum Directorate, have visited the island of Hopen in southeastern Svalbard regularly for the last six summers. Detailed lithological sections throughout the island have been measured (Klausen and Mørk, 2014; Mørk et al., 2013; Lord et al., 2014), in addition to biostratigraphic, palynological and magnetostratigraphic sampling. This has provided the basis for a considerable dataset, from which it has been possible to identify a new member unit within the De Geerdalen Formation, the Hopen Member. In the construction of this member an interdisciplinary approach has been applied within its definition and this comprises primarily of; outcrop observation, sedimentology, magneto-stratigraphy, palynology and photomosaic modelling.

Hopen is a narrow and elongate island consisting entirely of Late Triassic aged strata, which protrudes from the northern Barents Sea in the southeastern most corner of the Svalbard Archipelago (Fig. 1) (Mørk et al., 2013). At 32 km long and no wider than 2.5 km, Hopen features as somewhat of an oddity for the region, moreso given its relatively detached position from the archipelago. The islands topographical expression is a result of the regional tectonic style, present in the eastern and southeastern areas of Svalbard, where the island represents the exposed tip of a tectonic high, within a fault system (Doré, 1995; Grogan et al., 1999). These faults trend northeast – southwest and extend throughout the offshore areas of south-eastern Svalbard and Kong Karls Land (Doré, 1995; Grogan et al., 1999), thus providing the basis for the islands axial orientation, with fault blocks down stepping to the southeast towards the Olga Basin.

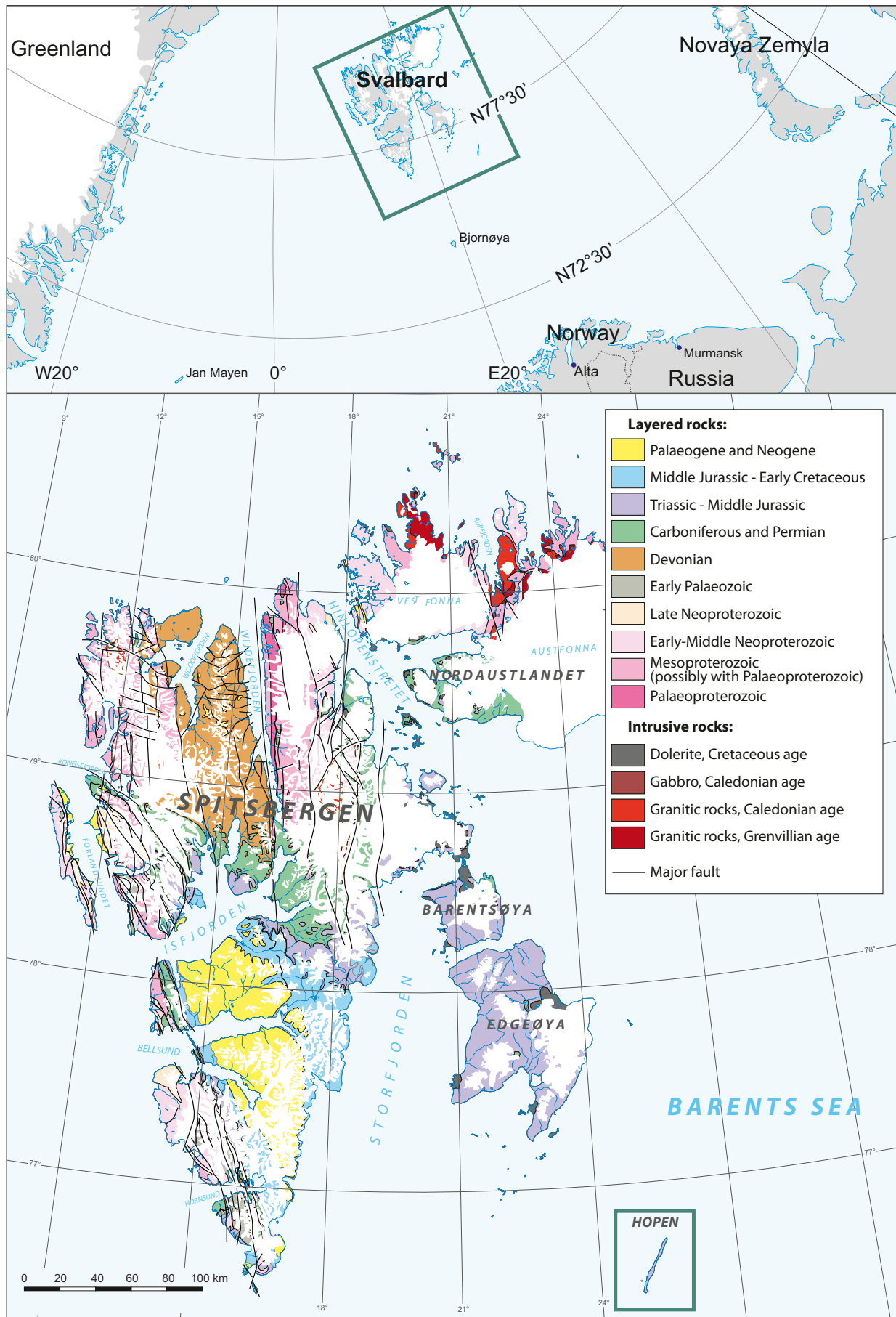


Figure 1. Overview areal map showing the position of Svalbard and basic bedrock geological map displaying the outcropping Mesozoic strata in purple with the position of Hopen denoted in the southeast. Map modified after Dallmann (in press).



The island is dissected by a series of NW-SE trending normal faults, which cut through the island at various intervals along its axis. Beds however are relatively horizontal with dips being in an order of no more than 1-2°, mainly to the NNE. The thickest exposures of the De Geerdalen Formation can be found at the southernmost mountain, Iversenfjellet, whilst in the north, the overlying Flatsalen and Svenskøya Formations are present (Mørk et al., 2013).

Pčelina (1972, 1983) noted the presence of her then defined Isfjorden 'Formation', from Central Spitsbergen, to represent the entirety of the De Geerdalen Formation on Hopen. She stated that the unit can be seen to extend over the entire archipelago, with the exception of Southern Spitsbergen. Her terminology included a much greater part of the succession within her Isfjorden 'suite' than in present nomenclature. Pčelina's Isfjorden 'Formation' and her Hahnfjella 'Formation' represented the Upper Triassic stratigraphic interval, which today is subdivided into the Tschermakfjellet and overlying De Geerdalen Formations. The revised lithostratigraphy of Mørk et al. (1999), have resulted in Pčelina's Isfjorden 'Formation' being downgraded to member status, within the De Geerdalen Formation, with its stratotype defined at Storfjellet in Sabine Land according to the section logged by Knarud (1980).

Mørk et al. (1999) (Fig. 2) did not recognise the Isfjorden Member outside of Spitsbergen, primarily due to poor constraints on stratigraphical thickness of the De Geerdalen Formation, its internal facies distributions and lithological variations in the eastern areas of Svalbard. Following a series of field studies and the creation of a computer based 3D geological model of Hopen, using photomosaics by Solvi (2013), the abrupt change in depositional style seen in the uppermost part of the De Geerdalen Formation became apparent. The 3D geological model of Hopen implemented a large photo dataset of the entire island (Solvi, 2013) and was made using Photomodeler™ software.

Mapping the lateral distribution of the base of the member, characterised by a notable colour change from light coloured yellow and grey, sands and shale to dark grey shale, was conducted using the 3D model, and this base could be followed all around the island. The surface was shown to be a more regional event unlike those more local facies variations of the stacked minor parasequences seen within the rest of the De Geerdalen Formation at Hopen (Klausen and Mørk, 2014; Lord et al., 2014). This also implies that the base of the Hopen Member may represent a major sequence stratigraphic boundary, expressing the onset of a marine transgression where the paralic deposits of the De Geerdalen Formation give way to more marine influenced deposition as a result of base level rise.

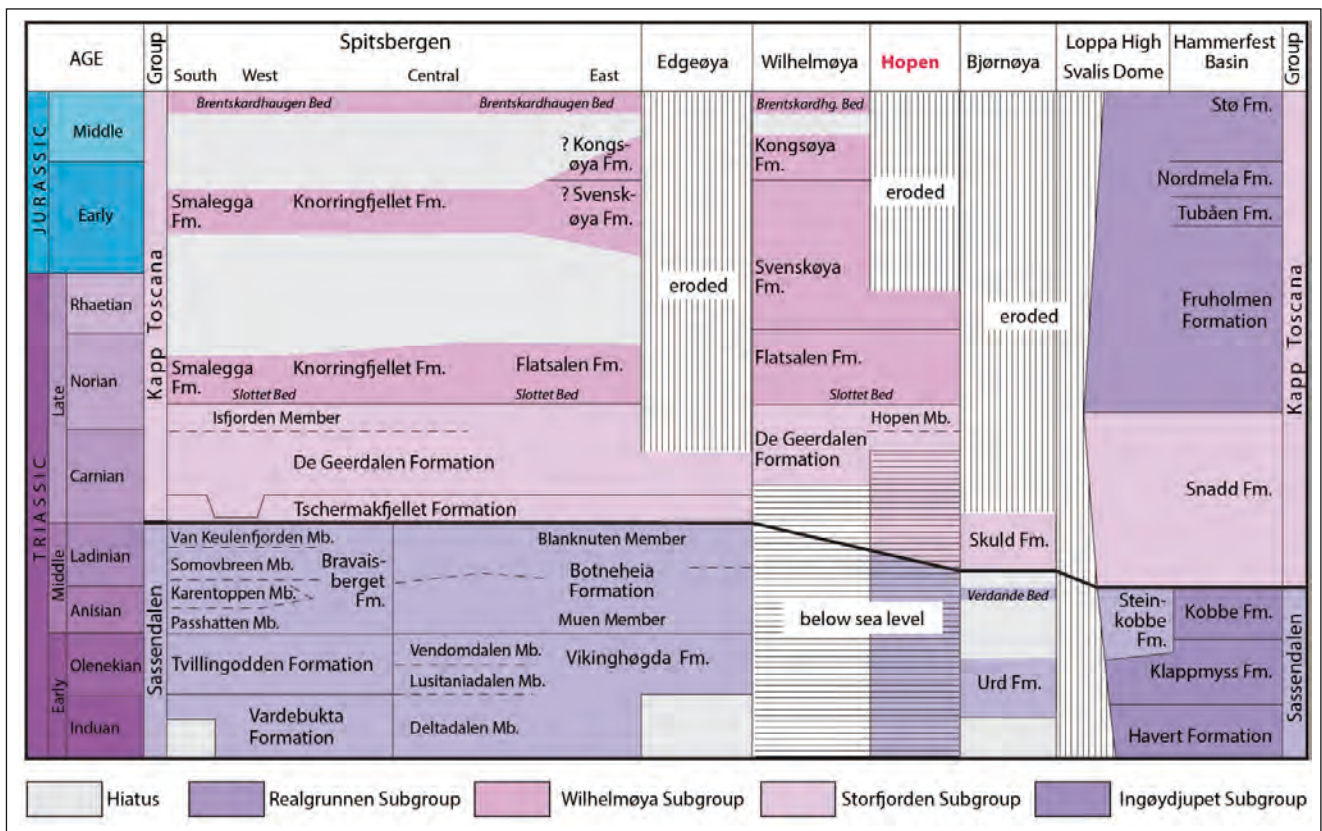


Figure 2. Stratigraphic subdivisions for the Triassic to mid-Jurassic succession of Svalbard and Barents Sea, with the Hopen Member included. Figure from Mørk et al. (2013).

## Stratigraphy

Three formations are present on the island (Fig. 2) (Mørk et al., 2013). The thickest succession being the Carnian aged De Geerdalen Formation, deposited in a fluctuating deltaic environment close to an ancient shoreline (Klausen and Mørk, 2014). Overlying this is the Norian aged Flatsalen Formation, with the pronounced carbonate Slottet Bed at its base. Overlying this is the Svenskøya Formation of Norian to possibly Rhaetian age, a prominent, white and grey, cliff-forming succession of deltaic sandstones.

The De Geerdalen Formation in the region of Hopen is interpreted to be approximately 650 m thick based on data from the Hopen 2 well, an onshore well drilled by the Norsk Fina Group in 1973. A total of 165 m is exposed above sea level in the north of the island, while some 325 m (Smith et al., 1975) is exposed in the southern part of Hopen. This is in relatively strong contrast to the 200-300 m thickness of the entire formation seen in areas of central Spitsbergen; however, this is more akin to the development of the correlative Snadd Formation seen in the Barents Sea, which is considerably thicker (Worsley et al., 1988, Riis et al., 2008). The thickness of the De Geerdalen Formation on Edgeøya and Barentsøya is presently undefined, as the uppermost part of the formation is considered to have been significantly eroded during the Cenozoic.

Minor NW-SE trending normal faults on the island and the general dip of strata to the NNE have resulted in overlying units to the De Geerdalen Formation being exposed in some locations, most predominantly in the north of the island. The De Geerdalen Formation is overlain on Hopen, by the Norian aged marine mudstones of the Flatsalen Formation (Fig. 3). This formation consists entirely of dark marine shales, with a prominent hard carbonate bed at its base, the Slottet Bed (Mørk et al., 1999). The Flatsalen Formation represents a series of discrete, upwards-coarsening packages forming a 62 m thick, dark-shale dominated succession. The Flatsalen Formation's stratotype is also defined by Mørk et al. (1999) on the mountain of Flatsalen, in the northeast of Hopen.

The Flatsalen Formation is overlain with a low angle unconformity, by a thin ca. 45 m thick package of highly cross-stratified sandstones, featuring a coarse-grained erosive base. Interpreted as having been deposited in a fluvial to deltaic depositional environment; these prominent, cliff-forming, white and grey beds represent the Svenskøya Formation, as defined on Kong Karls Land (Smith et al., 1976; Mørk et al., 1999).

The island's underlying stratigraphic units at depth have been interpreted from information provided by the Hopen 2 well log. The base of the Kapp Toscana Group is at present suggested to be approximately 685 m below sea

level. The deeper underlying units are un-interpreted, but are suggested to represent the Sassendalen Group. The base Triassic is interpreted in the well log to be at a depth of 1050 m below sea level (-1325 m on well log), where marine shales abruptly change to hard, silicified shale and sandstone of the Permian Kapp Starostin Formation. The proposed Hopen Member represents the upper ~70 m of the De Geerdalen Formation (Fig. 3) where it's notable, dark, cliff forming succession can be seen at numerous locations throughout the entire island. The thickness of the member is also seen to be relatively uniform, as measured in both in field sections and the Photomodeler™ 3D geological model.

## Sedimentology

The base of the Hopen Member is marked by clear indication of marine facies being dominant in this interval, at all locations in northern Hopen where sedimentological logs (Figs. 3 and 4) have recorded the Hopen Member. Several logs document the nature of sediments and although facies types are seen to vary, they are all associated with marine deposition. There is seen to be a notable change in lithological type where stacked heterolithic packages are observed to become more mud rich, with a loss of any plant fragments, fossil leaves, root beds, palaeosols and minor coal beds, as seen in the underlying strata. A greater increase in the presence and intensity of bioturbation is observed in the basal beds of the Hopen Member.

The sedimentological logs have been acquired by various geologists, throughout successive visits to the island since 1995 and include sections at Blåfjellet, Lyngfjellet, Binnedalen and Nørdstefjellet (Fig. 4). Additional logs of the southern part of the island are presented by Mørk et al. (2013) and Lord et al. (2014). Alike the rest of the De Geerdalen Formation, the Hopen Member is composed of layered, heterolithic clastic rocks, in beds of varying lateral continuity and facies (Fig. 5). However, unlike the underlying strata, the facies are genetically related over the entirety of the island; whereas those lower in the succession are laterally discontinuous and facies types vary considerably over relatively short distances, at the same stratigraphic level. The member consists predominantly of minor upwards coarsening packages dominated by dark mudstones that are interspersed with thin sandstone beds.

The base of the member is most prominently seen from a distance (Fig. 5) due to the overall, highly heterolithic nature of the De Geerdalen Formation. Its base is defined where the presence of root structures and subordinate coal beds with associated palaeosols become absent, approximately 70 m below the Slottet Bed. A notable change in the colour of strata is observed at this level where the underlying heterolithic packages of light coloured sand and shale give way to a much darker,

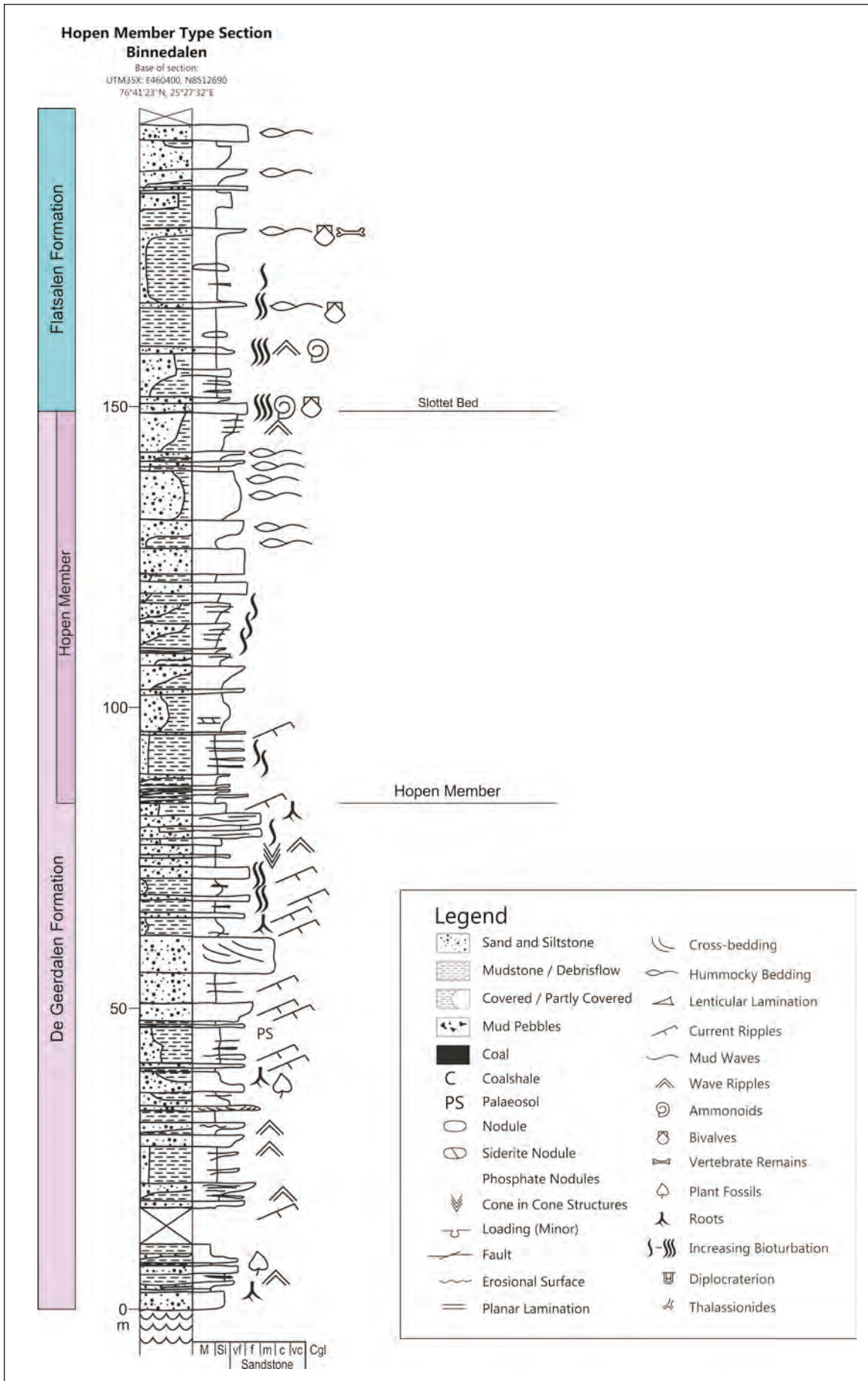


Figure 3. Stratigraphic and sedimentological log of the Hopen Member type section, Binnedalen, eastern face of Lynggefjellet, northern Hopen.



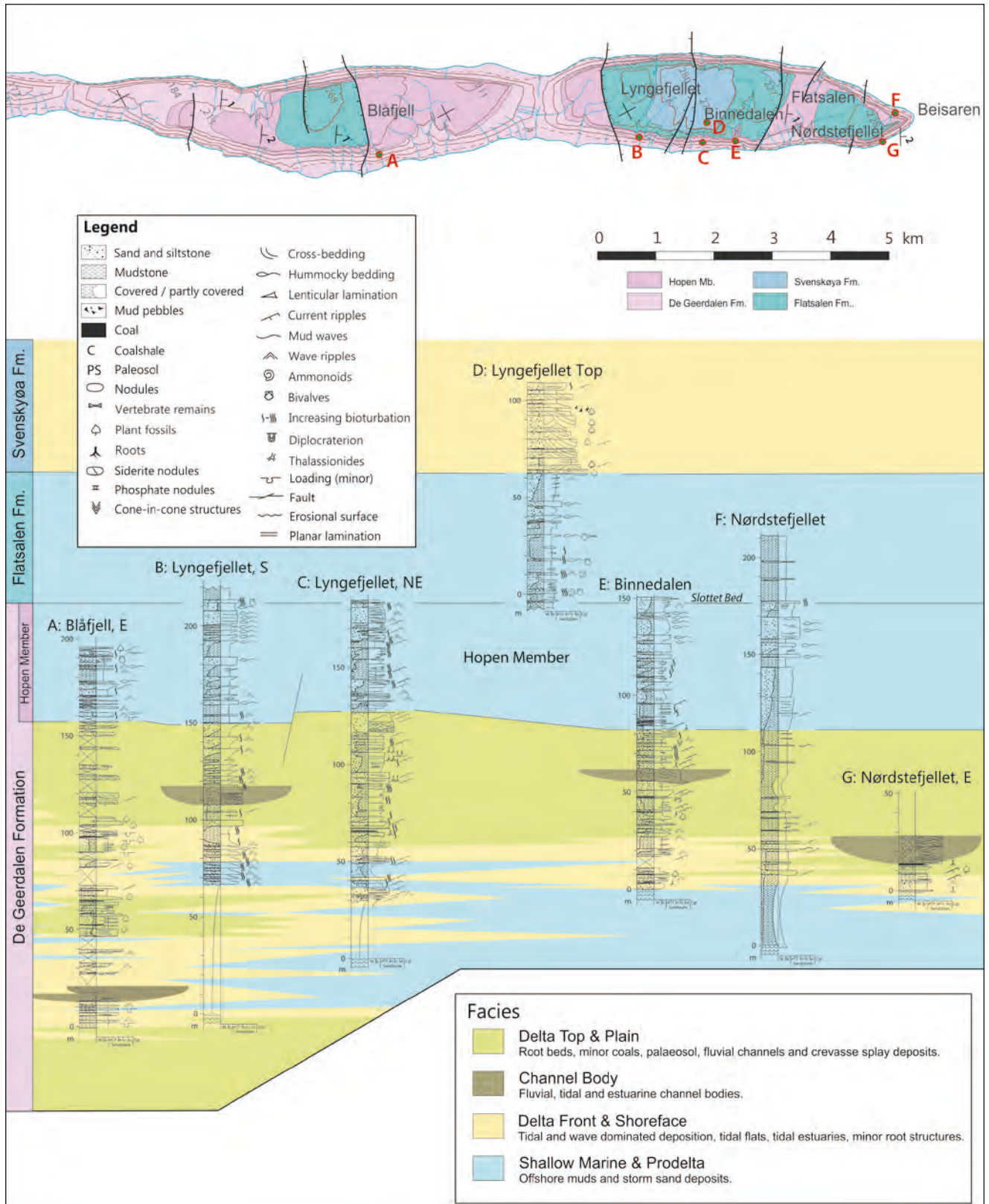
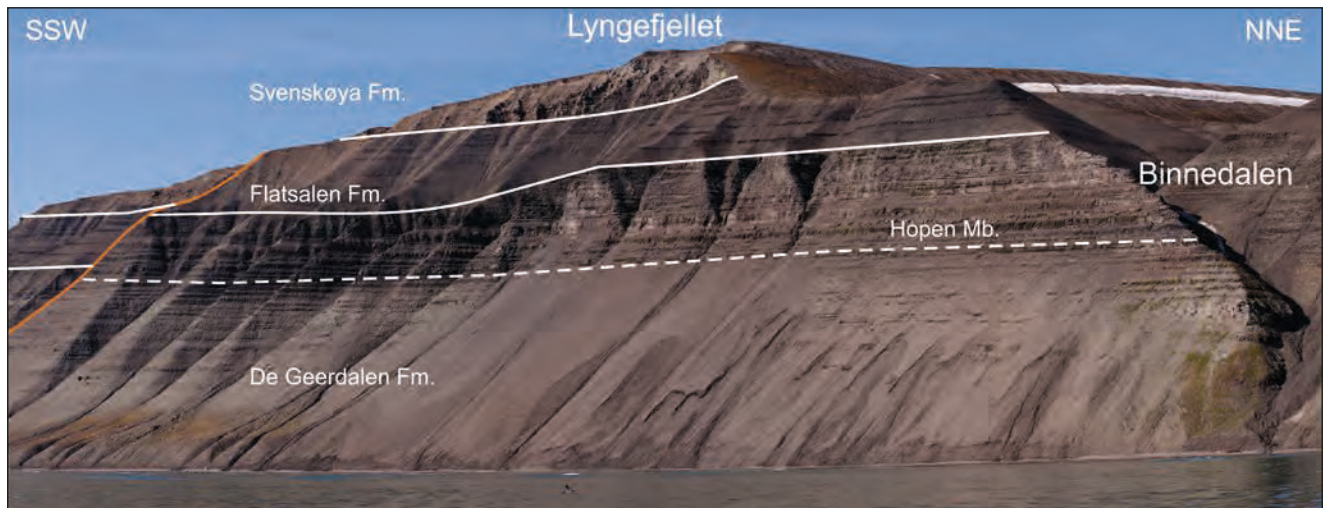


Figure 4. Facies association diagram throughout sections seen at Lyngefjellet in northern Hopen. Note the highly variable facies distribution in the De Geerdalen Formation below the base of the Hopen Member. A minor amendment has been made following the inclusion of palynological data, where the base of the Hopen Member has been set slightly lower in the Lyngefjellet NE log than previously shown in Mørk et al. (2013).





**Figure 5.** A panoramic view of Lyngfjellet displaying the stratigraphic subdivision of the Mesozoic strata on Hopen. The base of the Hopen Member is defined where the De Geerdalen Formation becomes notably darker in colour, in the upper cliffs of the formation. The type section is measured within the valley of Binnedalen in the right half of the picture. Photo: Terje Hellem.

laterally extensive succession (Figs. 5, 6, 7) that is visible in the Photomodeler™ 3D geological model. These lower beds, rich in mud and bioturbation, feature thin sandstones with both current and wave ripple structures, suggesting a relatively low energy environment of deposition. They most probably represent an inter delta lobe bay with fine grained sediments being deposited within the sub-tidal zone, with lamina and thin beds of sand representing reworked storm disrupted deposits.

Hummocky cross stratification is prolific throughout the sandstones within this interval, often being confined to more heterolithic sediment packages or thin sand beds in the uppermost part of the member. Wave and current ripples are also in abundance both in monolithic and heterolithic beds. In the case of Nørdstefjellet, a minor component of hummocky bedding is observed, in a more sandstone dominated package. Bioturbation is common and minor occurrences of bivalves are present. This suggests a slightly nearshore depositional environment



**Figure 6.** Photograph showing the nature of the Hopen Member at the type section within Binnedalen, Lyngfjellet. Note the darker colouration of this interval, with bioturbated shales hosting subordinate, rippled, sandstone laminae.





*Figure 7. Photograph depicting the nature of the shale within the Hopen Member. This is the dominant lithology throughout the unit and is seen to be highly bioturbated with the presence of minor sandstone laminations featuring wave and current ripples. Larger sandstone beds are also apparent and feature hummocky cross stratification.*

for the upper part of the member, below or just within the range of normal wave base, but still within the depth for storm wave energy to both re-work and introduce sediments into the environment.

The northern most exposures of the Hopen Member at Binnedalen and Nørdstefjellet (Figs. 3, 4) are seen to feature larger proportions of sandstone in comparison to the sections logged in the southern part of the island at Russevika and Iversenfjellet (Mørk et al., 2013; Lord et al., 2014). This may suggest a very subtle, lateral facies change along the islands axis, where the Hopen Member represents more deeper facies in the southwest, gently shallowing to the northeast.

Based on the sedimentological logs (Figs. 3, 4), the facies within the Hopen Member are interpreted as being indicative of an extensive, yet fluctuating, storm influenced shallow marine environment. This is most probably an inter delta lobe bay or a very large scale inter distributary bay, formed as a result of delta lobe switch due to the avulsuion of primary channels on the delta flood plain. In this setting, calm periods have allowed for the deposition of dark marine mud and shales, below tidal range and normal wave base. The presence of disturbed sands, interspersed within the succession, suggests the influence of wave action below wave base, aggravating the sediments during storms or periods of higher energy. These become more abundant in the upper part of the member, suggesting a relative shallowing of the depositional environment, from deeper and calmer deposition offshore, to more wave and storm disturbed sedimentation in the upper part of the member.

## Distribution and geometry

The clear, dark colouration of the Hopen Member allows for its visual profile to be traced throughout the entire island and by following the base of the boundary with the Photomodeler™ 3D geological model its distribution is seen to be widespread. The member also appears at a stratigraphically consistent level, with a similarly consistent thickness between 68-72 m. The basal surface is considered to be flat without evidence for underlying topography,

The member is present on nearly all of the major topographical highs of the island (Fig. 8). Due to the nature of faulting on the island the base of the Hopen Member has been used in order to reconstruct the islands stratigraphy, where erosion has removed significant proportions of the overlying formations, proving itself as a useable marker horizon. The most prominent locations for the change can be seen on the mountains of Iversenfjellet in the southwest and on the southern flank of Lyngefjellet in the northeast of Hopen.

The unit has been included in the Norwegian Polar Institute's geological map of Hopen (Mørk et al., 2013), due to its visual profile and pronounced continuous exposure on the island (Fig. 8).

## Ammonoid biostratigraphy

Ammonoids from the Flatsalen Formation are determined to be sirenitid ammonoids, largely of the genus *Neosirenites* (now *Norosirenites*; Bragin et al., 2012), which were previously also named as *Argosirenites*.





Figure 8. Geological map of Hopen displaying the overall distribution of the Hopen Member throughout the island. The type section location is marked in Binnedalen on eastern Lyngefjellet. Map modified after Mørk et al. (2013).

Sirenitid genera largely occur in Siberia and NE Asia, but do have representatives in Canada. They range in age, through the Boreal lower Norian with the last sirenitid ammonoids being either in the oldest parts of the NE Asian mid-Norian (within boreal ammonoid zone *Otapiria ussuriensis*; Zacharov 1997) or Siberian latest early-Norian (Konstantinov, 2008).

Korčinskaja (1980) describes *N. nelgehensis*, *N. obruchevi* and “Sirenites” *nabeshi* from the Flatsalen Formation on Hopen, which in NE Asia occurs in the *Pinacoceras verchojanicum* Zone. Bragin et al. (2012) and Konstantinov and Klets (2009) correlate this zone with the mid parts of the early Norian. The occurrence of the conodont *Norigondolella navicula* in the same beds bearing the *P. verchojanicum* Zone ammonoid fauna in NE Asia (Bragin et al., 2012), suggests much the same correlation, with *N. navicula* corresponding to the interval approximately from near the base of Lacion-I (Tethyan Jandianus Zone), to mid parts of Lacion-2 (Tethyan *Paulcke* Zone), of Krystyn et al. (2009) Norian sub-stage divisions (Orshard, 2010). This suggests the Hopen Member is at the very least, earliest Norian or older.

## Palynological Age and Characteristics

Palynological investigation of the sedimentary succession on Hopen was initiated in the early 1970s. The first study was conducted by Smith (1974) who proposed that Rhaetian and possibly Norian to Hettangian aged strata are represented on Hopen, an age which was maintained by Smith et al. (1975). However based upon further palynological investigation, Bjærke and Manum (1977) supported the Rhaetian age assignment proposed by Smith et al. (1975); however, no palynological evidence supporting either a Norian or Hettangian age was found during their study. Recently, Hopen has been the subject of renewed palynological studies (Ask, 2013; Vigran et al., 2014), and below we present preliminary data from these ongoing studies.

In general, assemblages recovered from the lower part of the De Geerdalen Formation are dominated by spore taxa, while those from the Hopen Member are more pollen-rich. Marine palynomorphs are consistently present but become more abundant in samples from the Hopen Member. Many samples contain acritarchs assigned to *Michrystidium* and *Veryhachium* spp. Dinoflagellate cysts belonging to *Rhaetogonyaulax arctica* and *R. rhaetica* are also present in samples from the De Geerdalen Formation, but are exceptionally rare. Freshwater algae *Botryococcus* spp. and *Plaesiodyctyon moesellaneum* are also present, with the latter becoming particularly abundant in samples from the Hopen Member.

Based upon semi-quantitative palynology, two distinct palynological zones are recognised in samples from the De Geerdalen Formation on Hopen (Fig. 9); these are

the lower *Leschikisporis aduncus* Acme Zone and the upper *Protodiploxypinus* spp. Acme Zone. The transition between the two zones closely approximates the base of the Hopen Member.

Assemblages of the *Leschikisporis aduncus* Acme Zone have been recovered in samples from the lower portion of the De Geerdalen Formation on Hopen from the three sections investigated. The assemblages from this zone are characterised by the dominance *L. aduncus*. Other spore taxa present in this interval include: *Aratrisporites* spp., *Aulisporites astigosus*, *Calamospora tener*, *Camerozonosporites rudis*, *Conbaculatisporites* spp., *Deltoidospora* spp., *Dictyophyllidites mortonii*, *Duplexisporites problematicus*, *Porcellispora longdonensis* and *Zebrasporites interscriptus*. Pollen comprises a relatively minor component of assemblages in this zone. Species recorded include: *Araucariacites australis*, *Chasmatosporites* spp., *Cycadopites* spp., *Eucommiidites* spp., *Illinites chitinoides*, *Ovalipollis ovalis*, *Triadispora verrucata* and *Vesicaspora fuscus*.

The *Protodiploxypinus* spp. Acme Zone is recognised in samples from the Hopen Member from Binnedalen, Blåfjell and Lyngfjellet. The diversity of assemblages from this zone is markedly higher than from those below. Assemblages from this zone are characterised by the dominance of pollen, particularly of *Protodiploxypinus* spp. Other pollen taxa present include: *Araucariacites australis*, *Chasmatosporites* spp., *Cycadopites* spp., *Eucommiidites* spp., *Illinites chitinoides*, *Ovalipollis ovalis*, *Triadispora verrucata* and *Vesicaspora fuscus*. *Leschikisporis aduncus* still occurs in assemblages from this zone but in significantly reduced numbers. The spore assemblage includes: *Annulispora folliculosa*, *Aratrisporites* spp., *Cingulizonates rhaeticus*, *Deltoidospora* spp., *Kyrtomisporis gracilis*, *K. laevigatus*, *K. speciosus*, *Ricciisporites tuberculatus*, *R. umbonatus*, *Rogalskisporites cicatricosus*, *Semiretisporis gothae*, *Striatella seebergensis*, *Uvaesporites* spp., *Velosporites cavatus* and *Zebrasporites interscriptus*. Assemblages from the *Protodiploxypinus* spp. Acme Zone are also rich in freshwater algae, particularly *Plaesiodyctyon moesellaneum*. Marine palynomorphs including the acritarchs *Michrystidium* and *Veryhachium* spp. and foraminifera test-linings are a consistent feature of this zone.

Bjærke and Manum (1977) reported the dominance of *Leschikisporis aduncus* in a coal sample from the lower De Geerdalen Formation near Iversenfjellet on the south of Hopen. Common to abundant *L. aduncus* is also a characteristic feature of the early to mid Carnian *Aulisporites astigosus* Composite Assemblage Zone of Vigran et al. (2014). Those authors also report common bisaccate pollen with an abundance peak of *Protodiploxypinus* spp. in the upper part of the zone. These observations are consistent with the *Leschikisporis aduncus* Acme Zone and the *Protodiploxypinus* spp. Acme Zone as recognised here.

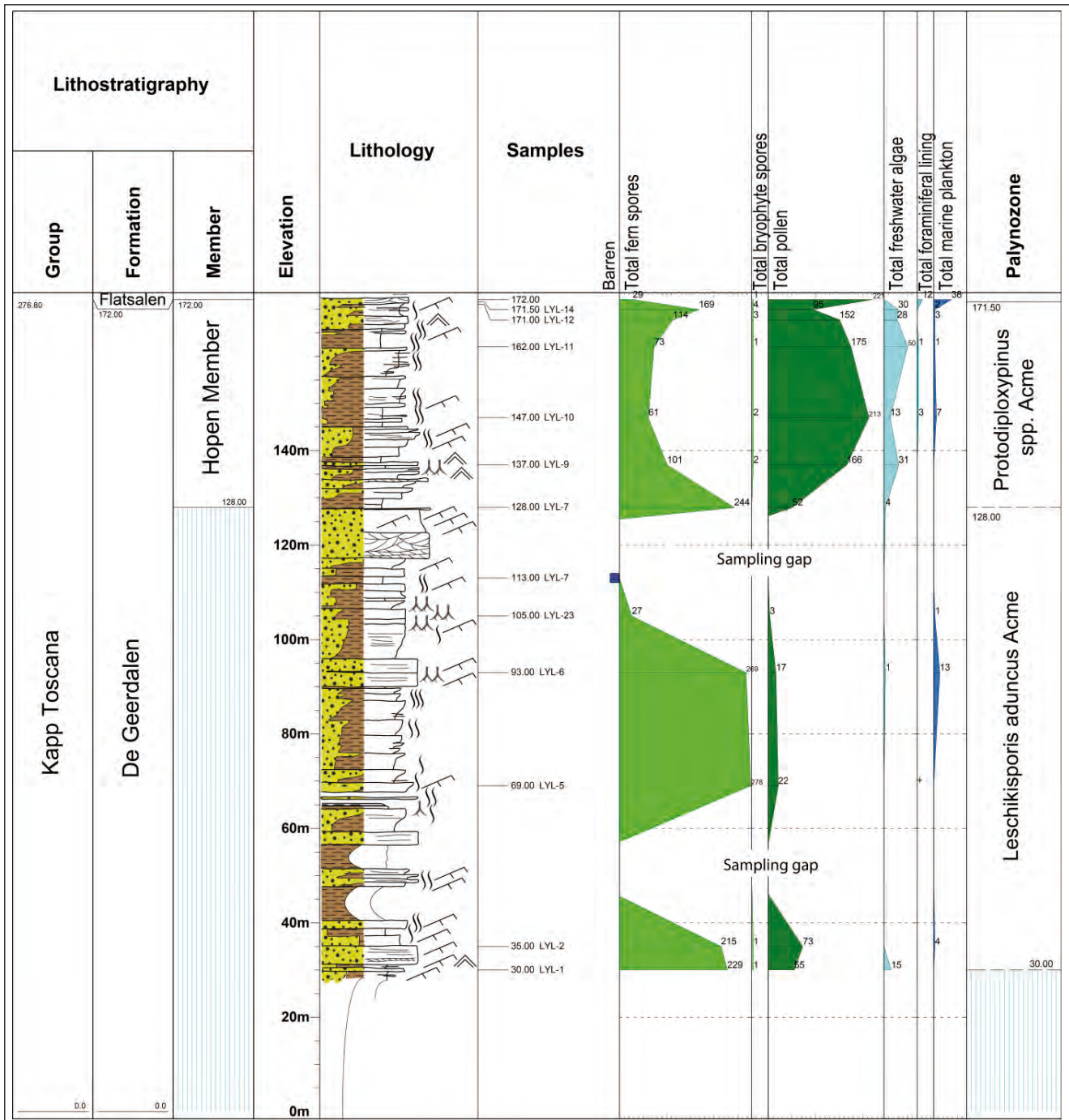


Figure 9. Relative abundances of main palynomorph groups from the De Geerdalen Formation, Lynggefjellet, Hopen. Samples and log from "Lete-samarbeidet 1995".

The occurrence of *Triadispora verrucata* in assemblages assigned to the *Protodiploxyipinus* spp. Acme Zone in the current study is indicative of a late Carnian age for the assemblage (Hochuli et al., 1989). Additionally, the common occurrence of the freshwater alga *Plaesiodyctyon moesellaneum* within this zone is indicative of an age no younger than Norian (Hochuli et al., 1989). Combining ammonoid and palynology data we suggest that the Hopen Member is of late Carnian age, possibly continuing into the earliest Norian.

The Hopen Member coincides with a major transition in the composition of palynomorph assemblages on Hopen. Assemblages from lower De Geerdalen Formation are dominated fern spore taxa such as *Leschikisporis aduncus*. However, assemblages from the Hopen Member are dominated by conifer pollen (Fig. 9). This trend has been noted elsewhere in the region (Hochuli and Vigran, 2010; Hochuli et al., 1989). *L. aduncus* was produced by plants growing under humid conditions (Hochuli and Vigran, 2010) in a near-shore, deltaic environment (Pott,



2014; Launis et al., 2014). In general, high abundances of fern spores in palynomorph assemblages signify a close proximity to the fluvio-deltaic source, rapid deposition close to their provenance and humid climatic conditions to allow significant pteridophyte growth (Tyson, 1995).

The transition to the conifer pollen dominated assemblages of the Hopen Member may reflect a change to coastal vegetation dominated by conifers, possibly due to cooler or more arid conditions in the region during the latest Carnian. Alternatively, the increased relative abundance of gymnosperm pollen in palynomorph assemblages may also signify more distal deposition from the fluvio-deltaic source (Tyson, 1995), the so-called “Neves effect” of Chaloner and Muir (1968). The latter interpretation would be consistent with deposition of the Hopen Member in a more distal marine environment.

Coinciding with the increased abundance of conifer pollen, the alga *Plaesiodyctyon moesellaneum* also increases in relative abundance in the Hopen Member. Modern coenobial algae are common constituents in freshwater environments but are typically transported by rivers into marine settings (Brenner and Foster, 1994). *P. moesellaneum* has been reported fluvial-lacustrine, marginal marine and offshore marine facies from ?Anisian-Norian-?Rhaetian age strata (Wood and Benson, 2000). The increased abundance of *P. moesellaneum* in the Hopen Member probably indicates redeposition from areas of freshwater input (Tyson, 1995). Marine palynomorphs such as acritarchs are slightly more common in the Hopen Member but are still relatively rare due to the dominance of terrestrial organic matter in the assemblages. The low abundance and diversity of acritarchs in the Hopen Member is consistent with reduced salinities and freshwater input from a fluvio-deltaic source.

## Magnetostratigraphy

The magnetostratigraphy on Hopen was constructed by sampling from the Binnedalen and Nørdstefjellet sections in northern Hopen. The sample-level data from these two sections were merged using a photo and log-based intersection correlation of the cliff sections. Data from the Nørdstefjellet section extends to slightly older intervals than that in the Binnedalen section. These data define parts of 8 major R-N magnetozone couplets, with 22 separate R plus N magnetozones plus sub-magnetozones (Fig. 10).

The reverse-polarity dominated interval HO3r to HO5r (Fig. 10) is one of the keys to understanding how the polarity may match the geomagnetic polarity timescale (GPTS). There are two intervals in the Late Triassic which have a reverse-dominated polarity pattern with three briefer normal polarity magnetozones within it.

These are within the early Norian and across the Norian-Rhaetian boundary (Hounslow and Muttoni, 2010). This later possibility is implausible, since it would push the Flatsalen Formation *Norosirenites* fauna into the late Rhaetian. A third possibility using the ammonoid-age of the Flatsalen Formation in the middle parts of the early Norian pushes all of the De Geerdalen Formation on Hopen into the Carnian. This option, preferred here, fully satisfies the age constraints from the *Norosirenites* fauna in the Flatsalen Formation as well as the palynology, which should correspond to the upper part of Lacion-1 and lower part of the Lacion-2 sub-stage divisions (Fig. 10). The magnetostratigraphic match to the GPTS is broadly satisfactory for the interval HO3n to HO8n, but less so below HO3n- some sub-magnetozones have a match in the GPTS and some not. The GPTS of Hounslow and Muttoni (2010) through the mid Carnian is derived only from the non-marine Stockton Formation of the Newark Super-group, so the validity of the GPTS remains uncertain in this interval. We have chosen to remove the Stockton Formation data from our GPTS composite. Our preferred age option places the De Geerdalen Formation all within the Carnian, and the Slottet Bed on Hopen corresponds closely to the Carnian-Norian boundary.

The magnetostratigraphic data from the Isfjorden Member in central Spitsbergen (Hounslow et al., 2007) can now be considered in the light of this new data, since this unit is widely thought to correlate to the units on Hopen. The best magnetostratigraphic match is with the interval over the base of the Hopen Member and into its lower parts (Fig. 10). The relative stratigraphic thicknesses in metres of these two intervals are also quite similar.

## Relationship to Isfjorden Member

The Hopen Member is prevalent on the island at which it is defined, Hopen in the southeast of the Svalbard archipelago. However, its notable similarity in stratigraphical position and thickness lends itself well to correlation with Triassic units elsewhere in the archipelago, most notably central and eastern Spitsbergen. In these regions the uppermost part of the De Geerdalen Formation is dominated by sediments of a marginal marine to lagoonal nature defined as the Isfjorden Member. These feature stacked heterolithic deposits of sandstone and shale as well as subordinate thin carbonates, nodular beds of siderite and phosphatic nodules (Mørk et al., 1999, Vigran et al., 2014). The most prominent features within the Isfjorden Member relate to its coloured, green and red beds, which are frequent in the upper strata of the member, below the Slottet Bed.

The Slottet Bed represents either a metre-scale hard carbonate bed in eastern Spitsbergen or a decimetre-scale bed of nodular phosphatic pebbles in central and western Spitsbergen (see logs in Vigran et al., 2014).

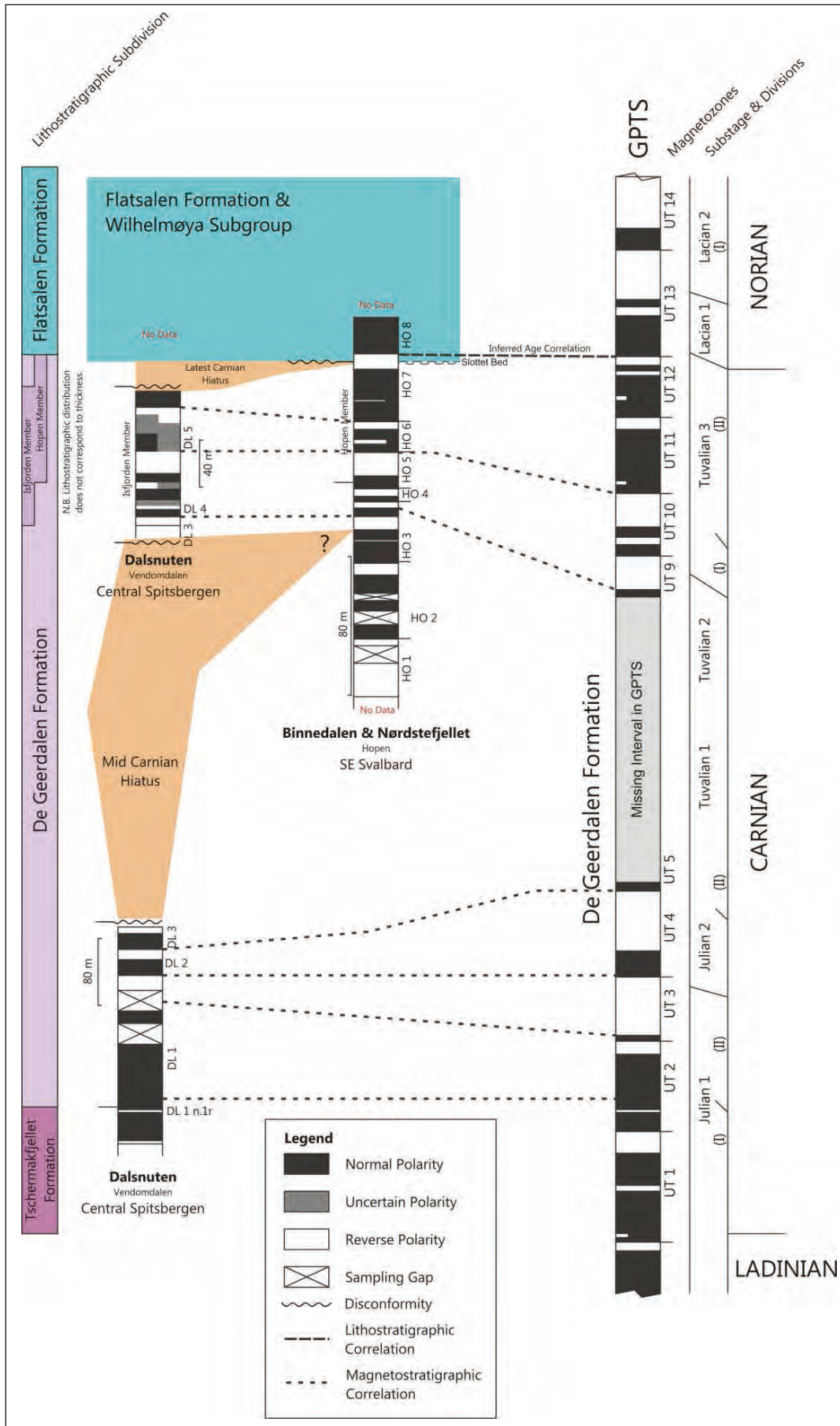


Figure 10. Summary of lithostratigraphy, age and magnetostratigraphy of the late Triassic of Svalbard based on data from Nørdstefjellet at Hopen (HO) and Dalsnuten (DL) in central Spitsbergen.

Palynology and magnetostratigraphy indicate that both member units represents the same period in time however it is unclear if the base of Isfjorden Member is synchronous to that of the Hopen Member as it is not directly observed or defined. The Isfjorden Member represents the onset of a lagoonal environment overlying a distal deltaic setting. The Hopen Member represents a dominantly shallow marine setting with inherently different lithological properties and facies, overlying a more proximal and paralic deltaic setting. This abrupt alteration seen in the De Geerdalen Formation shows a clear break and change in sediment style to marine facies, prior to the onset of a marine transgression, displayed by the Flatsalen Formation at Hopen and the Knorringsfjellet Formation, in Spitsbergen.

Neither of these member units are reported to be present in the eastern areas of Svalbard, on either Barentsøya or Edgeøya, primarily due to the fact that considerable erosion has occurred into the De Geerdalen and the overall stratigraphic thickness is unascertained. On the island of Wilhelmøya, the upper part of the De Geerdalen Formation features bivalve coquina beds and consists of dark shale, resembling the Hopen Member.

The Hopen Member may be equivalent to the upper "Carnian clinoform unit" reported from seismic studies by Riis et al. (2008), Glørstad-Clark (2010, 2011), Høy and Lundschieen (2011) and Lundschieen et al. (2014).

## Conclusions

The Hopen Member represents a widespread and abrupt variation in the depositional environment of the upper part of the De Geerdalen Formation on Hopen. Lithological changes and sedimentary structures suggest that the member has been deposited in a marine environment of variable energy and biota. Slow and relatively low energy depositional processes define the lowermost of the member, whilst offshore muds and storm deposits dominate the uppermost bed packages. The stratigraphical thickness of the member is relatively uniform throughout the entire island, at approximately 68-72 m.

The prominent change from the lower, paralic facies of the De Geerdalen Formation to those deposited in a more extensive marine and lagoonal setting (as shown by the occurrences of the Hopen and Isfjorden Members), suggests that both of these member units represent a response to a regime change at their time of deposition. This can arguably represent a surface that may be traceable into the Barents Sea. This is also reflected in the nature of palynomorphs seen at the onset of this interval, where the presence of marine algae becomes apparent.

Ammonoid stratigraphy shows that the overlying Flatsalen Formation of the Hopen Member is at its earliest

Norian in age and magnetostratigraphic correlation with sections in central Spitsbergen, show that the base of the member correlates well to an interval of reverse polarity at the same period in time. Palynological studies show a clear increase in the presence of marine palynomorphs within the Hopen Member. This also co-incides with an increase in the abundance of terrestrial palynomorphs and algae, interpreted as being flushed into the marine environment, palynological dating also defines the Hopen Member as being Carnian in age and possibly earliest Norian but no younger.

The Hopen Member has not been extended to eastern islands of the archipelago, e.g. Edgeøya and Barentsøya, but may occur on the island of Wilhelmøya, indicating that the member is an extensive marine equivalent to the more lagoonal sediments of the Isfjorden Member defined on Spitsbergen. The marine transgression resulting in the Hopen and Isfjorden members may be equivalent to the uppermost transgression of the Snadd Formation, that initiate the uppermost clinoform unit seen within Snadd Formation on the Barents Shelf. We further argue for a separate definition of this unit, aside from the Isfjorden Member (instead of simple stratigraphic correlation), as the presence of green and red beds, nodular sideritic beds and carbonate beds used in the definition of the Isfjorden Member in central Spitsbergen are not observed on Hopen, where the lithologies are predominantly dark grey clastic shales.

### Acknowledgements.

We thank all participants on the various Hopen expeditions. Part of the palynological data and several measured sections are from "Letesamarbeidet 1995", a joint project, undertaken in association with; The Norwegian Petroleum Directorate (NPD), Statoil, Norsk Hydro and Saga Petroleum, who carried out fieldwork in 1995.

## References

- Ask, M. 2013: *Palynological dating of the upper part of the De Geerdalen Formation on central parts of Spitsbergen and Hopen*. Master Thesis, University of Bergen, 78 pp.
- Bjærke, T. & Manum, S.B. 1977: Mesozoic palynology of Svalbard - I. The Rhaetian of Hopen, with a preliminary report on the Rhaetian and Jurassic of Kong Karls Land. *Norsk Polarinstitutt Skrifter*, 165, 1-48.
- Bragin, N.Y., Konstantinov, A.G., & Sobolev E.S. 2012: Upper Triassic Stratigraphy and Paleobiogeography of Kotel'nyi Island (New Siberian Islands). *Stratigraphy and Geological Correlation*, 20, 6, 54-80.
- Brenner, W. & Foster, C.B. 1994: Chlorophycean algae from the Triassic of Australia. *Review of Palaeobotany and Palynology*, 80, 209-234.
- Chaloner, W.G. & Muir, M. 1968: Spores and floras. In Murchison, D.G. & Westoll, T.S. (eds.): *Coal and coal-bearing strata*. Edinburgh, Oliver and Boyd, 127-146.
- Dallmann, W.K. (ed.) in press: *Geoscience atlas of Svalbard*. Norsk Polarinstitutt, Tromsø.
- Doré, A.G. 1995: Barents Sea Geology, Petroleum Resources and Economic Potential. *Arctic*, 48, 3, 207-221.



Formal Definition Hopen Member	
STATUS OF UNIT:	Formal
FIRST USE OF NAME:	Geological map of Hopen, Mørk et al., 2013.
CURRENT DEFINITION:	Here
SYNONYM:	None
ORIGIN OF NAME:	The island Hopen where the member is defined.
TYPE SECTION:	Stratotype Binnedalen – UTM 35X E460400, N8512690 – 76° 41' 23"N, 25° 27' 32"E.
DEPOSITIONAL AGE:	latest Carnian possibly lowermost Norian.
REFERENCES FOR AGE:	Here; Vigran et al., 2014, overlying and underlying beds dated by Korčinskaja, 1980.
OVERLYING UNIT:	Flatsalen Formation
UNDERLYING UNIT:	Un-named; remainder part of De Geerdalen Formation
SUPERIOR UNIT:	De Geerdalen Formation
OTHER USE OF NAME:	None
THICKNESS:	68-72 m, Type section is 68 m
MAIN LITHOLOGIES:	Dark shale and fine-grained sandstones
LOWER BOUNDARY DEFINITION:	Where grey shale and fine-grained sandstones are overlain by dark grey shales with fine-grained sandstones
DESCRIPTION:	Dark grey shale with subordinate fine grained sandstones. The unit represent marine sediments deposited in a fluctuating energy environment.
The Hopen Member has been approved by the Norwegian Committee on Stratigraphy, April 2014.	

- Glørstad-Clark, E., Faleide J.I., Lundschieen, B.A. & Nystuen, J.P. 2010: Triassic sequence stratigraphy and paleogeography of the western Barents Sea area. *Marine and Petroleum Geology*, 27, 1448-1475.
- Glørstad-Clark, E., Birkeland, E.P., Nystuen, J.P., Faleide J.I. & Midtkandal, I. 2011: Triassic platform-margin deltas in the western Barents Sea area. *Marine and Petroleum Geology*, 28, 1294-1314.
- Grogan, P., Østvedt-Ghazi, A.-M., Larssen, G.B., Fotland, B., Nyberg, K., Dahlgren, S. & Eidvin, T. 1999: Structural elements and petroleum geology of the Norwegian sector of the northern Barents Sea. In Fleet, A.J. & Boldy, S.A.R. (eds.): *Petroleum Geology of Northwest Europe: Proceedings of the 5th Conference*, 247-259.
- Hochuli, P.A. & Vigran, J.O. 2010: Climate variations in the Boreal Triassic – Inferred from palynological records from the Barents Sea. *Palaeogeography, Palaeoclimatology, Palaeoecology*, 290, 20-42.
- Hochuli, P.A., Colin, J.P. & Vigran, J.O. 1989: Triassic biostratigraphy of the Barents Sea area. In Collinson, J.D. (ed.): *Correlation in Hydrocarbon Exploration*. Norwegian Petroleum Society (Graham & Trotman, 1989), 131-153.
- Hounslow, M.W., Hu, M., Mørk, A., Vigran, J.O., Weitschat, W. & Orchard, M.J. 2007: Magneto-biostratigraphy of the lower part of the Kapp Toscana Group (Carnian), Vendomdalen, central Spitsbergen, arctic Norway. *Journal of the Geological Society, London*, 164, 581-597.
- Hounslow, M.W. & Muttoni, G. 2010: The Geomagnetic Polarity Timescale for the Triassic: linkage to stage boundary definitions. In Lucas, S. (ed.): *The Triassic Time scale*. Geological Society, London, *Special Publications*, 334, 61-102.
- Høy, T. & Lundschieen, B.A. 2011: Triassic deltaic sequences in the northern Barents Sea. In Spencer A.M., Embry, A.F., Gautier, D.L., Stopakova, A.V. & Sørensen, K. (eds.): *Arctic Petroleum Geology*. Geological Society, London, *Memoirs*, 35, 249-260.
- Klausen, T. G., & Mørk, A. 2014: The Upper Triassic paralic deposits of the De Geerdalen Formation on Hopen: Outcrop analog to the subsurface Snadd Formation in the Barents Sea. *American Association of Petroleum Geologists Bulletin*, 98, 1911-1941, doi:10.1306/02191413064.
- Knarud, R. 1980: *En sedimentologisk og diagenetisk undersøkelse av Kapp Toscana Formasjonens sedimenter på Svalbard*. Cand. Real. Thesis, University of Oslo, 208 pp.
- Konstantinov, A.G. 2008: Triassic Ammonoids of Northeast Asia: Diversity and evolutionary stages. *Stratigraphy and Geological Correlation*, 16, 490-502.
- Konstantinov A.G. & Klefs T.V. 2009: Stage Boundaries of the Triassic in Northeast Asia. *Stratigraphy and Geological Correlation*, 17, 173–191.
- Korčinskaja, M.V. 1980: Rannenorijskaja fauna arhipelaga Sval'bard (Early Norian fauna of the Archipelago of Svalbard). In D.V. Semevskij (ed.): *Geologija osadočnogo čehla arhipelaga Sval'bard (Geology of the sedimentary platform of the Archipelago of Svalbard)*, NIIGA, Leningrad, 30-43. (In Russian).
- Krystyn, L., Mandl, G.L. & Schauer, M. 2009: Growth and termination of the Upper Triassic platform margin of the Dachstein area (Northern Calcareous Alps, Austria). *Austrian Journal of Earth Sciences*, 102, 23-33.
- Launis, A., Pott, C. & Mørk, A. 2014: A glimpse into the Carnian: Late Triassic plant fossils from Hopen, Svalbard. *Norwegian Petroleum Directorate Bulletin*, 11, 81-96.
- Lord, G.S., Solvi, K.H., Klausen, T.G. & Mørk, A. 2014: Channels on Hopen, Svalbard: Their spatial distribution and paralic setting within the Triassic De Geerdalen Formation. *Norwegian Petroleum Directorate Bulletin*, 11, 41-59.
- Mørk, A., Dallmann, W.K., Dypvik, H., Johannessen, E.P., Larssen, G.B., Nagy, J., Nøttvedt, A., Olausen, S., Pčelina, T.M. & Worsley, D. 1999: Mesozoic Lithostratigraphy. In Dallmann, W.K., (ed.): *Lithostratigraphic Lexicon of Svalbard, Upper Palaeozoic to Quaternary Bedrock – Review and recommendations for nomenclature use*. Norwegian Polar Institute, Tromsø, 127-214.
- Mørk, A., Lord, G.S., Solvi, K.H. & Dallmann, W.K. 2013: Geological Map of Svalbard 1:100 000, sheet G14G Hopen. *Norsk Polarinstitutt Temakart No. 50*.
- Orchard, M.J. 2010: Triassic conodonts and their role in stage boundary definition. In Lucas, S.G. (ed.): *The Triassic timescale*. Geological Society, London, *Special Publications*, 334, 139-162.
- Pčelina, T.M. 1972: K voprosu o vozraste osadočnoj tolščiči ostrova Nadeždy (Sval'bard). (On the age of the sedimentary succession of the island of Hopen (Svalbard)). In V.N. Sokolov & N.D. Vasilevskaja (eds.): *Mezozoiskie otloženija Sval'barda (Mesozoic deposits of Svalbard)*, NIIGA, Leningrad, 75-81. (In Russian).

- Pčelina, T.M. 1983: Novye dannye po stratigrafii mezozoja arhipelaga Špicbergen (New data on the Mesozoic stratigraphy of the Spitsbergen Archipelago). In Krasilščikov, A.A. & Basov, V.A. (eds.): *Geologija Špicbergena (The Geology of Spitsbergen)*. PGO Sevmorgeologija", Leningrad, 121-141. (In Russian).
- Pott, C. 2014: The Upper Triassic flora of Svalbard. *Acta Palaeontologica Polonica*, 59, 709-740. doi: 10.4202/app.2012.0090.
- Riis, E., Lundschieen, B.A., Høy, T., Mørk, A. & Mørk, M.B.E. 2008: Evolution of the Triassic shelf in the northern Barents Sea region. *Polar Research*, 27, 318-338.
- Smith, D.G. 1974: Late Triassic pollen and spores from the Kapp Toscana Formation, Hopen, Svalbard - A preliminary account. *Review of Palaeobotany and Palynology*, 17, 175-178.
- Smith, D.G., Harland, W.B. & Hughes, N.F. 1975: Geology of Hopen, Svalbard. *Geological Magazine*, 112, 1-23.
- Smith, D.G., Harland, W.B. & Hughes, N.F. & Pickton, C.A.G. 1976: The Geology of Kong Karls Land, Svalbard. *Geological Magazine*, 113, 193-304.
- Solvi, K.H. 2013: *Visualize and interpret the geometry, heterogeneity and lateral continuation of channel bodies in the De Geerdalen Formation at Hopen*. Master Thesis, Norwegian University of Science and Technology, 122 pp.
- Tyson, R.V. 1995: *Sedimentary organic matter: Organic facies and palynofacies*. Chapman and Hall, London, 615 pp.
- Vigran, J.O., Mangerud, G., Mørk, A., Worsley, D. & Hochuli, P.A. 2014: Palynology and geology of the Triassic succession of Svalbard and the Barents Sea. *Geological Survey of Norway Special Publication*, 14, 270 pp.
- Wood, G.D. & Benson, D.G. Jr. 2000: The North American occurrence of the algal coenobium *Plaesiodyctyon*: Paleogeographic, paleoecologic, and biostratigraphic importance in the Triassic. *Palynology*, 24, 9-20.
- Worsley D. Johansen, R. & Kristensen, S.E. 1988: The Mesozoic and Cenozoic succession of Tromsøflaket. In Dalland et al. (eds.): *A lithostratigraphy scheme for the Mesozoic and Cenozoic succession offshore mid and northern Norway*. Norwegian Petroleum Directorate Bulletin, 4, 42-65.
- Zakharov, Y.D. 1997: Carnian and Norian sirenitid ammonoids of the NW circum-pacific and their role in the late Triassic faunal successions. *Memoires de Geologie (Lausanne)*, 30, 137-144.

# The first recovered ichthyosaur from the Middle Triassic of Edgeøya, Svalbard

Jørn H. Hurum<sup>1</sup>, Aubrey Jane Roberts<sup>1,2</sup>, Hans Arne Nakrem<sup>1</sup>, Jan A. Stenløkk<sup>3</sup> & Atle Mørk<sup>4,5</sup>

<sup>1</sup> Natural History Museum (Geology), University of Oslo, P.O. Box 1172 Blindern, NO-0318 Oslo, Norway.  
e-mail: h.a.nakrem@nhm.uio.no j.h.hurum@nhm.uio.no aubrey.roberts@nhm.uio.no

<sup>2</sup> Ocean and Earth Science, The National Oceanography Centre, University of Southampton, European Way, Southampton SO14 3ZH, Hampshire, UK.  
e-mail: ajr1g13@soton.ac.uk

<sup>3</sup> Norwegian Petroleum Directorate, P.O. Box 600, 4003 Stavanger, Norway.  
e-mail: jan.stenlokk@npd.no

<sup>4</sup> SINTEF Petroleum Research, NO-7465 Trondheim, Norway.  
e-mail: atle.mork@sintef.no

<sup>5</sup> Department of Geology and Mineral Resources Engineering, NTNU, Norwegian University of Sciences and Technology, NO-7491, Trondheim, Norway

The Blanknuten Member of the Botneheia Formation preserves ichthyopterygians of various body-sizes. Due to the fragmentary nature of their remains, their systematic positions are controversial. The most complete skeleton of a mixosaur from Svalbard (PMO 219.250) described in this paper adds new data to the *Phalarodon-Mixosaurus* controversy, which is directly connected to the Svalbard taxa, starting with the description of *Ichthyosaurus nordenskiöldii* by Hulke in 1873. The ratios of the posterior dorsal vertebrae to the mid caudal vertebrae are a mixture of what is stated to be typical for *P. callawayi*, *M. nordenskiöldii* and *M. cornalianus*. We conclude that PMO 219.250 most likely should be assigned to the genus *Phalarodon*, but refrain from further assignment to a species.

**Key Words:** Ichthyosaurs, Mixosauridae, Ichthyopterygia, Triassic, Edgeøya, Svalbard.

## Introduction

The earliest discoveries of vertebrate fossils from the Triassic of the Svalbard archipelago were made by the Nordenskiöld expeditions in 1864 and 1868 (Hulke, 1873), and the Russian-Swedish expedition in 1898 (Yakowlew, 1903). Expeditions in the early 20<sup>th</sup> century added more material (Wiman on the de Geer expedition in 1908; Stensiö and Wiman in 1912-1918; the Hamberg Swedish Expedition 1927; for history see Buchan et al., 1965 and Hagström, 2007). The ichthyopterygians found on these expeditions were thoroughly described by Carl Wiman in a series of papers (Wiman, 1910, 1916 a, b, 1928, 1933). In 1969 the Musée Nationale d'Histoire Naturelle, Paris conducted an expedition to Spitsbergen to collect fossil vertebrates from the Lower and Middle Triassic. The ichthyopterygians from this collection were described by Mazin (1981a, b, 1983a, 1984) and Maisch and Matzke (2002). More material has been collected randomly by different geological expeditions to Svalbard over the years but the Wiman collection has remained the

core collection and has been redescribed several times (for historical background see Maxwell and Kear, 2013). Even so, Maxwell and Kear concluded (2013:9): “*The persistent nomenclatural issues surrounding the Svalbard Triassic ichthyopterygians cannot be solved without the discovery of more diagnostic material.*”

Most collections of Triassic ichthyopterygians from the Svalbard archipelago have so far been focused on the Isfjorden area. Vertebrate fossils from the Triassic of Edgeøya are less studied, mainly due to the island's remote location. A list of fossils was given by Cox and Smith (1973), who also briefly mentioned a jaw of *Pessosaurus*. Lock et al. (1978) reported large numbers of vertebrate fossils, but did not carry out any further investigations.

The Svalbard archipelago, being a late Mesozoic and Cenozoic uplifted area of the Barents Sea shelf, is a unique location for studying the sedimentology and development of the northern Barents Sea. For several



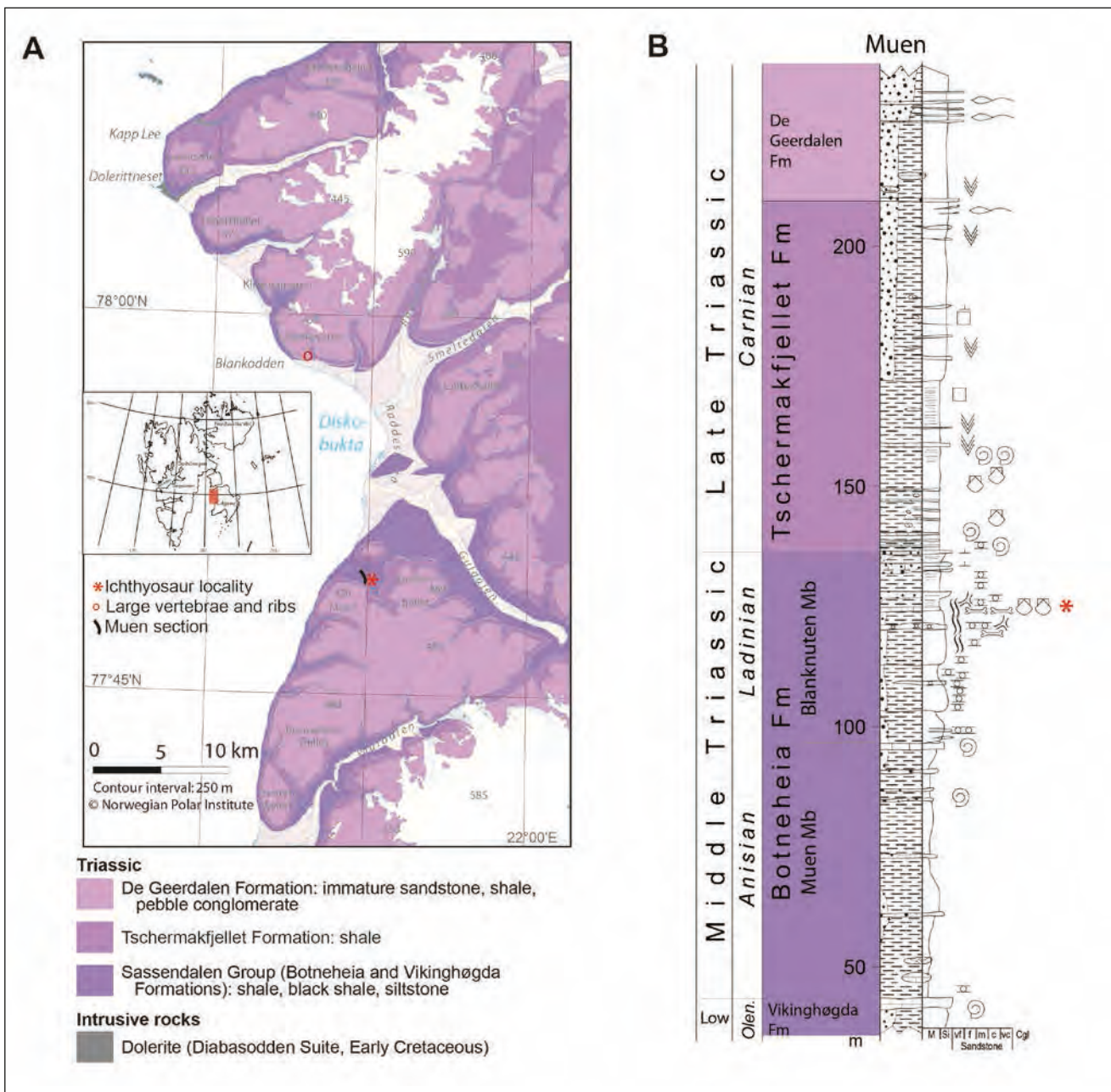


Figure 1. A. Geologic map of studied area at Edgeøya. B. Stratigraphic column of the Muen Section.

years, the Norwegian Petroleum Directorate (NPD) has worked on the geological sections as part of understanding of the Barents Sea area, in cooperation with Russian colleagues from VNIIOkeangeologia (All-Russia Research Institute for Geology and Mineral Resources of the World Ocean) and the Geological Institute, Russian Academy of Science on terrestrial and marine geology and geophysics. SINTEF Petroleum Research has participated as scientific and logistic supervisor. Other academic institutions have also been invited on the yearly expeditions (since 2006) and have contributed to the interpretation of results.

During the 2007 expedition, the team worked on a plateau at Muen, a mountain on western Edgeøya (Fig. 1), and discovered several bluish bones of ichthyosaurs. An articulated skeleton was found by the two Russian geologists Andrey Fedyaevskiy and Pavel Luner and the Polish geologist Krzysztof P. Krajewski (photo in Krajewski, 2008, fig. 9E). Further skeletons and articulated bones were also discovered by other members of the group, and were GPS marked for possible excavation the following summer. As a co-operation between NPD, The Natural History Museum of Oslo and SINTEF Petroleum Research, permission from the Governor of Svalbard (Sysselmannen) was granted

to collect the skeletons. In 2008, one of us (HAN), with assistance from the remainder of the field group (AM and JAS) excavated the ichthyosaur. The skeleton described in this paper was collected together with several other parts of ichthyosaurs and other fossils (bivalves and ammonoids).

### Triassic ichthyopterygians from Svalbard

Ichthyopterygians, the group including the less inclusive clade Ichthyosauria and their Early and Middle Triassic ancestors, were a group of globally distributed marine reptiles which thrived during the Mesozoic (Motani, 1999a). Ichthyopterygians evolved from a group of terrestrial diapsid amniotes, which adapted towards aquatic lifestyle during the Permian/Triassic transition and were fully marine by the Early Triassic (Sander, 2000; Maisch and Matzke, 2002). The Triassic ichthyosaurs show great variability in body shape and size (Sander, 2000; Motani, 2005). Although some species of Triassic ichthyosaurs show traces of their terrestrial heritage, they developed a mosaic of increasingly specialized adaptations to marine life through the Triassic (Motani et al., 1996).

The Triassic ichthyopterygian assemblages of Svalbard were recently summarized and discussed by Maxwell and Kear (2013). Of the numerous named ichthyopterygian taxa from the Triassic of Svalbard, Maxwell and Kear (2013) only regard *Grippia longirostris*, *Pessopteryx nisseri*, *Quasianosteosaurus vikinghoegdai*, *Omphalosaurus* sp., *Isfjordosaurus minor*, *Phalarodon* cf. *callawayi* and *Phalarodon* cf. *fraasi* as potentially valid. However they also recognized some additional morphologically differentiated specimens such as *Cymbospondylus* (Sander, 1992), the toretocnemid reported by Maisch and Blomeier (2009) and the shastasaurid formerly recognized as *Pessosaurus polaris* (sensu Sander and Faber, 1998).

The ichthyopterygian fossils from Svalbard are found in beds which span the Early to earliest Late Triassic and can be stratigraphically divided into six horizons, with age estimates from Mørk et al. (1999). Only selected papers are listed here; for a more complete publication list see Maxwell and Kear (2013).

1. "Fish Niveau" Lusitaniadalen Member, Vikinghøgda Formation, early Olenekian (Smithian): only isolated material (Wiman, 1933).
2. "Grippia Niveau" Vendomdalen Member, Vikinghøgda Formation, late Olenekian: *Quasianosteosaurus vikinghoegdai* Maisch and Matzke, 2003 and *Grippia longirostris* Wiman, 1928, Motani (1998, 2000).
3. "Lower Saurian Niveau" Vendomdalen Member, Vikinghøgda Formation, late Olenekian: *Pessopteryx nisseri* Wiman, 1910, *Isfjordosaurus minor* Motani, 1999a, and *Omphalosaurus* sp. (Wiman, 1910). Based on a tooth, the presence of a mixosaurid was reported

from core 7327/07-U-04 by Mørk and Elvebakk (1999) from the Svalis Dome, in the central Barents Sea. This core is dated as late Olenekian (late Spathian) (Vigran et al., 1998).

4. Lower Botneheia Formation (Anisian): a toretocnemid reported by Maisch and Blomeier (2009), *Phalarodon* sp. (Maxwell and Kear, 2013).
5. "Upper Saurian Niveau" Blanknuten Member, uppermost Botneheia Formation and the boundary beds to the Tschermakfjellet Formation, late Ladinian–early Carnian: *Phalarodon* cf. *callawayi* and *Phalarodon* cf. *fraasi*. (Hulke, 1873; Merriam, 1910; Wiman, 1910; Schmitz, 2005; Schmitz et al., 2004), a shastasaurid formerly recognised as *Pessosaurus polaris* (sensu Sander and Faber, 1998) and *Cymbospondylus* sp. (Sander, 1992).

### The Mixosauridae of Svalbard

The most common Middle Triassic ichthyosaurs are those belonging to the family Mixosauridae (Baur, 1887). The family Mixosauridae is diagnosed primarily on differences in limb and tooth structure (see systematic palaeontology section). Mixosaurids had a wide distribution including Canada, China, France, Germany, Timor, New Zealand, Poland, Russia, Svalbard (Norway), Switzerland, Turkey and the United States (McGowan, 1978; Mazin, 1983a, b; 1988; Zammit, 2010; Callaway and Massare, 1989; Sander and Mazin, 1993). Most mixosaurids are of Middle Triassic age, although undiagnostic fragments of *Mixosaurus* sp. have been reported from the Early Triassic of Canada (Callaway and Brinkmann, 1989). They are seen as an intermediate between the primitive Triassic and the more derived Jurassic body forms (Motani, 2005). Despite retaining several primitive morphological characters, mixosaurids show evidence of viviparous behavior (Brinkman, 1996). Until recently, Mixosaurids were the earliest indication of such a trait in ichthyopterygians. The recent discovery of embryos in the 248 million year old basal ichthyopterygian *Chaohusaurus geishanensis*, has pushed the evolution of this behavior back even further (Motani et al., 2014). Some of the first ichthyosaurs from the Triassic worldwide were collected by the Nordenskiöld expeditions in 1864 and 1868. The fossils, from what is now known as the Blanknuten Member of the Botneheia Formation, were described by Hulke in 1873. Hulke assigned the very fragmentary material to two new species, a large form named *Ichthyosaurus polaris* and a smaller one *Ichthyosaurus nordenskiöldii*. The two vertebral series of *Ichthyosaurus polaris* have a long history of different affinities since the first description are now recognized as material belonging to *Shastasauridae* indet (see discussion and references in Sander and Faber, 1998, and Maxwell and Kear, 2013). Dames (1895) referred the smaller species, *Ichthyosaurus nordenskiöldii*, to *Mixosaurus*. The better material found in 1908 and 1909 and described by Wiman in 1910 was also attributed to *Mixosaurus nordenskiöldii*, but Merriam in the following year identified jaw



fragments of *Phalarodon fraasi* among the specimens figured (Merriam, 1911). In 1916 Wiman summarized the findings and agreed with Merriam (Wiman, 1916 b). Several mixosaurid species have been described and these have been synonymized and reinstated over the years (Callaway, 1997; McGowan and Motani, 2003; Jiang et al., 2006). The review by McGowan and Motani (2003) recognized five species: *M. avatus* (Quenstedt, 1852), *M. nordenskiöldii* (Hulke, 1873), *M. cornalianus* (Bassani, 1886), *M. fraasi* (Merriam, 1910) and *M. kuhnschnyderi* (Brinkmann, 1998). In Jiang et al. (2006) and Liu et al. (2013) there is a disagreement on the genera and species definitions, but they both separate the family Mixosauridae into two genera, *Mixosaurus* and *Phalarodon*. Jiang et al. (2006) propose that the genus *Mixosaurus* contains three species; *M. cornalianus*, *M. kuhnschnyderi* and *M. panxianensis*. The second genus *Phalarodon* is often synonymized with *Mixosaurus* (see e.g. Schmitz et al., 2004), but proposed as a separate genus by Jiang et al. (2006) and later discussed in detail by Liu et al. (2013), with three species *P. avatus*, *P. callawayi* (Schmitz et al., 2004) and *P. fraasi* (Merriam, 1910).

The validity of *Mixosaurus nordenskiöldii* has been debated for many years and this is now considered a nomen dubium, due to non-diagnostic type material (see discussion in Schmitz, 2005). Schmitz (2005) attributed all Svalbard mixosaurids to *Phalarodon fraasi* and *P. callawayi*, on the basis of differing height to length ratio of vertebrae centra. This attribution was later followed by Maisch (2010). Maxwell and Kear (2103)

noted inconsistencies in the dentition between the type material of *P. fraasi* from Nevada and the Svalbard material, but regarded the Svalbard material of *P. fraasi* and *P. callawayi* to be potentially valid; we briefly discuss the problematic taxonomy of *Mixosaurus nordenskiöldii* in this paper.

## Geological setting

The exposed strata on Edgeøya consist entirely of rocks of Triassic age (Fig. 1) from the Sassendalen and Kapp Toscana groups, except for two small areas eroded down into the top Permian. Falcon (1928) named the dark shales at the island the Oil Shale member (now the Botneheia Formation) with its overlying Purple shale (Tschermafjellet Formation). Detailed fieldwork in 1969 resulted in a map and short description (Flood et al., 1971), which extended the Triassic stratigraphic nomenclature from Spitsbergen with minor modifications. A more thorough description, based on the same work, was later used to define a local stratigraphy for Barentsøya and Edgeøya (Lock et al., 1978). This scheme was further modified by Mørk et al. (1982) as they focused on the similarities of these two islands with the surrounding islands. In the revision of Svalbard's post Caledonian succession, Mørk et al. (1999) coordinated these earlier stratigraphical schemes to demonstrate the similarities and differences between the different areas of Svalbard (Fig. 2).

The Sassendalen Group of Early to Middle Triassic

AGE		Group	Spitsbergen			Edgeøya
			Horn-Sørk.	West	Central	
TRIASSIC	Late	Kapp Toscana	Isfjorden Member			eroded
			De Geerdalen Formation			
			Tschermafjellet Formation			
	Middle	Sassendalen	Van Keulenfjorden Mb.	Bravais-berget Fm.	Blanknuten Member	Botneheia Formation
			Somovbreen Mb.		Muen Member	
			Karentoppen Mb.			
			Passhatten Mb.			
	Early	Sassendalen	Tvillingodden Formation		Vendomdalen Mb.	Vikinghøgda Fm.
			Vardebukta Formation		Lusitaniadalen Mb.	
	Induan		Hiatus	Deltadalen Mb.		Hiatus

Figure 2. A correlation of the stratigraphic formations and groups of the Triassic of Svalbard (modified from Mørk et al., 1999).



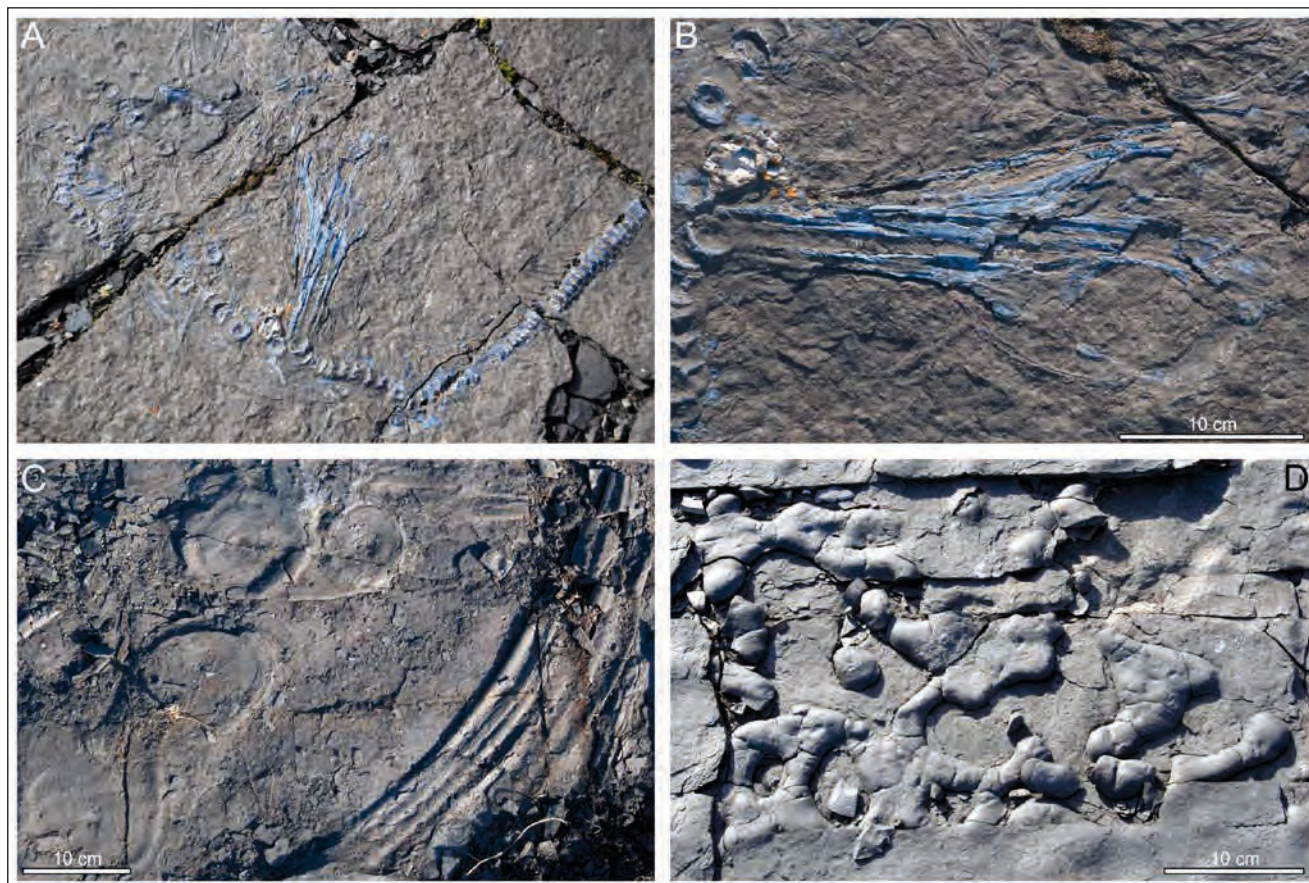


Figure 3. A. Specimen PMO 219.250 before excavation. B. Skull of PMO 219.250 before excavation with abundant bivalves around (*Daonella*). C. Ribs and imprints of vertebrae from a large ichthyopterygian from the same level (not excavated). D. Typical trace fossils from the level of the skeletons (*Thalassinoides*).

age is dominated by dark grey and black shales, and therefore Lock et al. (1978) grouped these units in the Barentsøya Formation. This scheme was retained by Mørk et al. (1982). During the total revision of the Mesozoic stratigraphy of Svalbard Mørk et al. (1999) again separated out the Botneheia Formation, as a practical mapping unit that also can be followed offshore. For Edgeøya and Barentsøya, Krajewski (2008) has given a thorough description of the formation, redefined type localities, and erecting the lower Muen Member overlain by the revised Blanknuten Member, and this subdivision is followed herein.

The ichthyopterygians recovered in 2008 on Edgeøya are found in the uppermost part of the Botneheia Formation (Figs. 1, 2). Lock et al. (1978) were the first to report the presence of vertebrate remains in this unit on Edgeøya, noting mainly ichthyosaur vertebrae. Fish fossils also occur in the laterally equivalent Bravaisberget Formation, and are irregularly dispersed throughout the Sassendalen Group (Mørk et al., 1982). All the articulated specimens described herein are from one level high in the Botneheia Formation (Figs. 1, 3). Most specimens have relatively small vertebrae, but a specimen found by AM in 1979 at Blanknuten has several large ribs and vertebrae ca. 10 cm in diameter. Large vertebrae were also observed by JAS just

above the specimen described in this paper (Fig. 3C). The association of fossils in the upper part of the Botneheia Formation demonstrates a special taphonomic environment. Very high organic content, from 8 to 12 % organic material for the upper part of the Blanknuten Member, was demonstrated by Mørk and Bjørøy (1984), and Brekke et al. (2014). Vigran et al. (2008) have shown that much of this organic material is derived from algae, mainly *Tasmanites*. The high organic content in the sediment, abundant *Thalassinoides* and a rich benthic fauna of bivalves (*Daonella*) indicate alternating anoxic and oxic conditions, as suggested by Mørk and Bromley (2008). Similar variations in bottom conditions have also been suggested by Krajewski et al. (2007) for the time equivalent unit along western Spitsbergen, and for Edgeøya by Krajewski (2008).

## Material and methods

### Fieldwork

An application from the Natural History Museum, University of Oslo, was sent to the Governor of Svalbard in 2008 to obtain permission to collect and conserve the ichthyopterygian fossils. Permission was granted (2008/00489-3 a.512).

The collection and field conservation of the fossils met two major challenges: frost weathering causing congelifraction made the fossilized bones rather brittle, and the compaction of the shale beds during diagenesis had also compressed and fractured them.

The commonly used vertebrate paleontological excavation technique to embed the bones and surrounding sediments in field jackets made of plaster and burlap was selected, in order to reduce further breakage during transport from the field to the laboratory. The studied specimen, occupying approximately 1.4 m x 1.1 m, was split in seven parts to make it possible to carry it from the field to the expedition ship. It was mainly split along natural fractures or using a knife. The bed housing the fossils is 5-10 mm thick.

The collected material comprises:

- Specimen 1. The main specimen, PMO 219.250 (described in this paper, Figs. 3A, B, 4).
- Specimen 2. A vertebral column and a collection of weathered ribs and gastralia.
- Specimen 3. A long vertebral column (33 vertebrae and 39 imprints of eroded vertebrae).
- Specimen 4. Scattered vertebrae and bones from the shoulder and lower jaw.
- Specimen 5. A vertebral column and heavily weathered skull and (jaw) bones with eroded teeth.

All specimens, in part split, were embedded in plaster and enforced with bandage and metal rods.

The main specimen (PMO 219.250), nick-named "ODa", was selected for subsequent laboratory preparation and description. This is an acronym for Oljedirektoratet (The Norwegian name of the Norwegian Petroleum Directorate) which supported the excavation and preparation of the specimen.

### Laboratory work

The main specimen was prepared at the Löwentor Museum in Stuttgart, Germany, by technician May-Liss Knudsen Funke (NHM, Oslo) under the supervision of Dr. Rainer Schoch and technician Isabell Rosin. The slabs were strengthened with polyester and fibre glass on their back side before being transported to Germany. The fossil and surrounding shale was very fragile and it was decided to use a sandblasting technique to remove rock matrix from the bones. Iron particles smaller than 0.2 mm were used and the work carried out under a Leitz Wild M3Z binocular microscope. A vibrotool was used in places where the sandblasting was unsuccessful. The bones were reinforced with "pioloform" (polyvinylbutyral) after the mechanical preparation.

The characteristic blue colour of the bones, caused by surface mineralization of vivianite, a hydrated iron phosphate, during years of frost weathering was lost

during the sandblasting process (Figs. 3A, B and 4 for comparison before and after treatment).

### *Institutional abbreviations:*

- FMNH Field Museum of Natural History, Chicago, USA.
- PMO Palaeontological museum, Natural History Museum, University of Oslo, Norway.
- PMU Palaeontological Museum, University of Uppsala, Sweden.

## Description

### Systematic Palaeontology

Family Mixosauridae Baur, 1887

Subfamily Mixosaurinae Baur, 1887

Specimen PMO 219.250 is a partially articulated medium-sized mixosaurid ichthyosaur from the Middle Triassic of Edgeøya, Svalbard (Fig. 4). It is flattened laterally and is in a curled up position as the skull is disarticulated from the rest of the axial skeleton. It is preserved in seven slabs labeled 1-7. Slab 1 (PMO 219.250/1) consists of vertebrae, a partial femur, and an impression of a femur with a partial paddle and numerous rib fragments. Slab 2 (PMO 219.250/2) consists of tail vertebrae along with several neural arches. Slab 3 (PMO 219.250/3) consists of articulated and disarticulated tail vertebrae. Slab 4 (PMO 219.250/4) consists of the skull, vertebrae, neural arches, ribs and gastralia. Slab 5 (PMO 219.250/5) consists of rib fragments and part of forefin. Slab 6 (PMO 219.250/6) consists of individual ribs and possible gastralia (not figured). Slab 7 (PMO 219.250/7) contains a partial pectoral girdle, two partial forefins, vertebrae and ribs. The articulated skeleton is estimated to have been 170-180 cm long, based on skull length and the vertebral column compared to other well known mixosaurids (see e.g. Sander, 2000; Maisch and Matzke, 2000; McGowan and Motani, 2003; Schmitz et al., 2004; Jiang et al., 2006; Liu et al., 2013).

### *Skull*

The skull has undergone ventral-lateral compaction, resulting in a flattening of all elements of the cranium and mandible. The right lateral and ventral side of the skull is visible, although most of the individual elements are in too poor condition to be described. See Table (1) for individual skull measurements.

*Dermatocranium* - The premaxilla is the dominant rostrum element, terminating posteriorly at the ventral and anterior border of the external naris. It bears small teeth with enamel ridging throughout the entire length, with little room between the individual teeth. It overlaps the maxilla in line with the external naris. The dorsal process of the maxilla is eroded, but it appears to exclude the lacrimal from the external naris, forming the posterior border. It bears large conical teeth, larger





Figure 4. The specimen PMO 219.250. A. prepared skeleton on slabs 1-5 and 7. Slab 6 is not figured as only a few disarticulated ribs were present. B. Schematic drawing of the skeleton. Abbreviations: cl-clavicula, f-femur, fi-fibilla, h-humerus, i-intermedium, lac-lacrimal, mx-maxilla, pmx-premaxilla, r-radius, ra-radiale, sa-surangular, sc-scapula, ti-tibia, u-ulna, ul - ulnare.



**Table 1.** Selected skull element measurements of PMO 219.250.

Selected skull element measurements	mm
Preserved skull length (Postorbital to preserved anterior of premaxilla)	280
Anteroposterior length of orbit	66
Maximum dorsaventral height of orbit	58
Anteroposterior length of postorbital bar	21
Preserved length of lower jaw (right)	310
Jugal length	~70
Maximum height of the posterior ramus	9
Articular anteroposterior length	12

than the teeth present in the premaxilla. There are significantly fewer teeth in the maxilla than in the premaxilla. Posteriorly it contacts the jugal, just ventral to the lacrimal. The lacrimal forms the anteroventral border of the orbit. It is small and somewhat eroded, missing the dorsal edge. There is no contact with the external naris. The external naris is anteroposteriorly longer than dorsoventrally high, measuring 21 mm in length and 3 mm in maximum height. The nasal is severely eroded and only the part in line with the external naris is preserved. However, there is a possible trace of a nasal terrace present. The prefrontal is almost entirely eroded and only the posterodorsal part is preserved, forming part of the orbital rim. There is no frontal preserved. The jugal is present as a gracile bar, forming the ventral part of the orbital rim. It articulates with the lacrimal anterodorsally and the maxilla anteriorly. The posterior terminal end articulating with the postorbital is missing. However, an impression is present and appears broad. The postfrontal is present although partially eroded, forming the posterodorsal border of the orbital rim. The postorbital appears to be a broad element, covering the other elements in the postorbital region. It is overlapped by the postfrontal anterodorsally and an eroded element which is either the squamosal or the supratemporal posterodorsally. An element possibly representing part of the parietal is present in the posterodorsal region of the skull. A disarticulated imprint of the basioccipital is also present, posterior to the skull.

**Mandible** - The dentary stretches along the rostrum and terminates posteriorly in line with the external naris, although it is partially covered by the splenial due to the ventral-lateral compaction. The element bears small conical teeth, set in sockets, throughout the entire length of the rostrum. There is little to no room between the individual teeth, except in the posteriormost region. The surangular is a robust element, dominating the mandible, appearing to extending anteriorly past the level of the bony nasal aperture. The surangular appears to form the posterior ramus of the lower jaw with the angular, however it is difficult to interpret how much is due to

the preservation. There is no sign of a coronoid process. The angular is a small element in comparison to the surangular, making up the posteroventral region of the mandible. An articular is also preserved disarticulated posterior to the mandible, which is rounded in shape laterally.

## Appendicular skeleton

**Pectoral girdle** - There are several pectoral girdle elements preserved in Slab 7. The element in partial articulation with the left forefin represents a scapula. It appears to have been twisted 180 degrees. A second scapula impression is present in the proximity of the right forefin. The scapula bears two long extensions, one towards the anterior, the other posterior with a short glenoid process in between. A small element which could represent part of the clavicle is present, but due to the poor preservation this is equivocal.

**Forefin** - Two forefins are preserved in PMO 219.250, in slabs 5 and 7 (Fig. 4). They appear to be in ventral view. The left forefin is lying close to the articulated vertebral column. The right forefin is split between slabs 5 and 7. See Table 2 for selected forefin and hind fin measurements.

**Table 2.** Selected fore- and hind fin measurements of PMO 219.250.

Humeral measurements	Left in mm	Right in mm
Maximum proximodistal length	44	49
Maximum anteroposterior width, proximal end	?	29
Maximum anteroposterior width, distal end	~42	?
Length of ulnar facet	16	18
Length of radial facet	~26	?
Maximum height of the posterior ramus	9	9
Articular anteroposterior length	12	12
Autopodium measurements	Left in mm	Right in mm
Anteroposterior width of radiale	31	?
Proximodistal length of radiale	19	?
Anteroposterior width of intermedium	20	?
Proximodistal length of intermedium	20	23
Anteroposterior width of ulnare	14	18
Proximodistal length of ulnare	15	19
Femoral measurements	Left in mm	Right in mm
Maximum proximodistal length	35	36
Maximum anteroposterior width, proximal end	~17	12
Maximum anteroposterior width, distal end	?	26
Length of tibial facet	19	?
Length of fibular facet	?	10

The left forefin includes a humerus, with distally articulating radius and ulna and several autopodium elements. Details of the proximal end are not available due to coverage by scapula. The right forefin includes a humerus, distally articulating radius and ulna, proximal carpal elements and several phalanges. The humerus is proximodistally longer than anteroposteriorly wide. There is an extensive unnotched anterior flange (see Jiang et al., 2005). The humeri bear deltopectoral crests on the anteroventral surface, starting at the proximal margin and twisting posteriorly down the shaft. The distal surface bears two facets for the radius and ulna, the latter of which is the smaller (Table 2). The two facets are offset and enclose an angle of approximately 115 degrees. The radius and ulna are preserved in partial articulation with the humerus and distal elements. The proximal edge of the radius forms a straight facet to meet the humerus. The anterior edge is straight, ending in a point distally. The anterior edge bears a notch close to the proximal end. It is unlikely that the radius and the ulna had any proximal contact, due to the edge of the humerus separating the two facets. The posterior edge of the radius appears to be straight. There is a small spatium interosseum between the two elements, not as large as in other mixosaurids (see e.g. Maisch and Matzke, 2000), as only the ulna bears a concave edge. The distal surface of the radius bears a long straight facet for the radiale and a significantly smaller posterior facet for the intermedium. The proximal edge of ulna forms a straight facet for the posterodistal humeral facet. The ulna is concave anteriorly and convex posteriorly. The distal end bears two facets of similar size for the intermedium and ulnare. The posteroproximal part of the ulna is drawn out into a point-like projection.

The carpal series in the right forefin are near complete, lacking only the fifth metacarpal series and the most distal elements. There are three proximal carpals, the radiale, the intermedium and the ulnare and four preserved distal carpals although a fifth seems likely. The autopodium elements are better preserved in the left forefin and are less flattened. Individual measurements of the proximal elements are available in Table 2. The radiale is preserved on both fore fins. It is rectangular in shape, but with a small notch-like facet posterodistally. The radiale is anteroposterally wider than the intermedium and the ulnare and has two distal facets for the first and second carpals. The intermedium is polygonal with two proximal facets for the radius and ulna. The intermedium separates the ulna and radius by having a small proximal point between the two elements. It has two clear distal facets for third and fourth distal carpal. A small anteroproximal notch is present in the intermedium. The ulnare is rounder in shape than the other proximal carpals. The pisiform is rather large and square. It has two distal facets for the fourth and fifth carpals. The distal carpals are of similar size and square in shape. The first metacarpal series is the most complete, with five phalanges.

*Hind fin* - Two partial hind fins are preserved in specimen PMO219.250 in slabs 1 and 4, comprising mainly impressions and partial fragments of elements (Table 2). The hind fin furthest from the vertebral column in the bottom right of Fig. 4 consists of a single femur. An element which could represent the tibia was located distally to this femur, but was lost during excavation (see Fig. 4). This femur is the more complete of two, and based on a partially eroded mid-centered process appear to be exposed on its ventral side. The distal end of the femur has two facets for the tibia and fibula. As the anteriormost facet is the tibia, this femur is interpreted to be the left. The hind fin closest to the vertebral column is therefore interpreted to be the right. The right femur comprises of a fragment and an impression of the remaining part of the femur spread on both slabs (1 and 4). The element articulating to the right femur, which also comprises a partial impression and fragments, is interpreted to be the tibia, because the articular surface is broad and contacts the largest femoral facet, as well as on the basis of its size and the general morphology. There is another preserved element articulating distally to the tibia. This element is rectangular in shape and is significantly smaller than the tibia. A fibula is present articulating to the left femur, represented partially by bone and impressions. It appears to have an anterior notch along its anterior margin, proximal from the astragalus facet.

### Axial skeleton

*Vertebrae* - The preserved vertebral column consists of 86 complete to partial vertebrae (See Table 3 for details). One was removed during preparation to expose more of the forefin. Six impressions of vertebrae were also observed, giving a total of 92 vertebrae. There are 48 presacral vertebrae preserved (including the impressions and the removed vertebrae). The vertebrae anterior to the pectoral girdle are all disarticulated, and some of the cervical vertebrae, including the atlas-axis,

**Table 3.** Number of vertebrae identified on slab 1-7 of PMO 219.250.

Slab	Vertebral count	Vertebral impressions
PMO 219.250/6	0	0
PMO 219.250/7	27	0
PMO 219.250/5	0	0
PMO 219.250/4	19	1
PMO 219.250/1	13	0
PMO 219.250/2	15	2
PMO 219.250/3	11	3
Removed during prep. from PMO 219.250/7	1	0
Total	86	6
Sum	92	

**Table 4.** Measurements of all vertebrae.

Vertebrae number from pectoral region	Dorsal-ventral height	Anterior-posterior length	Height/length
1	2.20	1.30	1.69
2	2.30	1.40	1.64
3	2.30	1.30	1.77
4	2.20	1.20	1.83
5	2.20	1.20	1.83
6	2.20	1.50	1.47
7	2.50	1.50	1.67
8	2.70	1.50	1.80
9	2.50	1.60	1.56
10	2.50	1.60	1.56
11	?	?	?
12	?	?	?
13	?	?	?
14	?	?	?
15	2.00	1.20	1.67
16	?	?	?
17	2.50	1.30	1.92
18	2.50	1.40	1.79
19	?	?	?
20	2.20	?	?
21	2.30	?	?
22	2.40	?	?
23	2.20	?	?
24	2.30	1.60	1.44
25	2.20	1.30	1.69
26	2.10	1.30	1.62
27	2.40	1.30	1.85
28	2.20	1.30	1.69
29	?	?	?
30	2.30	?	?
31	?	?	?
32	?	?	?
33	?	1.30	?
34	?	1.20	?
35	?	?	?
36	?	1.10	?
37	2.10	1.10	1.91
38	?	1.20	?
39	2.20	1.20	1.83
40	2.10	1.20	1.75
41	2.00	1.20	1.67
42	2.00	1.20	1.67

appear to be missing. This number is consistent with the estimates by Sander (2000) of 45-50 presacral vertebrae for mixosaurids. There are 44 postsacral vertebrae preserved (including the impressions), but the posteriormost caudal vertebrae are missing (See Table 4 for vertebrae measurements). By measuring the distance between slabs, it was estimated that there are at least three vertebrae missing between slabs 5 and 7 and three missing between slabs 2 and 3. Depending on how many of the posteriormost caudal vertebrae and the anteriormost cervical vertebrae are missing, between 10-20 vertebrae are estimated to be lost based on the estimate of Sander (2000).

Each articulated vertebra was measured at its maximum dorsal-ventral height at the anterior end, and the measurements plotted in a graph using PAST (Hammer et al., 2001). The results are presented in Fig. 5). Vertebrae that could not be measured due to erosion and vertebrae missing between slabs were taken into account to give a more correct picture of the dorsal-ventral height change throughout the vertebral column. The figure clearly illustrates a higher dorsal-ventral height in mid-caudal region as is common for mixosaurids (Sander, 2000).

The vertebrae in the mid-caudal region (slab 2) are significantly dorsal-ventrally higher than the preceding vertebrae. These vertebrae also appear to have widely spaced intervertebral joints between the centra of each vertebra, which are now filled with sediment. Some of these intervertebral joints are up to 3.5 mm wide and are prominent in all the mid-caudal vertebrae. There are no clear gaps between the centra at the intervertebral joint in the anterior vertebrae.

*Neural arches* - Several neural arches are preserved from various regions of the axial skeleton, most being from the anterior region of the axial skeleton. These are distinctively tall compared to the height of the dorsal vertebrae, being approximately twice the height in the trunk region (Table 3). These appear robust at the base of the spine, but thin out towards the terminal end. Impressions of neural arches around the sacral region show the spines are slightly reduced in size and robustness. This is, however, equivocal because of the poor preservation of the neural arches in this region. In the mid-caudal region where the vertebrae increase in dorsal-ventral height, the neural arches also appear to be long, densely packed and thin in comparison to the anterior trunk neural arches.

*Ribs* - Numerous rib fragments are preserved in specimen PMO 219.250, and several chevrons in the mid-caudal region are complete.

*Gastralia* - Several small gastralia fragments are present in slab 7; these are about half the thickness of the ribs and appear more rounded. There are also several impressions present in slab 6, which are a third of the thickness of the ribs.



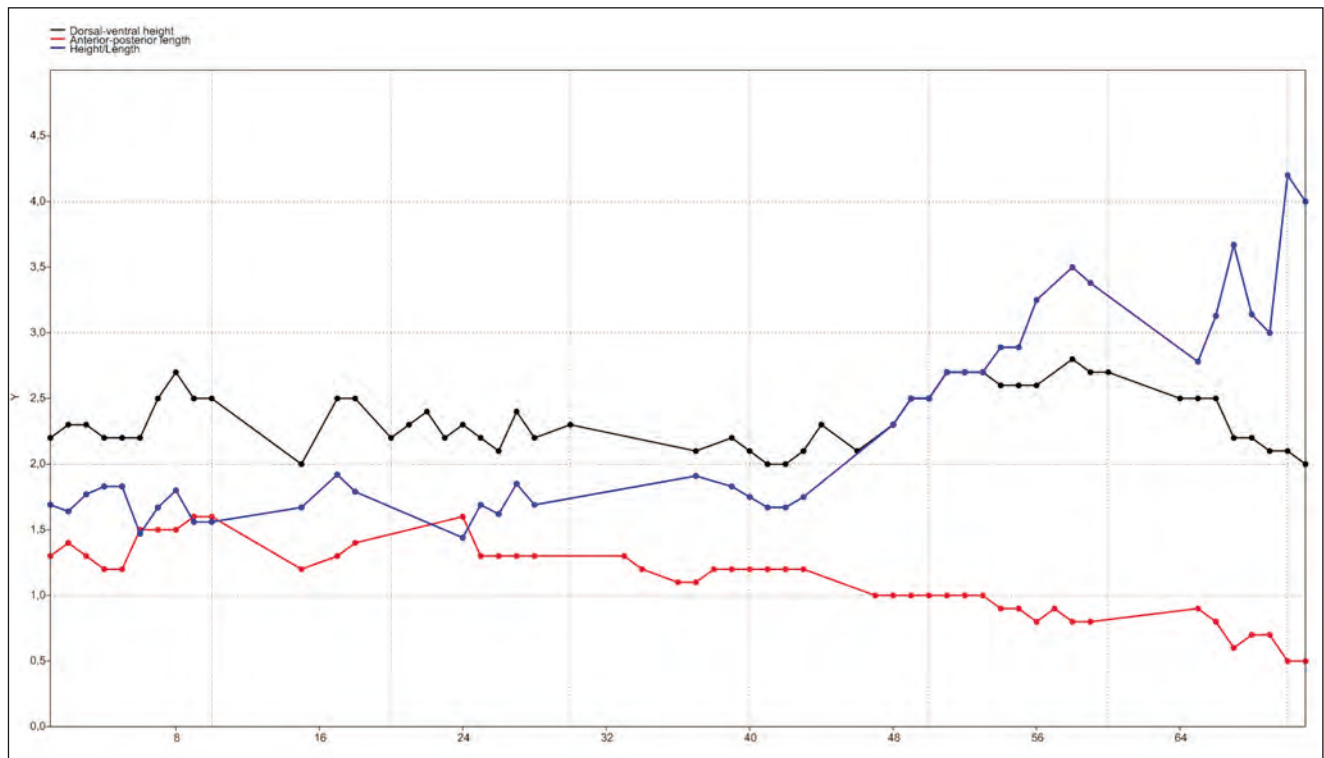


Figure 5. Graph illustrating dorsal-ventral height (black), anterior-posterior length (red) and the height/length ratio of the articulated vertebrae from the pectoral region to the caudal region of PMO 219.250. Vertebrae that could not be measured due to erosion and an estimated number of vertebrae lost between the slabs have been taken into account.

## Discussion

PMO 219.250 can be placed confidently in the family Mixosauridae on the basis of the following synapomorphies (taken from Liu et al., 2013 and references therein), which the specimen shares with members of the family:

- The premaxilla is posteriorly pointed.
- Distinctively high and narrow neural spines extend to the caudal peak.
- Mid-caudal vertebral centra have increased size (absent in some specimens of *M. cornalianus*).
- Posterior teeth are more robust than anterior ones (convergent in *Chaohusaurus* and *Grippia* and absent in *M. cornalianus* and *Phalarodon avatus*).
- Distal carpal 1 is slightly larger than other distal carpals.
- Humeri are relatively short but still retain constricted shafts (Sander, 2000; Maisch, 2010; Maisch and Matzke, 2000; McGowan and Motani, 2003; Schmitz et al., 2004; Jiang et al., 2006; Liu et al., 2013).
- Posterior dorsal and anterior caudal vertebrae are dicephalous (Nicholls et al., 1999).

Other characters that are shared with most mixosaurids are:

- The lacrimal has no contact with the external naris, similar to other Triassic mixosaurids (Schmitz et al., 2004; Jiang et al., 2005; Liu et al., 2013).
- The humerus has an extensive unnotched anterior flange, common in mixosaurids (Jiang et al., 2005).

*Skull* - The elements of the rostrum of specimen PMO 219.250 are displaced, and in some places covered by palate elements. Identifying the individual elements is therefore challenging. The premaxilla forms the anterior border and anteroventral border of the external naris, as in *P. avatus* and *P. callawayi* (Schmitz et al., 2004). This is different from *M. panxianensis* where although bordering the anterior region, the premaxilla does not form a subnasal process and the maxilla forms the entire ventral border of the external naris (Jiang et al., 2006). As with most mixosaurids, the maxilla excludes the lacrimal from externally bordering the external naris, with a postnasal process (Schmitz et al., 2004; Jiang et al., 2005; Liu et al., 2013). The external naris is located dorsally 50 mm anterior to the orbital rim, which is further anteriorly than most other members of the genus *Phalarodon* (Schmitz et al., 2004; Jiang et al., 2007; Liu et al., 2013). Little of the nasal is preserved on specimen PMO 219.250, so comparison is difficult. However there does appear to be a partial nasal terrace above the external naris, as in *Phalarodon* sp. (Liu et al., 2013). The lacrimal articulates ventrally with the jugal and the maxilla, as in *M. panxianensis* (Jiang et al., 2005, 2007). Even though the posterior region of the skull of PMO 219.250 is poorly preserved, the jugal has a broad articulating ramus to the postorbital similar to *P. fraasi*, but dissimilar to *M. panxianensis* which has a short posteroventral process (Jiang et al., 2005, 2006, 2007).

**Mandible** - The mandible of PMO 219.250 is so crushed and disarticulated that comparison is difficult. The dentary stretches along the rostrum and terminates in-line with the external naris, unlike *P. fraasi* where it ends posteriorly in-line with the anterior region of the orbit (Jiang et al., 2007). As in *P. fraasi* the surangular terminates anteriorly past the last tooth (Jiang et al., 2007). There is no presence of a coronoid process on the surangular as in *P. fraasi*, *M. cornalianus* and *M. kuhnschnyderi*, unlike the prominent coronoid process of *P. callawayi* (Schmitz et al., 2004).

**Dentition** - Similar to many of the members of the family, the maxilla bears more robust, conical, blunt teeth compared to the premaxilla dentition (Motani, 1997; Jiang et al., 2005; Liu et al., 2013). There is no sign of multiple maxillary tooth rows, but this may be due to poor preservation. The premaxilla bears smaller needle-like teeth, which are closely spaced as in *P. fraasi*, and unlike the widely spaced teeth of *M. panxianensis* and *M. nordenskiöldii* (Schmitz, 2005; Jiang et al., 2006, 2007). The teeth are set in sockets in the premaxilla and dentary similar to in *P. fraasi*, *P. avatus* and *P. callawayi* (Schmitz et al., 2004; Jiang et al., 2007; Liu et al., 2013), unlike *M. panxianensis* and *M. cornalius* where teeth are located in a dental groove (subthecodont) (Maisch and Matzke, 1997; Jiang et al., 2005).

**Appendicular skeleton** - The humeri are proximodistally longer than anteroposteriorly wide, as in *Phalarodon* (Jiang et al., 2006). There is an extensive anterior flange that lacks evidence of notching similar to *M. panxianensis*, unlike in *P. avatus* which has a weak notch (Jiang et al., 2006; Liu et al., 2013). There are two distal facets for the radius and ulna as in *M. panxianensis*, in contrast to the three distal facets of *P. avatus* (Liu et al., 2013). The anterior edge of the radius bears a notch close to the proximal end, whereas in *M. panxianensis* and *P. callawayi* there are two notches on the leading edge of the shaft (Jiang et al., 2006). The spatium interosseum is smaller than in other mixosaurids, as the posterior edges of radii shafts are straight (Jiang et al., 2005). The posterior margin of the ulna is rounded and convex as in *M. cornalianus*, while it is notched in *P. callawayi* (Motani, 1999b; Schmitz et al., 2004). As in *P. avatus* the radius facet of PMO 219.250 of the intermedium is significantly smaller than that for the radial. In contrast the intermedium proximal edge of *M. panxianensis*, has two equal facets for the radius and ulna. A small anteroproximal notch is present in PMO 219.250 and *P. avatus*. There are 5 distal carpals present in the described specimen as in *M. panxianensis*, whereas *P. avatus* has four distal carpals (Jiang et al., 2006; Liu et al., 2013). As in all mixosaurids the first distal carpal is the largest, and there are 5 metacarpal series (Maisch and Matzke, 2000).

The femora of PMO 219.250, as in *M. panxianensis*, *Phalarodon* and material described as *M. nordenskiöldii*

have two wide distal facets, where the tibia facet is the larger (Maisch and Matzke, 2000; Jiang et al., 2006; Liu et al., 2013). The anterior margin of the fibula of PMO 219.250 has an anterior notch as in *P. avatus* and *M. panxianensis* (Jiang et al., 2006; Liu et al., 2013).

**Axial skeleton** - There are 48 presacral vertebrae preserved in PMO 219.250; for mixosaurids this is rather high, considering that several of the cervical vertebrae are missing. Sander (2000) estimated that 40-50 presacral vertebrae are normal for mixosaurids, but this specimen could have up to 55. This may suggest a more undulatory movement than in other mixosaurids, as a reduction in this number is considered an adaptation to enhanced caudal propulsion (Motani et al., 1996). There are 44 postsacral vertebrae preserved in the described specimen, although the majority of the postflexural vertebrae are missing. An increase of the post-sacral vertebral count, thereby increasing the intervertebral joint count, increases the flexibility of the column (Buchholtz, 2001). The widely spaced mid-caudal intervertebral joints are not commonly observed, but are also present in the *Mixosaurus* sp. specimen FMNH PR 1804 from the Farvet Formation in the southern Tobian Range (USA) (Sander et al., 1994).

All previously described mixosaurid specimens from the Middle Triassic Blanknuten Member (also known as Upper Saurian niveau) have recently been referred to *Phalarodon callawayi* and *P. fraasi* (Schmitz, 2005; Maxwell and Kear, 2013; Schmitz et al., 2004). Schmitz et al. (2004) used the differing height to length ratio of the vertebral centra to discern between the two species. If we compare our plot (Fig. 5) to the plot made by Schmitz et al. (2004: fig 2), the specimen described here has a ratio of posterior dorsals closely comparable to *Mixosaurus cornalianus* and *M. nordenskiöldii* of 1.5-1.9. However, the mid caudal ratio extends to 4, while in *Mixosaurus cornalianus* and *M. nordenskiöldii* the ratio is about 2.5. The ratio of 3-4 for the mid caudals is between that of *P. callawayi* (up to 5) and the value cited for *Mixosaurus cornalianus* and *M. nordenskiöldii* in Schmitz et al. (2004).

The specimen from Svalbard designated as *P. callawayi* by Schmitz et al. (2004; PMU R 188) and figured by Wiman (1910: plate VI, fig. 1) consists of 59 posterodorsal and caudal vertebrae with a pelvic girdle and one hind fin. In size the specimen PMO 219.250 is similar, but the height to length ratios of the preserved vertebrae are significantly larger in PMU R 188. This could suggest either that PMO 219.250 is new species, or that there is more intraspecific variation in this region than previously anticipated; the latter explanation is considered to be more likely.

This specimen shows clearly the difficulties encountered when combining partial skeletons of mixosaurids and identifying species from partial individuals.

## Conclusion

PMO 219.250 resembles species referred to the genus *Phalarodon* (Merriam, 1910), based on the following synapomorphies (Jiang et al., 2007):

- Nasal region with pronounced narial shelf
- Maxillary teeth in sockets
- The premaxilla forms the anterior half of the ventral border of the external naris.

The specimen shares some anatomical traits with the previously described species from Spitsbergen (*P. fraasi* and *P. callawayi*), some of which could be synapomorphies. However, there are a number of differences between PMO 219.250 and the known species of *Phalarodon*, which suggests that the taxonomic relationships within Mixosauridae are more complex and less understood than previously anticipated. We refrain from erecting a new species, awaiting the preparation and description of the rest of the material collected from the site at Edgeøya.

### Acknowledgements.

Thanks to May-Liss Knudsen Funke and preparators at the Lowentor Museum in Stuttgart for doing a splendid job with a difficult specimen. Special thanks to NPD for inviting NHM to participate in the project and financing the field work and preparation.

Thanks to the two reviewers Benjamin Kear and David Worsley for constructive comments.

## References

- Bassani, F. 1886: Sui fossili e sull'età degli schisti bituminosi triasici di Besano in Lombardia. *Atti della Società Italiana di Scienze Naturali e del Museo Civico di Storia Naturale*, 29, 15-72.
- Baur, G. 1887: On the morphology and origin of the Ichthyopterygia. *American Naturalist*, 21, 15-72.
- Brekke, T., Krajewski, K.P. & Hubred, J.H. 2014: Organic geochemistry and petrography of thermally altered sections of the Middle Triassic Botneheia Formation on south-western Edgeøya, Svalbard. *Norwegian Petroleum Directorate Bulletin*, 11, 111-128.
- Brinkmann, W. 1996: A mixosaur (Reptilia, Ichthyosauria) with embryos from the Grenzbitumenzone (Middle Triassic) of Monte San Giorgio (Switzerland, Canton Ticino). *Eclogae Geologicae Helveticae*, 89, 1321-1344.
- Brinkmann, W. 1998: *Sangiorgiosaurus* n. g. – eine neue Mixosaurier-Gattung (Mixosauridae, Ichthyosauria) mit Quetschzähnen aus der Grenzbitumenzone (Mitteltrias) des Monte San Giorgio (Schweiz, Kanton Tessin). *Neues Jahrbuch für Geologie und Paläontologie Abhandlungen*, 207, 125-144.
- Buchan, S.H., Challinor, A., Harland, W.B. & Parker, J.R. 1965: The Triassic stratigraphy of Svalbard. *Norsk Polarinstitutt Skrifter*, 135, 1-94.
- Buchholtz, E. A. 2001: Swimming styles in Jurassic ichthyosaurs. *Journal of Vertebrate Paleontology*, 21, 61-73.
- Callaway, J.M. 1997: A new look at Mixosaurus. In Callaway, J. and Nicholls, E. (eds.): *Ancient marine reptiles*. Academic Press, San Diego, 45-59.
- Callaway, J.M. & Massare, J.A. 1989: Geographic and stratigraphic distribution of the Triassic Ichthyosauria (Reptilia: Diapsida). *Neues Jahrbuch für Geologie und Paläontologie, Abhandlungen*, 178, 37-58.
- Callaway, J. M. & Brinkman D.B. 1989: Ichthyosaurs (Reptilia, Ichthyosauria) from the Lower and Middle Triassic Sulphur Mountain Formation, Wapiti Lake area, British Columbia, Canada. *Canadian Journal of Earth Sciences*, 26, 1491-1500.
- Cox, C.B. & Smith, D.G. 1973: A review of the Triassic vertebrate faunas of Svalbard. *Geological Magazine*, 110, 405-418.
- Dames, W. 1895: Über die Ichthyopterygier der Triasformation. *Sitzungsberichte der Königlich Preussischen Akademie der Wissenschaften zu Berlin*, 46, 1045-1050.
- Falcon, N.L. 1928: Geology. In The Cambridge Expedition Edge Island. *Geographical Journal*, 72, 134-139.
- Flood, B., Nagy, J. & Winsnes, T.S. 1971: Geological map of Svalbard 1:500,000, sheet 1G Spitsbergen southern part. *Norsk Polarinstitutt Skrifter*, 154 A (with short description).
- Hagström, J. 2007: Palaeontological fieldwork on Spitsbergen - in the footsteps of Erik Stensiö. *Yearbook 2006. Swedish Polar Research Secretariat*, 67-70.
- Hammer, Ø., Harper, D.A.T. & Ryan, P.D. 2001: PAST: Paleontological Statistics Software Package for education and data analysis. *Palaeontologia Electronica*, 4, 9 pp.
- Hulke, J.W. 1873: Memorandum on some fossil vertebrate remains collected by the Swedish expedition to Spitzbergen in 1864 and 1868. *Bihang till Kungliga Svenska Vetenskapsakademiens Handlingar*, 1, Afdelning IV, 9, 1-11.
- Jiang, D.-Y., Hao, W.-C., Maisch, M.W., Matzke, A.T. & Sun, Y.-L. 2005: A basal mixosaurid ichthyosaur from the Middle Triassic of China. *Palaeontology*, 48, 869-882.
- Jiang, D.-Y., Schmitz, L., Hao, W.-C. & Sun, Y.-L. 2006: A new mixosaurid ichthyosaur from the Middle Triassic of China. *Journal of Vertebrate Paleontology*, 26, 60-69.
- Jiang, D.-Y., Schmitz, L., Motani, R., Hao, W.-C. & Sun, Y.-L. 2007: The mixosaurid ichthyosaur *Phalarodon* cf. *P. fraasi* from the Middle Triassic of Guizhou Province, China. *Journal of Vertebrate Paleontology*, 81, 602-605.
- Krajewski, K.P. 2008: The Botneheia Formation (Middle Triassic) in Edgeøya and Barentsøya, Svalbard: lithostratigraphy, facies, phosphogenesis, paleoenvironment. *Polish Polar Research*, 29, 319-364.
- Krajewski, K.P., Karcz, P., Woźny, E. & Mørk, A. 2007: Type section of the Bravaisberget Formation (Middle Triassic) at Bravaisberget, western Nathorst Land, Spitsbergen, Svalbard. *Polish Polar Research*, 28, 79-122.
- Liu, J., Motani, R., Jiang, D.-Y., Hu, S.-X., Aitchison, J.C., Rieppel, O., Benton, M. J., Zang, Q.-Y. & Zhou, C.-Y. 2013: The first specimen of the Middle Triassic *Phalarodon* avatus (Ichthyosauria: Mixosauridae) from South China, showing postcranial anatomy and Peritethyan distribution. *Palaeontology*, 56, 849-866.
- Lock, B.E., Pickton, C.A.G., Smith, D.G., Batten, D.J. & Harland, W.B. 1978: The geology of Edgeøya and Barentsøya, Svalbard. *Norsk Polarinstitutt Skrifter*, 168, 64 pp.
- Maisch, M.W. 2010: Phylogeny, systematics, and origin of the Ichthyosauria – the state of the art. *Palaeodiversity*, 3, 151-214.
- Maisch, M.W. & Blomeier, D. 2009: Filling the gap – an ichthyosaur (Reptilia: Ichthyosauria) from the Middle Triassic Botneheia Formation of Svalbard. *Neues Jahrbuch für Geologie und Paläontologie Abhandlungen*, 254, 379-384.
- Maisch, M.W. & Matzke, A.T. 1997: *Mikadocephalus gracilirostris* n. gen., n. sp., a new ichthyosaur from the Grenzbitumenzone (Anisian-Ladinian) of Monte San Giorgio (Switzerland). *Paläontologische Zeitschrift*, 71, 267-289.
- Maisch, M.W. & Matzke, A.T. 2000: *The Ichthyosauria*. Stuttgarter Beiträge zur Naturkunde, Serie B (Geologie und Paläontologie), 298, 159 pp.
- Maisch, M.W. & Matzke, A.T. 2002: The skull of a large Lower Triassic ichthyosaur from Spitsbergen and its implications for the origin of the Ichthyosauria. *Lethaia*, 35, 250-256.
- Maisch, M.W. & Matzke, A.T. 2003: Observations on Triassic ichthyosaurs. Part XII. A new Early Triassic ichthyosaur genus from Spitsbergen. *Neues Jahrbuch für Geologie und Paläontologie Abhandlungen*, 229, 317-338.
- Maxwell, E.E. & Kear, B.P. 2013: Triassic ichthyopterygian assemblages of the Svalbard archipelago: a reassessment of taxonomy and distribution. *GFF*, 135, 85-94.



- Mazin, J.-M. 1981a: *Svalbardosaurus crassidens* n.g.n. sp. un ichthyoptérygien nouveau du Spathien (Trias Inférieur) du Spitsberg. *Comptes Rendus de l'Académie des Sciences, Paris, Série III*, 293, 111–113.
- Mazin, J.-M. 1981b: *Grippia longirostris* Wiman, 1929, un Ichthyopterygia primitif du Trias inférieur du Spitsberg. *Bulletin du Muséum National d'Histoire Naturelle, Paris, C. Série IV*, 3, 317–340.
- Mazin, J.-M. 1983a: *Omphalosaurus nisseri* (Wiman, 1910), un ichthyoptérygien à denture broyeuse du Trias moyen du Spitsberg. *Bulletin du Muséum National d'Histoire Naturelle, Paris, C. Série IV*, 5, 243–263.
- Mazin, J.-M. 1983b: Répartition stratigraphique et géographique des Mixosauria (Ichthyopterygia). Provincialité marine au Trias moyen. In Bufféaut, E., Mazin, J. M. & Salmon, E. (eds.): *Actes du Symposium Paléontologique Georges Cuvier*, 1982. Motibéliard, France, 375–387.
- Mazin, J.-M. 1984: Les Ichthyopterygia du Trias du Spitsberg: Descriptions complémentaires à partir d'un nouveau matériel. *Bulletin du Muséum National d'Histoire Naturelle, Paris, C. Série IV*, 6, 309–320.
- Mazin, J.-M. 1988: Paléobiogéographie des reptiles marins du Trias. *Mémoires des Sciences de la Terre, Université Paris*, VI, 8/88, 1-313.
- McGowan, C. 1978: Further evidence for the wide geographical distribution of ichthyosaur taxa (Reptilia, Ichthyosauria). *Journal of Paleontology*, 52, 1152–1162.
- McGowan, C. & Motani, R. 2003: Ichthyopterygia In *Handbook of Paleoherpétology*, Verlag Dr. Friedrich Pfeil, München, 175 pp.
- Merriam, J.C. 1910: The skull and dentition of a primitive ichthyosaur from the Middle Triassic. *University of California Publications, Bulletin of the Department of Geology*, 5, 381–390.
- Merriam, J.C. 1911: Notes on the relationships of the marine saurian fauna described from the Triassic of Spitzbergen by Wiman. *University of California Publications, Bulletin of the Department of Geology*, 6, 317–327.
- Motani, R. 1997: Temporal and spatial distribution of tooth implantations in ichthyosaurs. In Callaway, J. & Nicholls, E. (eds.): *Ancient marine reptiles*. Academic Press, San Diego, 81–103.
- Motani, R. 1998: First complete forefin of the ichthyosaur *Grippia longirostris* from the Triassic of Spitsbergen. *Palaeontology*, 41, 591–599.
- Motani, R. 1999a: Phylogeny of the Ichthyopterygia. *Journal of Vertebrate Paleontology*, 19, 473–496.
- Motani, R. 1999b: On the evolution and the homologies of ichthyopterygian forefins. *Journal of Vertebrate Paleontology*, 19, 28–41.
- Motani, R., 2000: Skull of *Grippia longirostris*: no contradiction with a diapsid affinity for the Ichthyopterygia. *Palaeontology*, 43, 1–14.
- Motani, R. 2005: Evolution of fish-shaped reptiles (Reptilia: Ichthyopterygia) in their physical environments and constraints. *Annual review of Earth and Planetary Sciences*, 33, 395–420.
- Motani, R., You, H. & McGowan, C. 1996: Eel-like swimming in the earliest ichthyosaurs. *Nature*, 382, 347–348.
- Motani R., Jiang D.-Y., Tintori A., Rieppel O. & Chen G.-B. 2014: Terrestrial Origin of Viviparity in Mesozoic Marine Reptiles Indicated by Early Triassic Embryonic Fossils. *PLoS ONE* 9(2), e88640. doi:10.1371/journal.pone.0088640
- Mørk, A. & Bjørøy, M. 1984: Mesozoic source rocks on Svalbard. In Spencer, A.M. et al. (eds.): *Petroleum Geology of the North European Margin*. Norwegian Petroleum Society, Graham and Trotman, 371–382.
- Mørk, A. & Bromley, R.G. 2008: Ichnology of a marine regressive systems tract: the Middle Triassic of Svalbard. *Polar Research*, 27, 339–359.
- Mørk, A. & Elvebakk, G. 1999: Lithological description of subcropping Lower and Middle Triassic rocks from the Svalis Dome, Barents Sea. *Polar Research*, 18, 83–104.
- Mørk, A., Knarud, R. & Worsley, D. 1982: Depositional and diagenetic environments of the Triassic and Lower Jurassic succession of Svalbard. In Embry, A.F. & Balkwill, H.R. (eds.): *Arctic Geology and Geophysics- Canadian Society of Petroleum Geologists Memoir*, 8, 371–398.
- Mørk, A., Dallmann, W.K., Dypvik, H., Johannessen, E.P., Larssen, G.B., Nagy, J., Nøttvedt, A., Olaussen, S., Pcelina, M. & Worsley, D. 1999: Mesozoic lithostratigraphy. In Dallmann, W.K. (ed.): *Lithostratigraphic Lexicon of Svalbard: Upper Paleozoic to Quaternary Bedrock*. Review and recommendations for nomenclatural use, 127–214. Norsk Polarinstitut, Tromsø.
- Nicholls, E.L., Brinkman, D.B. & Callaway, J.M. 1999: New material of Phalarodon (Reptilia: Ichthyosauria) from the Triassic of British Columbia and its bearing on the interrelationships of mixosaurs. *Palaeontographica Abteilung A*, 252, 1–22.
- Quenstedt, F.A. 1852: *Handbuch der Petrefaktenkunde*. H. Laupp, Tübingen, 792 pp.
- Sander, P.M. 1992: *Cymbospondylus* (Shastasauridae: Ichthyosauria) from the Middle Triassic of Spitsbergen: filling a paleobiogeographic gap. *Journal of Paleontology*, 66, 332–337.
- Sander, P.M. 2000: Ichthyosauria: their diversity, distribution and phylogeny. *Paläontologische Zeitschrift*, 74, 1–35.
- Sander, P.M. & Faber, C. 1998: New finds of *Omphalosaurus* and a review of Triassic ichthyosaur paleobiogeography. *Paläontologische Zeitschrift*, 72, 149–162.
- Sander, P.M. & Mazin, J.-M. 1993: The paleobiogeography of the Middle Triassic ichthyosaurs: the five major faunas. *Paleontologia Lombarda, Nuova serie*, 2, 145–152.
- Sander, M., Rieppel, O.C. & Bucher, H. 1994: New marine vertebrate fauna from the Middle Triassic of Nevada. *Journal of Paleontology*, 68, 676–680.
- Schmitz, L. 2005: The taxonomic status of *Mixosaurus nordenskiöldii* (Ichthyosauria). *Journal of Vertebrate Paleontology*, 25, 983–985.
- Schmitz, L., Sander, P.M., Storrs, G.W. & Rieppel, O. 2004: New Mixosauridae (Ichthyosauria) from the Middle Triassic of Nevada (USA): implications for mixosaur taxonomy. *Palaeontographica Abteilung A*, 270, 133–162.
- Vigran, J.O., Mangerud, G., Mørk, A., Bugge, T. & Weitschat, W. 1998: Biostratigraphy and sequence stratigraphy of the Lower and Middle Triassic deposits from the Svalis Dome, Central Barents Sea, Norway. *Palyology*, 22, 89–141.
- Vigran, J.O., Mørk, A., Forsberg, A.W., Weiss, H.M. & Weitschat, W. 2008: *Tasmanites* algae – contributors to the Middle Triassic hydrocarbon source rocks of Svalbard and the Barents Shelf. *Polar Research*, 27, 360–371.
- Wiman, C. 1910: Ichthyosaurier aus der Trias Spitzbergens. *Bulletin of the Geological Institute of the University of Uppsala*, 10, 124–148.
- Wiman, C. 1916a: Ein Plesiosaurierwirbel aus der Trias Spitzbergens. *Bulletin of the Geological Institute of the University of Uppsala*, 13, 223–226.
- Wiman, C. 1916b: Notes on the marine Triassic reptile fauna of Spitsbergen. *University of California Publications, Bulletin of the Department of Geology*, 10, 63–73.
- Wiman, C. 1928: Eine neue marine Reptilien-Ordnung aus der Trias Spitzbergens. *Bulletin of the Geological Institute of the University of Uppsala*, 22, 183–196.
- Wiman, C. 1933: Über *Grippia longirostris*. *Nova Acta Regiae Societas Scientiarum Upsaliensis Serie IV*, 9, 1–19.
- Yakowlew, V., N. 1903: Neue Funde von Trias-Saurier auf Spitzbergen. *Verhandlungen der Russisch-Kaiserlichen Mineralogischen Gesellschaft*, 40, 179–202.
- Zammit, M. 2010: A review of Australasian ichthyosaurs. *Alcheringa*, 34, 281–2.

# Organic geochemistry and petrography of thermally altered sections of the Middle Triassic Botneheia Formation on south-western Edgeøya, Svalbard

Trond Brekke<sup>1</sup>, Krzysztof P. Krajewski<sup>2</sup> & Jørnar Heggsum Hubred<sup>3</sup>

<sup>1</sup> Brekke CHEMO, PB 151 6801 Førde, Norway, e-mail: trond.brekke@enivest.net

<sup>2</sup> Institute of Geological Sciences, Polish Academy of Sciences, Research Centre in Warsaw, Twarda 51/55, PL00818 Warsaw, Poland, e-mail: kpkr@twarda.pan.pl kpkr@poczta.onet.pl

<sup>3</sup> University of Oslo, Department of Geosciences, Oslo, Norway. Present adress: Aker Geo AS, Oslo, Norway, e-mail: jornar.hubred@akersolutions.com jornar@gmail.com

This study presents the results of analyses of outcrop samples of the organic carbon (OC)-rich succession of the Middle Triassic Botneheia Formation and the under- and overlying sedimentary units from two localities (Reddikeidet and Muen) in the south-western coastal exposures of Edgeøya, Svalbard. It documents a remarkably advanced maturity of the Triassic succession south of Diskobukta compared to the regional maturity in eastern Svalbard. This is believed to be caused by a very thick dolerite intrusion below sea level at the base of the Lower Triassic Vikinghøgda Formation, which might be a continuation of the Årdalstangen dolerite cluster located further south. These Early Cretaceous dolerites have caused profound thermal alterations on organic matter in the Triassic succession, including a nearly complete decomposition of alginite, a 1 – 3 ‰ positive shift of  $\delta^{13}\text{C}$  in the extracts, and total destruction of triterpanes and steranes in the saturated fraction and of mono- and tri-aromatic steroid hydrocarbons in the aromatic fraction. About 90 % of the original petroleum potential in the Botneheia Formation on SW Edgeøya was realized by the thermal alteration processes.

**Key Words:** Triassic, Organic geochemistry, Botneheia Formation, Svalbard, Edgeøya, Thermal alteration.

## Introduction

The Anisian–Ladinian Botneheia Formation on the islands of Edgeøya and Barentsøya, eastern Svalbard, is an organic carbon (OC)-rich, fine-grained clastic succession up to 100 m thick that forms the best petroleum source unit in the region (Krajewski, 2008, 2013). The total OC (TOC) content ranges from less than 1 wt % in silty/sandy lithologies in heavily altered mudrocks to nearly 12 wt % in less mature shale and mudstone successions. The Rock-Eval hydrogen index varies accordingly from less than 50 mg/g TOC (this study) to more than 600 mg /g TOC (Krajewski, 2011; Bjørøy et al., 2010). The Botneheia Formation is facies- and age- equivalent of the Bravaisberget Formation in western and southern Spitsbergen (Krajewski et al., 2007), and facies equivalent of the Mid-Olenekian and Anisian Steinkobbe Formation

on the Svalis Dome in the central Barents Sea (Mørk et al., 1999; Riis et al., 2008). On Bjørnøya a thin (20 cm) ?Early–Middle Triassic bed with remanié phosphate nodules (Isaksen, 1996, Mørk et al., 1990) is interpreted as reworked remains of condensed Botneheia Formation. According to Riis et al. (2008) the Botneheia Formation and its equivalents are developed as a diachronous facies over large parts of the Barents Sea, deposited first in the Olenekian as far south as the Loppa High, and up to Ladinian times in the north-eastern Svalbard area. It is thus a highly interesting source rock in petroleum prospecting in the Barents Sea.

This paper presents the effects of thermal alteration of organic matter in the Botneheia Formation source rocks related to Late Mesozoic intrusive activity in Svalbard. It involves organic geochemistry supported by petrographic

survey to document the thermal destruction of oil-prone maceral components and to characterize the chemical composition of residual organic fractions.

### Geological setting

Edgeøya and Barentsøya belong to a tectonic setting of the Eastern Svalbard Platform (Harland, 1997), which shows mostly flat-lying Triassic strata variably intruded by

dolerites in Early Cretaceous times (Figs. 1, 2). The Triassic succession is divided into the Lower–Middle Triassic Sassendalen Group embracing fine-grained, open shelf clastics of the Vikinghøgda and Botneheia formations, and the Upper Triassic Kapp Toscana Group that represents a deltaic system of the De Geerdalen Formation developed over marine shales of the Tschermakfjellet Formation (Mørk et al., 1999). Krajewski (2008) divided the Botneheia Formation into the lower Muen Member and the upper Blanknuten Member. The stratotypes for both

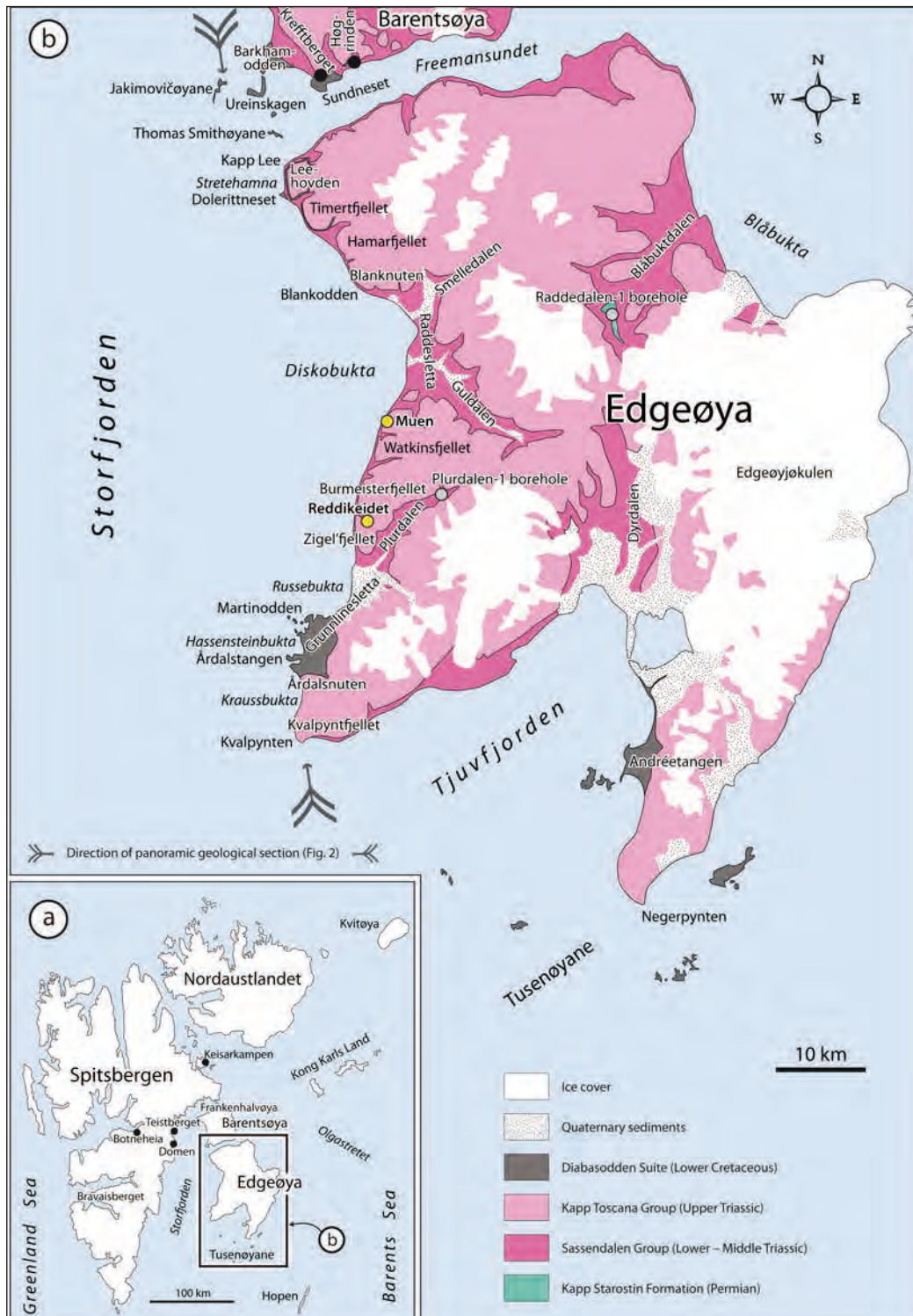


Figure 1. (a) Sketch map of Svalbard showing location of the study area on Edgeøya. (b) Geological map of Edgeøya and southern Barentsøya. The locations for the Reddikeidet and Muen sections of the Botneheia Formation are shown as yellow spots, the locations for the Plurdalen-1 and Raddedalen-1 boreholes are shown as grey spots, and the locations for the sections sampled by NPD in 1995 are shown as black spots. Geology after Winsnes (1981) and Dallmann et al. (2002), with new data.



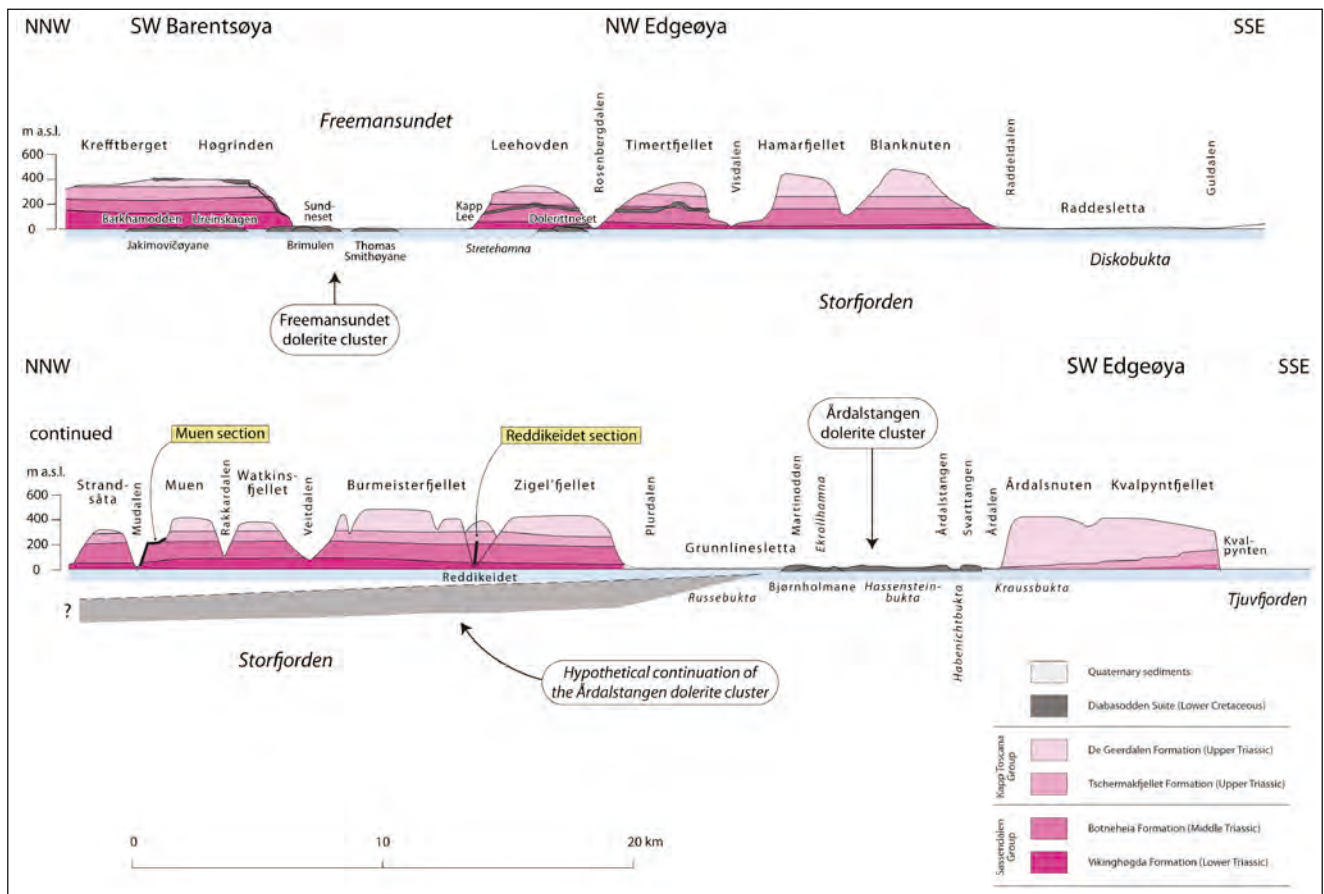


Figure 2. Panoramic geological section along western coast of Edgeøya and southern Barentsøya showing location of the Reddikeidet and Muen sections. Note the occurrence of two dolerite clusters at the entrance to Freemansundet and in the vicinity of Årdalstangen. The latter cluster is supposed to continue under the sea northward causing elevated maturity of the Triassic succession along the coastal range south of Diskobukta. Lithostratigraphic units of the Triassic succession after Mørk et al. (1999).

members are located on the western coast of Edgeøya. The uppermost part of the Muen Member is phosphorite bearing, as is the whole of the Blanknuten Member.

Edgeøya and Barentsøya are located within the Eastern Svalbard Dolerite Belt that shows many dolerite clusters composed mostly of sills in various morphological arrangements (Burov et al., 1975; Nejbort et al., 2011). The dolerites are dominantly of Early Cretaceous age, and are termed Diabasodden Suite in the local lithostratigraphic scheme (Mørk et al., 1999). Prominent dolerite clusters occur at Frankenhavøya at the northern tip of Barentsøya and at the western entrance to Freemansundet on Barentsøya. On Edgeøya, the clusters are located in the vicinity of Dolerittneset, Årdalstangen and Andrétangen, and further south throughout the Tusenøyane archipelago (Figs. 1, 2). They are believed to have caused local plumes of heating and maturing of the Botneheia Formation (Mørk and Bjørøy, 1984, Schou et al., 1984). While the background vitrinite reflectance of the Botneheia Formation in eastern Svalbard is in the range of 0.4 – 0.6 % Ro (Thronsdén, 1979 and personal communication; Hubred, 2006; Mørk and Bjørøy, 1984), the intrusives have increased the maturity significantly, to ca 1.1 % Ro

or more close to the clusters (Bjørøy et al., 2006). The extent of these plumes is, however, not well defined as only a few data points have been published (Thronsdén, 1979; Mørk and Bjørøy, 1984).

The Botneheia Formation records a second-order transgressive-regressive cycle in the Triassic succession of Svalbard that was associated with an event of high biological productivity on the Barents Sea Shelf (Krajewski, 2011, 2013). With the exception of the lower and middle parts of the Muen Member, which record an early transgressive phase dominated by terrestrial run-off, the formation contains mostly autochthonous, oil-prone organic matter (kerogen Types I and II) accumulated under conditions of enhanced bottom-water stagnation. Leith et al. (1993) discusses the organic geochemistry of the formation in a circum-Arctic perspective. Various aspects of the organic geochemistry and petroleum potential are further described and discussed in papers by Mørk and Bjørøy (1984), Abdullah (1999), Krajewski (2000, 2011, 2013), Bjørøy et al. (2006, 2010) and Vigran et al. (2008). Forsberg and Bjørøy (1983) investigated the effects on weathering on various organic parameters in surface and sub-surface samples. The Norwegian Geochemical Standard sample NGS SR-1

(Dahlgren et al., 1998) was collected from the Botneheia Formation at Teistberget in Eastern Spitsbergen (78° 20' 00" N, 18° 58' 34" E). The sampled section contained no phosphate nodules and therefore most likely belongs to the Muen Member. Hubred (2006) demonstrated the thermal effects of sills on the organic geochemistry of sample series from the Botneheia Formation at Botneheia in central Spitsbergen and Teistberget in eastern Spitsbergen, and at Krefftberget and Høgrinden on SW Barentsøya. An oil-filled ammonoid was found in the Botneheia Formation at Blanknuten on Edgeøya in 2006 (Smelror and Sollid, 2007), testifying that oil has been generated in this area. This is supported by a common occurrence of liquid bitumen in cracks of diagenetic carbonate concretions at Blanknuten and elsewhere in eastern Svalbard (Krajewski, 2013).

## Samples and methods

This study presents organic geochemical and petrographic data from two outcrops of the Botneheia Formation (Reddikeidet and Muen) in the western coastal exposures of Edgeøya (Fig. 3). The samples were collected during geological expeditions to Svalbard on board M/S Kongsøy, organized by the Norwegian Petroleum Directorate (NPD) in 2007 and 2009. Pilot samples for petrographic investigations were collected during geological expedition of the Polish Academy of Sciences to eastern Svalbard in 2005. No dolerites are visible at the two locations. The most extensive sampling was performed at Reddikeidet in 2009 (Fig. 4a) where 32 samples were taken for organic geochemistry, one of them in the Vikinghøgda Formation and the rest in

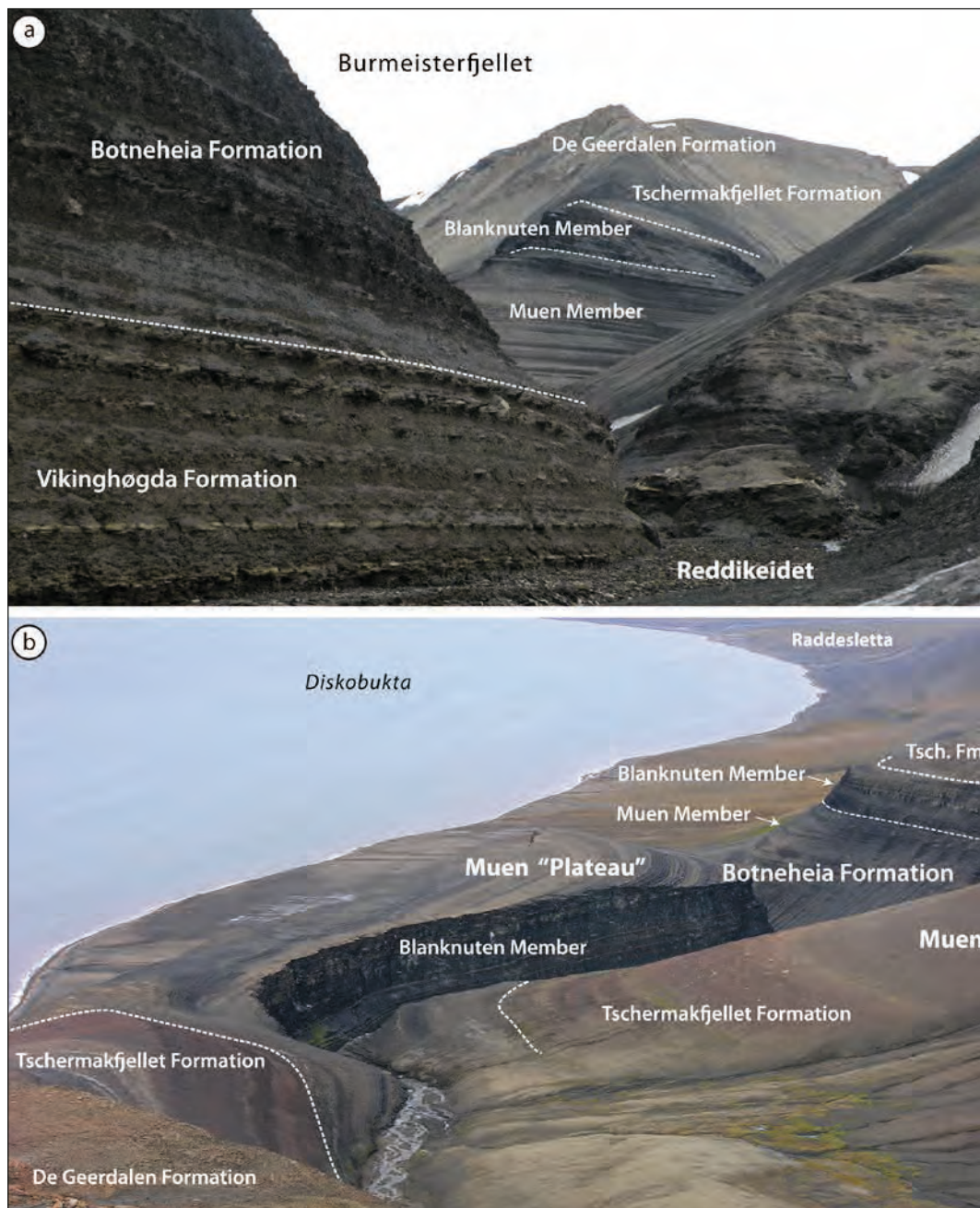
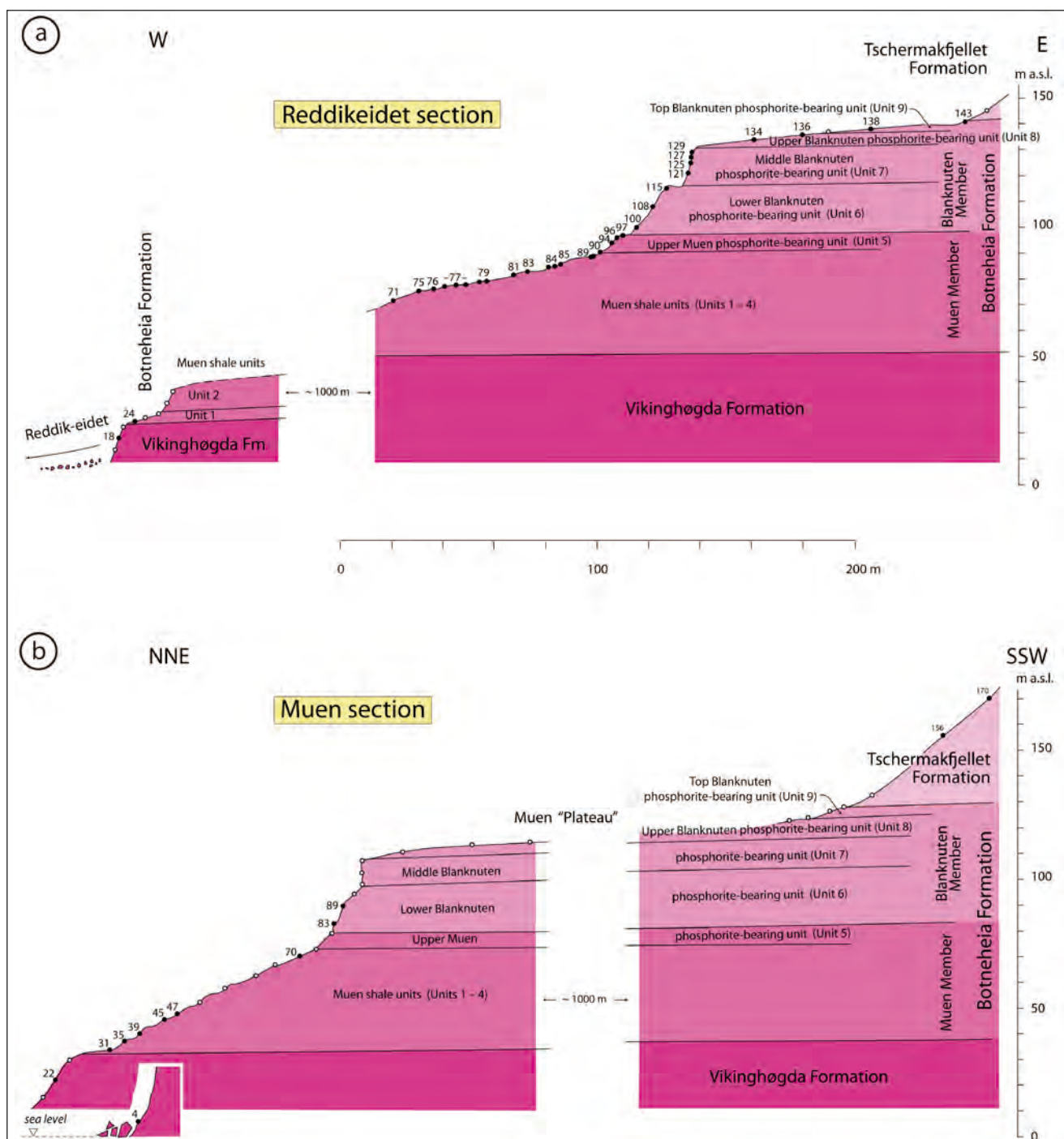


Figure 3. Field views of the Reddikeidet (a) and Muen (b) sections of the Botneheia Formation in western Edgeøya. Lithostratigraphic units of the Triassic succession after Mørk et al. (1999) and Krajewski (2008).





**Figure 4.** Reddikeidet (a) and Muen (b) sections of the Botneheia Formation on western Edgeøya showing its lithostratigraphic subdivision and location of samples analysed in this paper. Solid circles mark samples for organic geochemistry, some of which were also analysed using petrographic methods. Open circles are samples for petrography only. Numbers indicate elevations above sea level at sampling locations. Lithostratigraphic subdivision of the Botneheia Formation after Krajewski (2008).

the Botneheia Formation. The samples at Muen, ca 10 km north of Reddikeidet, were taken for comparative purposes and as reference to the Muen stratotype location (Fig. 4b). Here 12 samples for geochemical analyses were taken; two of them in the Vikinghøgda Formation, eight in the Botneheia Formation, and two in the Tschermafjellet Formation. Thorough sampling for petrographic investigations at Muen was done during earlier expeditions (Krajewski, 2008). In an attempt to

avoid surficial contaminations and diminish effects of weathering, sampling was done by digging through any loose cover and 20 – 30 cm into the rock below. A typical sample station is shown in Fig. 5. Geographical location and elevation at sample stations was recorded using a GARMIN GPSMap 60csx device with built-in atmospheric pressure recording. The elevation at sea level (0 m) was calibrated against atmospheric pressure before sampling started.





Figure 5. Photo of typical sample station in the black shale of the Muen Member at Reddikeidet.

The interpretations of thermal effects of sills on organic matter in the present study rely also on an earlier study made by the Norwegian Petroleum Directorate in co-operation with the University of Oslo. The samples for that study were collected in 1995 and most of the analytical work was also completed in 1995. Locations for the sampled sections are indicated in Fig. 1. The reader is referred to Hubred's thesis (Hubred, 2006) where further details about these data can be found, including all the data used in the present study.

For petrographic characterization of the Botneheia Formation source rocks and the contained organic matter polished thin sections were prepared from 62 samples, 34 and 28 from the Reddikeidet and Muen sections, respectively. Thin sections were analysed using transmitted (TLM), reflected (RLM), and fluorescent light microscopy (FLM). Selected samples (14 and 24 from the Reddikeidet and Muen sections, respectively) were analysed using X-ray diffraction (XRD). For details of the analytical procedure and the instruments used see Krajewski (2013). Qualitative maceral evaluations were performed following the ICCP nomenclature described in Taylor et al. (1998).

The analytical programme for the organic geochemical investigation consisted of screening and follow-up analyses. The screening included determination of the TOC content and Rock-Eval pyrolysis, and was carried

out on 32 samples from Reddikeidet and 12 samples from Muen. The follow-up programme on nine samples included solvent extraction, de-asphalting, and MPLC fractionation. Preparation of carbon dioxide of the saturated, aromatic, polar and asphaltene fractions for stable carbon isotope analysis was performed according to Sofer (1980), and the isotope analyses were conducted on a Micromass Optima Isotope Ratio mass spectrometer (IRMS). Originally the fractions from all nine samples were meant to be subjected to molecular analyses. However, due to very low extract yields the molecular compositions of hydrocarbon fractions from only two of these samples were further analysed using GC-FID and GC-MSD. GC-FID analysis was performed on the saturated fraction, while GC-MSD was performed on the saturated fraction and the aromatic fraction. The GC-MSD analyses included quantification of the  $C_{31}$  to  $C_{34}$  *n*-alkylcyclohexane series in order to test for the relative concentration of the  $C_{33}$  homologue, a diagnostic biomarker for the aftermath of the Permian/Triassic extinction event (Grice et al., 2005). The GC-FID and GC-MSD analyses were conducted at SINTEF Petroleum Research in Trondheim, Norway, while the remaining analyses were conducted at Applied Petroleum Technology at Kjeller, Norway.

All procedures for the organic geochemical analyses follow NIGOGA, 4<sup>th</sup> edition (Weiss et al., 2000).

## Results

### Reddikeidet and Muen sections

The Reddikeidet and Muen sections provide insight into a complete development of the Botneheia Formation in eastern Svalbard, with all the major facies and sedimentary units well exposed (Figs. 1, 2). The formation rests conformably with a sharp boundary on the Vikinghøgda Formation. It is subdivided into two formal members (Muen and Blanknuten members) and nine informal lithostratigraphic units (Krajewski, 2008). There are two major sedimentary facies of the formation: 1) the black (non-phosphogenic) shale facies forming the lower part of the succession (Units 1 – 4); and 2) the phosphogenic black shale facies forming the upper part of succession (Units 5 – 9). The boundary between the two facies is not coincident with the boundary between the members of the formation (Figs. 3, 4). At Muen and Reddikeidet it is accentuated by a thin dolomitic cementstone horizon containing the first phosphate nodules in the succession, accompanied by common, flattened ammonoid imprints. The boundary between the Muen and Blanknuten members was defined as the base of the upper, cliff-forming part of the succession that can easily be traced in the field (Mørk et al., 1982, 1999).

The black shale facies is represented by non-laminated

mud-shale, mudstone, silt-shale, and siltstone. The succession consists of 0.5 – 3 m thick coarsening-upward packages that terminate in silty horizons variably cemented by microcrystalline dolomite. The rock contains detrital quartz, feldspar and mica. Clay minerals are dominated by illite and chlorite, with a varying admixture of kaolinite. Noticeable amounts of iron (hydr)oxides and pyrite occur throughout the succession. Biogenic remnants embrace rare siliceous sponge spicules, arenaceous foraminifera, and reptilian and fish bones and bone debris. Flattened imprints of ammonoids are found in dolomitic cementstone beds.

The phosphogenic black shale facies embraces several sediment types, which are moderately to strongly enriched in sedimentary phosphate accumulations. Most of the lithologies are OC-rich and distinctly black in colour (Fig. 3). They are represented by mud-shale and mudstone, with subordinate siltstone, sandy siltstone, and silty sandstone. Quartz grains dominate the detrital fraction. Accessorial feldspar grains were observed in the lower and upper parts of the phosphogenic succession. Clay mineral representation is similar to the one observed in the underlying non-phosphogenic shale, though the content of detrital mica and kaolinite is far smaller. Iron (hydr)oxides do not occur in amounts detected by XRD. Pyrite constitutes a subordinate, but constant admixture. Common moulds of radiolaria are accompanied by bivalve shell detritus, rare sponge spicules, and arenaceous and calcareous foraminifera. Recurrent dolomitic cementstone beds and horizons of large carbonate concretions occur in the succession. Ammonoids occur both in the form of flattened imprints in the cementstone beds and as non-compressed phosphatic moulds in the shale.

The cliff-forming succession of the Blanknuten Member at Muen, Reddikeidet and elsewhere along western coast of Edgeøya is clearly tripartite, with the middle part made by a massive phosphatic mudstone classified as informal Unit 7 (Fig. 4). It is composed of OC-rich mudstone, with subordinate silty intercalations and recurrent phosphatic grainstone beds. The detrital components are dominated by quartz and the clay-rich matrix by illite. This mudstone is the best petroleum source rock in Svalbard (Krajewski, 2013).

The analysed samples of the Vikinghøgda Formation at Muen and Reddikeidet show microfacies and mineral composition similar to those of the non-phosphogenic black shale facies of the Botneheia Formation. However, the sediments are in general more silty and massive. The Botneheia Formation is overlain by the black sideritic shale succession of the Tschermakfjellet Formation.

The succession of the Sassendalen Group (Vikinghøgda and Botneheia formations) at Muen and Reddikeidet is enriched in diagenetic carbonate deposits. These occur in the form of cementstone beds and more or

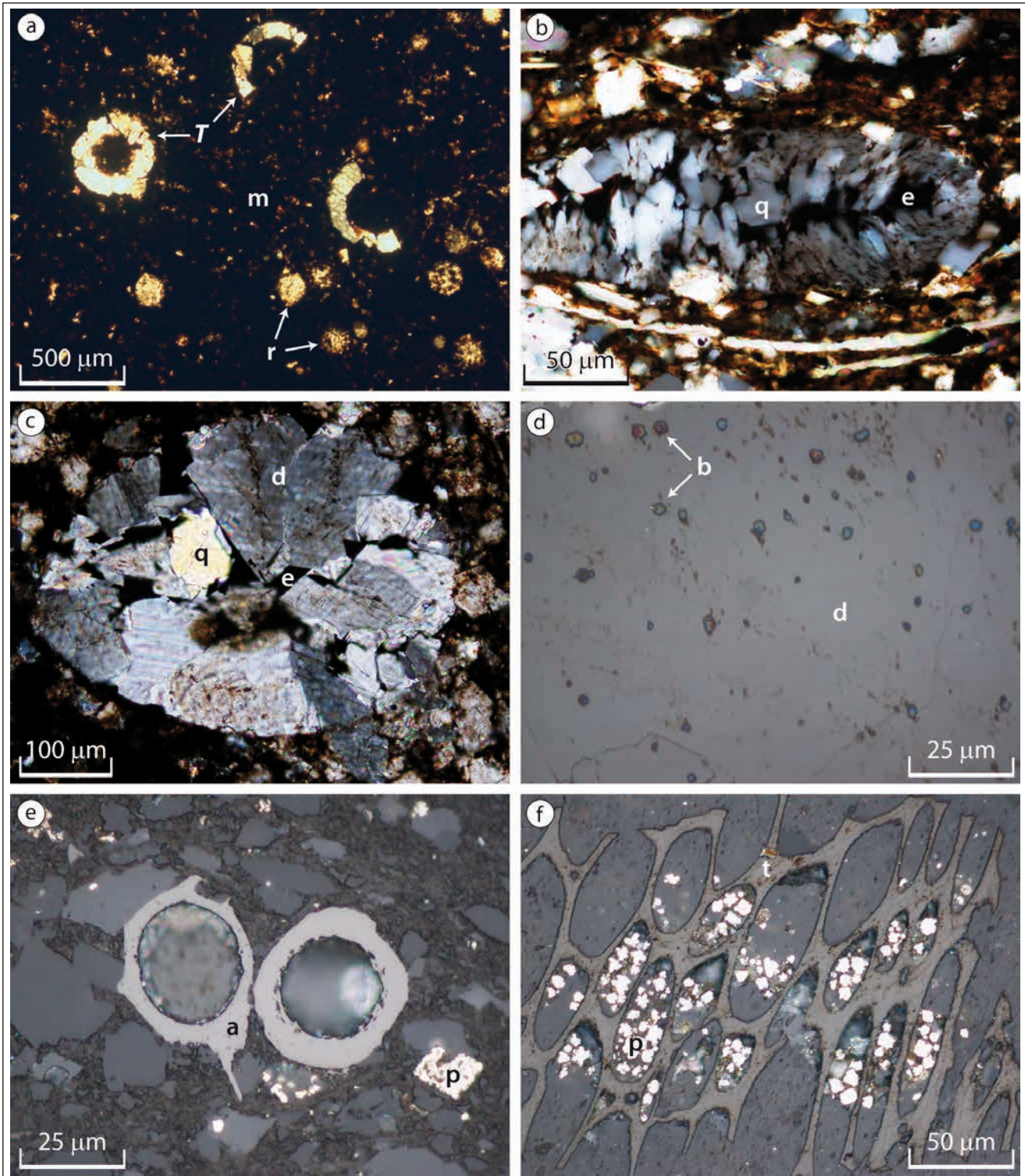
less regular horizons and lenticular bodies enriched in microcrystalline dolomite. The chemistry of the dolomite varies from non-ferroan dolomite through ferroan dolomite to ankerite. Microcrystalline dolomite also occurs as scattered microscopic crystals and their aggregates. There are at least two generations of dolomite cement. The first and most common consists of minute euhedral to subhedral crystals (5 – 100 µm) forming interlocking mosaics in matrices of cementstone beds, lenses, and cementation horizons. It is similar to the one observed elsewhere in the Botneheia and Bravaisberget formations (Krajewski and Woźny, 2009). The second generation forms irregular replacement zones and microscopic aggregates of usually larger crystals (> 100 µm) replacing mineral and organic particles, and cementing rudimentary pore space. This generation seems to have preferentially developed in areas of increased thermal alteration of organic matter. It occurs in association with late diagenetic sulphidic replacement structures composed of aggregates of skeletal pyrite and sphalerite crystals. Common bitumen inclusions in the second generation of dolomite and its association with late sulphide minerals suggest its formation in the catagenic environment during kerogen cracking and thermochemical sulphate reduction.

The other carbonate deposits in the Sassendalen Group are represented by large calcitic concretions forming indistinct horizons in the shaly succession. The concretions record stages of growth in the sediment, from early diagenetic, shallow subsurface environment to burial catagenic environment. They are usually heavily cracked forming septarian bodies, with the cracks filled by sequences of calcite and dolomite fringe cements. The remaining space of the cracks is at places filled by exudatinite and/or liquid bitumen. Calcite forming mosaics of large subhedral crystals also occurs in the form of void-filling cement in the shaly succession, mostly as infillings of sedimentary pore space in phosphate nodules and fossil moulds. Similar cement forms moulds developed after dissolution of radiolaria tests. This cement is at places associated with barite crystals.

## Organic petrography

The Botneheia Formation at Muen and Reddikeidet contains both sedimentary and secondary organic matter. Sedimentary organic matter comprises autochthonous marine and transported terrestrial fractions. Secondary organic matter comprises organic fractions generated from sedimentary organic matter during burial and products of their epigenetic transformations. Characteristic of the analysed sections is advanced thermal alteration of organic matter (Fig. 6). Most of the organic matter occurs in the form of amorphous material showing distinct black color in transmitted light and low reflectance in incident light (Fig. 6a). Fluorescence is usually absent in the Reddikeidet section, and absent to very weak in the Muen section. This





**Figure 6.** (a) Massive phosphatic mudstone of Unit 7 (Blanknuten Member of the Botneheia Formation) at Reddikeidet showing dolomite-replaced *Tasmanites* thalli (T) and calcite-cemented radiolaria moulds (r) in black matrix (m). This matrix contains residual amorphous organic fraction impregnated by exudatinite, which is the result of thermal decomposition of sedimentary marine organic matter (alginite, bituminite) and bitumen generation and migration in the succession. (b) Quartz-replaced *Tasmanites* in black phosphatic shale of Unit 6 (Blanknuten Member of the Botneheia Formation) at Muen. Note the acicular quartz crystals (q) growing from the thallus external surface towards the centre, and exudatinite (e) infilling the remaining space after thermal decomposition of alginite. (c) Dolomite-replaced *Tasmanites* in black phosphatic shale of Unit 6 (Blanknuten Member of the Botneheia Formation) at Reddikeidet. The rhomboidal dolomite crystals (d) grew from the thallus external surface towards the centre during and after thermal decomposition of alginite. Quartz crystal (q) occurs in the centre of the replacement structure. The remaining pores are filled by exudatinite (e). (d) Bitumen inclusions (b) in dolomite crystal (d) in the replacement structure of *Tasmanites* shown in photo (c). (e) Palynomorphs (a) in phosphatic black shale of Unit 6 (Blanknuten Member of the Botneheia Formation) at Muen. Grey bodies are detrital quartz grains and diagenetic dolomite crystals. Note the late diagenetic pyrite (p) replacing rhomboidal dolomite crystal. (f) Telinite particle (t) in black shale of Units 1–4 (Muen Member of the Botneheia Formation) at Reddikeidet. Re-crystallized pyrite frambooids and grains (p) occur in cellular voids in telinite. (a – c): transmitted light photomicrographs, nicols crossed; (d – f): reflected light photomicrographs, normal light.



**Table 1.** Rock-Eval and TOC screening data. (F): follow-up analyses (F+GC): follow-up analyses including GC and GC-MS

Locality	Lithostratigraphy	Elevation (m a.s.l.)	S1 (mg/g)	S2 (mg/g)	S3 (mg/g)	T <sub>max</sub> (°C)	PI (wt ratio)	HI (mg HC/ g TOC)	OI (mg CO <sub>2</sub> / g TOC)	TOC (wt%)
Reddikeidet	Blanknuten Mb, top Blanknuten phosphorite-bearing unit (9)	143	0.53	1.09	0.23	460	0.33	66	14	1.64
Reddikeidet (F)	Blanknuten Mb, top Blanknuten phosphorite-bearing unit (9)	138	1.26	2.95	0.41	462	0.3	86	12	3.42
Reddikeidet	Blanknuten Mb, upper Blanknuten phosphorite-bearing unit (8)	136	1.01	3.43	0.77	462	0.23	75	17	4.55
Reddikeidet	Blanknuten Mb, upper Blanknuten phosphorite-bearing unit (8)	134	1.1	4.16	0.43	462	0.21	98	10	4.24
Reddikeidet (F+GC)	Blanknuten Mb, middle Blanknuten phosphorite-bearing unit (7)	129	1.49	8.02	1.37	465	0.16	108	18	7.46
Reddikeidet	Blanknuten Mb, middle Blanknuten phosphorite-bearing unit (7)	127	0.68	4.88	1.21	461	0.12	81	20	6.04
Reddikeidet	Blanknuten Mb, middle Blanknuten phosphorite-bearing unit (7)	125	1.16	4.63	0.78	458	0.2	89	15	5.22
Reddikeidet (F)	Blanknuten Mb, middle Blanknuten phosphorite-bearing unit (7)	121	1.21	7.31	0.66	460	0.14	102	9	7.17
Reddikeidet	Blanknuten Mb, lower Blanknuten phosphorite-bearing unit (6)	115	0.67	4.24	0.98	457	0.14	75	17	5.68
Reddikeidet	Blanknuten Mb, lower Blanknuten phosphorite-bearing unit (6)	108	1.07	2.27	0.42	468	0.32	70	13	3.22
Reddikeidet (F)	Blanknuten Mb, lower Blanknuten phosphorite-bearing unit (6)	100	1.34	1.23	0.37	461	0.52	58	18	2.11
Reddikeidet	Muen Mb, upper Muen phosphorite-bearing unit (5)	97	1.12	3.72	0.78	462	0.23	80	17	4.64
Reddikeidet	Muen Mb, upper Muen phosphorite-bearing unit (5)	96	0.3	0.89	0.19	462	0.25	91	20	0.97
Reddikeidet (F)	Muen Mb, upper Muen phosphorite-bearing unit (5)	94	1.57	7.8	0.72	460	0.17	127	12	6.14
Reddikeidet	Muen Mb, upper Muen phosphorite-bearing unit (5)	90	0.27	1.56	1.21	462	0.15	53	41	2.96
Reddikeidet	Muen Mb, Muen shale units (1–4) (piece of carbonate concretion)	89	0.05	0.1	0.44	419	0.33	25	110	0.4
Reddikeidet	Muen Mb, Muen shale units (1–4)	89	0.37	0.64	0.57	458	0.37	47	42	1.37
Reddikeidet	Muen Mb, Muen shale units (1–4)	85	1.1	1.75	0.51	464	0.39	69	20	2.55
Reddikeidet	Muen Mb, Muen shale units (1–4)	84	1.11	3.3	0.59	469	0.25	82	15	4.04
Reddikeidet (F)	Muen Mb, Muen shale units (1–4)	84	1.25	2.51	1.52	469	0.33	75	46	3.34
Reddikeidet	Muen Mb, Muen shale units (1–4)	83	0.61	0.91	0.6	457	0.4	49	33	1.84
Reddikeidet	Muen Mb, Muen shale units (1–4)	81	1.06	1.78	0.4	462	0.37	63	14	2.84
Reddikeidet	Muen Mb, Muen shale units (1–4)	79	0.99	2.48	0.67	470	0.29	73	20	3.38
Reddikeidet	Muen Mb, Muen shale units (1–4)	79	1.03	2.18	0.64	466	0.32	65	19	3.33
Reddikeidet	Muen Mb, Muen shale units (1–4)	77	0.95	1.86	0.67	469	0.34	63	23	2.95
Reddikeidet	Muen Mb, Muen shale units (1–4)	77	0.89	2.12	0.45	466	0.3	74	16	2.86
Reddikeidet (F)	Muen Mb, Muen shale units (1–4)	77	1.35	2.95	0.55	470	0.31	74	14	3.99
Reddikeidet	Muen Mb, Muen shale units (1–4)	76	0.62	1.31	0.94	461	0.32	50	36	2.61
Reddikeidet	Muen Mb, Muen shale units (1–4)	75	0.96	1.46	0.59	464	0.4	51	21	2.86
Reddikeidet (F)	Muen Mb, Muen shale units (1–4)	71	1.19	2.04	0.37	467	0.37	72	13	2.85
Reddikeidet	Muen Mb, Muen shale units (1–4)	24	0.88	0.51	0.26	452	0.63	27	14	1.92
Reddikeidet	Vikinghogda Fm	18	0.38	0.3	0.38	448	0.56	28	35	1.08
Muen	Tschermakfjellet Fm	170	0.07	0.44	1.23	469	0.14	30	84	1.46
Muen	Tschermakfjellet Fm	156	0.28	0.81	0.41	458	0.26	62	32	1.3
Muen	Blanknuten Mb, lower Blanknuten phosphorite-bearing unit (6)	89	1.78	7.69	0.51	455	0.19	151	10	5.08
Muen	Blanknuten Mb, lower Blanknuten phosphorite-bearing unit (6)	83	1.94	3.43	0.31	459	0.36	116	10	2.96
Muen	Muen Mb, Muen shale units (1–4)	70	1.21	1.74	0.84	457	0.41	82	40	2.12
Muen	Muen Mb, Muen shale units (1–4)	47	1.23	3.53	0.82	462	0.26	92	21	3.84
Muen	Muen Mb, Muen shale units (1–4)	45	1.47	2.26	0.75	460	0.39	76	25	2.98
Muen	Muen Mb, Muen shale units (1–4)	39	1.53	4.28	0.48	463	0.26	106	12	4.04
Muen	Muen Mb, Muen shale units (1–4)	35	1.65	4.44	0.47	465	0.27	95	10	4.66
Muen	Muen Mb, Muen shale units (1–4)	31	1.28	2.25	0.33	463	0.36	97	14	2.31
Muen (F+GC)	Vikinghogda Fm	22	1.55	3.48	0.49	467	0.31	93	13	3.74
Muen	Vikinghogda Fm (silty shale with Euflemingites Romunderi from fresh rockslide by the sea)	4	0.66	0.84	0.19	359	0.44	90	20	0.93

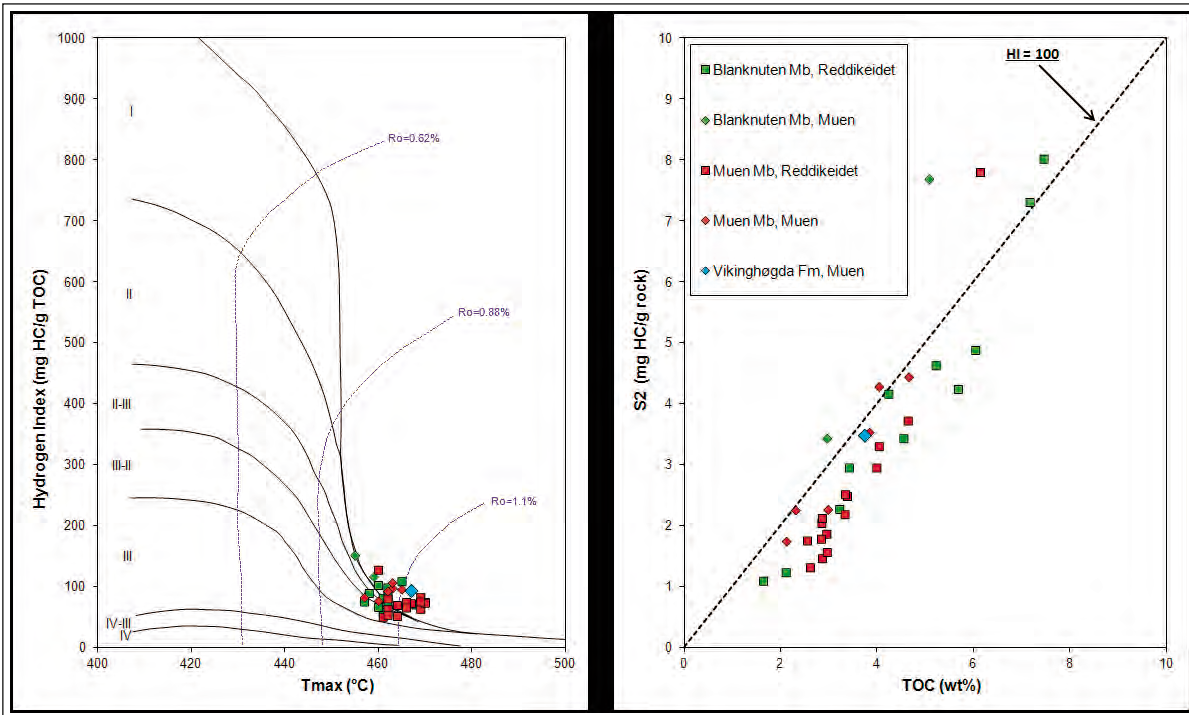


Figure 7. Hydrogen Index vs.  $T_{max}$  and Rock-Eval S2 vs. TOC content. Iso-reflectance lines on HI vs.  $T_{max}$  plot are according to Isaksen and Ledje (2001).

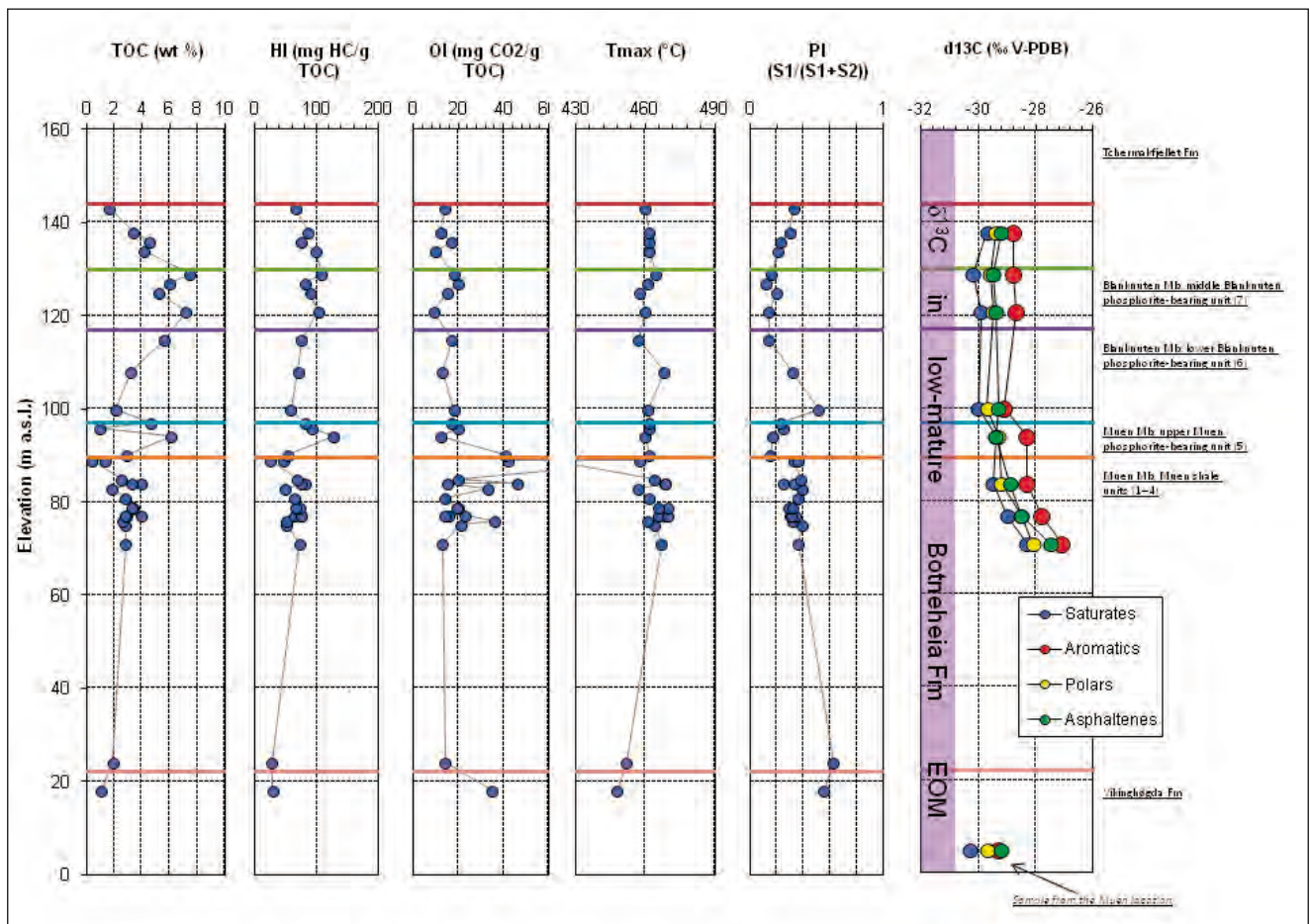


Figure 8. Rock-Eval and stable carbon isotope geochemistry in shales. The isotope fraction data in the Vikinghogda Formation from Muen is inserted for comparison (not to elevation); otherwise all data represent the Reddikeidet section.

**Table 2.** Calculated vitrinite reflectance ( $R_c$ ). Aromatic molecular parameters are from GC MSD analysis of aromatic fraction, peak height data.

Locality	Reddikeidet	Muen	Reddikeidet	Muen	
Lithostratigraphy	Blanknuten Mb, middle Blanknuten phosphorite-bearing unit (7)	Vikinghøgda Fm	Blanknuten Mb, middle Blanknuten phosphorite-bearing unit (7)	Vikinghøgda Fm	
Elevation (m a.s.l.)	129	22	129	22	
	Peak height ratios		$R_c$		$R_c$ formulae
MNR = 2-MN/1-MN	1.84	1.40	1.13	1.06	$R_c = 0.17 \cdot \text{MNR} + 0.82$ (Radke et al. 1982)
DNR 1 = 2,6DMN+2,7DMN/1,5DMN	9.52	7.01	1.33	1.21	$R_c = 0.046 \cdot \text{DNR} + 0.89$ (Radke et al. 1982)
MPI1 = (2MP+3MP)/(P+1MP+9MP)	1.02	0.99	1.01	1.00	$R_c = 0.6 \cdot \text{MPI1} + 0.4$ (Radke and Welte 1983)
F1 = (2MP+3MP)/(2MP+3MP+1MP+9MP)	0.56	0.50	1.08	0.97	$R_c = -0.166 + 2.242 \cdot \text{F1}$ (Kvalheim et al. 1987)
F2 = 2MP/(2MP+3MP+1MP+9MP)	0.33	0.29	1.12	0.96	$R_c = -0.112 + 3.739 \cdot \text{F2}$ (Kvalheim et al. 1987)
Average			1.14	1.04	

matter is mostly residual, reflecting thermal degradation of alginite and bituminite, which dominate the organic pool of the Botneheia Formation in sections of lower maturity (Abdullah, 1999; Krajewski, 2000, 2013). Its low reflectance corresponds to impregnation by exudatinitite, though micrinite particles were identified under high magnification in samples of the Blanknuten Member at Reddikeidet. All large alginite particles representing *Tasmanites* thalli are replaced by mineral matter. The replacement structures consist either of acicular quartz crystals (Fig. 6b) or rhomboidal dolomite crystals (Fig. 6c) or various combinations of the two. Pores between the crystals are filled by exudatinitite. In the Reddikeidet section the dolomite replacements are abundant. In the Muen section the quartz and dolomite replacements are equally common. The dolomite replacing *Tasmanites* is similar to the second generation of dolomite revealed in the host sediment. It shows common bitumen inclusions (Fig. 6d) that exhibit bright fluorescence under blue light excitation. The sedimentary organic components preserved in the Reddikeidet and Muen sections embrace various palynomorphs (Fig. 6e) and vitrinitic particles (Fig. 6f). The latter are represented by telinite and telocolinite particles, usually less than 200  $\mu\text{m}$  in size, as well as by vitrodetrinite. Inertinite is represented by inertodetrinite showing no fluorescence and very high reflectance.

## Rock-Eval data

The Rock-Eval and TOC data are given in Table 1, with selected parameters graphed in Figs. 7 and 8. The sample set includes a few samples from the Vikinghøgda and Tschermakfjellet formations below and above the Botneheia Formation, respectively. Of these, the sample from 22 m above sea level in the Vikinghøgda Formation at Muen was one of the two samples chosen for follow-up analyses (Fig. 4b).

The most striking feature in the results is the advanced maturity. The samples have  $T_{\text{max}}$  mostly in the range of 457 °C – 470 °C, corresponding to a vitrinite reflectance between 1.0 %  $R_o$  and 1.2 %  $R_o$  (Table 1, Fig. 7). Table 2 lists a number of calculated vitrinite reflectance ( $R_c$ ) based on GC-MSD aromatic maturity parameters from the two follow-up samples at Reddikeidet and Muen. Table 3 lists  $R_c$  values based on average  $T_{\text{max}}$  from Reddikeidet and Muen. There is a good agreement between  $R_c$  calculated from aromatic parameters and  $R_c$  calculated from  $T_{\text{max}}$  ( $R_c$ ; Isaksen and Ledje, 2001). Furthermore, the  $T_{\text{max}}$  data and the aromatic parameters both show slightly higher maturity at Reddikeidet compared to Muen. This difference is consistent with slightly lower TOC and HI values in the Reddikeidet location compared to the Muen location.

**Table 3.** Calculated vitrinite reflectance ( $R_c = 0.014 \cdot T_{\text{max}} - 5.3846$ ; derived from Isaksen and Ledje (2001)). The  $T_{\text{max}}$  values are averages for samples with  $S_2 > 1.0$  mg HC/g TOC.

	$T_{\text{max}}$ (°C)		$R_c$	
	Reddikeidet	Muen	Reddikeidet	Muen
Muen Mb average	465.4	461.6	1.13	1.08
Blanknuten Mb average	461.9	457	1.08	1.01
Botneheia Fm average	463.7	461.2	1.11	1.07



**Table 4.** Extractable Organic Matter (EOM), asphaltenes, and stable carbon isotope data.  
 $\delta^{13}\text{C-EOM}_{\text{calculated}} = 0.42 \cdot \delta^{13}\text{C-SAT} + 0.17 \cdot \delta^{13}\text{C-ARO} + 0.205 \cdot \delta^{13}\text{C-POL} + 0.205 \cdot \delta^{13}\text{C-ASPH}$ , where the coefficients are averages of the fraction data in Hubred's samples taken less than 1.5 times the sill thickness away from a sill contact.

Lithostratigraphy	Elevation (m a.s.l.)	Rock weight (g)	EOM (mg)	EOM (mg/kg rock)	ASPH (wt% of EOM)	$\delta^{13}\text{C-EOM}_{\text{calculated}}$ (‰ V-PDB)	$\delta^{13}\text{C-SAT}$ (‰ V-PDB)	$\delta^{13}\text{C-ARO}$ (‰ V-PDB)	$\delta^{13}\text{C-POL}$ (‰ V-PDB)	$\delta^{13}\text{C-ASPH}$ (‰ V-PDB)
Muen Mb, Muen shale units (1–4)	71	20.2	38	1878	2.4	-27.9	-28.3	-27.1	-28.1	-27.5
Muen Mb, Muen shale units (1–4)	77	21.1	50	2350	3.1	-28.6	-29.0	-27.8	-28.5	-28.5
Muen Mb, Muen shale units (1–4)	84	19.9	39	1946	3	-29.1	-29.5	-28.3	-29.2	-28.9
Muen Mb, upper Muen phosphorite-bearing unit (5)	94	21.2	74	3478	3.1	-29.2	-29.4	-28.3	-29.3	-29.4
Blanknuten Mb, lower Blanknuten phosphorite-bearing unit (6)	100	19.6	24	1229	4.6	-29.6	-30.0	-29.1	-29.7	-29.3
Blanknuten Mb, middle Blanknuten phosphorite-bearing unit (7)	121	20.8	46	2236	6.1	-29.5	-29.9	-28.7	-29.5	-29.4
Blanknuten Mb, middle Blanknuten phosphorite-bearing unit (7)	129	20.0	49	2432	6.4	-29.7	-30.2	-28.8	-29.6	-29.5
Blanknuten Mb, top Blanknuten phosphorite-bearing unit (9)	138	20.7	38	1828	5.1	-29.4	-29.7	-28.8	-29.4	-29.2
Vikinghøgda Fm, Sample from outcrop by the creek ca. 5 m below base Muen mb.	22	18.8	43	2260	4.6	-29.8	-30.3	-29.3	-29.7	-29.2

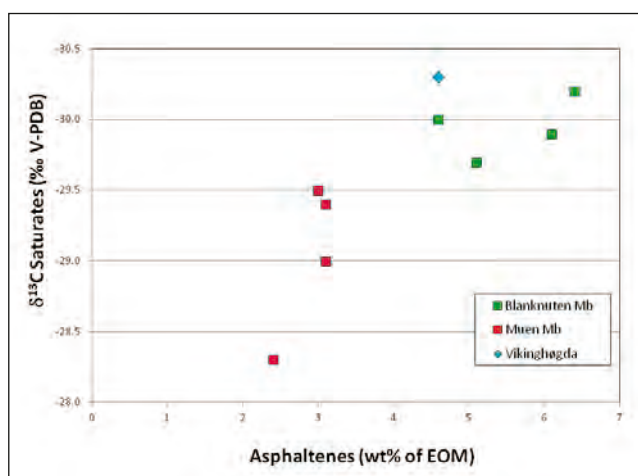


Figure 9. Asphaltene content vs. saturated fraction carbon isotopes.

Despite the advanced maturity and degradation there is still sufficient organic matter left to show clear trends in TOC content in the data from Reddikeidet (Fig. 8). The most organic-rich shales are seen in the phosphorite-bearing part of the succession, with up to 7.5 wt % in the middle and upper phosphorite-bearing units (Units 7 and 8) of the Blanknuten Member. These units also have the highest overall HI, although the single highest HI value is seen in the upper phosphorite-bearing unit of the Muen Member. The maximum HI in immature Botneheia Formation in the Barentsøya – Edgeøya outcrop belt is around 600 mg HC/g TOC (Schou et al., 1984; Vigran et al., 2008; Krajewski, 2011, 2013). If we assume that the

original HI was around 600 mg HC/g TOC in the richest samples in the Blanknuten Member at Reddikeidet we can tentatively calculate that the initial TOC content was up to 14 wt % in the richest sample. These calculations follow the method outlined in Justwan and Dahl (2005). They show that the transformation ratio from kerogen to petroleum has reached approximately 0.9, i.e. the remaining S2 represents only about 10 % of the original S2 value.

Most samples at Reddikeidet have oxygen index (OI) values in the range 10 – 20 mg CO<sub>2</sub>/g TOC. However, a number of samples in the Muen Member have substantially higher OI, suggesting episodes with more oxic conditions and/or more terrigenous input to the total organic matter preserved (Krajewski, 2013). The slightly higher T<sub>max</sub> seen in the Muen shales, especially in the non-phosphogenic part of the succession compared to the phosphogenic Blanknuten Member, also suggest more oxidized or terrigenous kerogen in the Muen Member (e.g. Hunt, 1995). This is consistent with microscopic observations that reveal elevated content of terrigenous and reworked fractions (vitrinitic and inertinitic particles) in the non-phosphogenic shale succession of the Muen Member (Fig. 6).

## Extract

Results from extraction, de-asphaltening and stable carbon isotope analyses of bulk fractions are given in Table 4. The asphaltene content is generally low in all samples, but it is consistently higher in the Blanknuten

Member and the sample from the Vikinghøgda Formation compared to the Muen Member. The  $\delta^{13}\text{C}$  values in samples and fractions span a range from -27.1 to -30.3 ‰. There are clear stratigraphic variations in these values. The Muen Member shows heavier isotopic compositions of organic carbon than the Blanknuten Member and the Vikinghøgda Formation in nearly all samples and fractions.

When  $\delta^{13}\text{C}$  values and asphaltene contents are cross-plotted (Fig. 9), the general picture is that the increasing asphaltene contents co-vary with lighter isotopic compositions of organic carbon. Similar data in a study of extracts from the Kimmeridge Clay in the North Sea (Macko and Quick, 1986) show the same kind of covariance. The reason for this relationship remains unclear, though it is noted here as an observation.

The GC-MSD analyses show no identifiable triterpanes or steranes in the saturated fraction and no identifiable mono- and triaromatic steroid hydrocarbons in the aromatic fraction. The  $\text{C}_{33}$  *n*-alkylcyclohexane was not found to occur in higher concentrations than the corresponding  $\text{C}_{34}$  compound. The polycyclic aromatic hydrocarbons are well developed.

## Discussion

### Weathering effects

There is always a possibility of weathering effects on organic matter in outcrop samples. At first sight, the relatively low contents of various organic constituents in the studied samples may indicate that weathering has had a major impact on organic matter preservation. Forsberg and Bjørøy (1983) made a thorough study of weathering effects on outcrop samples from the Botneheia Formation at Jinnbreen in central Spitsbergen. By comparing surface outcrop samples to shallow core samples they found that there was no significant weathering influence on the TOC and Rock-Eval characteristics in the surface samples, while the extractable organic matter (EOM) was reduced on average by 10 %. They suggested that a reduction in the ratio of aromatic constituents to saturated constituents was due to oxidation of the aromatics, while a reduction in the ratio of straight-chain isoprenoids to *n*-alkanes was attributed to mild biodegradation. The weathering effects were quite variable from sample to sample, and the isoprenoid/*n*-alkane ratio showed the most dramatic variations.

These relatively mild weathering effects are perhaps not surprising considering the quite short exposure times after the ice age, and the cold climate that has prevailed since then. Since the whole of Svalbard can be considered to have had roughly the same exposure time since the ice age and the same climate, there is no reason to believe that western Edgeøya should be any different from central Spitsbergen. This means that we can expect the

TOC and Rock-Eval analyses to be representative, while the GC and GC-MSD data should be considered with some caution.

### Thermal effect of dolerite intrusions

The most likely cause of the anomalous maturity in the area south of Diskobukta is obviously local heating by dolerite intrusions. Hubred (2006) found that the thermal effects on organic matter reached out as far as 1.5 times the dolerite thickness for some parameters. Aarnes et al. (2011) have shown that by interaction effects in space and/or time between multiple dolerite bodies the thermal effect can be up to seven times a single dolerite thickness. The sills in Svalbard vary in thickness from less than 1 m to more than 100 m, although most of them are about 10 to 30 m thick. (Nejbert et al., 2011). The observed lateral extent of individual sills attains 10 – 15 km (Mørk et al., 1999), but may be greater in extreme cases, e.g. in the Ginevrobotnen – Frankenhøya area between northern Barentsøya and Spitsbergen. The dolerites intruding the Botneheia Formation studied by Hubred (2006) range from 5 to 35 m in thickness. Rock-Eval, vitrinite reflectance, and other data in Hubred's study indicate a span in maturity from totally burnt-out organic matter at the dolerite contacts to normal background maturity in samples located more than 1.5 times the dolerite thickness away from the contacts.

The advanced maturity at Muen and Reddikeidet indicate the influence of intrusives close to the sampled sections. Since there are no visible dolerites at the studied localities, we conceive two scenarios that could have created the evident massive heat influence:

1. Several "normal sized" (10 – 30 m thickness) dolerite sills made up an interacting heat system as described by Aarnes et al. (2011). Today only the ones below sea level exist, and those that had occurred up the succession were eroded during the uplift of the islands.
2. There exists one major intrusive body, for example a dolerite sill of significant thickness and lateral extent below sea level south of Diskobukta.

The lack of visible remains of eroded doleritic rocks along the shorelines near the sampled locations indicate that no dolerite in the Sassendalen Group above sea level exist or existed close enough to have made a significant thermal impact on the Botneheia Formation south of Diskobukta. This leaves scenario 2, i.e. one large intrusive body below sea level in the Vikinghøgda Formation or deeper, as the most likely. This hypothetical intrusive body might be a northward continuation of the Årdalstangen dolerite cluster exposed between Martinodden and Svarttangen (Figs. 1, 2). The Årdalstangen dolerite cluster shows only the upper part of an extensive sill exposed to the surface, so its thickness is unknown. However, erosional cuts into the sill in Ekrollhamna and Habenichtbukta suggest that the intrusive body is considerably thick. The cluster intrudes into the Triassic succession separating the Årdalsnuten – Kvalpyntfjellet massif on the south from

the Burmeisterfjellet – Ziegel’fjellet massif on the north (Fig. 2). The Triassic strata in the two areas dip slightly towards the cluster and show different uplift, with the Vikinghøgda and Tschermakfjellet–Botneheia formations at sea level, respectively. This may be related to a fault zone in the area, which enabled extensive dolerite intrusions at Årdalstangen. The Årdalstangen cluster shows a composite internal structure and undulated morphology, though it dips gently northwards. Such a dipping sill (or cluster of sills) of considerable thickness would provide fading thermal effect on the sedimentary rock formations at sea level or above toward Diskobukta and eastward into the interior of Edgeøya. This is exactly what we observe in the maturity levels at Reddikeidet and Muen located ca. 15 and 30 km north of the Årdalstangen cluster. Based on the observed difference in maturity between the two locations the intrusive body should be thicker or closer to the surface at Reddikeidet than at Muen. Two boreholes located northeast of the Årdalstangen cluster (Plurdalen-1 and Raddedalen-1) provide further evidence of vanishing effects of dolerite intrusions from the western coast of Edgeøya eastward (Shvarts, 1985, Harland, 1997). The Plurdalen-1 borehole was located in the upper part of Plurdalen, ca 20 km northeast of the Årdalstangen dolerite cluster and ca 10 km east of Reddikeidet and Muen (Fig. 1). Its stratigraphic log embraces 2400 m of succession (?Pre-Devonian to Triassic), out of which the topmost 128 m in the Vikinghøgda Formation (Harland, 1997). No dolerite rock or thermally altered zones have been revealed in the obtained cores and cuttings. The Raddedalen-1 borehole was located in the outcrop area of the Permian Kapp Starostin Formation between Smelledalen and Blåbuktdalen, ca 55 km and 30 km northeast of the Årdalstangen dolerite cluster and Muen section, respectively. The borehole penetrated 2900 m of stratigraphic section (Ordovician – Permian) without any sign of intrusive activity or thermal alteration (Harland, 1997).

The analysed sections at Reddikeidet and Muen extend from the sea level to 170 m above. They show remarkably uniform and advanced maturity throughout. This could be a tail of the aureole from a very thick underlying dolerite sill. The most deviating shale sample is from the Vikinghøgda Formation at base of the sampled section at Muen. It is characterised by low TOC and an abnormally low  $T_{max}$ , both features can be associated with close proximity to a sill contact (Hubred, 2006). This is another support to our suggestion that there exists a very massive intrusive not far below sea level south of Diskobukta. While the heat from this intrusive was insufficient for hornfelsing and calcification in the exposed sections, it was evidently sufficient for major alterations of volatile constituents such as organic matter. However, enhanced dolomitization and precipitation of sulphidic minerals can be related to this heat flow and reactions associated with kerogen cracking, bitumen generation, and thermochemical reduction processes (Worden et al., 2000, 2003). It is clear that the heat from this intrusive must

have generated large amounts of petroleum in the area: about 90 % of the potential seems to have been realised (see above). Petroleum generation is confirmed by live oil within the formation (Smelror and Sollid, 2007), and by common liquid bitumen in cracks of diagenetic carbonate concretions and in micro-inclusions in burial carbonate cements (Krajewski, 2013).

The global carbon isotope record for the Triassic period is a complex one. A pronounced negative excursion began before the Permian/Triassic boundary event and continued into the earliest Triassic times. The succeeding 4 to 6 Ma time period during the Early Triassic (Induan – Olenekian) is marked by isotopic instability, with positive and negative excursions. Following a distinct positive Carbon Isotope Excursion (CIE) in the earliest Anisian, less isotopic variation is seen throughout the Anisian (Tanner, 2010, Hermann et al., 2010). Galfetti et al. (2007) provide a bulk OC isotope profile through the Lower Triassic Vikinghøgda Formation at Kongressfjellet (78° 33’ 40.3” N, 15° 19’ 07.2” E; coordinates provided by T. Galfetti, pers. comm., 2014) in central Spitsbergen that fits very well with the global pattern. The carbon isotopic data presented in this study show an abrupt deviation towards more positive values, which does not fit with the global isotopic record for the early Anisian. Data from Hubred (2006) show that this deviation can be explained in terms of thermal effects caused by the dolerite intrusions.

Hubred’s data on carbon isotopes in EOM from the Botneheia Formation on SW Barentsøya and in central Spitsbergen are graphed in Fig. 10. These data span a range from 32.2 ‰ to -28.1 ‰. The more positive values (-30.5 ‰ to -28.1 ‰) are only found in samples that were taken less than 1.5 times the sill thickness away from the contact. These isotopic compositions are very likely affected by the heat from the dolerite intrusions. The more negative range

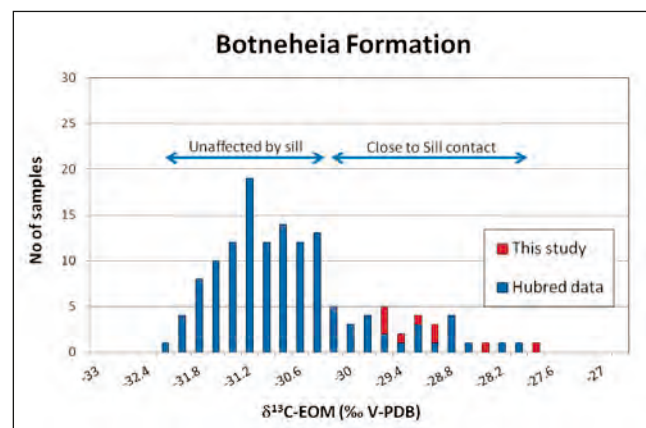
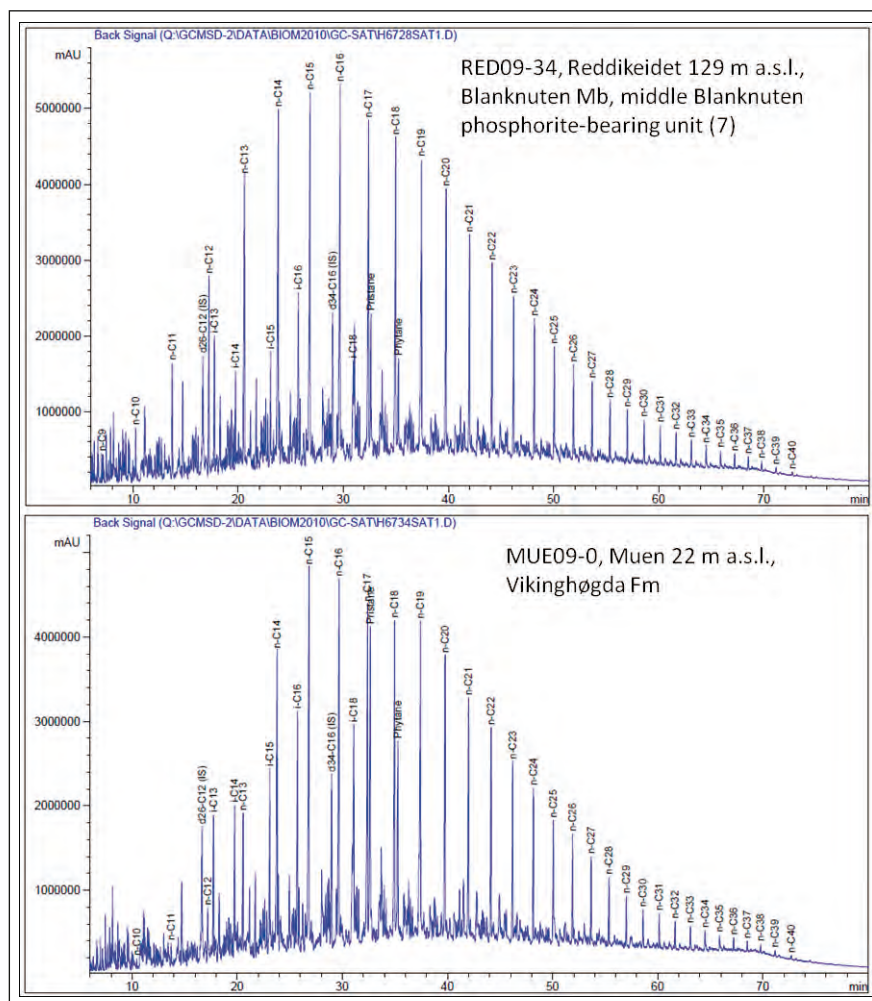


Figure 10. Frequency distribution of carbon isotopes in EOM. Data from Hubred (2006).

“Unaffected by sill” correspond to samples > 1.5 times the sill thickness away from sill. EOM isotopes were not measured in this study; they are calculated as weighted sums of the fraction isotope data (see caption, Table 4).



Figure 11. Gas chromatograms of the saturated fraction from two samples.



(-32.2 ‰ to -30.6 ‰) characterizes samples unaffected by the dolerites, thus representing the true carbon isotopic composition in the Botneheia Formation. It is therefore likely that the dolerite heat has caused a positive shift of 1 to 3 ‰ in  $\delta^{13}\text{C}$  for the extracts in thermally altered sections of the Botneheia Formation on SW Edgeøya, compared to the low-mature sections analysed by Hubred (2006).

Primary petroleum generation does not produce significant isotopic shifts in the expelled petroleum. However, large thermally induced positive isotope shifts (> 1 ‰) in oils and bitumen are known to be caused by oil cracking (Clayton, 1991). Hence, the heat from the dolerite intrusions must have caused not only primary kerogen cracking to oil, but also thermal cracking of the generated oil. The interesting implication of this is that large parts of the primary oil in fact may have been converted instantaneously to gas and that gas has constituted a major fraction of the petroleum that migrated out of the Botneheia Formation in the most thermally altered areas. Exudatinites are common throughout the studied sections (Fig. 6). It is the secondary maceral forming solid residuum after generation, maturation, and migration of bitumen in the source rock (Taylor et al., 1998). Oil cracking begins at 150 °C to 160 °C (see e.g. Hunt, 1995, page 152 or Peters et al., 2005 volume 1, page 159). The temperature required

for oil cracking also depends on the time period during which the oil is exposed to the heat (Hunt 1995). The heat spots caused by intrusions in the form of sills and dykes are short-lived compared to the regional heat flows in sedimentary basins related to burial (Tissot and Welte, 1984). Therefore the temperature required for oil cracking as a result of localized intrusion probably is higher than the one related to the regional heat flow.

The isotopically heavier composition of carbon in extracts from the Muen Member compared to the Blanknuten Member reflects a higher content of terrigenous organic matter and more oxic depositional conditions in the Muen Member, similar to the heterogeneous situation often seen in the Draupne Formation in the North Sea (Justwan et al., 2006; Keym et al., 2006).

Gas chromatograms of the two samples chosen for molecular analyses are shown in Fig. 11. One sample is from the Blanknuten Member of the Botneheia Formation at Reddikeidet, the other is from the Vikinghøgda Formation at Muen. The two samples show close similarities. The only noticeable difference is a depletion of *n*-alkanes relative to straight-chain isoprenoids in the sample from Muen. This difference can be caused either by minor biodegradation (Forsberg and Bjørøy, 1983), or by lower maturity, in the

Muen sample compared to the Reddikeidet sample. The latter interpretation is qualitatively in agreement with the Rock-Eval  $T_{\max}$  and the aromatic biomarker data at the two locations (Tables 2 and 3).

The mass fragmentograms of the saturated biomarkers (triterpanes and steranes) contain no identifiable peaks, which is normal for the high thermal maturity level (Tables 2 and 3). The  $C_{33}$  *n*-alkylcyclohexane was not found to occur in higher concentrations than the corresponding  $C_{34}$  compound. This may indicate that the globally high concentration of this compound seen in the earliest Triassic (Grice et al., 2005) has dropped to non-diagnostic levels in the early Anisian. However, due to the advanced maturity the present results cannot be taken as a definite proof of low concentrations of this age-diagnostic biomarker compound in the Vikinghøgda and Botneheia formations. The mass fragmentograms representing mono- and triaromatic steroid hydrocarbons show no identifiable peaks. The polycyclic aromatic hydrocarbons are well developed and the composition of the methylated naphthalenes and phenanthrenes is consistent with the high level of maturity.

The aromatics indicate a slightly lower maturity in the Vikinghøgda Formation sample 22 m above sea level at Muen, compared to the Blanknuten Member sample 129 m above sea level at Reddikeidet, testifying to the overall higher level of maturity of the Triassic succession at Reddikeidet than at Muen.

## Conclusions

- Two sections of the Botneheia Formation on SW Edgeøya, Svalbard (Reddikeidet and Muen) have been sampled and analysed by petrographic and organic geochemical methods. Both sections show anomalously advanced maturity compared to the regional maturity of the Botneheia Formation in eastern Svalbard. This is consistent with earlier reports (Krajewski, 2013; Mørk and Bjørøy, 1984; Schou et al., 1984).
- No significant weathering effects are believed to have affected the analysed samples.
- The advanced maturity is proposed to be due to a very thick dolerite intrusion occurring below sea level south of Diskobukta in the lower part of the Vikinghøgda Formation. This hypothetical dolerite body might be a continuation of the Årdalstangen dolerite cluster located further south.
- The thermal alteration of organic carbon is uniform throughout the sampled sections up to 170 m above sea level, suggesting an unusually thick intrusive body.
- The maturity profiles are different from the bell-shaped maturity profile often observed around sills of moderate thicknesses. The uniform advanced maturity level seen in the organic components is supported by the concentration of late diagenetic mineral phases related

to bitumen generation and thermochemical reduction processes throughout the sections studied.

- A consistent difference in maturity between the two locations is observed, with average calculated vitrinite reflectance ( $R_o$ ) equal to 1.14 % at Reddikeidet and 1.05 % at Muen. The dolerite intrusion is therefore supposed to be thicker, or closer to surface at Reddikeidet than at Muen, which is consistent with the postulated northward continuation of the Årdalstangen dolerite cluster.
- In the Triassic succession south of Diskobukta, the heat flow from the dolerite intrusion has transformed a major part of kerogen into petroleum. Assuming the original Hydrogen Index in the most OC-rich intervals was around 600 mg HC/g TOC, we find that ca 90 % of the original petroleum potential has been realized. All microscopically discernible alginite material (mostly *Tasmanites*) was thermally decomposed and replaced by mineral matter (dolomite, quartz) and exudatinitite.
- Due to the advanced maturity molecular analyses by GC-MS proved no detectable triterpanes and steranes in the saturated fraction and no mono- and triaromatic steroid hydrocarbons in the aromatic fraction. Methylated naphthalenes and phenanthrenes are well developed, showing maturity consistent with Rock-Eval  $T_{\max}$  and the content of organic carbon.
- The stable carbon isotopic composition of extracts, expressed as  $\delta^{13}C$  relative to V-PDB, was found to be 1 to 3 ‰ more positive than the one observed in extracts from low-mature sections of the Botneheia Formation. This is believed to be caused by secondary oil cracking due to the dolerite heat. An implication of this may be that a major part of the petroleum that migrated out of the Botneheia Formation as a result of dolerite intrusion was gas.
- An age-diagnostic biomarker,  $C_{33}$  *n*-alkylcyclohexane (Grice et al., 2005), abundant in marine organic matter in the aftermath of the end-Permian extinction, is not present in higher concentrations than the corresponding  $C_{34}$  compound. This indicates that the concentration of this compound has dropped to non-diagnostic levels in the early Anisian. Less mature sections should, however, be analysed to confirm this finding.

### Acknowledgements.

We are grateful to the Norwegian Petroleum Directorate (Oljedirektoratet) for inviting TB and KPK to its expeditions to Svalbard on board M/S *Kongsøy* in 2007 and 2009. We thank the crew of M/S *Kongsøy* for logistical support and the colleagues and friends from the Svalbard party for good company in the field. Marta Ślubowska-Woldengen helped us in sampling the Reddikeidet section in 2009. Bożena Łącka at the Institute of Geological Sciences, Polish Academy of Sciences in Warszawa prepared samples for XRD analysis, and Ewa Deput made thin sections. Professor Dag A. Karlsen at the University of Oslo, Department of Geosciences, is thanked for valuable input about the thermal effects of sills.

## References

- Abdullah, H.W. 1999: Organic facies variations in the Triassic shallow marine and deep marine shales of central Spitsbergen, Svalbard. *Marine and Petroleum Geology*, 16, 467-481.
- Bjorøy, M., Hall, P.B. & Mørk, A. 2006: Triassic hydrocarbon source rocks on Svalbard and in the Barents Sea. *Abstracts and Proceedings of the Norwegian Petroleum Society*, 3, 42-45.
- Bjorøy, M., Hall, P.B., Ferriday, I.L. & Mørk, A. 2010: Triassic Source Rocks of the Barents Sea and Svalbard. *Search and Discovery Article #10219* posted February 3, 2010 (Adapted from poster presentation at AAPG Convention, Denver, Colorado, June 7-10, 2009).
- Burov, Y.P., Krasil'scikov, A.A., Firsov, L.V. & Klubov, B.A. 1975: The age of Spitsbergen dolerites (from isotopic dating). *Årbok Norsk Polarinstitutt 1975*, 101-108.
- Clayton, C.J. 1991: Effect of maturity on carbon isotope ratios of oils and condensates. *Organic Geochemistry*, 17, 887-899.
- Dahlgren, S., Hanesand, T., Mills, N., Patience, R., Brekke, T. & Sinding-Larsen, R. 1998: *Norwegian Geochemical Standards Newsletter vol. 1, Norwegian Geochemical Standard samples: Svalbard Rock - 1 (NGS SR-1)*. The Norwegian Petroleum Directorate, Stavanger, Norway.
- Dallmann W. K., Ohta Y., Elvevold S. & Blomeier D. (eds.): 2002: *Bedrock Map of Svalbard and Jan Mayen*. Norsk Polarinstitutt Temakart 33.
- Forsberg, A.W. & Bjorøy, M. 1983: A sedimentological and organic geochemical study of the Botneheia Formation, Svalbard, with special emphasis on the effects of weathering on the organic matter in shales. In Bjorøy, M., Albrecht, P., Cornford, C. et al. (eds.): *Advances in Organic Geochemistry 1981*, 60-68, Wiley, Chichester.
- Galfetti, T., Hochuli, P.A., Brayard, A., Bucher, H., Weissert, H. & Vigran, J.O. 2007: Smithian-Spathian boundary event: Evidence for global climatic change in the wake of the end-Permian biotic crisis. *Geology*, 35, 291-294.
- Grice, K., Twitchett, R.J., Foster, C.B., Alexander, R. & Looy, C. 2005: A potential biomarker for the Permian-Triassic ecological crisis. *Earth and Planetary Science Letters*, 236, 315-321.
- Harland, W.B. 1997: *The Geology of Svalbard*. Geological Society London Memoir, 17, 521 pp. ISBN: 1-897799-93-4.
- Hermann, E., Hochuli, P.A., Bucher, H., Vigran J.O., Weissert, H. & Bernasconi, S.M. 2010: A close-up view of the Permian-Triassic boundary based on expanded organic carbon isotope records from Norway (Trøndelag and Finnmark Platform). *Global and Planetary Change*, 74, 156-167.
- Hubred, J.H. 2006: *Thermal effects of basaltic sill emplacement in source rocks on maturation and hydrocarbon generation*, Cand. Scient. Thesis, University of Oslo. Permanent link: <http://urn.nb.no/URN:NBN:no-12609>, direct link to PDF document: [https://www.duo.uio.no/bitstream/handle/123456789/12406/jornar\\_thesis\\_small.pdf?sequence=1](https://www.duo.uio.no/bitstream/handle/123456789/12406/jornar_thesis_small.pdf?sequence=1),
- Hunt, J.M. 1995: *Petroleum Geochemistry and Geology*. W. H. Freeman and Company New York, ISBN: 0-7167-2441-3, 743 pp.
- Isaksen, H.I. 1996: Organic geochemistry and geohistory of the Triassic succession of Bjørnøya, Barents Sea. *Organic Geochemistry*, 24, 333-349.
- Isaksen, G.H. & Ledje, H.I. 2001: Source rock quality and hydrocarbon migration pathways within the greater Utsira High area, Viking Graben, Norwegian North Sea. *American Association of Petroleum Geologists Bulletin*, 85, 861-883.
- Justwan, H. & Dahl, B. 2005: Quantitative hydrocarbon potential mapping and organofacies study in the Greater Balder Area, Norwegian North Sea. In Doré, A.G. & Vining, B. (eds.): *Petroleum Geology: North-West Europe and Global Perspectives - Proceedings of the 6<sup>th</sup> Petroleum Geology Conference*, 1317 - 1329, Petroleum Geology Conferences Ltd. Published by Geological Society, London.
- Justwan, H., Dahl, B. & Isaksen, G.H. 2006: Geochemical characterisation and genetic origin of oils and condensates in the South Viking Graben, Norway. *Marine and Petroleum Geology*, 23, 213-239.
- Keym, M., Dieckman, V., Horsfield, B., Erdmann, M., Galimberti, R., Kuo, L.-C., Leith, L., & Podlaha, O. 2006: Source rock heterogeneity of the Upper Jurassic Draupne Formation, North Viking Graben, and its relevance to petroleum generation studies. *Organic Geochemistry*, 37, 220-243.
- Krajewski, K.P. 2000: Phosphorus concentration and organic carbon preservation in the Blanknuten Member (Botneheia Formation, Middle Triassic) in Sassenfjorden, Spitsbergen. *Studia Geologica Polonica*, 116, 139-173.
- Krajewski, K.P. 2008: The Botneheia Formation (Middle Triassic) in Edgeøya and Barentsøya, Svalbard: lithostratigraphy, facies, phosphogenesis, paleoenvironment. *Polish Polar Research*, 29, 319-364.
- Krajewski, K.P. 2011: Phosphatic microbialites in the Triassic phosphogenic facies of Svalbard. In Tewari, V.C. & Seckbach, J. (eds.): *Stromatolites: Interaction of Microbes with Sediments. Cellular Origin, Life in Extreme Habitats and Astrobiology*, 18, 187-222, Springer.
- Krajewski, K.P. 2013: Organic matter-apatite-pyrite relationships in the Botneheia Formation (Middle Triassic) of eastern Svalbard: Relevance to the formation of petroleum source rocks in the NW Barents Sea shelf. *Marine and Petroleum Geology*, 45, 69-105.
- Krajewski, K.P. & Woźny, E. 2009: Origin of dolomite-ankerite cement in the Bravaisberget Formation (Middle Triassic) in Spitsbergen, Svalbard. *Polish Polar Research*, 30, 231-248.
- Krajewski, K.P., Karcz, P., Woźny, E. & Mørk, A. 2007: Type section of the Bravaisberget Formation (Middle Triassic) at Bravaisberget, western Nathorst Land, Spitsbergen, Svalbard. *Polish Polar Research*, 28, 79-122.
- Kvalheim, O.M., Christy, A.A., Telnæs, N., & Bjørseth, A. 1987: Maturity determination of organic matter in coals using the methylphenanthrene distribution. *Geochimica et Cosmochimica Acta*, 51, 1883-1888.
- Leith, T.L., Weiss, H.M., Mørk, A., Århus, N., Elvebakk, G., Embry, A.F., Brooks, P.W., Stewart, K.R., Pchelina, T.M., Bro, E.G., Verba, M.L., Danyushevskaya A. & Borisov, A.V. 1992: Mesozoic hydrocarbon source-rocks of the Arctic region. In Vorren, T.O. et al. (ed.): *Arctic Geology and Petroleum Potential*, Norwegian Petroleum Society (NPF) Special Publication, 2, 1-25, Elsevier, Amsterdam.
- Macko, S.A. & Quick, R.S. 1986: A geochemical study of oil migration at source rock reservoir contacts: Stable isotopes. *Organic Geochemistry*, 10, 199-205.
- Mørk, A. & Bjorøy, M. 1984: Mesozoic source rocks on Svalbard, In Spencer A.M. et al. (eds.) *Petroleum Geology of the North European Margin*, 371-382, Norwegian Petroleum Society (Graham & Trotman).
- Mørk A., Knarud R. & Worsley D. 1982: Depositional and diagenetic environments of the Triassic and Lower Jurassic succession of Svalbard. In Embry, A.F. & Balkwill, H.R. (eds): *Arctic Geology and Geophysics*. Canadian Society Petroleum Geologists Memoir, 8, 371-398.
- Mørk, A., Vigran, J.O. & Hochuli, P.A. 1990: Geology and palynology of the Triassic succession of Bjørnøya. *Polar Research*, 8, 141-163.
- Mørk, A., Dallmann, W.K., Dypvik, H., Johannessen, E.P., Larssen, G.B., Nagy, J., Nøttvedt, A., Olaussen, S., Pchelina, T.M. & Worsley, D. 1999: Mesozoic lithostratigraphy. In Dallmann, W. K. (ed.) *Lithostratigraphic Lexicon of Svalbard. Review and Recommendations for Nomenclature Use. Upper Palaeozoic to Quaternary Bedrock*. Norsk Polarinstitutt, Tromsø, 127-214.
- Nejbert, K., Krajewski, K.P., Dubińska, E. & Pécskay, Z. 2011: Dolerites of Svalbard, north-west Barents Sea Shelf: age, tectonic setting and significance for geotectonic interpretation of the High-Arctic Large Igneous Province. *Polar Research*, 30, 7306 - DOI: 10.3402/polar.v30i0.7306., [http://www.polarresearch.net/index.php/polar/article/download/7306/pdf\\_216](http://www.polarresearch.net/index.php/polar/article/download/7306/pdf_216)
- Peters, K.E., Walters, C.C. & Moldowan, J.C. 2005: *The Biomarker Guide - Second Edition - Volume 1 Biomarkers and Isotopes in the Environment and Human History*. Cambridge University Press, ISBN 978-0-521-78697-3, 1155 pp.



- Radke, M. & Welte, D.H. 1983: The Methylphenanthrene Index (MPI): A maturity parameter based on aromatic hydrocarbons. In Bjorøy, M. et al. (eds.): *Advances in Organic Geochemistry 1981*, 504-512, Wiley.
- Radke, M., Willsch, H., Leythaeuser, D. & Teichmüller, M. 1982. Aromatic components of coal: relation of distribution pattern to rank, *Geochimica et Cosmochimica Acta*, 46, 1831- 1848.
- Riis, F., Lundschieen, B.A., Høy, T., Mørk, A. & Mørk, M.B.E. 2008: Evolution of the Triassic shelf in the northern Barents Sea region. *Polar Research*, 27, 318-338, <http://www.polarresearch.net/index.php/polar/article/download/6198/6877>
- Schou, L., Mørk, A. & Bjorøy, M. 1984: Correlation of source rocks and migrated hydrocarbons by GC-MS in the middle Triassic of Svalbard. *Organic Geochemistry*, 6, 513-520.
- Shvarts, V. L. 1985: Litologo-stratigraficeskoe rasclenienie razreza skvaziny Raddedalen-I (ostrov Edz, archipelag Spitsbergen) [Lithostratigraphic division of the section of the Raddedalen-I drilling hole (Edgeøya, Archipelago of Svalbard)]. In: Geologiceskoe stroenie Barentsevo-Karskogo sel'fa. Sbornik nauenykh trudov. (Geological structure of the Barents-Kara Shelf) Collection of scientific papers, 44- 58, Sevmorgeologija, Leningrad [in Russian. Translated into English 1986 by Norsk Polarinstitut].
- Smelror, M. & Sollid, K. 2007: Blekkspruter fulle av olje. GEO 2, 26-28, Geopublishing, Trondheim, in January 2012 available at: <http://www.geo365.no/sfiles/0/37/4/file/blekksprut26.pdf> (In Norwegian).
- Sofer, Z. 1980: Preparation of carbon dioxide for stable carbon isotope analysis of petroleum fractions. *Analytical Chemistry*, 52, 1389-1391.
- Tanner, L.H. 2010: The Triassic isotope record. Geological Society, London, *Special Publications*, 334, 103-118.
- Taylor, G.H., Teichmüller, M., Davis, A., Diessel, C.F.K., Littke, R. & Roberts, P. 1998: *Organic Petrology: A New Handbook Incorporating Some Revised Parts of Stach's Textbook of Coal Petrology*. Gebrüder Bornträger, Berlin, Stuttgart, 704 pp.
- Thronsen, T. 1979: Kerogen Maturation of Triassic Deposits in Svalbard. Presentation at NPF Norwegian Sea Symposium, Tromsø.
- Tissot, B.P. & Welte, D.H. 1984: *Petroleum Formation and Occurrence*. 2<sup>nd</sup> edition. Springer-Verlag, Berlin, Heidelberg, 699 pp.
- Vigran, J.O., Mørk, A., Forsberg, A.W., Weiss, H.M., & Weitschat, W. 2008: *Tasmanites* algae—contributors to the Middle Triassic hydrocarbon source rocks of Svalbard and the Barents Shelf. *Polar Research*, 27, 360-371, <http://www.polarresearch.net/index.php/polar/article/viewFile/6196/6875>
- Weiss, H.M., Wilhelms, A., Mills, N., Scotchmer, J., Hall, P.B., Lind, K. & Brekke, T. 2000: *NIGOGA -The Norwegian Industry Guide to Organic Geochemical Analysis* [online]. Edition 4.0. Published by Norsk Hydro, Statoil, Geolab Nor, SINTEF Petroleum Research and the Norwegian Petroleum Directorate. Electronic document only, available from World Wide Web: <http://www.npd.no/engelsk/nigoga/nigoga4.pdf>
- Winsnes, T.S. 1981: Geological Map of Svalbard 1:500 000. Sheet 2G Edgeøya. *Norsk Polarinstitut Skrifte*, 154B.
- Worden, R.H., Smalley, P.C. & Cross, M.M. 2000: The influence of rock fabric and mineralogy on thermochemical sulfate reduction: Khuff Formation, Abu Dhabi. *Journal of Sedimentary Research*, 70, 1210-1221.
- Worden, R.H., Smalley, P.C. & Barclay, S.A. 2003: H<sub>2</sub>S and diagenetic pyrite in North Sea sandstones: due to TSR or organic sulphur compound cracking? *Journal of Geochemical Exploration*, 78-79, 487-491.
- Aarnes, I., Svensen, H., Polteau, S. & Planke, S. 2011: Contact metamorphic devolatilization of shales in the Karoo Basin, South Africa, and the effects of multiple sill intrusions. *Chemical Geology*, 281, 181-194.

# A glimpse into the Carnian: Late Triassic plant fossils from Hopen, Svalbard

Ahti Launis<sup>1,2</sup>, Christian Pott<sup>3</sup> & Atle Mørk<sup>4,5</sup>

<sup>1</sup> Department of Biological and Environmental Sciences & Botanical Museum, P.O. Box 7, FI-00014 University of Helsinki, Finland, e-mail: ahti.launis@helsinki.fi

<sup>2</sup> UNIS, The University Centre in Svalbard, NO-9171 Longyearbyen.

<sup>3</sup> Swedish Museum of Natural History, Department of Palaeobiology, Box 50007, SE-104 05 Stockholm, Sweden, e-mail: Christian.Pott@nrm.se

<sup>4</sup> SINTEF Petroleum Research, NO-7465 Trondheim, Norway, e-mail: atle.mork@sintef.no

<sup>5</sup> NTNU, Norwegian University of Science and Technology, Department of Geology and Mineral Resources Engineering, NO-7491 Trondheim, Norway.

A small number of well-preserved plant fossils have been collected during recent fieldwork on Hopen in the Svalbard archipelago. The assemblage shows a composition typical of Carnian floras from central Europe and complements a recent study of old collections of Upper Triassic plant fossils from Svalbard. The new findings include already described species and some possibly new for Svalbard. The plant fossils are from well-dated Carnian beds on Hopen and confirm the earlier assumed Carnian age for plants collected on Svalbard from Upper Triassic sediments. A remarkable feature of this flora is the high number of plants, which are also described from Carnian floras from Austria and Switzerland, but also recorded from Franz Josef Land and other Arctic areas. The stratigraphic value of this flora is discussed.

**Key words:** *Pterophyllum*, *Taeniopteris*, *Leguminanthus*, Triassic, Arctic fossil flora, Svalbard, Lunz, Neuwelt.

## Introduction

Collection of fossils on Svalbard started with the large scientific expeditions to the archipelago in the second half of the 19th century. During subsequent geological exploration, mainly in search for natural resources and mapping of the archipelago, fossils were sampled to fill the collections of the upcoming natural history museums and collections all over Europe (e.g. Albert I of Monaco, 1899; Nathorst, 1900). Svalbard yields plant fossils from the Devonian to the Oligocene (Denk et al., 1999). Some periods (e.g. Jurassic/Cretaceous and Cenozoic) show fossil diversity and high abundance. Upper Triassic plants are widely distributed on Svalbard, but represent rather fragmentary floras (Pott, 2014). Accounts on the Upper Triassic flora (Vasilevskaja, 1972, 1983, 1987; Dobruskina, 1980, 1994) were published exclusively in Russian. Pott (2014) recently revised the Russian collections of Upper Triassic floras from the 1960–70s, stored in the A.P. Karpinsky Russian Geological Research Institute (VSEGEI), St. Petersburg, together with old collections obtained by Scandinavian explorers in 1896–1929, stored in the Swedish Museum of Natural History (NRM),

Stockholm. These older collections were re-assessed using the locality information given on the old labels. The assumed Carnian age of the Upper Triassic floras from Svalbard has been deduced from index fossils and the composition of the flora, as well as on the basic geological information for the sampled localities.

First plant fossils from Hopen were collected by Prince Albert I of Monaco at Nørdstefjellet in 1898 (Fig. 1). Sporadic collections have later been made by Høeg (1926), who described compressed foliage remains, Vasilevskaja (1983), Strullu-Derrien et al. (2014), who described silicified wood and peat deposits, the latter with arthropod remains in a fossil root system. However, these fossils occur on loose rocks on the beaches or elsewhere on the island and, given the fact that Hopen above sea level entirely consists of Upper Triassic rocks, were considered possibly Carnian. In this paper, we report on a small assemblage of plant fossils collected from well-dated beds in situ at Kollerfjellet (Figs. 1, 2) confirming the Carnian age assumed earlier (e.g. Vasilevskaja, 1972, 1983; Dobruskina, 1980; Pott, 2014).

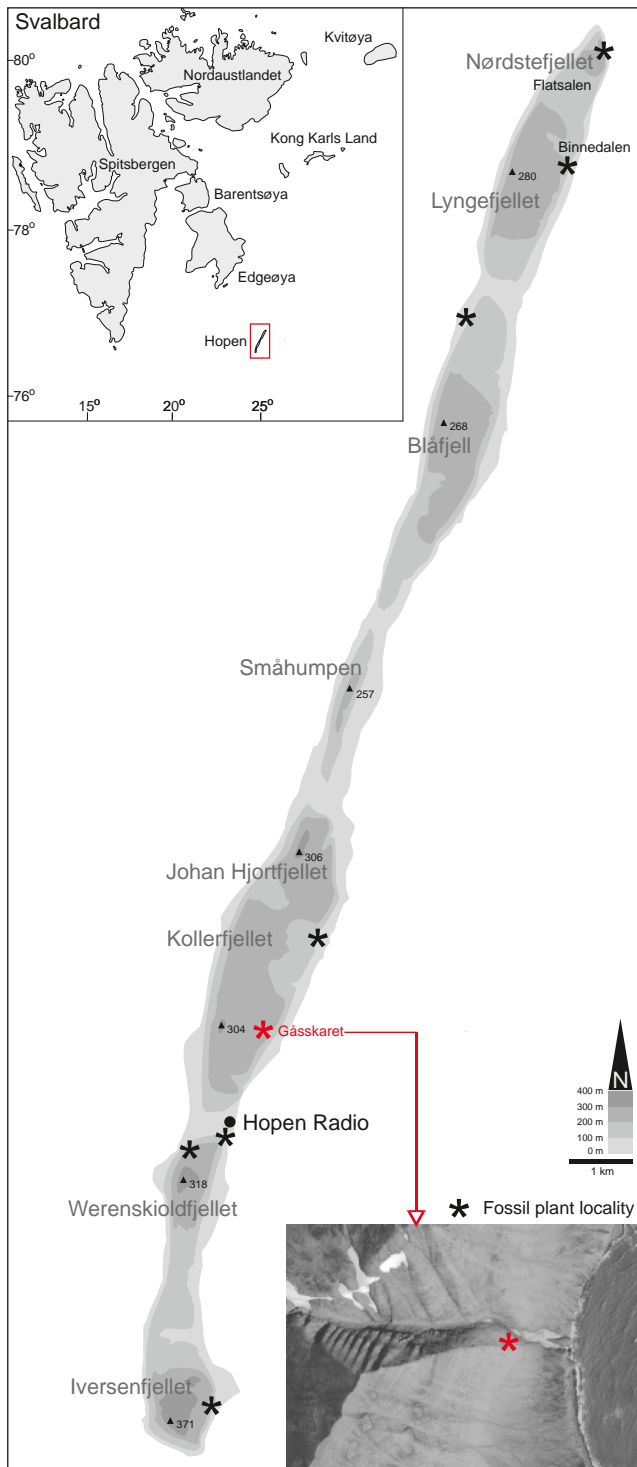


Figure 1. Map of the island of Hopen, Svalbard, depicting localities with plant fossils. The sampled locality is indicated by a red asterisk. Photo from Norwegian Polar Institute.

## Material and methods

Twenty-nine fossiliferous rock specimens, including three counterparts, exclusively yielding plant fossils, were collected by AL during a geological expedition to Hopen in August 2011. The location is 59–61 m above sea level at Gåsskaret, Kollerfjellet (Fig. 2), c. 20 m into the gully from its southern ridge (Fig. 1). The loose rock specimens were found within a 5–10 m wide area, and represent two separate beds within a metre of height. They are treated as recovered from one layer. Most rock specimens contain several fossils, assignable to different species. The fossil fragments are preserved as compressions or impressions with very little organic material left. A thin anthracitic layer covers some of the fossils. In total, there were 156 compressions or impressions. The specimens are stored in the paleontological collections of the Natural History Museum, Oslo, Norway, under accession numbers PMO 227.548–227.573.

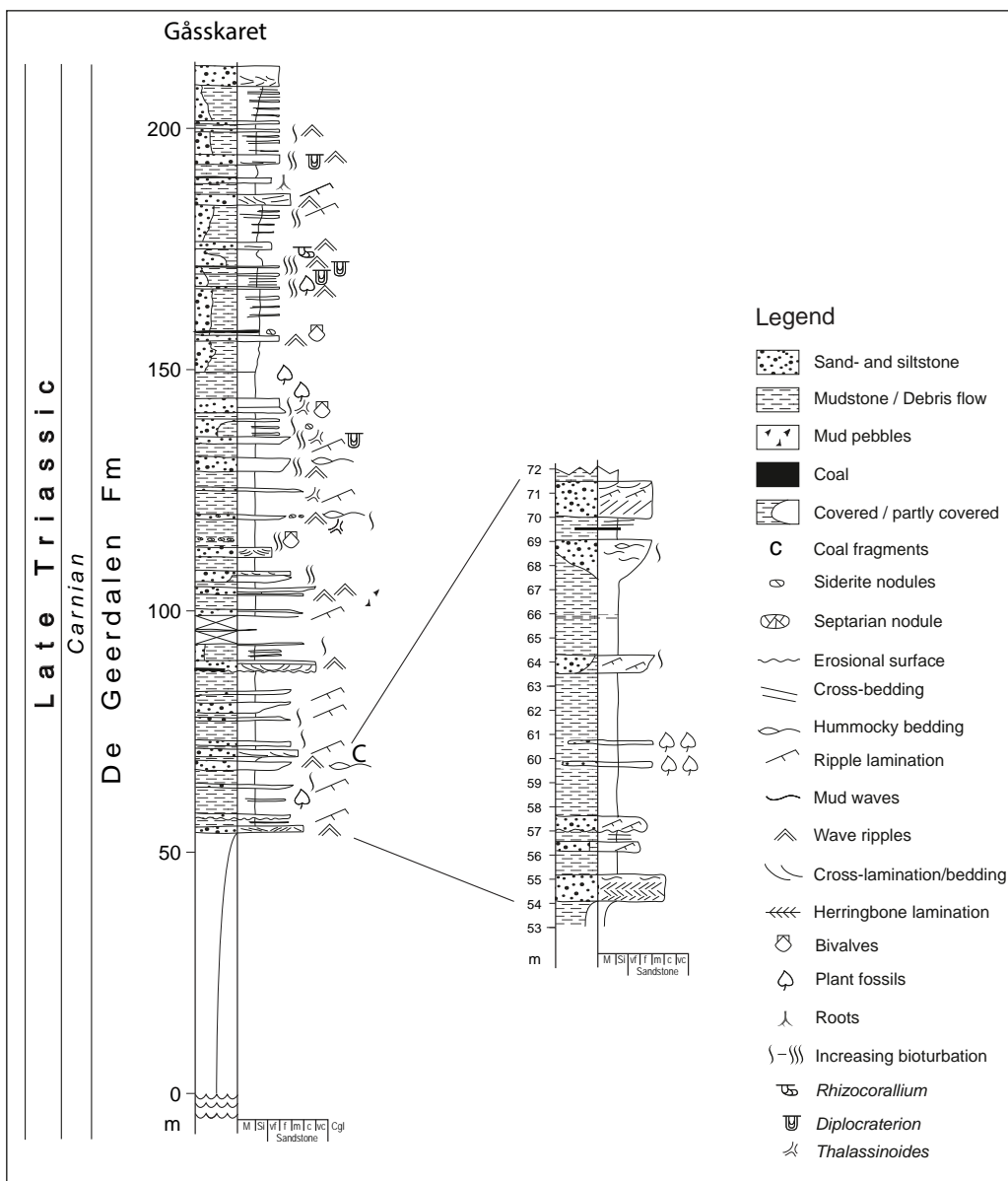
The hand specimens have been analysed under a dissecting microscope and were photographed with a Nikon D300/Sigma 50mm F2.8 EX DG Macro system digital camera at the Botanical Museum and the Department of Geosciences and Geography, University of Helsinki, Finland. Oblique lighting was used in order to enhance contrast. Some hand specimens were taken to the Swedish Museum of Natural History, Stockholm, for analysis with an Olympus BX-51 microscope under fluorescent light by CP, but no fluorescent cuticles were observed, and attempts to isolate cuticles with standard methods (cf. Pott and McLoughlin, 2009) failed.

## Geological setting

The exposures of the De Geerdalen Formation on Hopen represent the upper part of the formation, as most part of the unit occurs below sea level (Riis et al., 2008; Mørk et al., 2013). The formation represents paralic sediments, which in this lower part of the section, are mainly deltaic top sediments (Klausen and Mørk, 2014; Lord et al., 2014 a, b). The layers with plant fossils are in the lower part of these deposits (Fig. 2). The successions on Hopen all belong to the Kapp Toscana Group of Late Triassic age, which overlies the Sassendalen Group and is elsewhere on Svalbard divided into the Tschermakfjellet Formation and the overlying De Geerdalen Formation (Mørk et al., 1999, 2013). Both are assigned a Carnian age (e.g. Dobruskina, 1994; Tozer and Parker, 1968; Dagys and Weitschat, 1993; Hounslow et al., 2007; Vigran et al., 2014), although the De Geerdalen Formation extends into the Norian. The latter is overlain by the Norian–Rhaetian Wilhelmøya Subgroup (Worsley, 1973; Smith et al., 1975; Dypvik et al., 1985; Mørk et al., 1999; Hounslow et al., 2007). The plant fossils occur in two beds within the De Geerdalen Formation, layers dated as of late Carnian age (Lord et al., 2014a; Vigran et al., 2014). The correlated age agrees with an early Norian age for the overlying Flatsalen Formation



**Figure 2.** The geological section of Gåsskaret with emphasis on the interval with the beds yielding the plant fossils studied (at the level of the double leaves indicated). Bivalves, trace fossils and hummocky cross-bedding indicate a shallow shelf depositional environments. Section measured by B.A. Lundschieen, T. Solbakk and M. Ask.



as suggested by Korčinskaja (1982) based on ammonoids and bivalves.

## Results

The fossil remains are fragmentary, but allow in most cases satisfying identification and correlation with species reported from Carnian floras of Svalbard (Pott, 2014).

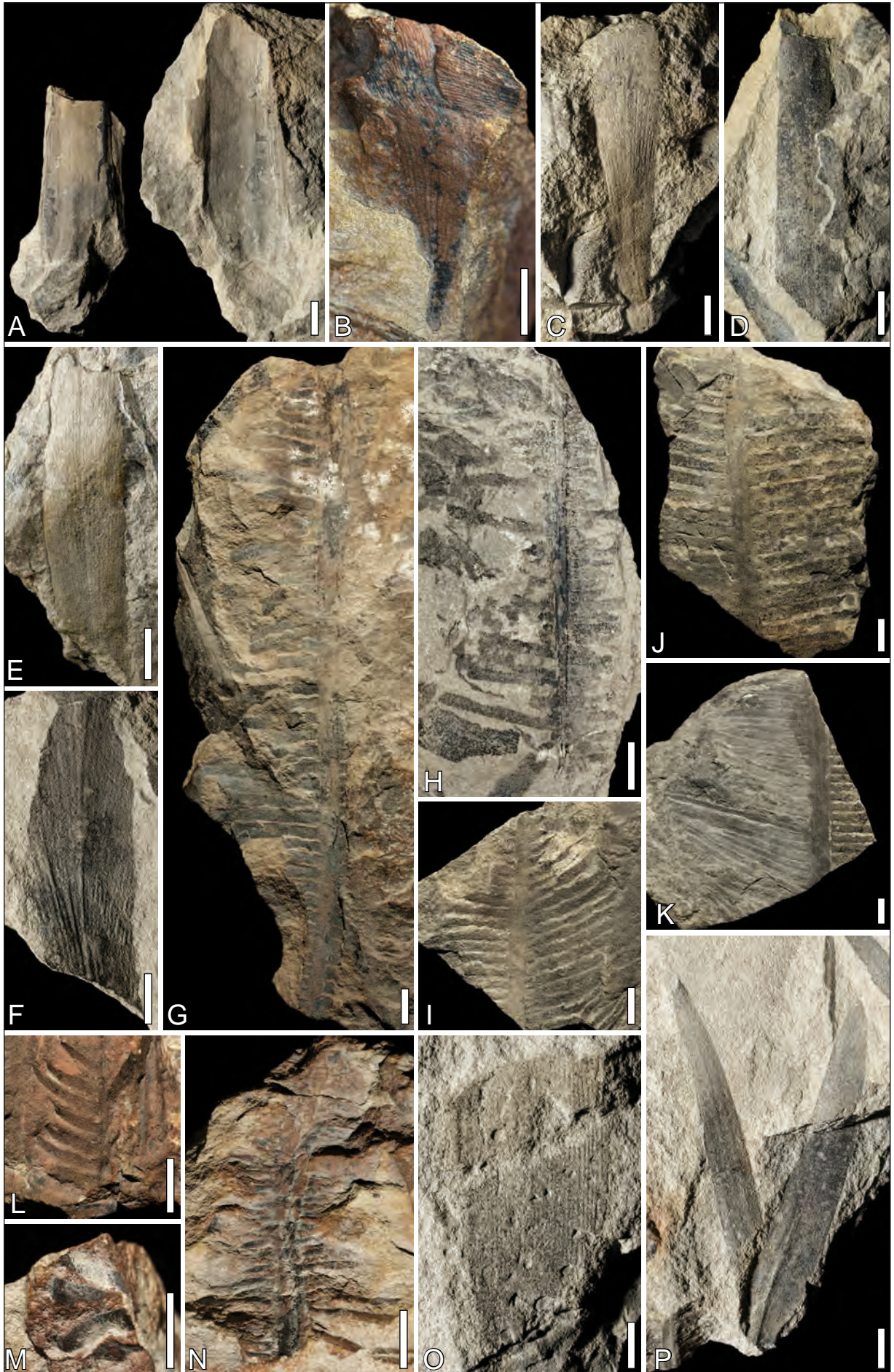
### Pteridophytes

Four specimens (PMO 227.560, 227.563, 227.569A+B, 227.571) provide impression of 17–24 mm wide sphenophyte axis portions assignable to *Neocalamites* (Fig. 3A). Diagnostic characters, such as internodes or leaves are absent, and further identification is impossible. *Neocalamites merianii* seems a good option given the size

ranges and the structure of the axes (cf. Pott, 2014; Pott et al., 2008a). Two fragments on slab PMO 227.553 were identified as *Dictyophyllum* sp. and *Clathropteris* sp., but are too ill-preserved to be confidently identified.

### Pteridosperms

Peltaspermalean foliage assigned to *Paratatarina* has been found on several specimens (PMO 227.548, 227.552, 227.553, 227.556A, 227.559, 227.572; e.g. Figs. 3B–F). The preserved leaves, up to 18 mm wide and 124 mm long, are all in the range of those identified as *Paratatarina ptchelinae* by Pott (2014). They also display the typical shape and venation of this species (Figs. 3E–F). We regard the ones from Hopen conspecific with *Paratatarina ptchelinae* from elsewhere on Svalbard. *Paratatarina korchinskajae* reported by Vasilevskaja (1983) as endemic for Hopen has been regarded conspecific





with *Paratatarina ptchelinae* by Pott (2014). PMO 227.556A+B yields a small 51 mm long and 11 mm wide cone with a slightly undulating central axis, and small structures (Fig. 4H) interpreted as spirally arranged sporangia or synangia. The morphology of the cone resembles *Peltaspermum madygenicum* described by Dobruskina (1980) from the Upper Triassic Madygen Formation of Uzbekistan. A few poorly preserved scales of PMO 227.556B might represent seeds or sporangia belonging here, but further identification is impossible.

## Cycadophytes

Similar to the remainder of the Carnian flora of Svalbard (Pott, 2014), also that from Hopen is dominated by well-preserved bennettitalean foliage. Several rock specimens (PMO 227.548–227.552, 227.556A, 227.559, 227.560, 227.569A+B, 227.572) yield large fragments of *Pterophyllum filicoides* foliage (Fig. 3G–L; Pott et al., 2007), whereof the longest fragment reaches 190 mm. The parallel-sided leaflets, inserted perpendicularly to the lateral edges of the rachis, are 2.6–3.6 mm wide and up to 58 mm long. The fossils are easily identified by size ranges and appearance with the material reported from several localities all over Svalbard including three localities on Hopen (Pott, 2014).

One of the specimens from Hopen (PMO 227.552) has four leaflets in a position suggesting that the rock portion with the connecting rachis is broken apart (Fig. 3M). The leaflets are 3 mm wide and 11 mm long and fall well within the range of the leaflets of *Pterophyllum brevipenne* as described from Svalbard by Pott (2014). The fragmentary specimen PMO 227.570 has leaflets attributable to *Pterophyllum brevipenne*, but since no further material is preserved, it is assigned with reservation. Leaf portions with more slender leaflets occur on a few rock specimens (PMO 227.552, 227.554, 227.556A, 227.559) and match specimens assigned to *Pterophyllum* sp. cf. *firmifolium* by Pott (2014). The largest fragment is 54 mm long with a 4–5 mm wide

rachis (Fig. 3N). Leaflets are 1.2–2.0 mm wide, inserted very close to each other perpendicularly and laterally to the rachis.

On three specimens (PMO 227.556A, 227.561, 227.573), entire-margined leaves up to 15 cm long and 21 mm wide at their widest point are preserved (Figs. 4C, E–F). The leaves have a sharply pointed apex; the base is contracted, proceeding into a short 10 mm long petiole, up to 3 mm wide. The lamina appears robust and is retaining its width throughout the middle portion of the leaf. It is characterised by straight margins and a central, 2–4 mm wide rachis, which gives off delicate, densely spaced, parallel lateral veins at angles of 70–80°. The veins occasionally bifurcate close to the rachis and proceed straight to the leaf margin (Fig. 4F). The specimens are very similar to leaves from other localities on Svalbard, earlier reported as *Taeniopteris* sp. by Vasilevskaja (1972). These have been included in *Nilssoniopteris angustior* by Pott (2014), but the new findings reveal that they belong to a different species instead. Assignment to either Bennettitales or Cycadales is equivocal since epidermal anatomy is unknown and, therefore, we refrain to assign the species to either order until epidermal information becomes available.

One specimen (PMO 227.556A+B) yields an opened pod very similar to *Leguminanthus siliquosus* from Neuwelt and Lunz (Kräusel and Schaarschmidt, 1966) that is 140 mm long and 44 mm wide (Fig. 4D). The pod is characterised by a strong lamina suggesting a leathery (or woody) texture that inserts laterally to a strong, 3–4 mm wide rachis, and is folded ad- or abaxially. The outer margins do not touch each other ventrally, but they do touch in leaves from Lunz and Neuwelt and were apparently connected or connate. The lamina is further characterised by densely arranged veins, 4–5 per cm, emerging almost perpendicularly from the rachis and proceeding straight to the margin. Besides brachyparacytic stomata in the cuticles of these pods from Lunz, Kräusel and Schaarschmidt (1966) described pollen sacks and pollen grains from their inside, both features identifying the pods as male fructifications of Bennettitales.

## Ginkgophytes

Ginkgophytes are another common element in Carnian flora from Svalbard (Pott, 2014). Several of the leaf fragments from Hopen match well with two ginkgophyte leaves described from Svalbard, *Arberophyllum spetsbergensis* (PMO 227.554; Fig. 3O) and *Arberophyllum substrictum* (PMO 227.548–227.551, 227.553–227.556A+B, 227.558, 227.559, 227.567A+B, 227.569A, 227.572, 227.573; Figs. 3P, 4A–B; Vasilevskaja, 1972; Pott, 2014). The leaves found on Hopen display the same shapes and outlines as those from elsewhere on Svalbard. Both species differ by the different shape and outline of their leaves, as well as in venation details (Pott, 2014).

◀ **Figure 3.** Plant fossils from the Carnian (Upper Triassic) at Gåsskaret. A. *Neocalamites* sp.; specimens PMO 227.569A+B. B–F. *Paratatarina ptchelinae*; specimens PMO 227.552, 227.572, 227.549, 227.559, 227.553. G–L. *Pterophyllum filicoides*; specimens PMO 227.548, 227.559, 227.551, 227.549, 227.550, 227.552. M. *Pterophyllum brevipenne*; specimen PMO 227.552. N. *Pterophyllum* sp. cf. *Pterophyllum firmifolium*; specimen PMO 227.552. O. *Arberophyllum spetsbergensis*; specimen PMO 227.554. P. *Arberophyllum substrictum*; specimen PMO 227.554. Scale bars – 1 cm.







Strap-shaped leaf portions, 2.2–2.9 mm wide, up to 38 mm long, without venation occur on specimens PMO 227.561, 227.564, 227.565 and 227.571 (Fig. 4G). The lowermost portion of one 3 mm wide leaf displays a bifurcation reminiscent of a *Sphenobaiera* leaf (Fig. 4G, arrow). Leaves appear identical with leaves from Neuwelt that Leuthardt (1903) described as *Baiera furcata* later transferred to *Sphenobaiera* by Florin (1936). Identification is equivocal as the remains are further undeterminable.

### Coniferophytes

Two rock specimens (PMO 227.557, 227.559) yield remains interpreted as ovuliferous structures reminiscent of conifer-like cones. The fragments, up to 73 mm long, 1.1–1.6 mm wide, consist of a central axis, 2–3.5 mm wide, with perpendicular, bracts, up to 6 mm long and 2.5 mm wide, spaced at intervals of 3–4 mm. The bracts consist of a proximal petiole, up to 7 mm long, widening into a triangular, and probably seed-bearing, abaxially keeled, slightly expanded, median portion (Fig. 4H–I). The cone morphology and dimensions of the two fragments from Hopen allow comparison with the far better preserved specimens of *Voltzia novomundensis* described from Neuwelt (Kräusel and Leschik, 1955). The latter have seeds, bracts and scales; the two fragmented specimens from Hopen show the same type of bract axes and longitudinal striation of scales. They are kept unassigned to species level since the complete shape of the bracts or scales, the seeds and seed number are unknown.

Specimen PMO 227.556A yields cones, 17–32 × 9 mm, characterised by a surface pattern of rhomboid scale heads, c. 2 × 1 mm (Fig. 4K). Specimen PMO 227.558 has a different type of cone, 36 × 11 mm, with a 9 mm long petiole. Parts of the cone have c. 2 × 1.5 mm large rhomboidal scale heads. A straight central axis is visible in the lower portion of the cone and there are some scales, 4 × 2 mm, possibly bearing seeds or sporangia (Fig. 4L). The poorly preserved cones most likely are of coniferalean affinity. Similar material so far is unknown in the Carnian floras of Neuwelt, Lunz and Svalbard and a further assignment has been avoided.

A number of rock specimens (PMO 227.553, 227.554, 227.556A+B, 227.558, 227.561, 227.562, 227.564, 227.566, 227.568, 227.570, 227.571) yield branching and simple axes without leaves in organic connection and thus of unknown affinity (e.g. Figs. 4J, M).

### Discussion

The older collections from the widely distributed Upper Triassic floras on Svalbard show that they are rather fragmentary and information is scarce. Pott (2014) re-assessed these floras, where distinct stratigraphic information is missing, and based the Carnian age on available geological information about the localities with the fossiliferous beds and on the occurrence of identical species in much better known Carnian floras from central Europe (viz. Lunz and Neuwelt). Especially the Lunz flora is well-dated as Julian (Dunay and Fisher, 1978). The present stratigraphically well-dated Carnian plant material from Hopen allows now confident dating of the material.

The obtained plant fossils from Hopen expand the range of species present in the Upper Triassic flora from Svalbard, Lunz and Neuwelt. Of the 28 species recorded for Svalbard, at least 10 species are present in Neuwelt and Lunz. The ferns (pteridophytes) from the Lunz flora are currently being revised and may increase this number since at least 4–5 species may be present in both locations (CP, own observation, January 2014). Some species present in the flora from Svalbard have earlier only been found either in Neuwelt or Lunz, but not in both. However, future research may reveal new taxa in the Lunz flora and elucidate more details of the character and composition of the Lunz and Neuwelt floras. The collection of plants from Hopen studied for this publication is from a single locality representing a deltaic environment, in close association to shallow marine influence, as indicated by hummocky cross bedding and sparse trace fossils (Lord et al., 2014b). The Lunz and Neuwelt floras thrived in similar environments, and the slight differences in the composition of these remote but in other aspects very similar floras point to very local differences arguing for spatially very restricted plant communities (Pott, 2014; Pott et al., 2008b).

### Acknowledgements.

AL would like to thank Jorunn Os Vigran, Trondheim, Norway, for comments and encouragement, the Botanical Museum of Helsinki for providing the working and storage facilities, and Aleksis Karme, Department of Geosciences and Geography, University Helsinki, for providing the access to photography facilities. CP acknowledges financial support by the Swedish Research Council (Vetenskapsrådet), Stockholm, Sweden. We thank Hans Arne Nakrem and Franz-Josef Lindemann, UiO Natural History Museum, Oslo, Norway, for the good and straightforward cooperation. The fieldwork was supported by the Norwegian Petroleum Directorate and five exploration licences.

◀ **Figure 4.** A Plant fossils collected from the Carnian (Upper Triassic) at Gåsskaret. A–B. Arberophyllum substrictum; arrows pointing to potential galls (B); specimens PMO 227.553, 227.556A. C. Taeniopteris sp.; specimen PMO 227.561. D. Leguminanthus siliquosus; specimen PMO 227.556A. E–F. Taeniopteris sp.; specimens PMO 227.556A, 227.573. G. Ginkgoalean leaves; arrow: bifurcation; specimen PMO 227.565. H. ?Peltaspermalean cone cf. Peltaspermum madygenicum; specimen PMO 227.556A. I–J. Coniferalean cones cf. Voltzia novomundensis; specimens PMO 227.557, 227.559. K–L. Small cones of uncertain affinity; arrows pointing to details of seed scales; specimens PMO 227.556A, 227.558. M. Branched axis with triangular leaf scars; specimen PMO 227.562. Scale bars – 1 cm.

## References

- Albert I of Monaco. 1899: Première campagne de la 'Princesse-Alice II'. *Comptes Rendus Hebdomadaires des Séances de l'Académie des Sciences*, 128, 212–214.
- Dagys, A. & Weitschat, W. 1993: Correlation of the Boreal Triassic. *Mitteilungen des geologisch-paläontologischen Instituts der Universität Hamburg*, 75, 249–256.
- Denk, T., Wanntorp, L. & Manum, S.B., with the assistance of Haglund O. 1999: *Catalogue of the Tertiary plant fossils from Spitsbergen housed in the Swedish Museum of Natural History*, Stockholm. Stockholm: Swedish Museum of Natural History.
- Dobruskina, I.A. 1980: Stratigraphical position of Triassic plant-bearing beds of Eurasia. *Trudy GIN Akademiâ Nauk SSSR*, 346, 1–164. (In Russian).
- Dobruskina, I.A. 1994: *Triassic floras of Eurasia*. Wien: Springer.
- Dunay, R.F. & Fisher, M.J. 1978: The Carnian palynofloral succession in the Northern Calcareous Alps, Lunz-am-See, Austria. *Pollen et Spores*, 20, 177–187.
- Dypvik, H., Hvoslef, S., Bjærke, T. & Finnerud, E. 1985: The Wilhelmøya Formation (Upper Triassic–Lower Jurassic) at Bohemanflya, Spitsbergen. *Polar Research*, 3, 155–165.
- Florin, R. 1936: Die fossilen Ginkgophyten aus Franz-Joseph-Land nebst Erörterungen über vermeintliche Cordaitales mesozoischen Alters. II. Allgemeiner Teil. *Palaeontographica Abt. B* 82, 1–72.
- Høeg, O.A. 1926: Fossil plants. In T. Iversen (ed.): *Hopen (Hope Island), Svalbard – Results of a reconnaissance in the summer 1924. Resultater av de norske statsunderstøttende Spitsbergenekspeditioner*, 32–33. Oslo: Det Norske Videnskaps-Akademi.
- Hounslow, M.W., Hu, M., Mørk, A., Vigran, J.O., Weitschat, W. & Orchard, M.J. 2007: Magneto-biostratigraphy of the Middle to Upper Triassic transition, central Spitsbergen, Arctic Norway. *Journal of the Geological Society, London*, 164, 581–597.
- Klausen, T. G., & Mørk, A. 2014: The Upper Triassic paralic deposits of the De Geerdalen Formation on Hopen: Outcrop analog to the subsurface Snadd Formation in the Barents Sea. *American Association of Petroleum Geologists Bulletin*, 98, 1911–1941, doi:10.1306/02191413064.
- Korčinskaja, M.V. 1982: Explanatory note to the stratigraphic scheme of Mesozoic (Triassic) Svalbard, 40–99. Leningrad: Ministerstvo geologii SSSR, PGO "Sevmorgeologia". (In Russian).
- Kräusel, R. & Leschik, G. 1955: Die Keuperflora von Neuwelt bei Basel – I. Koniferen und andere Gymnospermen. *Schweizer Paläontologische Abhandlungen*, 71, 1–27.
- Kräusel, R. & Schaarschmidt, F. 1966: Die Keuperflora von Neuwelt bei Basel – IV. Pterophyllen und Taeniopteriden. *Schweizer Paläontologische Abhandlungen*, 84, 3–44.
- Leuthardt, F. 1903: Die Keuperflora von Neuwelt bei Basel – I. Teil Phanerogamen. *Abhandlungen der Schweizer Paläontologischen Gesellschaft*, 30, 1–23.
- Lord, G.S. Solvi, K.H., Ask, M., Mørk, A., Hounslow, M.W. & Paterson, N.W. 2014a: The Hopen Member: A new lithostratigraphic unit on Hopen and equivalent to the Isfjorden Member of Spitsbergen. *Norwegian Petroleum Directorate Bulletin*, 11, 81–96.
- Lord, G.S., Solvi, K.H., Klausen, T.G. & Mørk, A. 2014b: Triassic channel bodies on Hopen, Svalbard: Their facies, stratigraphical significance and spatial distribution. *Norwegian Petroleum Directorate Bulletin*, 11, 41–60.
- Mørk, A., Dallmann, W.K., Dypvik, H., Johannessen, E.P., Larssen, G.B., Nagy, J., Nøttvedt, A., Olausson, S., Pchelina, T.M. & Worsley, D. 1999: Mesozoic lithostratigraphy. In W.K. Dallmann (ed.): *Lithostratigraphic lexicon of Svalbard. Review and recommendations for nomenclature use. Upper Palaeozoic to Quaternary bedrock*. 127–214. Tromsø: Norsk Polarinstitut.
- Mørk, A., Lord, G.S., Solvi, K.H. & Dallmann, W.K. 2013: *Geological map of Svalbard 1:100 000, sheet G14G Hopen*. Norsk Polarinstitut Temakart No. 50.
- Nathorst, A.G. 1900: *Två somrar i Norra Ishafvet. Första delen: Kung Karls land, Spetsbergens kringsegling*. Stockholm: Beijers.
- Pott, C. 2014: The Upper Triassic flora of Svalbard. *Acta Palaeontologica Polonica*, 59, 709–740. doi: 10.4202/app.2012.0090.
- Pott, C. & McLoughlin, S. 2009: Bennettitalean foliage from the Rhaetian–Bajocian (latest Triassic–Middle Jurassic) floras of Scania, southern Sweden. *Review of Palaeobotany and Palynology*, 158, 117–166.
- Pott, C., Van Konijnenburg-van, Cittert J.H.A., Kerp, H. & Krings, M. 2007: Revision of the *Pterophyllum* species (Cycadophytina: Bennettitales) in the Carnian (Late Triassic) flora from Lunz, Lower Austria. *Review of Palaeobotany and Palynology*, 147, 3–27.
- Pott, C., Kerp, H. & Krings, M. 2008a: Sphenophytes from the Carnian (Upper Triassic) of Lunz am See (Lower Austria). *Jahrbuch der Geologischen Bundesanstalt Wien*, 148, 183–199.
- Pott, C., Krings, M. & Kerp, H. 2008b: The Carnian (Late Triassic) flora from Lunz in Lower Austria: Palaeoecological considerations. *Palaeoworld*, 17, 172–182.
- Riis, F., Lundschieen, B.A., Høy, T., Mørk, A. & Mørk, M.B.E. 2008: Evolution of the Triassic shelf in the northern Barents Sea region. *Polar Research*, 27, 318–338.
- Smith, D.G., Harland, W.B. & Hughes, N.F. 1975: Geology of Hopen, Svalbard. *Geological Magazine*, 112, 1–112.
- Strullu-Derrien, C., McLoughlin, S., Philippe, M., Mørk, A. & Strullu, D.G. 2012: Arthropod interactions with bennettitalean roots in a Triassic permineralized peat from Hopen, Svalbard Archipelago (Arctic). *Palaeogeography, Palaeoclimatology, Palaeoecology*, 348–349, 45–58.
- Tozer, E.T. & Parker, J.R. 1968: Notes on the Triassic biostratigraphy of Svalbard. *Geological Magazine*, 105, 526–542.
- Vasilevskaja, N.D. 1972: The Late Triassic flora of Svalbard. In Sokolova, V.N. & Vasilevskaja, N.D. (eds.): *Mezozojskie otloženija Svalbarda*. Leningrad: NIIGA. (In Russian).
- Vasilevskaja, N.D. 1983: Late Triassic plants from the Island of Hopen (Svalbard). In Vasilevskaja, N.D. (ed.): *Geologija Špicbergena*. Leningrad: Ministerstvo geologii SSSR, PGO "Sevmorgeologia". (In Russian).
- Vasilevskaja, N.D. 1987: A new Late Triassic representative of peltaspermic pteridosperms from Spitsbergen. *Paleontologičeskij Žurnal*, 16, 131–133. (In Russian).
- Vigran, J.O., Mangerud, G., Mørk, A., Worsley, D. & Hochuli, P.A. 2014: Palynology and geology of the Triassic succession of Svalbard and the Barents Sea. *Geological Survey of Norway Special Publication*, 14, 270 p.
- Worsley, D. 1973: The Wilhelmøya Formation – a new lithostratigraphic unit from the Mesozoic of Eastern Svalbard. *Norsk Polarinstitut Årbok 1971*, 7–16.



# Calcareous microbialites in the Upper Triassic succession of Eastern Svalbard

Marina A. Tugarova & Andrey G. Fedyaevsky

VNIIOkeangeologia, St. Petersburg, e-mail: tugarova@mail.ru

Carbonate bodies with possible microbial genesis have been found and described in the Upper Triassic Tschermakfjellet and De Geerdalen formations in the eastern islands of Svalbard. They have a specific morphology and clearly stand out against a background of clastic sedimentary facies. The microbialites are associated with carbonatized discontinuity surfaces in the clastic succession and show common calcareous crustifications with cone-in-cone texture. The microbialites were investigated in both optical and electronmicroscopes to reveal the micro- and ultrastructures. The revealed ultrastructures indicate contribution of microbial communities in their formation. The most abundant ultrastructures are attributed to cyanobacteria, and dominate calcareous microbialites with cone-in-cone crustifications. The investigation of group and molecular (GC-MS) composition of sedimentary organic matter (OM) and isotopic analysis of carbon and oxygen were focused on identifying geochemical imprint of microbial communities in the carbonate bodies. The obtained results support the role of microorganisms in the biochemical formation of the carbonates and led us to conclude that they developed during very early diagenesis in shallow marine clastic facies.

**Key words:** Svalbard, Triassic, Calcareous microbialites, Cyanobacteria, Cone-in-cone structures, Biomarkers, Carbon and oxygen isotopes.

## Introduction

The present work is based on data and samples acquired during the field work seasons of 2007-2013 in the eastern part of Svalbard (Fig. 1). The research was carried out within a framework of the Russian-Norwegian project "Field work on Svalbard and Franz Josef Land – specialized research" with participation of the Norwegian Petroleum Directorate (NPD) and Sintef Petroleum Research from Norway and the Geological Institute of Russian Academy of Science (GIN RAS), Association "Sevmorgeologia" and VNIIOkeangeologia from Russia.

During the field work we focused on the process of carbonatization of sedimentary rocks and their occurrences as calcareous concretions and carbonatized beds and discontinuity surfaces. We described their morphology, character of relationship with the host rocks and macroscopic structural and compositional features.

Our attention was mainly focused on the carbonatized surfaces, single nodules and horizons of concretions or mounds. Nearly all these objects are characterized by the presence of cone-in-cone structures. Usually the formation of these structures is interpreted as a result

of recrystallization under pressure (e.g. Whitten and Brooks, 1979), but several observations point to their early diagenetic origin.

This paper is a preliminary report on carbonate bodies from the Upper Triassic of eastern Svalbard, and the interpretation is supported by petrographic and geochemical data.

## Analytical methods

The analyses were focused on structural and compositional features of the carbonate bodies, with an emphasis on identifying traces of microorganisms and their possible role in the mineral deposition. The analyses include: petrographic analysis of thin sections, fluorescent test on laser scanning confocal microscope, electron-microscopic analysis, chemical X-ray fluorescent analysis, investigation of group and molecular composition of organic matter with biomarker identification, and isotopic analysis of carbon and oxygen.

Petrographic analysis was done using a Leica DMPL microscope, and more than 170 thin-sections were

analysed. Laser scanning confocal microscope Leica SPE (LSCM) was used for fluorescent tests.

Detailed study of ultrastructures and mineral composition was done in the interfaculty educational-scientific laboratory of St. Petersburg State University under the leadership of A.R. Nesterov. Sample preparation included ultrasonic cleaning of rock chips that were then coated with silver by plasma spray SC 500 (Emscope). The research was performed on a scanning electron microscope – microprobe analyser SEM-501B (Philips) with back scatter electron detector.

Semi-quantitative X-Ray spectral fluorescent silicate analysis was carried out by A.P. Borozdin using ARL ADVANT’X (tube with Rh-anode, 50 kV, 24 mA) analyser in the laboratory of the Department of Geology of St. Petersburg State University.

The bitumen fraction was studied in the laboratory of organic geochemistry in VNIIOkeangeologia under supervision of V.I. Petrova. Eight samples of concretions of different morphology were analysed. The analysis included: determination of insoluble fraction of organic matter and the TOC content, chloroform and benzene-alcohol extraction of bitumen and humic acids and determination of their group composition.

Fractions of saturated and aromatic hydrocarbon (CH) were separated using GC-MS on Hewlett Packard 5973/6850 equipment with quadrupole mass detector and software package for processing the analytical information. The biomarker analysis (n-alkanes, isoprenoids, naphthenes, arenas (poly aromatic hydrocarbon)) was carried out using GC-MS on Hewlett Packard 6850/5973 equipment.

The carbon and oxygen isotopic analysis was performed by E.M. Prasolov at the Center of Isotopic Research of the All-Russia Scientific Research Institute. Twenty-nine samples from carbonate bodies of different morphological types were analysed using a mass spectrometer DELTA plus XL, equipped with preparative attachment GasBench (produced by the ThermoFinnigan Company). Approximately 0.5 mg of grounded carbonate sample was reacted with anhydrous orthophosphoric acid for 2 hours at 72° C. The extracted CO<sub>2</sub> was analysed in the mass spectrometer for isotopic ratios <sup>13</sup>C/<sup>12</sup>C and <sup>18</sup>O/<sup>16</sup>O. The obtained data were calculated using the internal standard KH-2 (limestone, δ<sup>13</sup>C = +1.97±0.09 ‰<sub>PDB</sub>; δ<sup>18</sup>O = +27.81±0.13 ‰<sub>VSMOW</sub> or δ<sup>18</sup>O = -2.96±0.13 ‰<sub>PDB</sub>). The results are presented as δ<sup>13</sup>C and δ<sup>18</sup>O deviations related to V-PDB standard. The measurement error (1σ) is within the limits of 0.1-0.2 ‰ for carbon and 0.1-0.3 ‰ for oxygen.

## Geological materials

During the field work, detailed layer-by-layer description and sampling of sections were carried out. Special attention was paid to concretions and nodules in the whole Triassic succession, and to carbonatized surfaces and cone-in-cone structures in the Upper Triassic formations, focusing on description of their morphology and compositional features, and the relationship with the host rocks. Stratigraphic terminology of Mørk et al. (1999) is used in the present paper, where the Lower Triassic is represented by the Vikinghøgda Formation, the Middle Triassic by the Botneheia Formation, and the Upper Triassic by the Tschermakfjellet and De Geerdalen formations. A total of 300 samples were analysed for this study.

Our attention was mainly focused on the Upper Triassic calcareous beds and bodies that we have divided into six types. The three first types were revealed in the Tschermakfjellet Formation, mainly on Edgeøya (Fig. 2), and the three additional types in the De Geerdalen Formation, mainly on Hopen (Fig. 1).

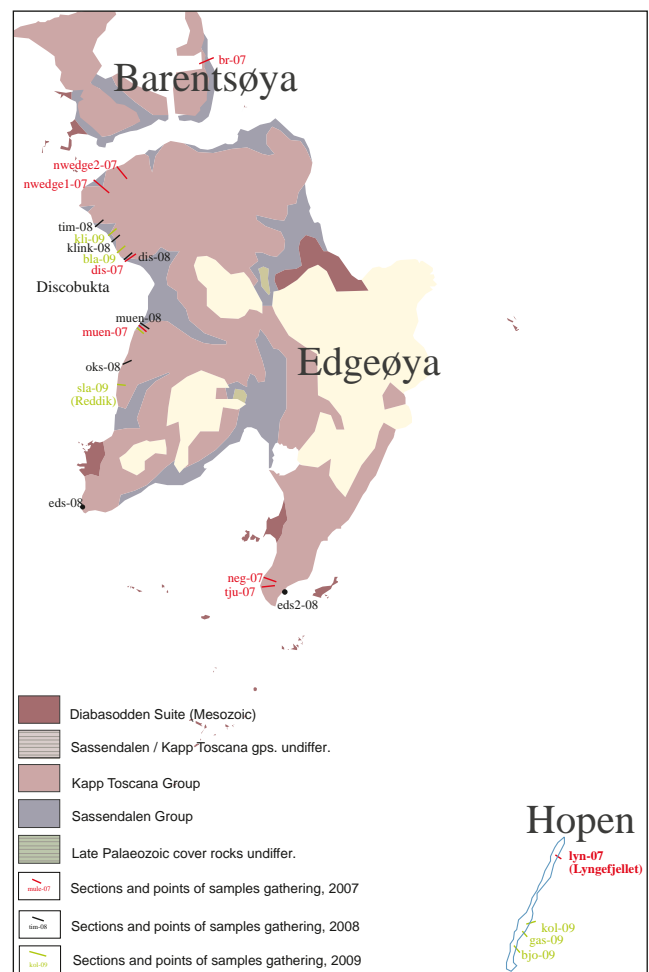


Figure 1. Geological map with sites of studied sections (from Norwegian Polar Institute, 1992)

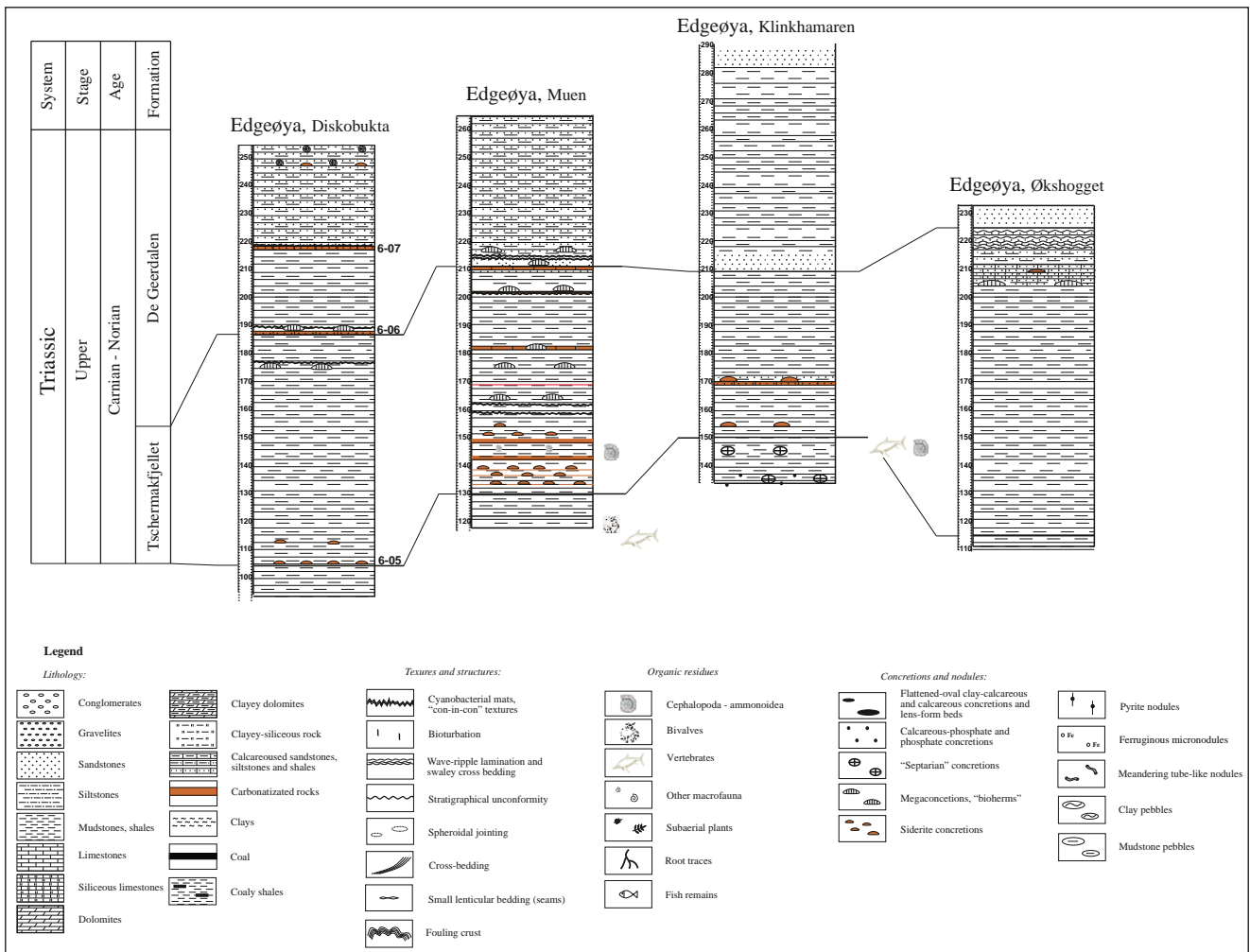


Figure 2. The positions of carbonatized surfaces, different types of concretions and microbialites in the Upper Triassic sections of Edgeøya.

The first three discerned types are as follows:

*Type-1.* Carbonatized surfaces in terrigenous sediments.

*Type-2.* Calcareous bodies characterized by small thickness and relatively large diameter along the long axis (up to 4 m), with typical cone-in-cone fouling along the surface. Usually they are confined to carbonatized surfaces.

*Type-3.* Calcareous mounds with isometric form, and dimensions up to 1-1.5 m, showing complex internal alternation of terrigenous and carbonate layers with cone-in-cone structures.

Carbonatized surfaces in the Upper Triassic succession are represented by siderite nodules or as carbonate impregnation zones in the clastic rocks. At Muen on Edgeøya, the surfaces at the altitude 137, 139, 143, 149 m above sea level contain siderite nodules, which is typical for the Upper Triassic sections. Higher up the section, at 159 and 162 m above sea level another type of carbonatized surfaces with cone-in-cone textures have been observed (Fig. 3).

At Blanknuten in Diskobukta (Edgeøya) a similar flattened surface occurs at 187 m above sea level. On this surface, a single calcareous body with the thickness up to 0.5 m and diameter up to 4 m represents type 2 (Fig. 4). The domed undulations of the structure show 20-40 cm thick elevations. On the surface of the domes, cone-in-cone structures have been observed. The structures are multidirectional, often showing radial orientation of the "cones".

Isometric calcareous bodies (type 3) can be observed at Muen on Edgeøya at 182 and 210 m above sea level (Figs. 5a, b). At 210 m, alternations of calcareous and terrigenous layers are present under the surface of carbonatized sandstones.

Detached "mounds" rise above the planar surface (Fig. 6). Their sizes reach 1.5-2.5 m along the long axis, and the thickness varies from 0.6 to 1.5 m.

Both subsurface bioherm and "mounds" have a complex internal structure, showing layers with cone-in-cone

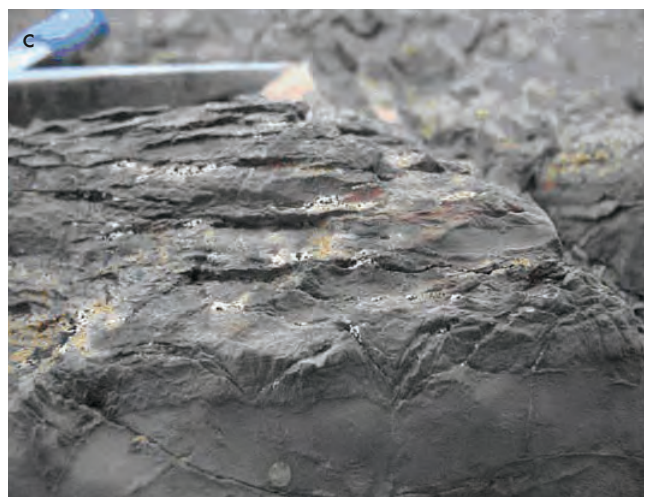




**Figure 3.**  $T_3$  Tschermakfjellet Formation, 162 m above sea level at Muen on Edgeøya. Carbonatized surface with cone-in-cone structures.



**Figure 4.**  $T_3$  Tschermakfjellet Formation at Blanknuten, Edgeøya, 187 m above sea level; a - carbonatized sandy-clay-siltstones; b - calcareouse body – type 2; c - cone-in-cone crustification.





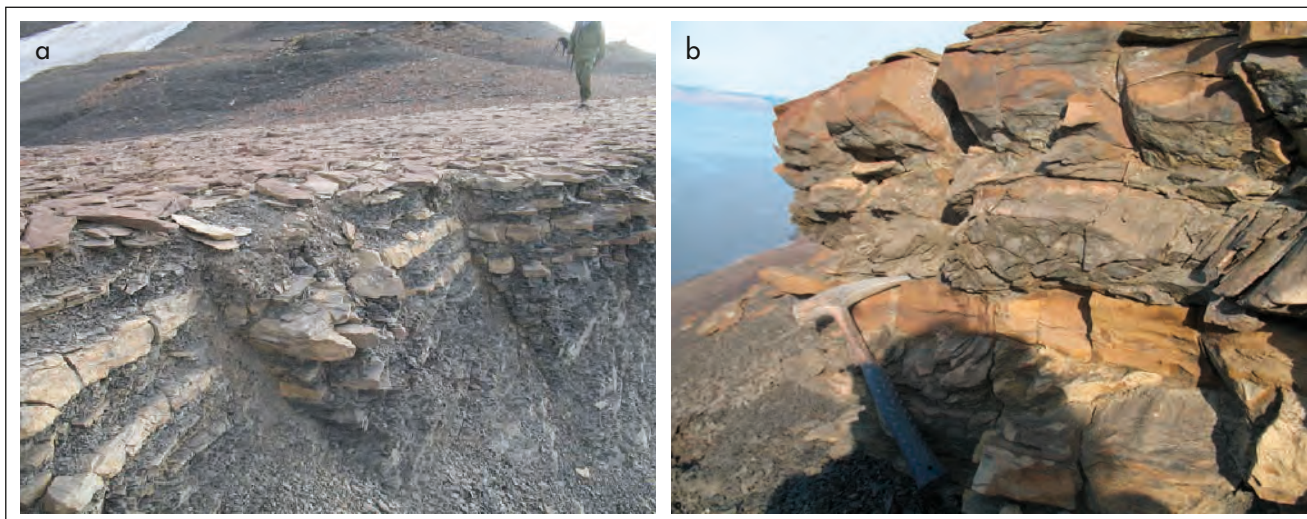


Figure 5. Tschermakfjellet Formation at Muen on Edgeøya.  $T_3$ , 210 m above sea level; **a** - the alternating calcareous and lime-terrigenous layers under the surface of carbonatized sandstones, **b** - bioherm.

structures that alternate with layers of carbonatized clastic rocks. In flanks, the layers of the “bioherms” may pinch out into the surrounding strata. The relationship with the host rocks, the type of bedding and rock

structures indicate their sedimentary genesis, and the nature of changes in the mineral composition gives the evidence of early diagenetic formation.



Figure 6. Tschermakfjellet Formation at Muen on Edgeøya  $T_3$ , 212 m above sea level. Calcareous “mound”.



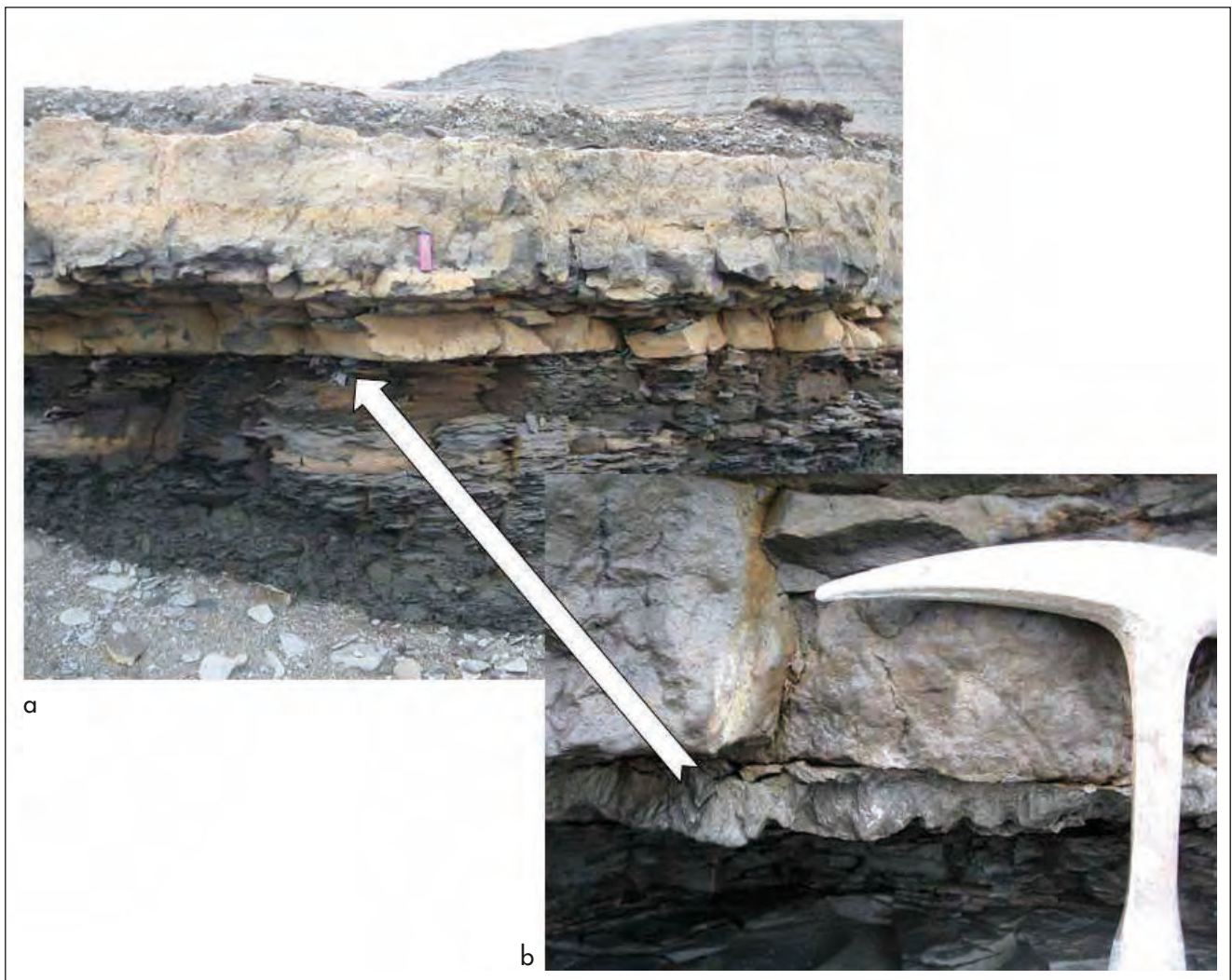
In addition to the above described types of calcareous bodies, the numerous cone-in-cone structures in the form of individual lenses and foulings occur in the Upper Triassic De Geerdalen Formation on Hopen. They can be classified into three types:

- Type-4.* Extensive calcareous layers - lenses, with a thickness of a few tens of centimetres and a length of up to 70 m – herein considered as possible cyanobacterial mats.
- Type-5.* Local calcareous bodies similar to calcareous «mounds» from the Tschermakfjellet Formation.
- Type-6.* Nodular calcareous edifices (small stromatolite like bodies), confined to carbonate strata.

Calcareous layers and lenses of about 20 meters in length occur 0.7 m above sea level in the Iversenfjellet section (Fig. 7). Black calcareous rocks are developed upon a background of the black carbonaceous shales. Their apparent thickness is about 0.5 m, and the contacts with the host rock are sharp due to abrupt change of their

chemical and mineral composition. At the bottom of the carbonate lenses, there are cone-in-cone structures. Bivalves are present in the calcareous rock. The lens is overlain by a thin layer of carbonaceous mudstone and coal. Above there are clastic regressive sequences (Fig. 7 a).

The distinct horizon of 16 carbonate lenses with cone-in-cone structures can be traced at 100 metres above sea level at Småhumpen. One of them shows a lateral extent of 70 m, with the thickness of 0.25 m (Fig. 8). This lens has a calcareous composition and cone-in-cone texture. Lateral to this lens, a chain of elongated lenses (type-5) occurs. They are up to 2 m long, with the maximum thickness of about 0.7 m (Fig. 9). These nodules/lenses differ from one another with respect to their internal structure, especially with the frequency of alternation of massive micrite and textured layers, and by the character of cone-in-cone crustification.



**Figure 7.** Iversenfjellet on Hopen. a - calcareous layer – lens at a height of 0.7 m above sea level; b – cone-in-cone at the base of the carbonate layer.



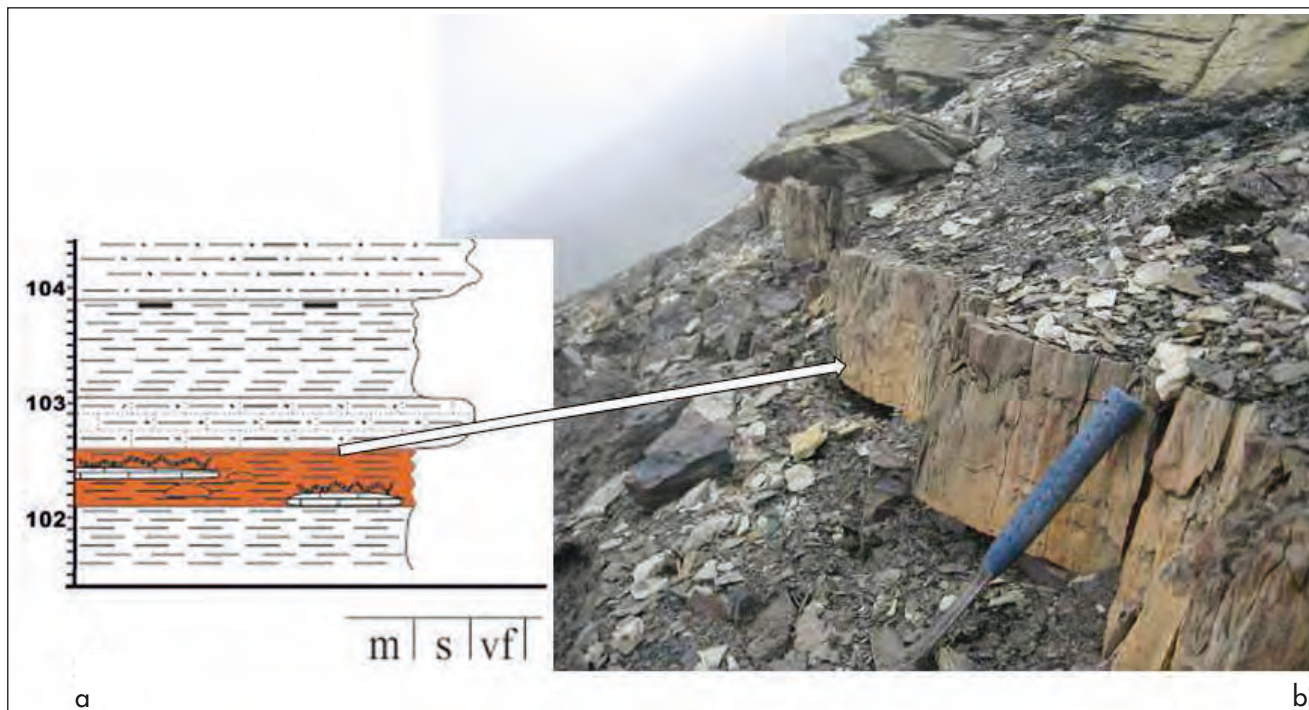


Figure 8. Småhumpen on Hopen. a – lithological column (legend in Fig. 2); b – calcareous layer – lens with cone-in-cone structure.



Figure 9. Småhumpen on Hopen. Calcareous layers and lenses with cone-in-cone structures; a – a lens with cone-in-cone fouling over the entire surface; b – Cone-in-cone forming roof crustification; c – “multistoried” structure with cone-in-cone crustification over the entire surface.



Several varieties of nodules-lenses have been observed:

- 1) Micrite calcareous layers – lenses with cone-in-cone fouling over the entire surface (Fig. 9a);
- 2) Micrite calcareous layers – lenses with roof cone-in-cone crustification (Fig. 9b);
- 3) “Multistoried” structures with several cone-in-cone layers inside and cone-in-cone crustification over the entire surface (Fig. 9c). Some thin layers within these bodies have a layered texture, grading into more massive and thick micritic layers.

Similar carbonate bodies are present in all the studied sections on Hopen. For comparative purposes, one carbonate body from the Hugosøkket section is presented (Fig. 10).

Nodular calcareous edifices (type 6) are morphologically similar to the classical forms of stromatolites with nodulated structures. Similar forms also occur in the Hugosøkket section on Hopen (Fig. 11).

The nodular bodies are confined to a thin carbonate layer, which looks like an accumulation of nodules with different morphologies, including stromatolitic morphology (Fig. 12). The laminated bodies at Hugosøkket occur as thin beds, and many of them represent stromatolites.

Thus, in the Upper Triassic succession of Eastern Svalbard several morphological types of carbonate beds can be identified. The bodies showing bioherm morphology are characterized by a flat bottom and a dome-like roof.

The “mounds” are found in all the studied Upper Triassic sections. The laterally extensive layers or lenses are confined to sections of the De Geerdalen Formation. This is also the case for the nodulated fouling carbonates that may represent stromatolites. All these carbonate bodies show cone-in-cone textures.

## Structural and microstructural features of microbialites

The petrographic investigation has been focused on gaining possible evidence of microbial origin of the carbonate beds. The bases of the carbonate-rich beds have a mixed lime-terrigenous composition. Petrographically, they are sandy-silty-clayey limestones with algal detritus (Fig. 13a). Carbonate is present as micritic peloids up to 0.5 mm in size occurring within micrite-sparite cement. The carbonate grains are recrystallized to pure lime composition and show radial-fibrous internal structure (Fig. 13b). These structures can develop locally in micritic areas or they completely replace the rock, showing gradations to cone-in-cone structures. Another structure of carbonatized surfaces is the stromatolite-like lamination (Fig. 13c).

Extensive calcareous layers – lenses and local calcareous bodies in the Småhumpen section (Figs. 8, 9) – are compositionally diverse and have varying structural features. Composition of the rocks is predominantly calcareous

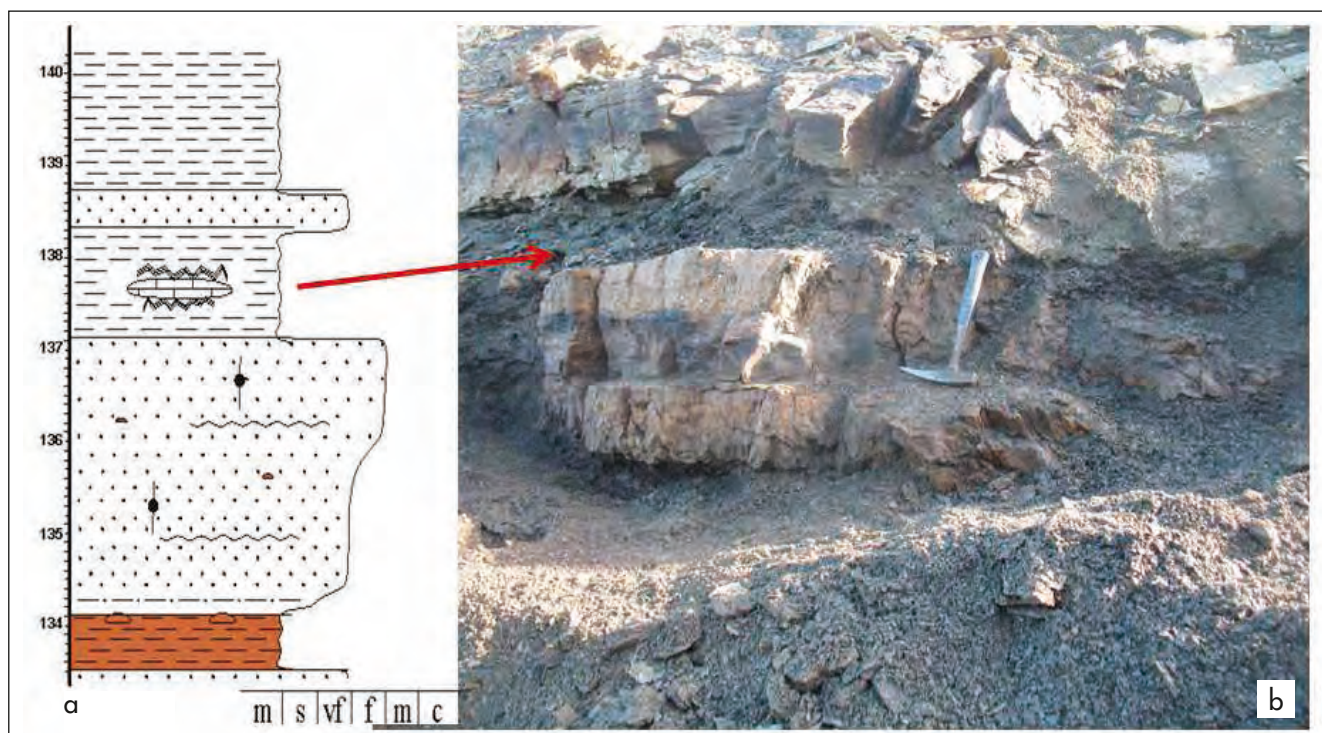


Figure 10. Hugosøkket on Hopen. a – lithological column (legend in Fig. 2); b – calcareous layer – lens with cone-in-cone structure.



Figure 11. Hugosøkket on Hopen. Nodular calcareous edifice (type 6).

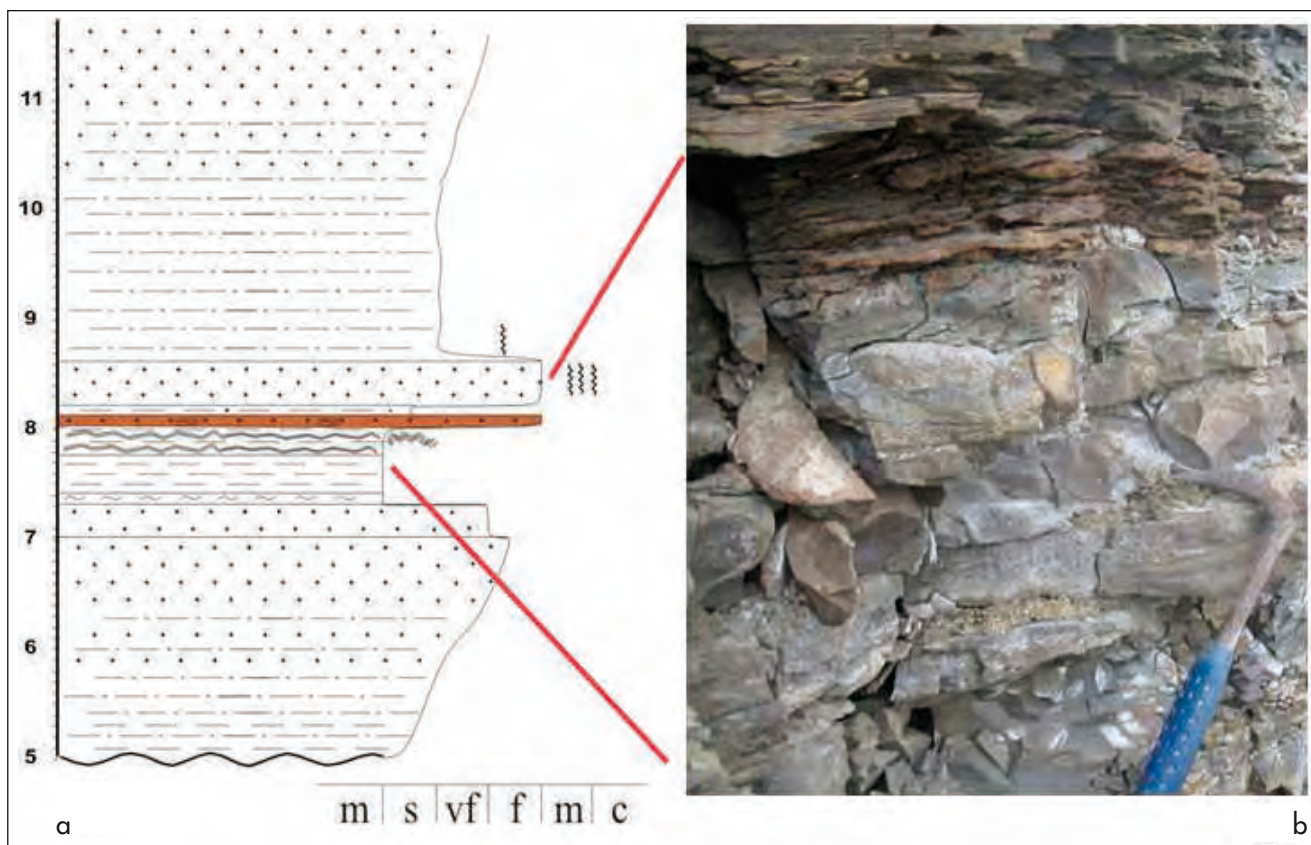
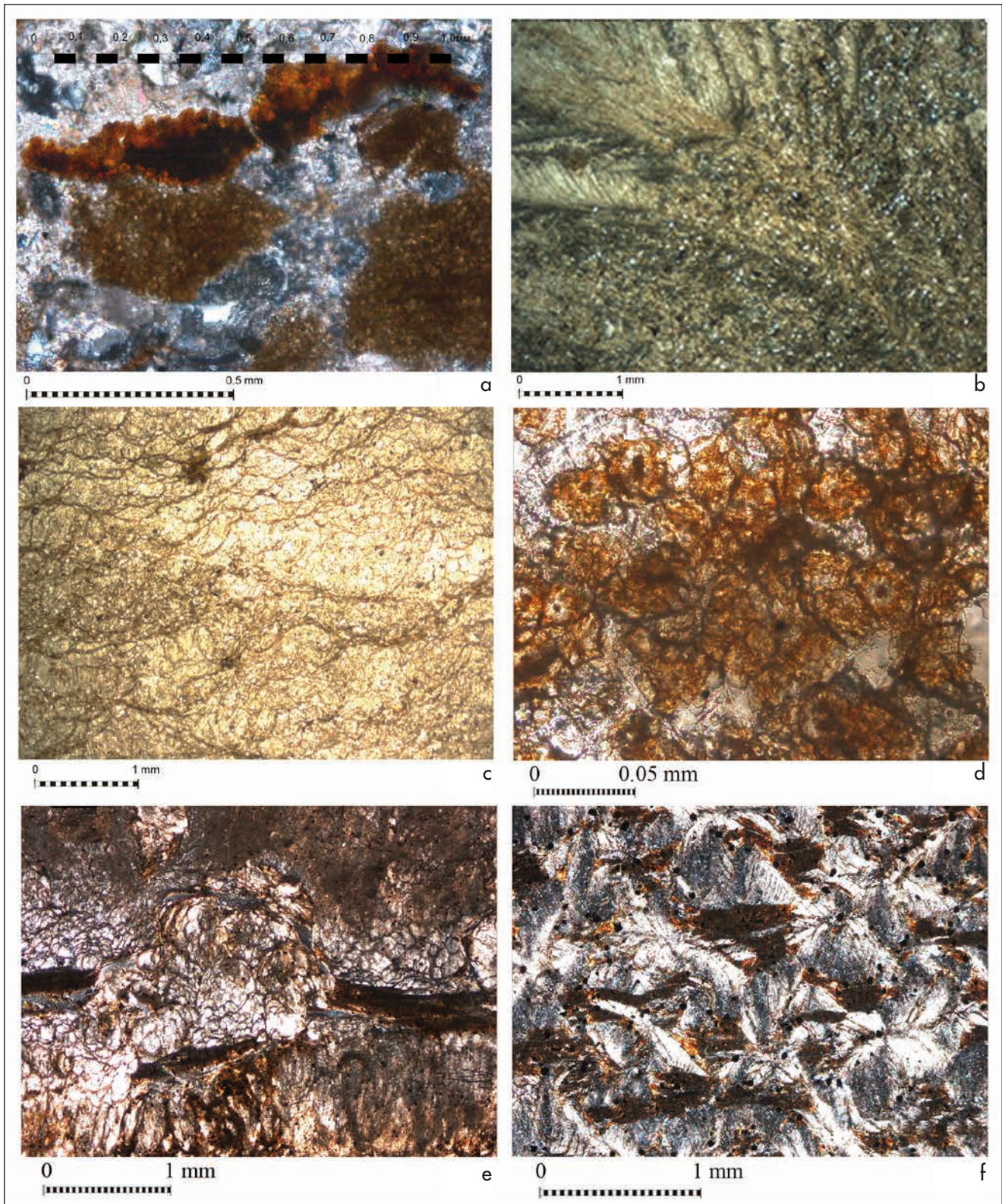


Figure 12. Hugosøkket on Hopen. a – lithological column (legend in Fig. 2); b - calcareous layer containing «nodulated» stromatolites.

with subordinate contribution of clay minerals. The lower part of the layer (Fig. 9a), up to 0.1 m thick, shows a layered-massive texture. Petrographically, it is a limestone

with carbonate-bituminous aggregates constituting up to 50% of the rock (Fig. 13d). This rock is smoothly covered by the next layer, which is characterized by flow structure





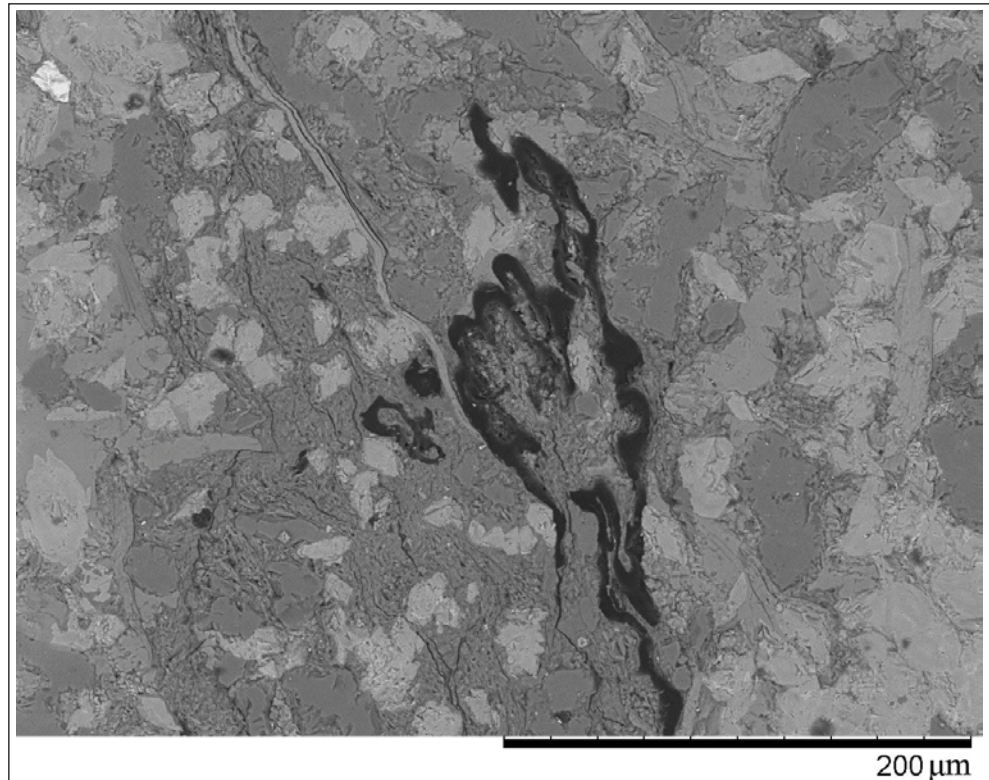
**Figure 13.** Photos of thin-sections. Rock from the carbonatized surfaces: *a* – algae fragments in terrigenous-calcareous rock, *nic. X*; *b* – fibrous calcite structure, *nic. X*; *c* – stromatolite-like lamination from the lens in Fig. 9a, *nic. II*; *d* – carbonate-bituminous aggregates, *nic. X*; *e* – «flow structure»; *nic. X*; *f* – sheaf-like structure with bituminization along crystal growth cracks, *nic. X*.

(Fig. 13e). There are common sparitic replacements with “sheaves” crustifications around small mineral-bituminous aggregates (Fig. 13 f). In thin-sections of the upper

layer, the cone-in-cone structure with bitumen impregnation along crystal growth cracks is present.



**Figure 14.** SEM photos of lime lens (Fig. 9 a), bitumen are forming the texture of fluidization.



Scanning electron microscopic (SEM) studies have revealed numerous liquid bitumen inclusions (Fig. 14), and show the presence of abundant pyrite framboids, whose genesis may be interpreted as a result of biochemical processes with the participation of sulfate-reducing bacteria (e.g. Postfai et al., 1998; Astafieva et al., 2004).

Another object (concretion) with typical cone-in-cone fouling from Lyngefjellet shows mineral-bituminous aggregates, which constitute most of the rock. Around the aggregates, split growth of calcite crystals is observed (Fig. 15a). Numerous kerogen grains in chain-like arrangement are present in the rock (Fig. 15b). Similar grains were identified by Korde (1950) as the coccoid cells of cyanobacteria.

Nodular stromatolites, confined to the carbonate layers (Fig. 11) have a complex composition and structure. The rock from the interior, massive part of stromatolite is mainly characterized by cryptocrystalline structure, with individual microlenses dominated by recrystallized and encrusted microfossils (*Tasmanites?*) (Fig. 15c). Massive rock is replaced by homogeneous micritic and fibrous sparite partings (Fig. 15d). Some layers have a stromatolite-like lamination (Figs. 15e, f). In thin sections made parallel to bedding of cover fouling black-brown-bitumen zone, “clean” areas of sparite crystallization are present. In the overlying rocks numerous fragments of stromatolite-laminas are recorded. Similar structures are common in Precambrian stromatolites (e.g. Varaksina and Habarov, 2007).

SEM and microprobe analysis confirmed that all our studied microbialites have calcite mineral composition (Fig. 16a), and also contain numerous pyrite framboids (Fig. 16).

Dark aggregates (Fig. 15f) indicate the presence of microtextures that have a fluidal occurrence (Fig. 16a), formed by a distribution of black amorphous mass, which according to microprobe analysis, comprises carbonaceous material, presumably bitumen and their oxidation products. Fluidal texture is always accompanied by intensive development of sulphides (Fig. 16a), which can be regarded as the result of authigenic mineralization during bacterial breakdown of organic matter (anaerobic digestion).

Many individual aggregates, which were observed in the polarizing microscope, have a concentric structure. The main part of aggregates have calcareous or calcareous-siliceous composition (Figs. 16b, c), and silica is present in the form of semi-crystalline chalcedony that replaces primary carbonate minerals. Threads are sometimes developed around the aggregates, and units appear as “balls” (Figs. 16b, c). Microprobe analysis shows that these “threads” are almost entirely composed of carbon. This association may indicate that they represent microbial aggregates.

A collection of structural features of the studied microbialites shows layering structure at macro-, micro- and ultra-levels, and a high content of components whose



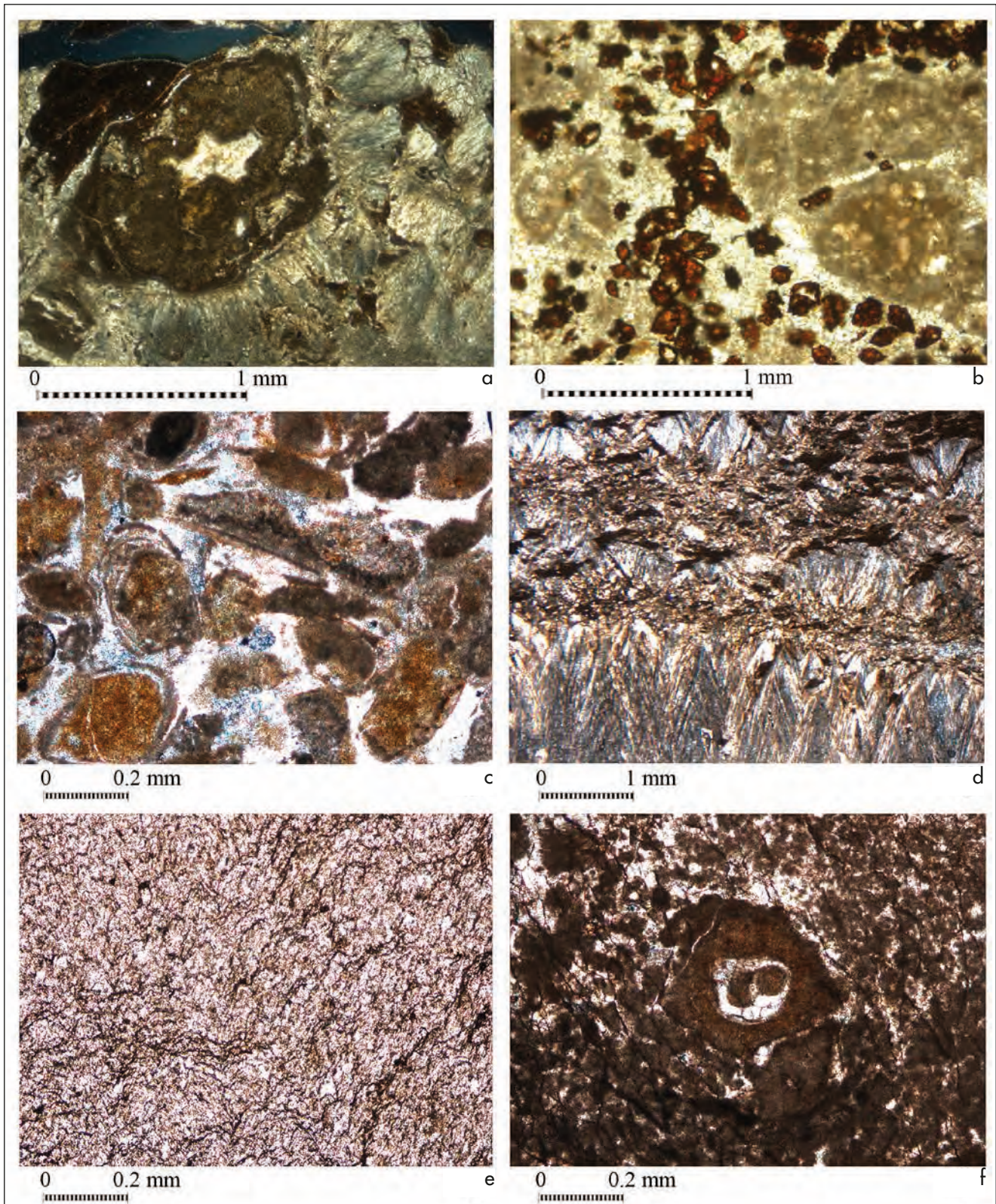
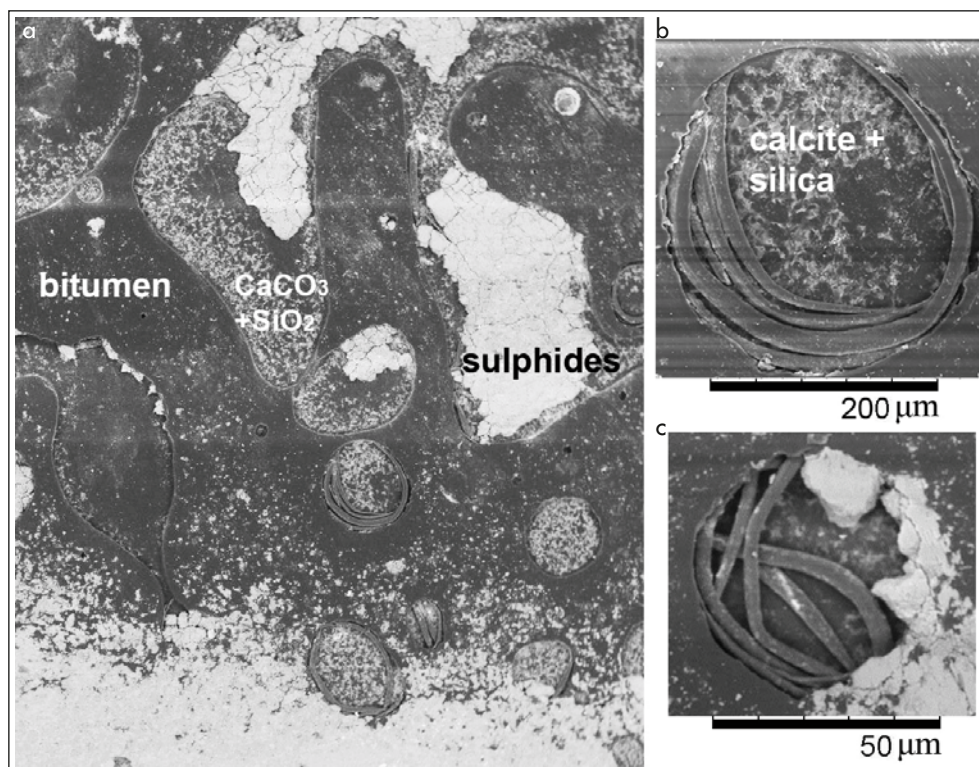


Figure 15. Photos of thin sections. Microbialite with cone-in-cone fouling: a – radial and sheaf-like recrystallization around carbonate-bituminous aggregates, *nic. X*; b – brown kerogen grain forming a chains, *nic. X*. «Nodulated» stromatolite (Fig. 11): c – recrystallized and crustified microfossils (Tasmanites?), *nic. X*; d – alternating of micritic and fibrous sparite partings, *nic. X*; e – stromatolite-like lamination in the section perpendicular to the bedding, *nic. II*; f – stromatolite-like lamination in the section along the bedding, black – bitumen saturation, *nic. X*.



**Figure 16.** SEM photos of nodulated stromatolite (Fig. 11):  
*a* - fluidal microtexture;  
*b, c* - carbonate-siliceous aggregates in amorphous carbon rock mass (bitumen).



morphological and chemical characteristics indicate their microbial origin. The high content of bitumen components is genetically associated with the primary components of the rocks. Secondary mineral transformations, first of all the replacement of carbonates by silica, indicate geochemical non-equilibrium (change from medium alkaline to acid) due to transformation of the initial organic matter.

## Geochemical data

This paper focuses on the morphology, structures and microstructures of the microbialites, but some preliminary geochemical data are presented to support the discussion of the genesis of these structures. These data include results from organic geochemistry as well as X-ray fluorescent analysis, investigations of group and molecular composition of sedimentary organic matter (OM) by GC-MS and also isotopic analysis of carbon and oxygen.

The microbialites are characterized by a very pure limestone composition (concentration of calcium up to 48.9%), which distinguishes them sharply against the Upper Triassic siderite nodules and, indirectly, is further evidence of their biogenic nature.

Dispersed OM in our samples has been characterized by biomarkers. TOC content for carbonatized beds varies from 0.15 to 1.06% (average 1.1%), limestone "mounds"

from 0.62 to 1.46% (average 1.1%), minimum TOC values present in cone in-cone structures are 0.09-0.65% (average 0.2%). The average concentration of organic carbon (OC) in carbonate rocks is 0.2%; so for most samples the values of OC exceeded the average concentration. Contents of chloroform-extracted bitumen (Achl) are high in most of the carbonate "mounds" - up to 0.2% (the average concentration of Achl - 0.03%). Bitumen index  $\beta$  ( $\beta = (\text{Achl} / \text{TOC}) \times 100$ ) is used to determine syngenetic or epigenetic HC genesis in the rocks. For syngenetic bitumen in carbonate rocks, its value does not exceed 5-10 (Neruchev et al., 1998). This coefficient is maximum for any "mound"-bioherms-microbialites (9.1 - 19.5, average 12.8) and in the cone-in-cone structures (4.8-11.4), which allows to suggest the presence of migrated HC in these rocks. All microbialites are characterized by high content of methane-naphthenic hydrocarbon fractions (over 59%).

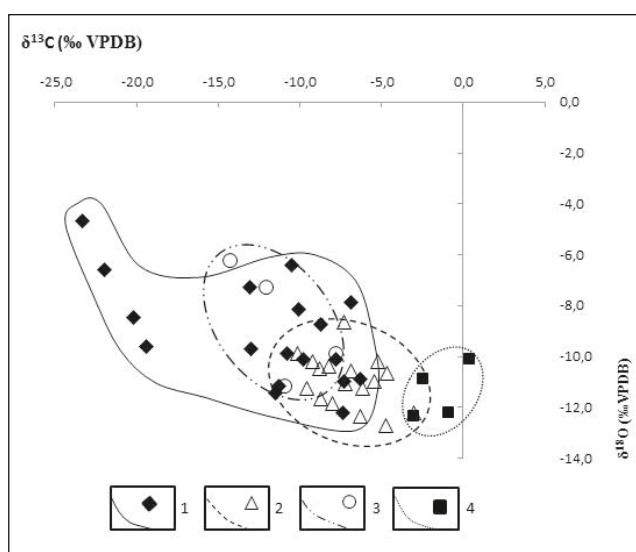
Variations in the molecular composition of n-alkanes and isoprenoids reflect genetic specificity of DOM. There are three main types of n-alkanes distributions in the DOM of the Upper Triassic possible microbialites. The first one, with a maximum in a low molecular HC ( $C_{17}$ - $C_{19}$ ), indicates that the hydrobiont OM (Peters et al., 2004) represent bioherms-"mounds" and cone-in-cone foulings. The second type of distribution has two main modes in the low molecular ( $C_{17}$ - $C_{19}$ ) and high molecular HC ( $C_{25}$ - $C_{29}$ ) - with mixed sapropelic-humic OM present in the carbonatized surfaces. Additional "blurred" maximum at  $C_{20}$ - $C_{22}$ , reflecting the contribution of bacterial

OM, is common in n-alkanes distribution in all types of microbialites.

The contribution of protozoa in the formation of OM is indicated by the values of 17 $\alpha$ -hopanes (prokaryotes markers), and regular steranes (H<sub>30</sub>/St<sub>29</sub>) - eukaryotes markers (Peters et al., 2004), which are quite high for all samples. Among triterpens the number of sapropelic markers is significant with high content of norhopanes (S<sub>29</sub>/S<sub>30</sub> to 0.7) and tricyclanes (C<sub>tri</sub> / H to 11.1). Elevated levels of tricyclic terpanes are typical for a large part of the studied samples. Peters et al. (2004) associate tricyclanes with cell membranes of prokaryotes. In some samples tricyclanes form a stable homologous distribution of C<sub>19</sub>-C<sub>36</sub> typical for bacterial-algal OM (Neruchev et al., 1998).

In addition to "bacterial" signs, HC biomarkers fix correspondence to mature oil (homologous series of alkylcyclohexanes, high value content of cyclanes, naphthidic PAHs, etc.) and the intense thermal effects on the OM of microbialites (index of sterans; metilphenanthrene index, etc.), which exceeds the Upper Triassic level of catagenesis.

We observe some trends in the variations of the isotopic composition of various carbonate edifices of our material (Fig. 17). Minimum values of  $\delta^{13}\text{C}$  are present in the type-2, -3 and -4 microbialities, especially in carbonate bodies with indications of "protozoa-bacterial" signs (Gåsskaret, Hugosøkket, Småhumpen sections). In calcareous rocks with cone-in-cone structures the lightest  $\delta^{13}\text{C}$  values are typical for massive pieces of rocks while cone-in-cone



**Figure 17.** Plot of  $\delta^{13}\text{C}$  (‰ V-PDB) versus  $\delta^{18}\text{O}$  (‰ V-PDB).  
 Legend: 1 - microbialites - bioherms, "mounds", lenses without cone-in-cone crustifications (types 2, 3, 5); 2 - cone-in-cone structures; 3 - cyanobacterial mats (type 4); 4 - carbonatized surfaces with cone-in-cone structures (type-1).

isotopic compositions are heavier. It may be explained by the participation of the inorganic seawater carbon in the formation of fouling at the surfaces of cyanobacterial bodies.

For reliable diagnosis of methane-derived carbonate bodies, the negative carbon isotopic composition should be below -40 ‰ (Whiticar, 1999; Peckmann and Thiel, 2004; Hovland et al., 2005; Jenkins et al., 2007). However, isotopic values may vary within a wide range in different components of the same rock (e.g. Jenkins et al., 2007). Relatively low values of  $\delta^{13}\text{C}$  ‰ in combination with organic geochemistry data allow us to assume the influence of the HC-emanation processes on the microbial activity, and as a final result the genesis of microbial-seep carbonate bodies. Of course, these assumptions require strong, statistically supported evidence.

## Summary and Conclusions

The position of the studied microbialites in the Upper Triassic sedimentary succession of Eastern Svalbard suggests their origin in shallow marine to supralittoral or littoral environments (c.f. Mørk et al., 2013).

In general, the Upper Triassic microbial carbonates, irrespective of their morphology, show specific microstructures and the presence of numerous microbial traces. Fluid ultra- and micro-textures recorded in some of the "microbialites" indicate paragenetic relationship of hydrocarbons and secondary mineral phases. Based on the field and analytical data, the major stage of formation of the microbialites is related to early diagenetic processes.

Carbonatized beds are confined to the supralittoral paleoenvironments. The studied sections of thin beds and their underlying rocks are similar to the sections of cyanobacterial mats described by Reading et al. (1986) in a sequence from the bottom-up as: lagoonal deposits enriched by algal carbonate "moors" and actual algal mats. In our study we trace a similar pattern (Fig. 18).

Apparently bioherms - "mounds" with macro-bedding - alternating layers of pure lime and carbonate layers doped with terrigenous material are characteristic of the littoral zone. Presumably, alternating layers in this type of microbialites were related to alternating periods of growth of micro-organisms, accumulation of terrigenous material, and redistribution of the decomposition products of organic matter and its mineralization. The first two processes are determined by fluctuations in the position of the shoreline.

Microbialites-lenses may be found in these same sedimentary paleoenvironments. Cone-in-cone fouling is typical for them. It can be developed either in the roof or on the entire surface of the carbonaceous bodies. The last



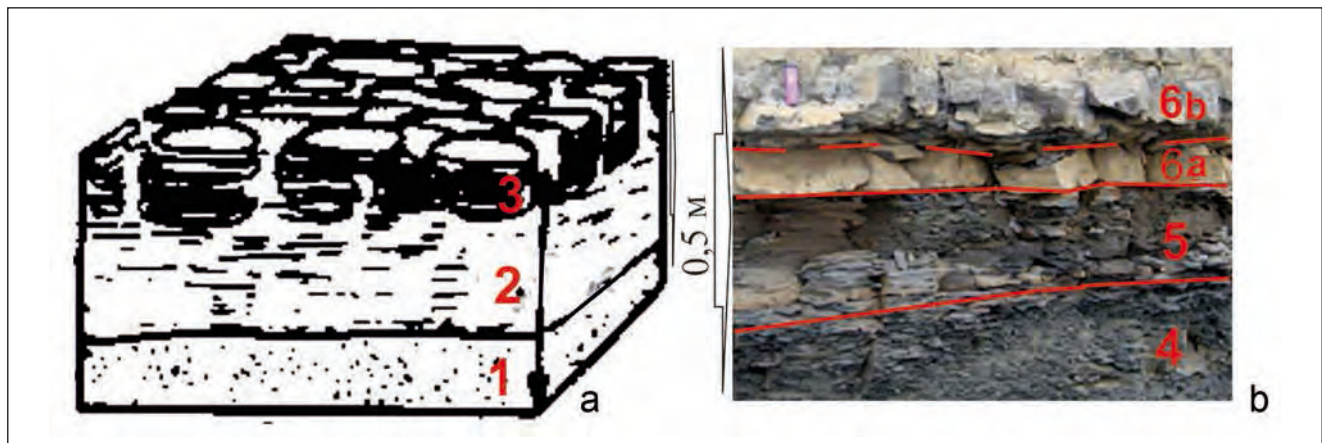


Figure 18. Construction of cyanobacterial mats. a – block map (from Reading et al., 1986); b – the section of cyanobacterial mat (Iversenfjellet, Hopen, Fig. 7). Legend: 1 – lagoonal sands or mud; 2 – dark stratified, carbonates enriched algal turf moor; 3 – algal mat; 4 – lime mudstone with coalificated plants residuals; 5 – mixed silty-clay-limestone with algal-bacterial fragments; 6a – fine-crystalline limestone with cone-in-cone structure; 6b – algal-bacterial mat.

type of crustification clearly indicates an early diagenetic origin. By our assumption, cone-in-cone fouling seems to reflect the biochemical conditions of very early diagenesis, and it is the result of shifting the equilibrium in carbonate - bicarbonate system towards the crystallization of carbonate mineral phases under the influence of biological conditions.

Crystallogenic radiating growths of calcite, which are commonly called “cone-in-cone”, represent thin split crystals. Split growth phenomenon is well known and confirmed experimentally (e.g. Nassif et al., 2005). All forms of cleaved growth occur directly during crystallization. One of the main reasons for splitting is the presence of mechanical impurity in the environment of crystallization, commensurable with the thickness of increased layers of a crystal. The firm particles absorbed by the growing side force new accruing layers to deviate parallel position (Glikin, 2009; Shubnikov and Parvov, 1969). Involving clastic sedimentation, such conditions could be preferred in the littoral environment. Split crystal growth can be realized only in free volume, i.e. this process can occur either during sedimentation or early diagenesis in water-saturated sediments.

In general, the cones fouling around the microbial structures formed by complex communities of different algae and other microorganisms can be regarded as a process of biochemical precipitation of calcite (or aragonite), which is controlled by the presence of bicarbonate in the sediment environment and biological factors - liming and extraction of  $\text{CO}_2$  during photosynthesis.

Morphological and microstructural characteristics and the composition of components indicate the essential role of microbiological communities in formation of the studied sedimentary edifices. The biological nature

is indicated in real structural features (fragments of algae, the microbial cells, microspherolites, and others). Mineralized protozoa components were reported by Astafieva et al. (2011), Lowenstam and Weiner (1989) and Starr et al. (1981). Active development of cyanobacterial mats and local hilly bodies is, on the one hand, predetermined by depositional environment, and, on the other hand, has to be due to any additional factors, like the bio-mineralization processes and interactions between the organic matter and microbial processes.

#### Acknowledgements.

The authors are grateful to the Norwegian Petroleum Directorate for financial support of the research. The authors express their gratitude to H. Brekke and A.V. Zayonchec for organization of the work during the joint Russian-Norwegian project, colleagues B.A. Lundschieen, J. Stenløkk, T. Høy, R.S. Rød, M.S. Woldengen (NPD), and K.P. Krajewski (Geological Institute of Polish Academy of Science) for fruitful communication during fieldwork. We also thank the referees Øyvind Hammer (University of Oslo) and Krzysztof P. Krajewski for their critical remarks and good recommendations. A special note of thanks should be expressed to A. Mørk (Sintef Petroleum Research) for the excellent geological and scientific management of the investigations, for his thorough editorial work and contribution to the final version of the manuscript.

## References

- Astafieva, M.M., Hoover, R. & Rozanov, A.Yu. 2004: Framboidal structures in Earth rocks and in astromaterials. *Proceedings of SPIE Proc. SPIE*. V. 5163, 36–47.
- Astafieva, M.M., Gerasimenko, L.M., Geptner, A.R., Zhegallo, E.A., Zhmur, S.I., Karpov, G.A., Orleanskiy, V.K., Ponomarenko, A.G., Rozanov, A.Yu., Sumina, E.L., Ushatinskaya, G.T., Huver, R. & Shkolnik, E.L. 2011: *Iskopaemye bakterii i drugie mikroorganizmy v zemnyih porodah I astromaterialah (Fossilized bacteria and other microorganisms in terrestrial rocks and astromaterials)*. Moscow: Paleontological Institute of the Russian Academy of Sciences PI RAS, 172 pp. (in Russian).



- Jenkins, R.G., Kaim, A., Hikida, Y. & Tanabe, K. 2007: Methane-flux-dependent lateral faunal changes in a Late Cretaceous chemosymbiotic assemblage from the Nakagawa area of Hokkaido, Japan. *Geobiology*, 5, 127–139.
- Hovland, M., Svensen, H., Forsberg, C.F., Johansen, H., Fichler, C., Fossa, J.H., Jonsson, R. & Rueslåtten, H. 2005: Complex pockmarks with carbonate-ridges off mid-Norway: Products of sediment degassing. *Marine Geology*, 218, 191–206.
- Glikin, A.E. 2009: *Polimineral-Metasomatic Crystallogenesis*. Springer Science, 312 pp.
- Korde, K.B. 1950: Mikroskopicheskaja struktura nasloenij stromatolitov i tipy sohrannosti iskopaemyh Cyanophyceae (Microscopic structure of stromatolites stratifications and types of safety of Cyanophyceae). *Reports of AS USSR*, V. LXXI, № 6, 1950, 1109–1112. (In Russian).
- Lowenstam, H.A. & Weiner, S. 1989: *On biomineralization*. Oxford: Oxford Univ. Press, 324 pp.
- Mørk, A., Dallaman, W.K., Dypvik, H., Johannessen, E.P., Larsen, G.B., Nagy, J., Nøttvedt, A., Olausson, S., Pchelina, T.M. & Worsley, D. 1999: Mesozoic lithostratigraphy. In Dallmann W.K. (ed.): *Lithostratigraphic lexicon of Svalbard. Review and recommendations for nomenclature use. Upper Palaeozoic to Quaternary bedrock*. Norsk Polarinstittutt, Tromsø, 127–214.
- Mørk, A., Lord, G.S., Solvi, K.H. & Dallmann, W.K. 2013: *Geological map of Svalbard 1:100 000, sheet G14G Hopen*. Norsk Polarinstittutt Temakart No. 50.
- Nassif, N., Gehrke, N., Pinna, N., Shirshova, N., Tauer, K., Antonietti, M. & Colfen, H. 2005: Synthesis of stable aragonite superstructures by a biometric crystallization pathway. *Angewandte Chemie*, 117, 6158–6163.
- Neruchev, S.G., Rogosina, E.A., Shimanskiy, V.K., Sobolev, V.S., Yakutzeni, V.P., Parparova, G.M. & Prasolov, E.M. 1998: *Spravochnik po geohimii nefti i gaza (Handbook of geochemistry of oil and gas)*. St. Petersburg: Publishing house Nedra, 576 pp. (In Russian).
- Peckmann, J. & Thiel, V. 2004: Carbon cycling at ancient methane-seeps. *Chemical Geology*, 205, 443–467.
- Peters, K., Walters, C. & Moldowan, J. 2004: *The biomarker guide*. Cambridge University Press, 1155 pp.
- Postfai, M., Buseck, P.R., Bazylinski, D.A. & Frankel, R.B. 1998: Iron sulfides from magnetotactic bacteria: Structure, composition, and phase transitions. *American Mineralogist*, 83. № 11–12(2), 1469–1481.
- Reading, H.G. (ed.), 1996: *Sedimentary environments: processes, facies, and stratigraphy*. 3<sup>rd</sup> ed., Blackwell Scientific Publications, 688 pp.
- Shubnikov, A.V. & Parvov, V.F. 1969: *Zarozhdenie i rost kristallov (Origin and growth of crystals)*. Moscow, publishing house "Nauka", 70 pp. (In Russian).
- Starr, M.P., Stolp, H., Truger, H.G., Balows, A. & Schlegel, H.G. (eds.), 1981: *The Prokaryotes. A Handbook on Habitats, Isolation, and Identification of Bacteria*. Springer-Verlag Berlin Heidelberg, New York, 1102 pp.
- Varaksina, I.V. & Habarov, E.M. 2007: Mikrostruktury, litologicheskie assotsiatsii i usloviya obrazovaniya rifejskikh stromatolitov Bajkitskoj anteklizy (zapad Sibirskoj platformy) (Microstructure, lithological association and environments of Riphean stromatolites of Baikit antecline (West Siberian platform)). *Litosfera (Lithosphere)*, № 4, 59–72. (In Russian).
- Whiticar, M.J. 1999: Carbon and hydrogen isotope systematics of bacterial formation and oxidation of methane. *Chemical Geology*, 161, 291–314.
- Whitten, D.G.A. & Brooks, J.R.V. 1979: *A Dictionary of Geology*, Penguin Books Ltd., 518 pp.

# An infrazonal ammonite biostratigraphy for the Kimmeridgian of Spitsbergen

Mikhail A. Rogov

Geological Institute of Russian Academy of Science (RAS), Moscow, Russia, e-mail: russianjurassic@gmail.com

An infrazonal ammonite-based *biostratigraphy* for the Kimmeridgian of Spitsbergen is reviewed in detail. The *Bauhini Zone*, *bayi* horizon, aff. *beau-grandii* and *norvegicum* horizon have been recognized in this area for the first time. The presence of separate *decipiens* and *elegans* horizons has been demonstrated for the Myklegardfjellet section. The Kimmeridgian ammonite succession of Spitsbergen resembles that of Franz Josef Land and consists mainly from Boreal cardioceratids and oppeliids. In contrast to East Greenland and the Norwegian Sea, the sub-Boreal aulacostephanids are restricted to a few narrow stratigraphic intervals. This difference suggests a very limited exchange by ammonite faunas through the Greenland-Norwegian Seaway during the Kimmeridgian. The evolutionary trend of Boreal oppeliid genus *Suboxydiscites* is briefly outlined.

**Key words:** Kimmeridgian, Jurassic, Spitsbergen, Svalbard, Ammonites, Infrazonal biostratigraphy.

## Introduction

Numerous studies of Kimmeridgian high-latitude ammonite successions have been conducted during the previous three decades. Successions of biohorizons, mainly based on the cardioceratid lineage, were established through the whole Arctic from East Greenland to Barents Sea, and north of Siberia (Birkelund and Callomon, 1985; Wierzbowski and Smelror, 1993; Rogov and Wierzbowski, 2009; Wierzbowski et al., 2002). Spitsbergen is well-known for its rich Jurassic ammonite faunas (including Kimmeridgian ones) and geographical position along the migrational pathways of ammonites, making study of ammonite successions of this region very important for both stratigraphical and paleogeographical aims.

The first data on Kimmeridgian ammonites of the region were published by Spath (1921), who recorded some species of *Pictonia*, *Rasenia* and *Amoeboceras*, collected at Festningen<sup>1</sup> by Dr. J. W. Gregory during the 1896 expedition led by Martin Conway. Re-examination of ammonites from this collection, currently curated at the British Museum of Natural History, reveals the presence of at least one specimen of *Pictonia* (pl.1, fig. 4.1). Additional Kimmeridgian ammonites from the same section were reported by Frebold (1928), who

recognized a few species of Kimmeridgian “*Cardioceras*” from bed 7. Two years later, Frebold described Kimmeridgian ammonites from various localities on Spitsbergen, including *Cardioceras* cf. *nathorsti* var. *robusta* (Frebold, 1930, pl. VIII, figs.1-2 = *Euprionoceras sokolovi* (Bodylevski)), *Rasenia* sp. indet. aff. *groenlandica* (Frebold, 1930, pl. IX, fig. 3-4; fig. 3 = *Zonovia* sp., fig. 4 = *Zenostephanus (Xenostephanoides)* cf. *thurrelli* (Arkell et Callomon)), *Rasenia* sp. indet. cf. *groenlandica* (Frebold, 1930, pl. XXII, fig. 2 = *Zenostephanus (Xenostephanoides)* *thurrelli* (Arkell et Callomon)) and *Cardioceras* sp. indet. aff. *cricki* (Frebold, 1930, pl. IX, figs. 1-2; fig. 1 = *Amoebites* ex gr. *subkitchini* Spath) The following year, Sokolov and Bodylevski (1931) published a description of Jurassic and Cretaceous fossils from Spitsbergen, collected primarily from the Festningen section (including all described Kimmeridgian ammonites). They figured numerous specimens of *Amoebites* cf. *subkitchini* (Spath) (as *Cardioceras* cf. *kitchini*) and described a new species *A. sokolovi* (Bodylevski).

<sup>1</sup> Jurassic and Cretaceous ammonites from this collection are mainly labeled as collected from “Kapp Starostin”, but only Paleozoic rocks are cropped out near to this cape, while Jurassic and Cretaceous deposits are exposed some three kilometers eastwards, near to Cape Festningen.

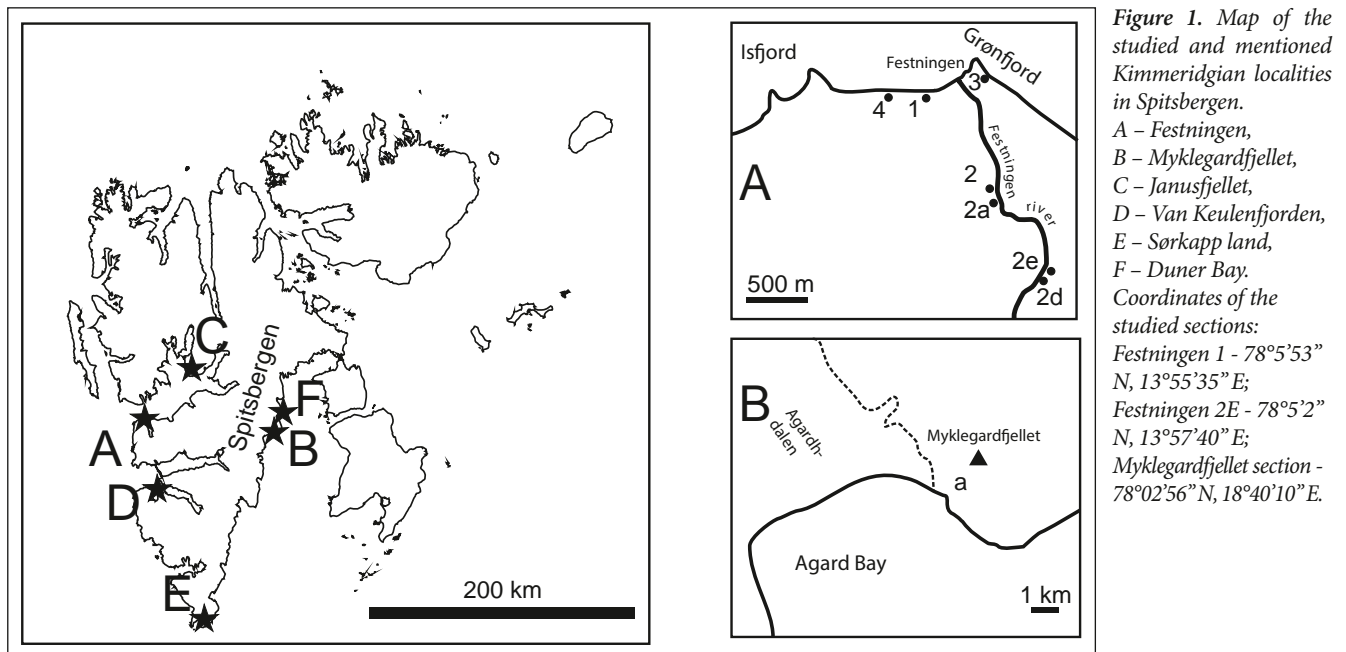


Figure 1. Map of the studied and mentioned Kimmeridgian localities in Spitsbergen.

A – Ffestningen,  
B – Myklegardfjellet,  
C – Janusfjellet,  
D – Van Keulenfjorden,  
E – Sørkapp land,  
F – Duner Bay.

Coordinates of the studied sections:

Festningen 1 - 78°5'53" N, 13°55'35" E;

Festningen 2E - 78°5'2" N, 13°57'40" E;

Myklegardfjellet section - 78°02'56" N, 18°40'10" E.

During the last few decades, abundant new data regarding Kimmeridgian ammonites and biostratigraphy of Spitsbergen has been gained during the geological survey by Russian geologists (since early 60s) and by field trips by Polish Spitsbergen Expedition. New data published in 1980s, significantly improved the existing knowledge of the Kimmeridgian ammonite succession of Spitsbergen. Birkenmajer et al. (1982) described the Jurassic and Lower Cretaceous succession of Myklegardfjellet. Fossils were collected from 20 fossiliferous horizons from this section, including two levels with Kimmeridgian ammonites; the lower level with *Amoebites* cf. *kitchini* and *Zonovia evoluta* (re-identified by Wierzbowski (1989) as *A. subkitchini* and *Rasenia cymodoce*) and the upper level with *Amoebites* cf. *salfeldi* (re-classified as *A. kitchini* by Wierzbowski, 1989). The following year, "Explanatory notes on the biostratigraphical scheme for the Jurassic and Cretaceous of Spitsbergen" were published by Ershova (1983). This included a description of all Jurassic-Lower Cretaceous zones and beds recognized during the geological survey, and figured most of the typical ammonite taxa. Ershova subdivided the Kimmeridgian Stage of Spitsbergen based on beds with *Rasenia borealis* and *Amoeboceras kitchini* (Lower Kimmeridgian), overlain by the *Mutabilis* Zone and beds containing *Amoeboceras decipiens* and *A. kochi* above (Upper Kimmeridgian). Unfortunately, this paper lacks accurate data regarding the ammonite ranges in the sections and their relative stratigraphical positions within zones and beds. The most important ammonites, figured in the paper by Ershova (1983), are index-taxa of zones, subzones and biohorizons, recently recognized in the Boreal Kimmeridgian by Birkelund and Callomon (1985) and Wierzbowski (Wierzbowski, 1989; Wierzbowski and Smelror, 1993; Wierzbowski et al., 2002). These are *Plasmatites bauhini* (Opp.) (*Amoeboceras bauhini* in Ershova, 1983, pl. V, fig. 7 only; refigured herein, Fig.

4. 2), *Amoebites pingueforme* (Mesezhn. et Romm), *A. subkitchini* (Spath), *A. kitchini* (Salf.), *Rasenia* spp., *Zenostephanus* spp. (for details see Wierzbowski, 1989), *Euprionoceras sokolovi* (Bodyl) (= *A. sokolovi* (Bodyl.) and *A. kochi* (Spath)), and *Hoplocardioceras* spp. Ershova also reported *Aulacostephanus* from the Upper Kimmeridgian. However, all ammonites from her collection recorded as *Aulacostephanus* (including those figured in Ershova, 1983, pl. XV, fig.5) should be re-classified as *Zenostephanus* and therefore could be assigned to the separate *Zenostephanus* horizon, as has been proposed previously by Wierzbowski (1989). Among stratigraphically important taxa, which were not figured, Ershova mentioned "*Streblites* sp." from the Upper Kimmeridgian, reassigned to the Boreal oppeliid genus *Suboxydiscites* (see below). Later, Wierzbowski (1989) described the Kimmeridgian ammonite succession of the Sassenfjorden area. Here he recognized a succession of ammonite faunal horizons similar to that from East Greenland, but also noted differences including the relative scarcity of aulacostephanids, which are common in two levels only, and the impossibility to subdivide *decipiens* and *elegans* horizons. Wierzbowski also critically reassessed previous identifications and age assignments of Kimmeridgian ammonites from Spitsbergen. A paper devoted to analysis of very interesting Kimmeridgian ammonite assemblage has been published by Birkenmajer and Wierzbowski (1991). All ammonites described here were collected by K. Birkenmajer from the relatively thin band (~1 m in thickness) in the southern part of Holmgardfjellet, ca. 7 km NW from the Myklegardfjellet section. This ammonite assemblage includes only cardioceratids showing high intraspecific variability and including morphologies close to *Hoplocardioceras elegans*, *H. decipiens*, *Euprionoceras sokolovi* and ?*E. uralense*. Wierzbowski interpreted this assemblage as



a highly variable biospecies *A. uralense* and concluded that this assemblage is probably slightly older than the fauna with *H. elegans* and *H. decipiens* which he previously described, and that close phyletic relations are suggested between *Amoebites s.s.*, *Hoplocardioceras* and *Euprionoceras*. Alternatively, the record of strictly separated *decipiens* and *elegans* faunas in East Greenland (Birkelund and Callomon, 1985) and in Spitsbergen (Rogov, 2010b) suggests a revised age interpretation for assemblages with *H. elegans* and *H. decipiens* as described from Janusfjellet (Wierzbowski, 1989) and Holmgardfjellet (Birkenmajer and Wierzbowski, 1991). These assemblages could correspond to the intermediate level between *decipiens* and *elegans* faunas.

This study is based on the results of the field works of the years 2006 and 2007 (conducted at the famous Festningen and Myktagardfjellet sections, see Fig. 1), which were part of joint project by NPD (Norway) and Geological Institute of RAS (Moscow, Russia). Fieldwork and analysis of published data and results of studying of collections from Spitsbergen, collected during the geological survey are presented. Ammonites are not very common in either of the studied sections, and their records are mainly restricted to particular beds or their parts only. Ammonite ranges and recognized zonal and infrazonal units are shown in Figs. 2 and 3. In terms of lithostratigraphical units the Kimmeridgian includes the Lardyfjellet and Oppdalssåta members of the

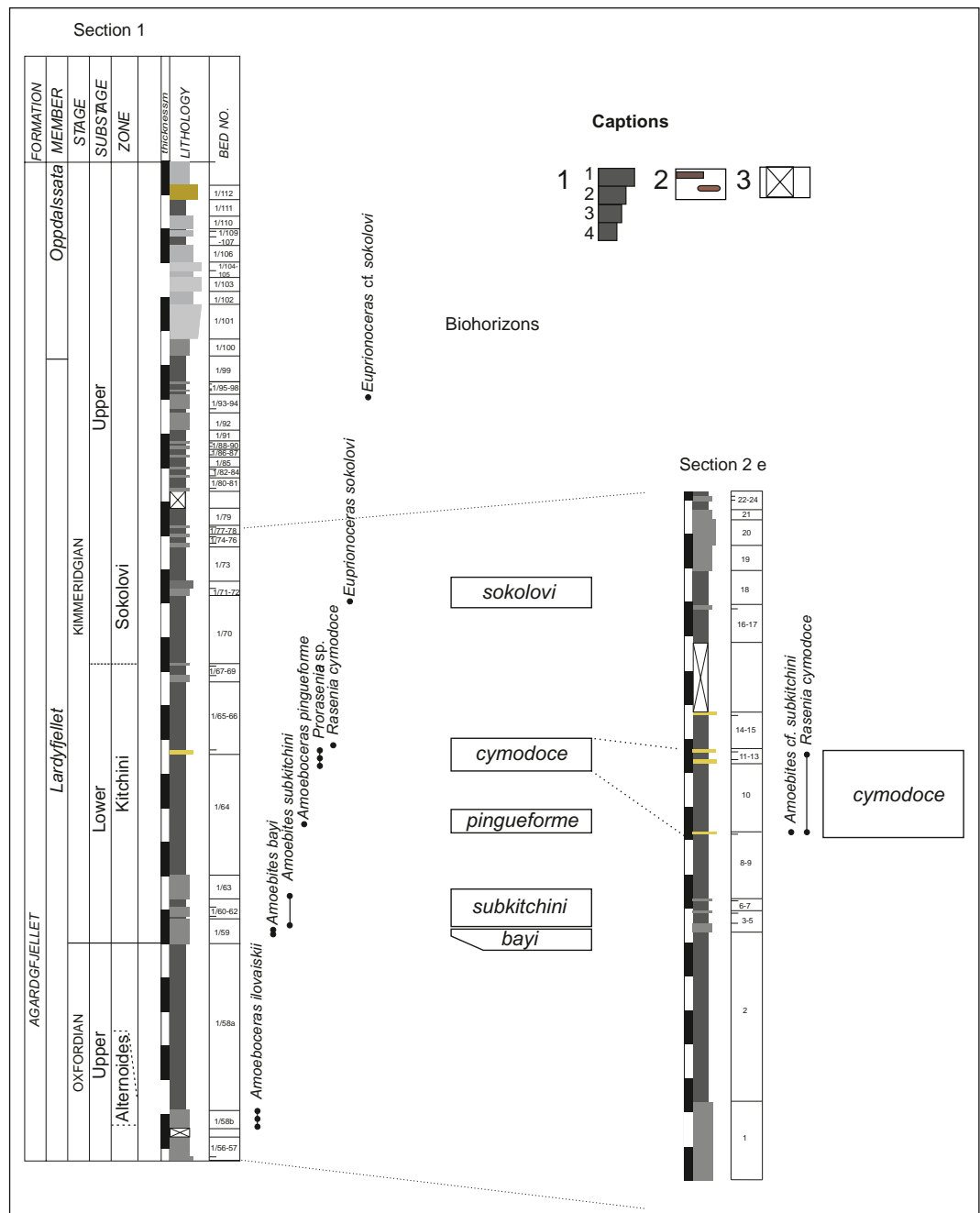
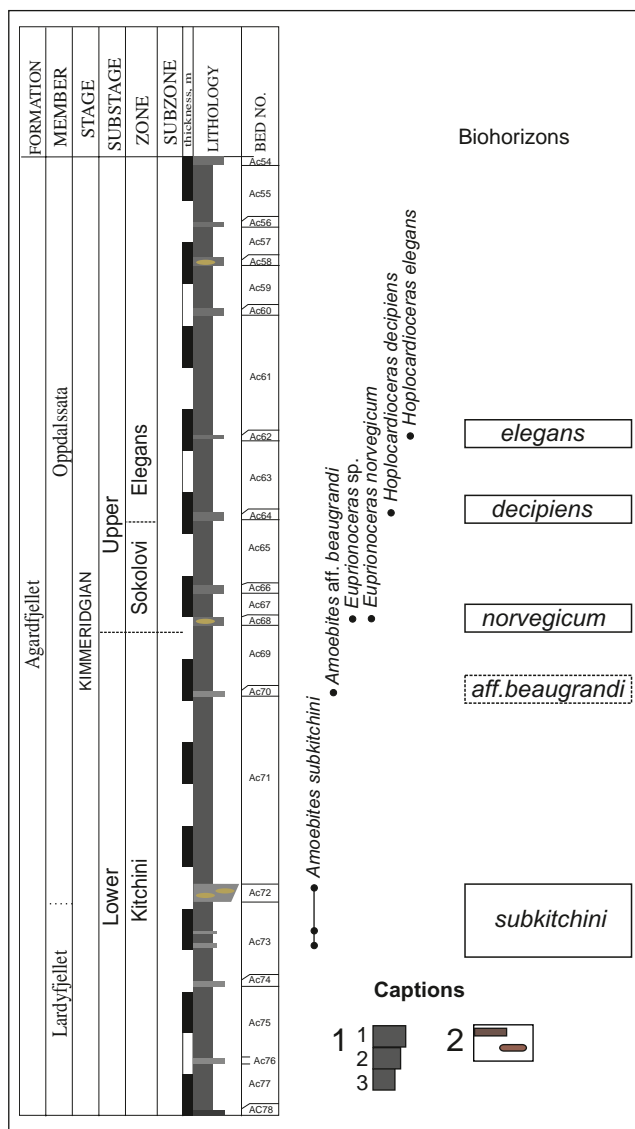


Figure 2. Kimmeridgian ammonite ranges, litho- and biostratigraphy of the Festningen sections 1 and 2e. 1 - thickness of beds in the log corresponding to the granulometric composition of rocks: (1) sandstones, (2) siltstone, (3) silty shale, (4) shale; 2 carbonate nodules (mainly dolomite), 3 gaps in observations.

Agardhfjellet Formation (Dypvik et al., 1991). The more coarse-grained Oppdalssåta Member is easily recognized in the Festningen section by the occurrence of thick sandstone bands, but in Myklegardfjellet it could only be tentatively recognized by the presence of relatively coarse-grained siltstone bands.

Ammonites studied in this investigation are currently curated in the Vernadsky State Geological Museum in Moscow (SGM...), in the VNIGRI Museum, Saint-Petersburg (VNIGRI...), CNIGR Museum, Saint-Petersburg (CNIGR...), Geological Museum of the University of Copenhagen (MGUH...) and in the Natural History Museum, London (NHM...).



**Figure 3.** Kimmeridgian ammonite ranges, litho- and biostratigraphy of the Myklegardfjellet section. 1 - thickness of beds in the log corresponding to the granulometric composition of rocks: (1) siltstone, (2) silty shale, (3) shale; 2 - carbonate nodules and bands (mainly dolomite).

## Ammonite succession and infrazonal biostratigraphy

The ammonite succession and preliminary zonal scheme is summarized below. The rarity of aulacostephanid ammonites and abundance of cardioceratids allows using cardioceratid-based zonal and infrazonal schemes (Wierzbowski and Smelror, 1993) and, in some cases only, the sub-Boreal aulacostephanid-based zonation (Table 1).

### Lower Kimmeridgian

#### *Bauhini* Zone

Ammonites typical of this interval, were absent in both studied sections, but were recognized previously by Ershova (1983), who figured *Plasmatites bauhini* (Opp.) (Ershova 1983, pl.V, fig.7, refigured here: Fig. 4.2) from Van Keulenfjorden. *Pictonia* (*Pictonia*) sp. from Spath's collection (Fig. 4.1) could be also assigned to this zone or, alternatively, to the overlying *bayi* horizon of the *Kitchini* Zone.

#### *Kitchini* Zone

This zone is well-recognized based on the range of *Amoebites* sensu stricto. Aulacostephanid ammonites (*Rasenia cymodoce* (d'Orb.) and corresponding microconchiate *Prorrasenia*) occur within a relatively narrow interval within the zone. The upper boundary of the *Kitchini* Zone closely coincides with upper boundary of the *Mitabilis* Zone in Subboreal succession. Subdivision of the *Kitchini* Zone in 3 subzones, proposed by Wierzbowski and Rogov (2013) is used here.

#### *Bayi* Subzone

*Bayi* horizon: *Amoebites bayi* (Birkelund & Callomon) has been recognized at Festningen section (Figs. 4.3-4).

#### *Subkitchini* Subzone

*Subkitchini* horizon: This subzone is well-exposed at Janusfjellet section (Wierzbowski, 1989) as well as at Myklegardfjellet (Figs. 4.6-7). At Festningen, small-sized *Amoebites subkitchini* (Spath) with looped ribs (Fig. 4.5, comparable with records from the East Taimyr, Fig. 4.9) appear directly above *A. bayi*. A small ammonite with narrow umbilicus, found above the figured specimen (Fig. 4.8), could be assigned to fine-ribbed variety of this species. There are some uncertainties regarding the full range of the *A. subkitchini* species, which co-occurs with *Rasenia cymodoce* in East Greenland (Birkelund and Callomon, 1985) and (at least *A. ex. gr. subkitchini*) in Spitsbergen. Earliest forms of *A. subkitchini* are characterized by a narrower umbilicus and could be compared with *A. alticarinatum* (Mesezhnikov & Romm). In Spitsbergen, the range of *A. subkitchini* possibly overlaps with the ranges of coarse-ribbed small-sized *A. mesezhnikovii* and *A. pingueforme* species.

**Table 1.** Kimmeridgian ammonite zonation of Spitsbergen (preliminary) and East Greenland.

Subboreal zonation	East Greenland horizons (cardioceratid horizons were chosen when possible, succession after Birkelund, Callomon, 1985)	Spitsbergen horizons (letters indicates sections: M - Myklegardfjellet, F - Festningen, J - Janusfjellet (Wierzbowski, 1989))	Franz-Josef Land horizons (based on data published by Shulgina, 1960; Mesezhnikov, Shulgina, 1982; Repin et al. 2007)	Boreal zonation
Aulacostephanus autissiodorensis	Aulacostephanus cf. kirghisensis			Suboxydiscites taimyrensis
Aulacostephanus eudoxus	Hoplocardioceras elegans	Hoplocardioceras elegans	Hoplocardioceras elegans	Hoplocardioceras decipiens
	Hoplocardioceras decipiens	Hoplocardioceras decipiens	Hoplocardioceras decipiens	
Aulacostephanoides mutabilis	Amoebites kochi	Euprionoceras sokolovi	Euprionoceras sokolovi	Euprionoceras sokolovi
	Aulacostephanoides mutabilis	Euprionoceras norvegicum		Amoebites kitchini
	Amoebites cf. beaugrandi	Zenostephanus sachsi	Zenostephanus sachsi	
	Amoebites aff. beaugrandi			
Rasenia cymodoce	Amoebites aff. rasenense	Rasenia cymodoce		Amoebites kitchini
	Amoebites aff. subkitchini	Amoebites pingueforme		
	"Pachypictonia"	Amoebites mesezhnikovi		
	Amoebites subkitchini	Amoebites subkitchini	Amoebites subkitchini	
Pictonia baylei	Amoebites bayi	Amoebites bayi		Plasmatites bauhini

*Mesezhnikovi* horizon: recognized at Janusfjellet by Wierzbowski (1989), characterized by *Amoebites mesezhnikovi* (Sykes & Surlyk).

*Pingueforme* horizon: Firstly recognized at Janusfjellet (Wierzbowski, 1989) as *Rasenia cymodoce* - *Amoebites pingueforme* horizon and also recognized at Festningen by the presence of *Amoebites pingueforme* (Mesezhn.). Additional specimens of *A. pingueforme* from other parts of Spitsbergen were also figured by Ershova (1983). A photo of a previously unpublished specimen of *A. pingueforme* from Van Keulenford is given here (Fig. 4.12). At Festningen the ranges of coarse-ribbed *A. pingueforme* (Figs. 4.10-11) and aulacostephanids, assigned to *Rasenia cymodoce*, do not overlap in contrast to Janusfjellet, where their ranges coincide. Perhaps the ranges of *R. cymodoce* and *A. pingueforme* horizons overlap only partially and thus it may be possibly to recognize two concurrent biohorizons, based on different lineages. Birkenmajer et al. (1982) also mentioned *Rasenia cymodoce* (figured as *R. evoluta* and later re-determined by Wierzbowski, 1989) from the Myklegardfjellet section, but neither *Amoebites pingueforme* nor *Rasenia* were found during the studies of the same section undertaken by the current author.

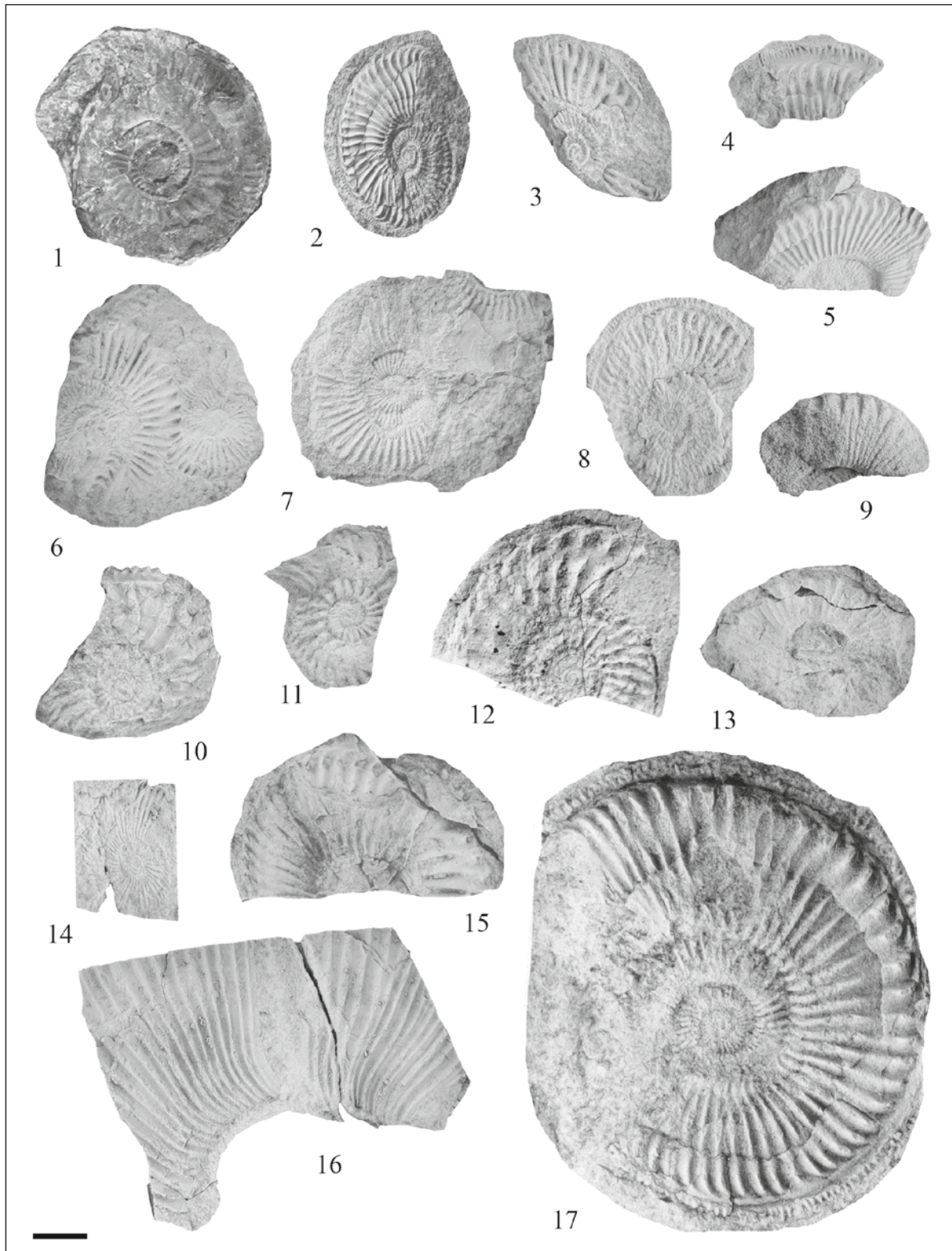
*Cymodoce* horizon: *Rasenia cymodoce* (d'Orb.) and corresponding *Prorasenia* microconchs are among the most common aulacostephanid ammonites in the Kimmeridgian of Spitsbergen (Figs. 5.1-4). The occurrence of these ammonites is restricted to a narrow interval, within which they are relatively abundant. In some cases other ammonites are absent, for instance

section 1A in Wierzbowski (1989), and interval between uppermost part of the bed 1/64 and lower part of the bed 1/66 in Festningen. Such a brief migrational event could be caused by short-term climate oscillation and/or palaeogeographical changes. It should also be noted that full-grown macroconchs of *Rasenia cymodoce* (d'Orb.) from Spitsbergen (Figs. 5.1-2) are characterized by a ribbed body chamber, while typical smooth bodied forms of *R. cymodoce* (d'Orb.) are unknown here. Specimens from Spitsbergen resemble *R. evoluta* Spath in this respect but are distinguishable by more involute whorls and the usual occurrence of relatively smooth middle whorls. Such ribbed morphotypes of *R. cymodoce* (d'Orb.) co-occur with typical specimens of this species in East Greenland (Birkelund and Callomon, 1985, pl.17, fig.2). In addition to aulacostephanids, *Amoebites* ex gr. *subkitchini* (Spath) also occurs in this horizon (Fig. 5.5). It is notable, that aulacostephanids occur only sporadically in Franz-Josef Land as well as in Spitsbergen, but *Rasenia cymodoce* (d'Orb.) is absent in Franz-Josef Land. Instead this region is characterized by records of *Rasenia inconstans* Spath (Mesezhnikov and Shulgina, 1982, pl.1, fig.6, pl.2, fig.3), which is typical of the underlying biohorizon in East Greenland (Birkelund and Callomon, 1985).

#### Modestum Subzone

The provisional *Amoebites* aff. *beaugrandi* biohorizon is tentatively recognized at Myklegardfjellet, where a single poorly preserved specimen of *A. aff. beaugrandi* (Sauvage et Rigoux) was recovered a few beds above the level with numerous *A. subkitchini* (Fig. 5.6). The stratigraphical range of this taxon is similar to that of *A. aff. beaugrandi*





**Figure 4.** Scale bar = 1 cm (as well as in Figs. 5, 6, 8). 1. *Pictonia* (*Pictonia*) sp., NHM C26969, Festningen, Lower Kimmeridgian, collected by Dr. J.W. Gregory (1896), mentioned by Spath (1921); 2. *Plasmatites bauhini* (Opp.), CNIGR 32/12210, Van Keulenford, collected by Pchelina (1979), figured by Ershova, 1983, pl. IV, fig. 7; 3-4 - *Amoebites bayi* (Birkelund et Callomon), Festningen, bayi horizon, 3 - SGM-1409-23/10356, 0.7 m above the base of bed 1/59; 4 - SGM-1409-24/10357, 0.5 m above the base of bed 1/59; 5-9. *Amoebites subkitchini* (Spath), subkitchini horizon, 5 - SGM-1409-05/10338, Festningen, 1 m above the base of bed 1/59; 6-7. SGM MK2776 (fig. 6), SGM-1409-49/10382 (fig. 7), Myklegardfjellet, 2 m below the top of the bed AC73; 8 - SGM-1409-12/ 10345, Festningen, 0.2 m above the base of the bed 1/63; 9 - SGM MK43, Chernokhrebnaya river, East Taimyr, collected by V. Egorov, 2006; 10-12. *Amoebites pingueforme* (Mesezhn. et Romm), pingueforme horizon; 10-11. Festningen, 3 m below the top of the bed 1/64, 10 - SGM-1409-11/10344; 11 - SGM-1409-04/10337; 12 - specimen lost, Duner Bay, collected by M. Burdykina, 1988; 13. *Euprionoceras* cf. *sokolovi* (Bodylevski), SGM-1409-25/10358, Festningen, bed 1/94, Sokolovi Zone; 14-17. *Euprionoceras sokolovi* (Bodylevski), sokolovi horizon, 14-16. Festningen, 0.5 m below the top of the bed 70, 14 - SGM-1409-17/10350, 15 - SGM-1409-16/10349, 16 - SGM-1409-15/10348; 17 - CNIGR 77/12210, Van Keulenford, figured by Ershova, 1983, pl.XII, f4.



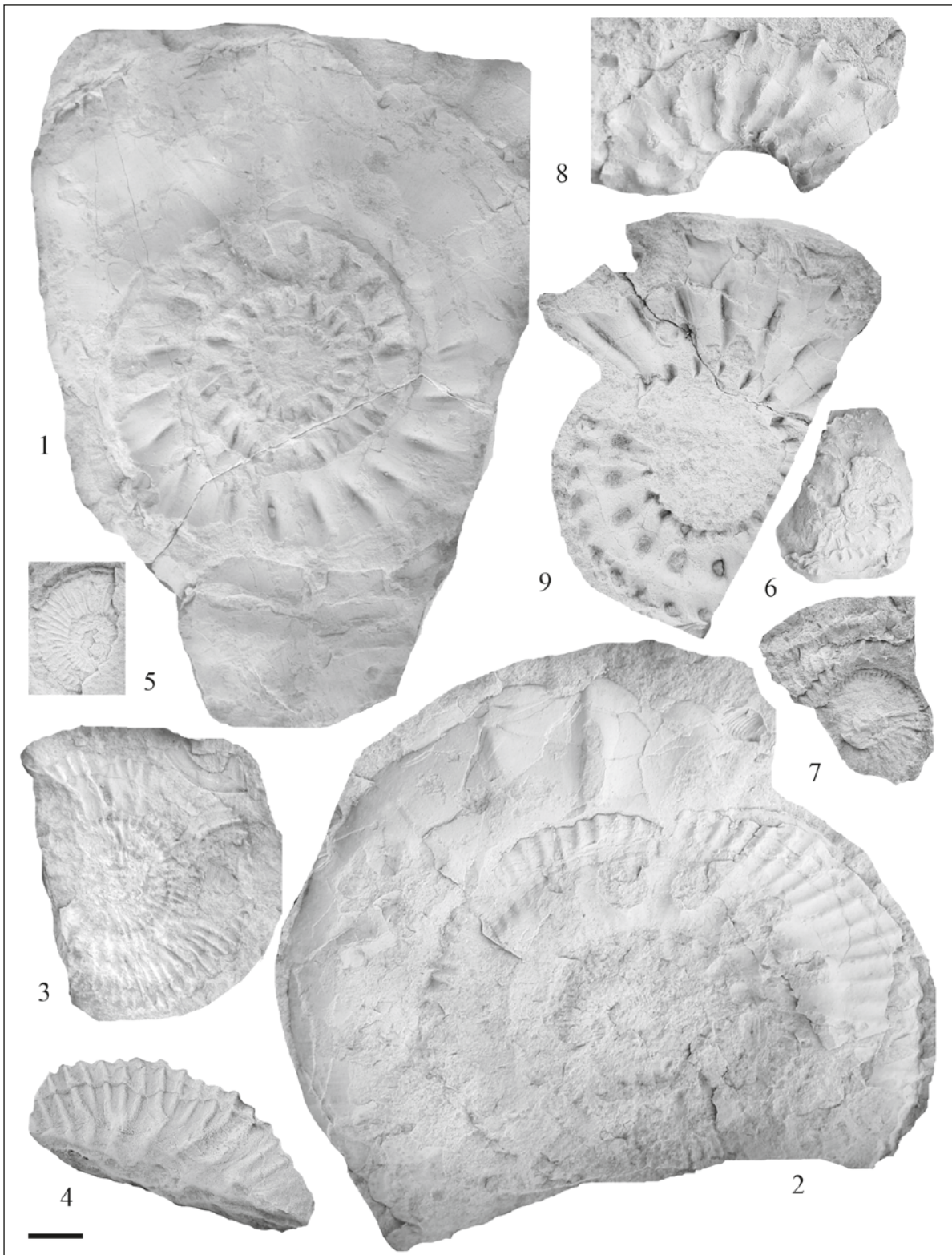


Figure 5.1-2. *Rasenia cymodoce* (d'Orb.) [M], *Festningen*, cymodoce horizon; 1 – SGM-1409-22/10355, bed 2E/9; 2 – SGM-1409-01/10334, bed 2E/13; 3-4. *Prorasenia* sp. [m], *Festningen*, cymodoce horizon; 3 – SGM-1409-14/10347, 0,7 m below top of the bed 1/64; 4 – SGM-1409-02/10335, bed 1/65; 5. *Amoebites* cf. *subkitchini* (Spath), SGM-1409-18/10351, *Festningen*, bed 2E/9, cymodoce horizon; 6. *A. aff. beaugrandi* (Savauge et Rigaux), SGM-1409-45/10378, *Myklegardfjellet*, bed AC70, aff. *beaugrandi* horizon; 7. *Euprionoceras norvegicum* (Wierzbowski), SGM-1409-29/10362, *Myklegardfjellet*, bed AC68, *norvegicum* horizon; 8-9. *Hoplocardioceras decipiens* (Spath), *Myklegardfjellet*, bed AC64, *decipiens* horizon, 8 – SGM-1409-51/10384, 9 – SGM-1409-46/10379.

(Sauvage & Rigoux) from East Greenland (Birkelund and Callomon, 1985, pl.4, fig. 6-8), however, the latter ammonites are characterized by more dense and regular ribbing. Thus the precise stratigraphical relationship between the “*aff. beaugrandi*” horizon of East Greenland and the level with *A. aff. beaugrandi* in Spitsbergen remains still uncertain but may be closely correlatable. Anyway these records marked older stratigraphical level compared with those of true *Hoplocardioceras beaugrandi* (Sauvage et Rigoux) which came from the *Eudoxus* Zone, and “*A. aff. beaugrandi*” from East Greenland and Spitsbergen should be ascribed to new species.

The precise position of the provisional *Xenostephanus* (= *Zenostephanus sachsii*, corrected) horizon proposed by Wierzbowski (1989) is uncertain, because although *Zenostephanus* (including species *Z. sachsii*, which is widely ranged in Arctic) are known from Spitsbergen (Fig. 6.6), these ammonites were collected by our precursors during the geological survey and their precise stratigraphic position within the succession is unclear. During 2012 new records of *Zenostephanus* at Sassenfjord were made by our colleagues, directly above the *Rasenia* occurrences. The same level, characterized by *Zenostephanus sachsii* in Franz-Josef Land (Repin et al., 2007, pl. XII, fig.1-2, pl.XIII, fig. 1,3,4; pl.XIV, fig.1,2,4,5) has been recently recognized as the “*Sachsii* Zone” (Repin et al., 2007), but this “zone” has been erected without reference to its type section and biostratigraphical characteristics, and is presented in the correlation chart only. In this author’s opinion, this unit may be comparable with the *Zenostephanus* horizon of Spitsbergen, and *Z. sachsii* (Fig. 6.6) could be used as its index species.

#### Sokolovi Zone

The *Sokolovi* Zone (proposed by Spath, 1935 as *Kochi* Zone) corresponds to the total range of the *Euprionoceras*. Its correlation with sub-Boreal aulacostephanid zonation still remains unclear. All known records of cardioceratids typical of this zone were known until now from the levels between records of *Aulacostephanus* of the *A. mutabilis* group and *Aulacostephanus* of the *A. eudoxus* (Birkelund and Callomon, 1985; Wierzbowski et al., 2002) or from the *Eudoxus* Zone (Mesezhnikov in Sachs, 1969). Recently, specimens of *Euprionoceras sokolovi* (Bodylevski) were recorded in the *Eudoxus* Zone of the Middle Volga area (Rogov and Shchepetova, 2011), but the full range of *Euprionoceras* in terms of sub-Boreal zonation still remains unclear.

*Norvegicum* horizon. *Euprionoceras norvegicum* (Wierzbowski) was designated as the marker species of a separate horizon of the Barents Sea Kimmeridgian (Wierzbowski and Smelror, 1993) recently reclassified as a subzone (Wierzbowski et al., 2002). This distinctive species is characterized by weakly ribbed inner whorls which became strongly ribbed on the outer whorls.

The presence of this horizon at Spitsbergen could be inferred on the basis of presence of *E. norvegicum* at the Myklegardfjellet section (Fig. 5.7), where it co-occurs with poorly preserved specimens of coarse-ribbed cardioceratid ammonites (*Euprionoceras* sp.)

*Sokolovi* horizon: *Euprionoceras sokolovi* (Bodylevski), considered here as senior synonym of the *E. kochi* (see Birkelund and Callomon, 1985; Wierzbowski and Rogov, 2013), is a very characteristic ammonite for Spitsbergen. A few specimens of this species have been collected at the Festningen section (Figs. 4.13-16) and more specimens were found in collections of VNIIOkeangeologiya (Saint-Petersburg) (Fig. 4.17).

#### Decipiens Zone

In the Boreal zonal succession of the Kimmeridgian Stage this zone is usually referred to as the *Elegans* Zone, as has been proposed by Wierzbowski (in Wierzbowski and Smelror, 1993). However, Spath (1935) previously recognized *Decipiens* assemblage (based on the other species of *Hoplocardioceras*) in highest part of Boreal Kimmeridgian. Thus the *Decipiens* Zone has a priority over the *Elegans* Zone. Previously, Wierzbowski (1989) based on his observations at Janusfjellet, suggested that in Spitsbergen the *decipiens* and *elegans* horizons, which are recognized in East Greenland, cannot be distinguished. Ammonites are rare in the upper part of the Kimmeridgian of the Festningen section, only a few ammonites resembling *Euprionoceras sokolovi* has been found here (Fig. 4.13). But at the Myklegardfjellet section late *Hoplocardioceras elegans* (Spath) (= *H. bodylevskii* (Schulgina)) occurs in the uppermost fossiliferous horizon within the Kimmeridgian ammonite succession and is clearly separated from band with *Hoplocardioceras decipiens* (Spath) which is located some 3.5 m below. These horizons are also clearly separated in the sub-Boreal succession of the Middle Volga area. Alternatively, the co-occurrence of both morphotypes of *Hoplocardioceras* within a narrow fossiliferous band (Wierzbowski, 1989; Birkenmajer and Wierzbowski, 1991, see above) suggests their ranges overlap. In Franz-Josef Land, Shulgina (1960) recognized a similar ammonite succession, with *H. decipiens* and *H. elegans* (= *bodylevskii* Schulgina) below and only *H. elegans* above (Figs. 6.4-5). Records of *H. elegans* and *H. decipiens* in reversed succession has been reported by Wierzbowski (in Wierzbowski and Smelror, fig.3, 5) from the Barents Sea cores 7227/08-U-03 and 7231/01-U-01, but in my opinion figured *H. elegans* (Spath) (loc.cit., pl.2, fig.9-12), characterized by absence of looped and rursiradiate ribs and presence of elongated secondaries seems to be more close to *E. sokolovi* (Bodylevski).

*Decipiens* horizon: typical specimens of *Hoplocardioceras decipiens* (Spath) were recognized from the bed AC64 at Myklegardfjellet (Figs. 5.8-9). This species is also known from the other sites of Spitsbergen.



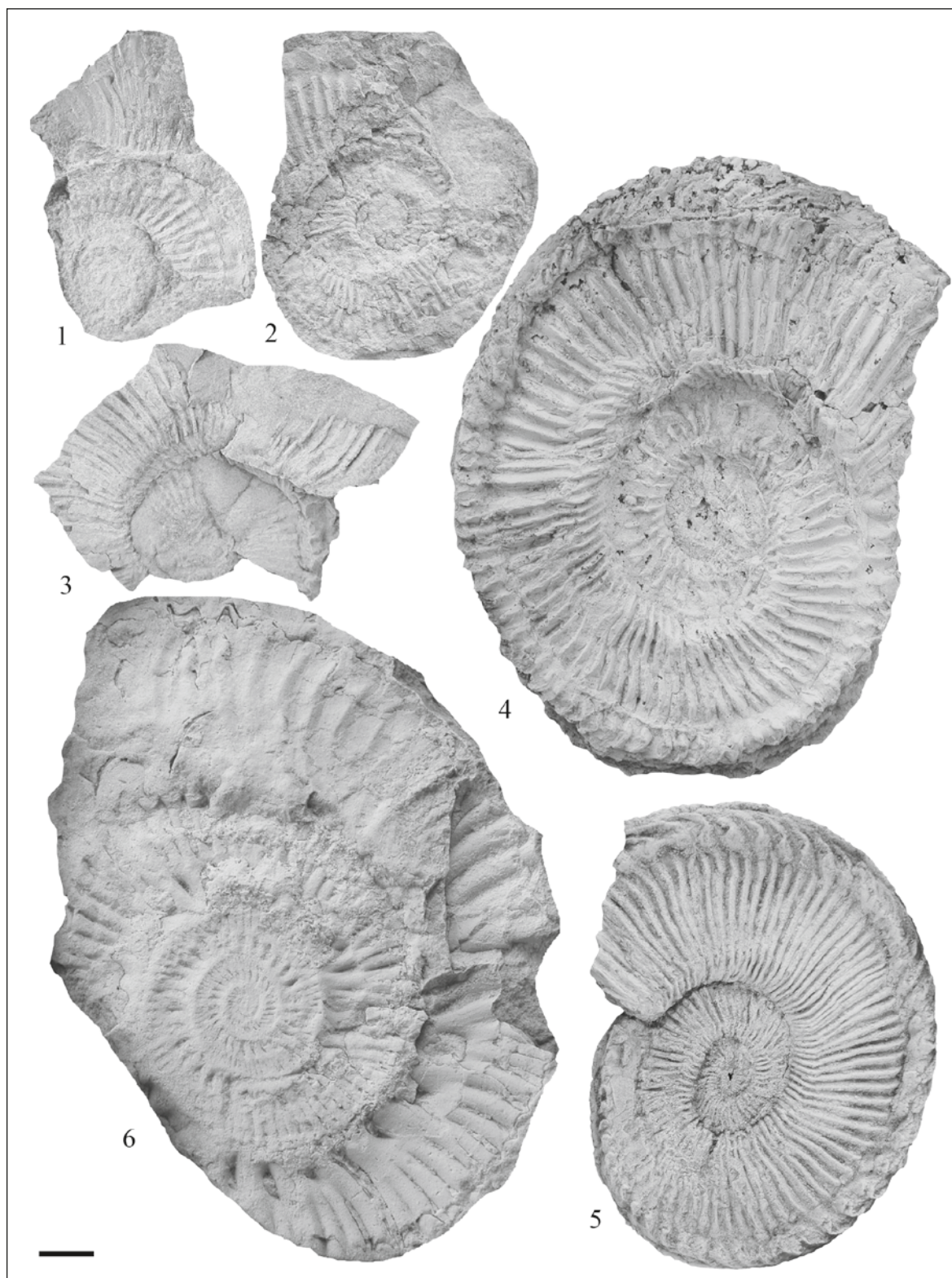


Figure 6.1-5. *Hoplocardioceras elegans* (Spath), *elegans* horizon; 1-3. Myklegardfjellet, bed AC/62, 1 – SGM-1409-41/10374, 2 – SGM-1409-48/10381, 3 – SGM-1409-27/10360; 4-5. Franz-Josef Land, Wilczek Land, Cape Hanza, 4 – SGM-1392-08/10327 (= *Amoeboceras* (*Amoebites*) *bodylevskii* sp. nov. var. nov.: Shulgina, 1960, pl. IV, fig. 2). 5 – SGM 652p/448 (= holotype of *Amoeboceras* (*Amoebites*) *bodylevskii* Shulgina: Shulgina, 1960, pl. IV, fig. 1); 6. *Zenostephanus sachsii* (Mesezhn.) SGM-1409-30/10363, Spitsbergen, precise locality unknown, *sachsii* horizon.

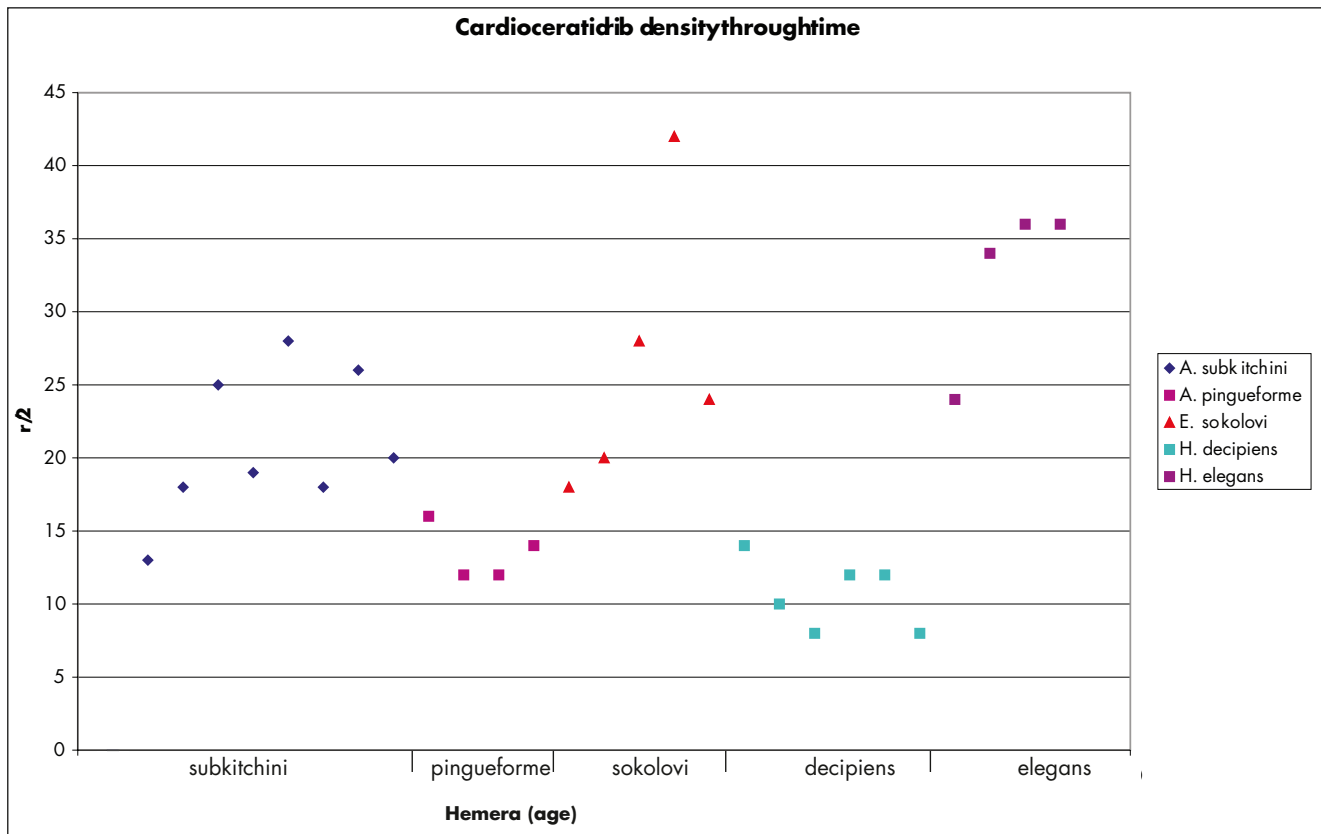


Figure 7. Oscillations in rib density through time within Kimmeridgian cardioceratid lineage of Spitsbergen.

*Elegans* horizon: *Hoplocardioceras elegans* (Spath) characterizes the uppermost fossiliferous level in the Kimmeridgian of Myklegardfjellet (Figs. 6.1-3).

Interestingly, through the Kimmeridgian cardioceratid succession recognized in Spitsbergen, changes of fine and densely ribbed taxa to those with rare and relatively thick ribbing and back occurs few times (Fig. 7). Such oscillations in development of one feature through evolution of the lineage have been recognized recently in cardioceratids from the Bathonian/Callovian boundary beds (Kiselev and Rogov, 2007).

#### Taimyrensis Zone

The Boreal oppeliid ammonite *Suboxydiscites taimyrensis* (Mesezhn.), is restricted in the Arctic to the uppermost zone of the Kimmeridgian. In the type succession in the Kheta depression the lower boundary of this zone is recognized by the disappearance of aulacostephanids. Cardioceratid ammonites from this zone in north Central Siberia were not figured or described and are missing in Mesezhnikov's collection. But taking into account the presence of *Hoplocardioceras* and *Nannocardioceras* in the lower part of zone (Mesezhnikov, 1984), at least a partial overlap of this zone with *Decipiens* Zone could be suggested. The upper part of *Taimyrensis* Zone lacks cardioceratids and is closely comparable to the *Autissiodorensis* Zone, which is characterized by

cardioceratid ammonites in the two lowermost horizons only (Rogov, 2010a). This conclusion is further supported by rare occurrences of *Suboxydiscites* in the *Fallax* Subzone of the *Autissiodorensis* Zone (Rogov, 2010a). It should be noted that the genus *Suboxydiscites*, as has been shown recently, ranged through the whole Kimmeridgian Stage and its successive species are very poorly known. Studying of the Ershova's collection revealed presence of few *Suboxydiscites* cf. *taimyrensis* (Mesezhn.) (Fig. 8.1), but their precise position within the succession remains unclear. *Suboxydiscites* is the single example of a true Boreal genus among oppeliids, which probably originated from sub-Mediterranean *Ochetoceras* (Rogov, 2001). Oppeliids occasionally inhabited Arctic regions during the Middle Jurassic, but these were short-time migrations which did not lead to the existence of endemic lineage. The oldest *Suboxydiscites* are known from the Upper Oxfordian of East Greenland (based on re-examination of an undescribed collection stored in CASP, Cambridge). Typical macroconchs, resembling *S. taimyrense* by shell coiling, but with a slightly wider umbilicus, weaker ribbing and smaller size, are known from the basal Kimmeridgian (*bauhini* horizon) of Swabia, where they co-occur with other ammonites of Boreal and sub-Boreal origin (Schweigert and Jantschke, 2001). These ammonites should be described as a new species. Lower Kimmeridgian *Suboxydiscites* were also recorded recently from Northern Siberia (Rogov and Wierzbowski, 2009),



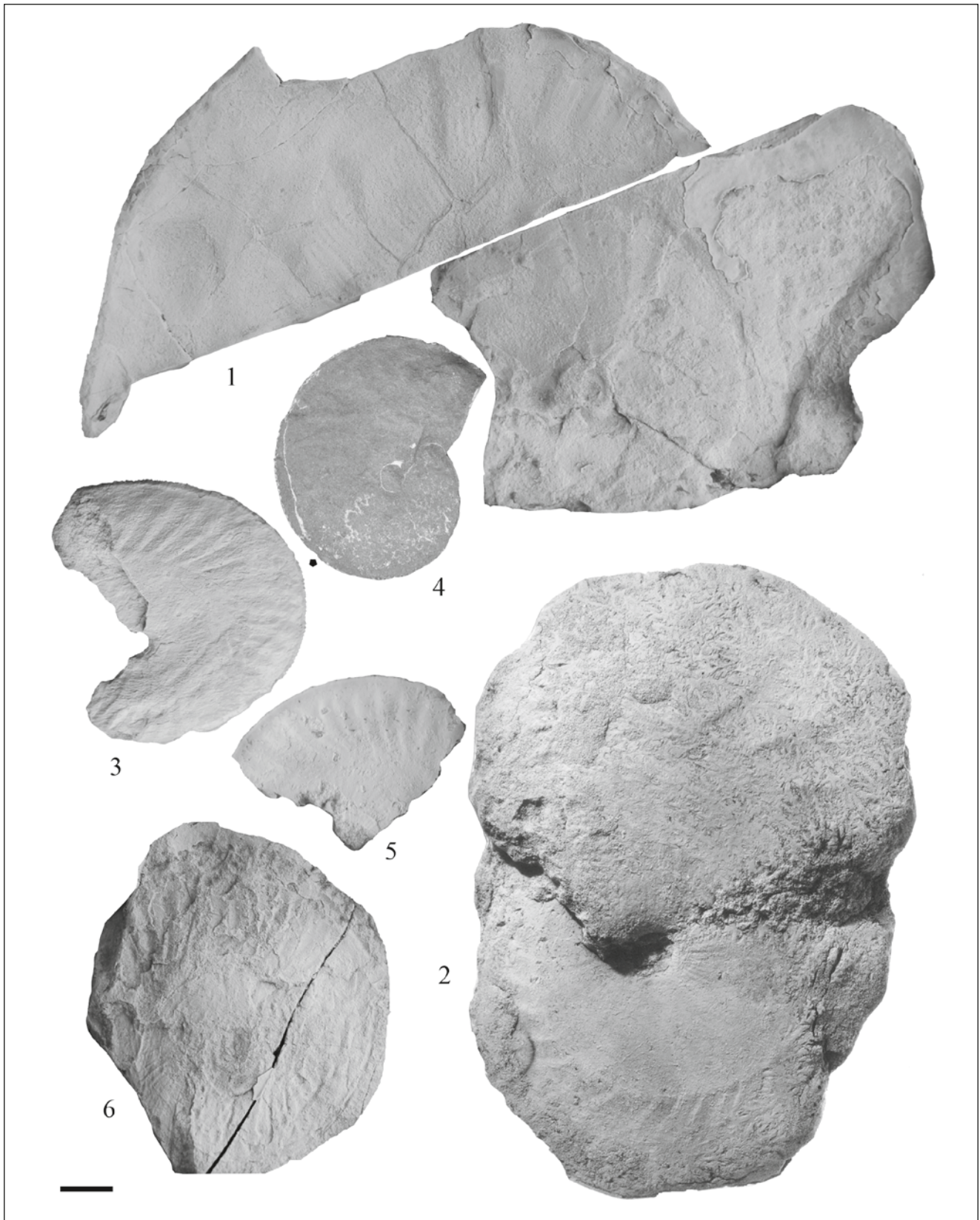


Figure 8.1. *Suboxydiscites cf. taimyrensis* (Mesezhn.) [M], SGM-1409-39/10372, Upper Kimmeridgian, Sørkapp Land, collected by E.S. Ershova in 1965; 2, 5. *Suboxydiscites taimyrensis* (Mesezhn.) [M], Eudoxus or Autissiodorensis Zone, Pechora area, left bank of the Pizhma river near Vyartkina spring; 2 – SGM MIV237, 5 – SGM-1409-66/10399 inner whorls of macroconch; 3. *Suboxydiscites* sp. [m], VNIGRI (specimen without number), Taimyrensis Zone, Malaya Podkamennaya river, East Taimyr, collected by M.S. Mesezhnikov; 4. *Suboxydiscites* sp. [m], MGUH 14348; East Greenland, Section 32, beds with fauna 19, Cardioceraskøft Member, Mutabilis Zone, black dot indicated beginning of the body chamber (=Streblites? (Oxydiscites?) cf. *taimyrensis* Mesezhnikov (m) in Callomon and Birkelund, 1980, pl.3, fig.5; Streblites? cf. *S. taimyrensis* in Birkelund and Callomon, 1985, fig.7); 6. *Suboxydiscites* sp. [m], SGM-1409-19/10352, Upper Kimmeridgian, Sørkapp Land, collected by E.S. Ershova.



but are typically badly preserved. Upper Kimmeridgian *Suboxydiscites* have a wide geographical distribution through the Arctic. They are known from the entire Upper Kimmeridgian of Northern Siberia (Sachs et al., 1969) and from the *Eudoxus-Autissiodorensis* zones of the north of European part of Russia (Mesezhnikov, 1984) and Middle Volga area (Rogov, 2010a). Additionally, microconchiate populations are known from the Upper Kimmeridgian of the Russian Far East (*S. elgense* (Chudoley & Kalacheva)), British Columbia (*S. manningense* (Poulton, Zeiss & Jeletzky)) and East Greenland (“*Streblites?* (*Oxydiscites?*) cf. *taimyrensis* Mesezhnikov (m)” in Callomon and Birkelund, 1980; Birkelund and Callomon, 1985). Through the evolution of the both micro- and macroconchs of *Suboxydiscites* their ribbing became more coarse and regular. Ribbing is unclear in early macroconchs (Schweigert and Jantschke, 2001, fig. 2-3) and microconchs from the *Mutabilis* Zone and (Callomon and Birkelund, 1980, pl.3, fig.5 a,b, refigured here in Fig. 8.4) but became well-revealed and regular in *Suboxydiscites* during the latest Kimmeridgian (Figs. 8.1-3, 5-6).

## Some biogeographical remarks

Spitsbergen is a key region for understanding the peculiarities of the faunal exchange through Greenland-Norwegian Seaway (GNS) during the Kimmeridgian. As has been demonstrated recently from analysis of ammonite latitudinal diversity gradient and presence of sub-Boreal/sub-Mediterranean faunal elements in Boreal faunal associations, Middle Russian Sea influence over the Arctic was of great importance, while Greenland-Norwegian Seaway was of minor significance (Rogov, 2012). Kimmeridgian assemblages of both East Greenland and the Norwegian Sea (Birkelund and Callomon, 1985; Wierzbowski et al., 2002) consist of a mixture of the Boreal cardioceratids and sub-Boreal aulacostephanids. The latter ammonites became rare in the Spitsbergen, Barents Sea shelf and Franz-Josef Land. Two well-recognized levels containing aulacostephanids recognized in Spitsbergen (*cymodoce* and *sachsi* horizons) perhaps can also be traced through the Barents Sea region, because both *Rasenia* and *Zonovia* are known from Barents Sea cores (Shulgina and Burdykina, 1992). Mutterlose et al. (2003) suggested that the Greenland-Norwegian Seaway during the Late Jurassic was relatively shallow and only became deeper in the Valanginian-Hauterivian. This interpretation corresponds well with the peculiarities of ammonite distribution around this seaway. It is possible that during the Late Jurassic ammonite migration through the Greenland-Norwegian Seaway were very restricted and mainly southward in direction, providing penetration of Boreal faunas to NW Europe. The appearance of aulacostephanids in Svalbard and Barents Sea shelf could be related to a brief migrational event from the Middle Russian Sea, coinciding with a warming climate. In the Middle Volga

area and Kostroma region this warming is marked by appearance of sub-Mediterranean ammonites, especially aspidoceratids.

### Acknowledgements.

This study has been supported by RFBR grant 12-05-00380 and Earth Science Division of RAS Program no.1. This is the part of the project “Late Mesozoic-Cenozoic tectono-magmatic history of the Barents Sea shelf and slope as a clue to paleodynamic reconstructions in the Arctic Ocean”. The author also expresses his thanks to colleagues who helped him during the field trip held at Spitsbergen and to those who help with access to collections in museums (Drs. S. Nikolaeva, A. McGowan, NHM London; A.R. Sokolov, CNIGR Museum, V.A. Basov, G.A. Cherkashov, VNIIOkeangeologiya, T.V. Dmitrieva, V.V. Bystrova, VNIGRI, Saint-Petersburg; P. Alsen, Geological Museum of the University of Copenhagen, S.R.A. Kelly, CASP, Cambridge).

## References

- Birkelund, T. & Callomon, J.H. 1985: The Kimmeridgian ammonite faunas of Milne Land, central East Greenland. *Grønlands Geologiske Undersøgelse Bulletin*, 153, 1–56.
- Birkenmajer, K., Pugaczewska, H. & Weirzbowski, A. 1982: The Janusfjellet Formation (Jurassic-Lower Cretaceous) at Myklegardfjellet, east Spitsbergen. *Palaeontologia Polonica*, 43, 107-140.
- Birkenmajer, K. & Wierzbowski, A. 1991: New Kimmeridgian ammonite fauna from east Spitsbergen and its phyletic significance. *Polar Research*, 9, 169-179. doi: 10.1111/j.1751-8369.1991.tb00612.x
- Callomon, J.H. & Birkelund, T. 1980: The Jurassic transgression and the mid-late Jurassic succession in Milne Land, central East Greenland. *Geological Magazine*, 117, 211-226. doi: 10.1017/S0016756800030442
- Dypvik, H., Nagy, J., Eikeland, T.A., Backer-Owe, K., Andresen, K., Haremo, P., Bjærke, T., Johansen, H. & Elverhøi, A. 1991: The Janusfjellet Subgroup (Bathonian to Hauterivian) on central Spitsbergen: a revised lithostratigraphy. *Polar Research*, 9, 21-43. doi: 0.1111/j.1751-8369.1991.tb00400.x
- Ershova, E.S. 1983: *Explanatory notes for the biostratigraphical scheme of the Jurassic and Lower Cretaceous deposits of Spitsbergen archipelago*. Leningrad, PGO Sevmorgeologia, 88 pp. (In Russian).
- Frebold, H. 1928: Das Festnungsprofil auf Spitzbergen. Jura und Kreide. II. Die Stratigraphie. *Skrifter om Svalbard og Ishavet*, 19, 1-39.
- Frebold, H. 1930: Verbreitung und Ausbildung des Mesozoikums in Spitsbergen. *Skrifter om Svalbard og Ishavet*, 31, 1-127.
- Kiselev, D.N. & Rogov, M.A. 2007: Stratigraphy of the Bathonian-callovia boundary deposits in the Prosek Section (Middle Volga Region). Article 1. Ammonites and Infrazonal Biostratigraphy. *Stratigraphy and Geological Correlation*, 15, 485–515. doi: 10.1134/S0869593807050036
- Mesezhnikov, M.S., 1984: *Kimmeridgian and Volgian Stages of north of the USSR*. Leningrad, Nedra, 224 pp. (In Russian).
- Mesezhnikov, M.S. & Shulgina N.I. 1975: On ecology of Late Jurassic and Neocomian Boreal ammonites. *Institute of marine biology, collection of papers*, 4, 66-81. (In Russian).
- Mesezhnikov, M.S. & Shulgina, N.I. 1982: On the Kimmeridgian ammonites and new data on the stratigraphy of the north of USSR. *Soviet Geology and Geophysics*, 10, 20-29. (In Russian).
- Mutterlose, J., Brumsack, H., Flögel, S., Hay, W., Klein, C., Langrock, U., Lipinski, M., Ricken, W., Söding, E., Stein, R. & Swientek, O. 2003: The Greenland-Norwegian Seaway: a key area for understanding Late Jurassic to Early Cretaceous paleoenvironments. *Paleoceanography*, 18, 1, 1010. 26 pp. doi: 10.1029/2001PA000625

- Repin, Yu.S. Fedorova, A.A., Bystrova, V.V., Kulikova, N.K. & Polubotko, I.V. 2007: Mesozoic of the Barents sea sedimentological basin. In Kirichkova, A.V. & Dmitrieva, T.V. (eds.): *Stratigraphy and its role in development of the oil and gas complex of Russia*, 112-161. VNIGRI, Saint-Petersburg. (In Russian).
- Rogov, M.A. 2001: Phylogenetic relations within Jurassic Ocheteratinae (Ammonoidea, Oppeliidae). *Bulletin of Moscow Society of Naturalists, series geology*, 75, 5, 38-42. (In Russian).
- Rogov, M.A. 2010a: A precise ammonite biostratigraphy through the Kimmeridgian-Volgian boundary beds in the Gorodischi section (Middle Volga area, Russia), and the base of the Volgian Stage in its type area. *Volumina Jurassica VIII*, 103-130.
- Rogov, M.A. 2010b: New data on the Kimmeridgian ammonite biostratigraphy of Spitsbergen. *Earth Science Frontiers* 17, Special Issue, 94-95.
- Rogov, M.A. 2012: Latitudinal gradient of taxonomic richness of ammonites in the Kimmeridgian-Volgian in the Northern Hemisphere. *Paleontological Journal*, 46, 148-156. doi: 10.1134/S0031030112020104
- Rogov, M.A. & Shchepetova, E.V. 2011: New data on sedimentology and biostratigraphy of the Upepr Kimmeridgian Eudoxus Zone near the border of Ulianovsk region and Tatarstan. In Zakharov V.A., Rogov M.A., Ippolitov A.P. (eds.): *Jurassic System of Russia: Problems of stratigraphy and paleogeography. Fourth All-Russian meeting. September 26-30, 2011, St.-Petersburg. Scientific materials*. 186-189. Lema, Saint-Petersburg. (In Russian).
- Rogov, M. & Wierzbowski, A. 2009: The succession of ammonites of the genus *Amoeboceras* in the Upper Oxfordian – Kimmeridgian of the Nordvik section in northern Siberia. *Volumina Jurassica VII*, 147-156.
- Sachs, V.N. (ed.), 1969: *Fundamental section of the Upper Jurassic of Kheta river basin*. Leningrad, Nauka. 207 pp. (In Russian).
- Schweigert, G. & Jantschke, H. 2001: Erstnachweis von *Suboxydiscites* Poulton, Zeiss & Jeletzky (Ammonitina, Oppeliidae) im Schwäbischen Oberjura (Hauffianum-Subzone, bauhini-Horizont). *Neues Jahrbuch für Geologie und Paläontologie – Monatshefte*, 11, 659-668.
- Shulgina, N.I. 1960: Ammonites from the Franz-Josef Land and Taimyr and their significance for zonal subdivision of the Kimmeridgian in Arctic. *Transactions of the Institute of the Geology of Arctic*, 111, 136-144. (In Russian).
- Shulgina, N.I. & Burdykina, M.D. 1992: Biostratigraphical scheme of Jurassic and Lower Cretaceous of shelves of Barents, Norwegian and North seas. In *Geological history of Arctic in Mesozoic and Cenozoic. Volume 1*. Materials of lectures in memory of V.N. Sachs, 106-114. VNIOkeangeologia. Saint-Petersburg. (In Russian).
- Sokolov, D. & Bodylevsky, W. 1931: Jura- und Kreideformationen von Spitzbergen. *Skrifter om Svalbard og Ishavet*, 35, 1-151.
- Spath, L.F. 1921: On Ammonites from Spitsbergen. *Geological Magazine*, 58, 347-356. doi: 10.1017/S0016756800104662
- Spath, L.F. 1935: The Upper Jurassic invertebrate faunas of Cape Leslie, Milne Land. I. Oxfordian and Lower Kimmeridgian. *Meddelelser om Grønland*, 99 (2), 1-78.
- Wierzbowski, A., 1989: Ammonites and stratigraphy of the Kimmeridgian at Wimanfjellet, Sassenfjorden. Spitsbergen. *Acta Palaeontologica Polonica*, 34, 355-378.
- Wierzbowski, A. & Rogov, M. 2013: Biostratigraphy and ammonites of Middle Oxfordian to lowermost Upper Kimmeridgian in northern Central Siberia. *Russian Geology and Geophysics*, 54, 1083-1102. doi: 10.1016/j.rgg.2013.07.021
- Wierzbowski, A. & Smelror, M. 1993: Ammonite succession in the Kimmeridgian of southwest Barents Sea, and the *Amoeboceras* zonation of the Boreal Kimmeridgian. *Acta Geologica Polonica*, 43, 229-249.
- Wierzbowski, A., Smelror, M. & Mørk, A. 2002: Ammonites and dinoflagellate cysts in the Upper Oxfordian and Kimmeridgian of the northeastern Norwegian Sea (Nordland VII offshore area): biostratigraphical and biogeographical significance. *Neues Jahrbuch für Geologie und Paläontologie Abhandlungen*, 226, 145-164.



# Norwegian Petroleum Directorate BULLETIN No. 11

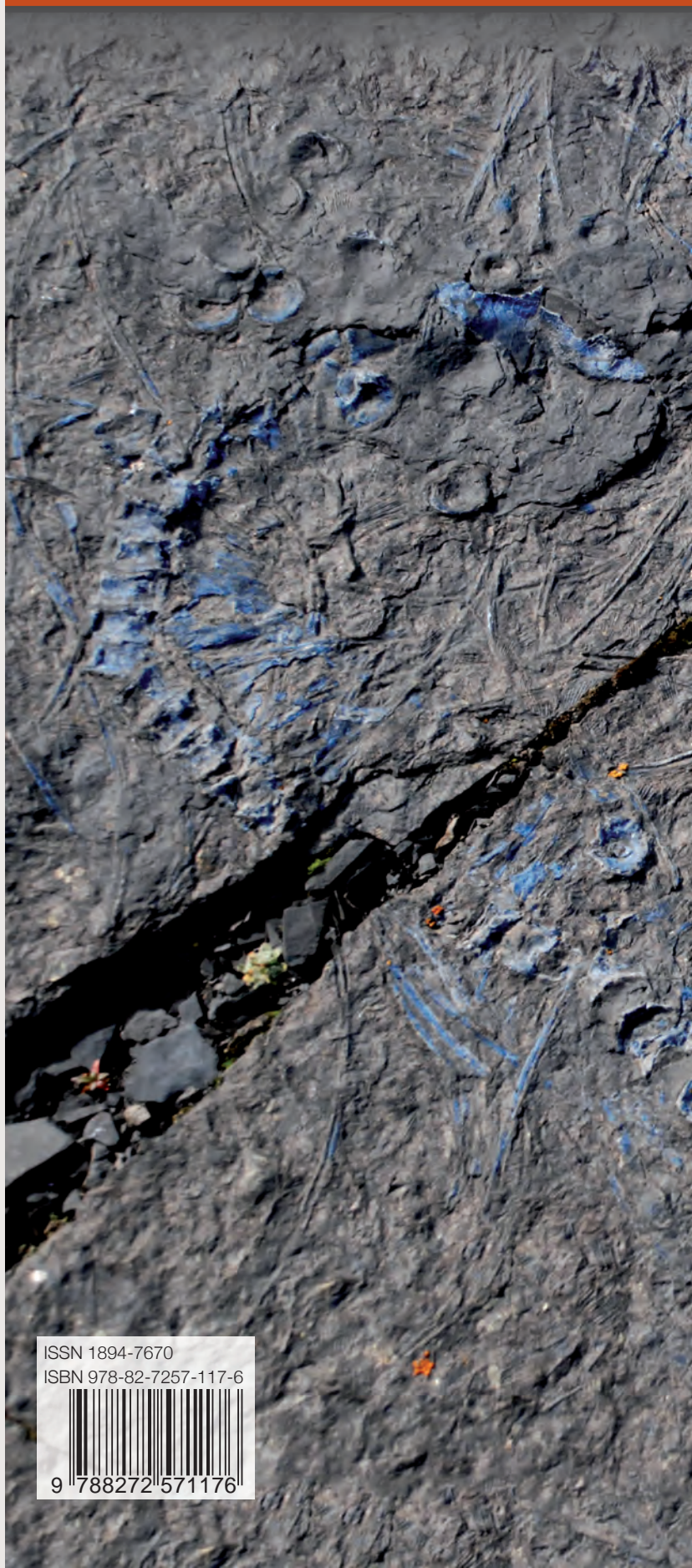
2014

<b>Bjørn Anders Lundschie, Tore Høy &amp; Atle Mørk</b> Triassic hydrocarbon potential in the Northern Barents Sea: integrating Svalbard and stratigraphic core data .....	3
<b>Rita Sande Rød, Ingrid Bjørnerheim Hynne &amp; Atle Mørk</b> Depositional environment of the Upper Triassic De Geerdalen Formation – An E-W transect from Edgeøya to Central Spitsbergen, Svalbard .....	21
<b>Gareth S. Lord, Kristoffer H. Solvi, Tore G. Klausen &amp; Atle Mørk</b> Triassic channel bodies on Hopen, Svalbard: Their facies, stratigraphical significance and spatial distribution .....	41
<b>Per Terje Osmundsen, Alvar Braathen, Rita Sande Rød &amp; Ingrid Bjørnerheim Hynne</b> Styles of normal faulting and fault-controlled sedimentation in the Triassic deposits of Eastern Svalbard .....	61
<b>Gareth S. Lord, Kristoffer H. Solvi, Marianne Ask, Atle Mørk, Mark W. Hounslow &amp; Niall W. Paterson</b> The Hopen Member: A new member of the Triassic De Geerdalen Formation, Svalbard .....	81
<b>Jørn H. Hurum, Aubrey Jane Roberts, Hans Arne Nakrem, Jan A. Stenløkk &amp; Atle Mørk</b> The first recovered ichthyosaur from the Middle Triassic of Edgeøya, Svalbard .....	97
<b>Trond Brekke, Krzysztof P. Krajewski &amp; Jørnar Heggsum Hubred</b> Organic geochemistry and petrography of thermally altered sections of the Middle Triassic Botneheia Formation on south-western Edgeøya, Svalbard .....	111
<b>Ahti Launis, Christian Pott &amp; Atle Mørk</b> A glimpse into the Carnian: Late Triassic plant fossils from Hopen, Svalbard .....	129
<b>Marina A. Tugarova &amp; Andrey G. Fedyaevsky</b> Calcareous microbialites in the Upper Triassic succession of Eastern Svalbard .....	137
<b>Mikhail A. Rogov</b> An infrazonal ammonite biostratigraphy for the Kimmeridgian of Spitsbergen .....	153



NORWEGIAN PETROLEUM  
DIRECTORATE

Return: NPD, Professor Olav Hanssens vei 10, NO-4003 Stavanger, NORWAY



ISSN 1894-7670  
ISBN 978-82-7257-117-6  
  
9 788272 571176